One-pot Carbonyl Reduction and Carbonate Formation using Sodium Borohydride in Dialkyl Carbonate Solvents and the Development of Ionophore-inspired Monomers and Polymers for Ion Sensing

A Dissertation

Presented in Partial Fulfillment of the Requirements for the

Degree of Doctor of Philosophy

with a

Major in Chemistry

in the

College of Graduate Studies

University of Idaho

by

Abdulakeem Osumah

Major Professor: Kristopher V. Waynant, Ph.D.

Committee Members: I. Francis Cheng, Ph.D.; Patrick Hrdlicka, Ph.D.;

Mark Roll, Ph.D.

Department Administrator: Ray von Wandruszka, Ph.D.

December 2020

Authorization to Submit Dissertation

This dissertation of Abdulakeem Osumah, submitted for the degree of Doctor of Philosophy with a Major in Chemistry, and titled "One-pot Carbonyl Reduction and Carbonate Formation using Sodium Borohydride in Dialkyl Carbonate Solvents and the Development of Ionophore-inspired Monomers and Polymers for Ion Sensing," has been reviewed in final form. Permission, as indicated by the signatures and dates below, is now granted to submit final copies to the College of Graduate Studies for approval.

Major Professor: _____Date:_____
Kristopher V. Waynant Ph.D.

Committee Members: _____Date:_____
I. Francis Cheng, Ph.D.

_____Date:_____
Patrick J. Hrdlicka, Ph.D.

_____Date:_____
Mark F. Roll, Ph.D.

Department Administrator: _____Date:_____
Ray von Wandruszka, Ph.D.

Abstract

This dissertation describes two separate projects. First is a convenient synthetic method for the conversion of ketones and aldehydes to unsymmetrical carbonates in refluxing dialkyl carbonate solvents using sodium borohydride in a single step. This one-pot method utilizes "greener" carbonate solvents and eliminates the need for toxic alkyl chloroformate reagents. An extensive substrate scope and reaction optimization are presented. The second part describes the development of flexible and printable calcium ion-selective electrodes (ISEs) and the use of commercially available conductive CNT inks as the ion-to-electron transducer. These electrodes were evaluated potentiometrically with the aim of retaining sensitivity while also evaluating the surface impedance. We found that ionophores were compatible and equally selective when printed with conductive ink, yet the binding agents were not compatible and needed to be added separately following jet-printing. This led to the synthesis of a novel ionophore-inspired monomer and its polymerization both in various copolymer blends and in bulk on surfaces using activators regenerated by electron transfer atom transfer radical polymerization (ARGET ATRP). The polymerization blends were used to explore the potential of replacing common binding agents found in solid contact ISEs with ionophore based binding agents. The ARGET ATRP polymer brushes were developed with the goal of growing the ion-sensing polymers directly onto carbon nanotubes (CNTs) as potential ion-sensing components to known CNT inks. Ultimately, it was found that the total average bond distances of the novel ionophore analog were within 0.5% difference of that of the known calcium ionophore ETH129, yet the stoichiometry differed. Overall, ionophore compatibility in jet-printing, sensing, and the monomer as a potential polymer candidate for device design were explored.

Vita

Abdulakeem Osumah, PhD 208-301-7407 | osum1316@vandals.uidaho.edu

EDUCATION

Ph.D. Candidate, Organic Chemistry, University of Idaho, Moscow ID 2015-2020
Advisor: Dr. Kristopher V. Waynant
Dissertation Title: One-pot Carbonyl Reduction and Carbonate Formation using Sodium Borohydride in Dialkyl Carbonate Solvents and Calcium Ion-Selective Electrode and Ionophore-inspired Monomers and Polymers for Calcium Ion Sensing

B.Sc. Industrial Chemistry, University of Ibadan, Ibadan Nigeria 2003-2007
Research Advisor: Dr. Odola
Thesis: "Preparation, Characterization and Antimicrobial Activity of Dithiocarbamate Complexes of Nickel (II)"

WORK EXPERIENCE

Graduate Teaching Assistant, Department of Chemistry, University of Idaho 2015-2020
Instructor for Organic Chemistry I and II labs

Customer Care Executive, Etisalat Nigeria (now 9mobile Nigeria) 201-2014
- Achieved a 5% increase in customer satisfaction by attending to and promptly resolving customer complaints
- Decreased rebound call traffic by 20% through careful troubleshooting and resolution of lingering customer device and service subscription issues
- Increased business intelligence data by 3%, recording all customer interactions using approved software and escalated unresolved issues to the relevant units using defined escalation channels

Mobile Financial Services Analyst, Etisalat Nigeria 2013
- Increased customer usage by 10% by promptly resolving unusual transactions and issues on the usage of the Mobile Money (MM) platform detected by analysis of the daily reports I prepared
- Contributed to the team's effort that added three new partners to the MM platform by interfacing the partners with the relevant Etisalat Products and Services teams

Instructor, AfriHUB Oba Akran Ikeja – Lagos, Nigeria. 2011
- Mathematics instructor for Diploma in Software Engineering students
- Trained students preparing for Cisco Certified Network Associates examination

PUBLICATION

- **Osumah, A.**, Magolan, J., Waynant, K. V., One-pot Carbonyl Reduction and Carbonate Formation using Sodium Borohydride in Dialkyl Carbonate Solvents. *Tetrahedron Letters* **2019**, 60, 151203.

Manuscripts under preparation

- **Osumah, A.**, Larson, G. E., Waynant, K. V. Conductive carbon nanotube ink formulation as a contact layer for calcium ion-selective electrodes.
- **Osumah, A.**, Hill C., Waynant, K. V. Development of Calcium Ionophore-inspired monomer and evaluation as a copolymer binding agent

Presentations

- **Osumah, A.**, Larson, G. E., Waynant, K. V., Synthesis of Ionophore-Inspired Monomers and Evaluation of Polymer-coated Carbon Nanotube Inks as Calcium Ion-sensitive Electrodes. *Oral* presentation at the 46th NOBCChE Annual National Conference, St. Louis Union Station, MO. November 18th - 21st, **2019**
- **Osumah, A.**, Larson, G. E., Waynant, K. V., Synthesis of Ionophore-Inspired Monomers and Evaluation of Polymer-coated Carbon Nanotube Inks as Calcium Ion-sensitive Electrodes. *Poster* presentation at the National Society of Black Engineers Region VI Fall Regional Conference, San Francisco, CA. November 8 - 10th**, 2019**
- **Osumah, A.**, Larson, G. E., Humayun MD. K., Waynant, K. V., Synthesis, and Evaluation of Polymer-Coated Carbon nanotube Inks as Calcium Ion-Sensitive Electrodes. *Poster* presented at the American Chemical Society Spring Annual National Meeting, Orlando, Fl. March 31st – April 4th, **2019**
- **Osumah, A.**, Larson, G. E., Waynant, K. V., Towards the Development of Polymer-coated Carbon Nanotubes for Printable Calcium Electrodes. 45th NOBCChE Annual National Conference, Orlando, Fl. October 30th – November 2nd, **2018**.

HONORS / AWARDS

- Rao Chemistry Scholarship 2019
- IDeA Network of Biomedical Research Excellence Travel Award 2018-2019
- NOBCChE 2018 Poster Presentation Outstanding Poster Awardee 2018
- NOBCChE Advancing Science Conference Grant Recipient 2017-2019
- Malcolm and Carol Renfrew Scholarship Summer Scholarship (Department of Chemistry, University of Idaho) 2015-2020

PROFESSIONAL AFFILIATIONS

- **President**, National Organization for the Professional Advancement of Black Chemists and Chemical Engineers (NOBCChE) University of Idaho Chapter 2018–2019
- **Member,** American Chemical Society (ACS) 2019-pres
- **Chief Justice**, University of Idaho Graduate and Professional Students' Association (GPSA) 2018–2019
- **Chemistry Department Representative**, University of Idaho GPSA 2017–2018

Acknowledgments

All praise is due to God, Lord of the worlds! I started my Ph.D. in the Spring of 2015. I am thankful that I can complete the program and lucky enough to have worked with two helpful research advisors. My sincere appreciation goes to my first research advisor, Dr. Jakob Magolan, for accepting me into his lab, where I developed my research skills and learned the basics of advanced organic chemistry. Dr. Magolan is a great mentor and advisor who taught me so much in organic chemistry, including the use of ChemDraw and SciFinder, how to design and give technical presentations, and exemplary leadership skills. Jakob made me feel at home in his lab as he cares about the well-being of his students and organizes team bonding events.

My profound gratitude goes to Dr. Kristopher Waynant for all my achievements in the later stage of my Ph.D. Dr. Waynant is a mentor and friend, whose open-door policy is outstanding! Kris (as he is popularly known) is a very friendly and caring supervisor who goes the extra mile for his students. He is a charismatic leader, a very ambitious scientist with diverse knowledge and experience in Chemistry. I am grateful for his trust in me as his first graduate and Ph.D. student, which exposed me to some aspect of chemistry research, namely polymerization and electrochemical sensing. I also did my first collaborative research under Kris, (the NASA EPSCoR-sponsored project) with other researchers at Boise State University. I am thankful for the experiences I gained and the skills I learned. I will miss our lab bonding events and the yearly waffle parties.

I thank my Dissertation committee members Prof. I. Francis Cheng, Prof. Patrick J. Hrdlicka and Dr. Mark Roll for finding time to serve on my committee and for their insightful inputs in my projects and also for their mentorship.

I wish to thank Dr. Alexander Blumenfeld for helping to analyze my NMR spectra and the NMR skills I learned from him. I owe any of my future success in an NMR position to Alexander, especially in the management of NMR magnets. I wish to thank Dr. Lee Deobald for helping to take the mass spectroscopy of my samples. My gratitude to Moubani Chakraborty and Rabina Pradhan for being good colleagues in the lab. I also want to thank Dr. Md Kabir Humayun, Dr. Charles Nwamba, Dipak Koirala, and Rabina Pradhan for their insights in my potentiometric setup.

Dedication

I dedicate this Ph.D. to the memory of my late dad, Yakubu Osumah (despite his illiteracy, did everything he could to get us educated), to my family and the family of Yakubu Osumah. I appreciate every member of Yakubu Osumah's family for the roles we have played in each other's lives. May we continue to be strong, healthy, and supportive of each other. I thank my wife, Amina, for her role in my life and her support all the way. May Allah reward her abundantly. And my kids, Abdurrahman, Farah, and the twins, may Allah bless you all. Ali Ali and Shamsa Njagi, thanks for your hospitality.

Table of Contents

List of Tables

List of Figures

List of Schemes

List of Abbreviations

Ac	Acetyl
Aq.	aqueous
Bn	Benzyl
Bz	benzoyl
t-Bu	*tert*-butyl
9-BBN	9-Borabicyclo[3.3.1]nonane
cat.	catalytic amount
CoA	Coenzyme A
d	doublet
DCM	dichloromethane
DDQ	2,3-Dichloro-5,6-dicyano-1,4-benzoquinone
DIBAL-H	diisobutylaluminum hydride
DIPEA	diisopropylethylamine
DMAP	4-dimethylaminopyridine
DMF	*N*,*N*-dimethylformamide
DMSO	dimethyl sulfoxide
d.r.	diastereomeric ratio
Et	Ethyl
Equiv	equivalents
FTIR	Fourier transform infrared
gem	geminal
h	Hour(s)

HMBC	heteronuclear multiple bond correlation
HRMS	high resolution mass spectrometry
Hz	Hertz
IR	infrared
KCN	potassium cyanide
LDA	lithium diisopropylamide
LHMDS	lithium bis(trimethylsilyl)amide
mL	milliliter
m	multiplet
M	Molar
Me	Methyl
MRSA	methicillin-resistant *Staphylococcus aureus*
m	*Meta*
m.p	melting point
N	Normal
NBS	N-bromosuccinimide
NMR	nuclear magnetic resonance
o	ortho
OTf	trifluoromethanesulfonate
p	Para
PG	unspecified protecting group
Ph	Phenyl
PPA	polyphosphoric acid

i-Pr	isopropyl
q	Quartet
R_f	relative to front
s	Singlet
r.t	Room temperature
SEM	scanning electron microscopy
SM	starting material
SN_{Ar}	nucleophilic aromatic substitution reaction
t	Triplet
TEA	triethylamine
THF	tetrahydrofuran
TLC	thin layer chromatography
TMEDA	tetramethylethylenediamine
TMS	trimethylsilyl
TMSCl	trimethylsilyl chloride
TMSCN	trimethylsilyl cyanide
Ts	*p*-toluenesulfonyl (tosyl)
TsOH	*p*-toluenesulfonic acid
w/w	weight per weight

Chapter 1: One-Pot Carbonyl Reduction and Carbonate Formation Using Sodium Borohydride in Dialkyl Carbonate Solvents

Chapter 1 is a more detailed adaptation of a published manuscript:

Osumah, A.; Waynant, K. V.; Magolan, J. *Tetrahedron Letters* **2019**, *60* (44), pp 151203-5

Abstract

Borohydride reduction of carbonyl derivatives in refluxing dialkyl carbonate solvents provides mixed alkyl carbonates directly from ketones and aldehydes via a facile one-pot, two-step sequence. The substrate scope of this reaction is demonstrated with twenty-one examples. It is hypothesized that residual borohydride reagents facilitate the second step in this reaction sequence. Therefore, the preparation of carbonates in high yields from alcohols using catalytic sodium hydride was also demonstrated and optimized. These two facile and general methodologies are efficient synthetic procedures for carbonate formation without the need for alkyl chloroformates.

Keywords: Carbonates, One-pot, Carbonyl reduction, Carbonate formation; green chemistry

1.1. Introduction

Concerns of step economy and synthetic efficiency have long been ubiquitous in multi-step, target-directed organic synthesis.[1, 2] From the perspective of efficiency, it is advantageous whenever more than one sequential transformation can be achieved in one-pot without isolation or purification of intermediates.[3-5] We were particularly interested in the reduction of steps in the formation of mixed carbonates directly from carbonyl derivatives. Organic mixed carbonates, often used as versatile alcohol protecting moieties, have received interest of late both as reagents and solvents for many catalytic reactions,[6-8] and have even been studied as co-solvents in Li-ion batteries.[9] Our laboratory has sought to develop procedurally advantageous

reaction methodologies characterized by simple, and usually filtrative, work-ups. In general, the aims of green chemistry can be fulfilled by the development of any vital chemical transformation that achieves multiple steps in a single pot, is catalytic, and uses commonly-sourced materials in atom-economical and mass-balanced manners.[10] Furthermore, for industrial applications, the minimization of reagents, short reaction times (under eight hours), and the use of green solvents are all desirable attributes.

In multi-step reaction sequences, it is not uncommon to see ketones or aldehydes reduced with borohydride followed by subsequent conversion of the resulting alcohol to an alkyl carbonate with the use of an alkyl chloroformate. The most common reagents for carbonate formation in this context are toxic and corrosive methyl- or ethyl chloroformates and these reactions have been extensively used in synthetic methods development[11-13], total syntheses[10, 14, 15], active pharmaceutical ingredients production[16], and in multiple patents even though the formation of mixed carbonates using milder dimethyl or diethyl carbonate solvents is well-established in the literature.[17-23] This observation led us to consider a borohydride-facilitated reduction of carbonyls in a dialkyl carbonate solvent as the optimal strategy for the direct one-pot formation of a mixed carbonate from a ketone or aldehyde.

Herein we report our investigation of a sodium borohydride-mediated carbonyl reduction and carbonate formation strategy that converts ketones and aldehydes directly to alkyl carbonates (methyl or ethyl) in a one-pot two-step strategy. This reaction requires minimal work-up and proceeds in good yields. Secondly, towards a more thorough mechanistic insight into this one-pot reaction procedure, a second reaction scheme was investigated on the conversion of alcohols directly to mixed carbonates in the presence of sub-stoichiometric

amounts of sodium hydride. This substrate scope and study, while left unpublished, helped determine the mechanism of this reaction, as described in **Figure 1.6**.

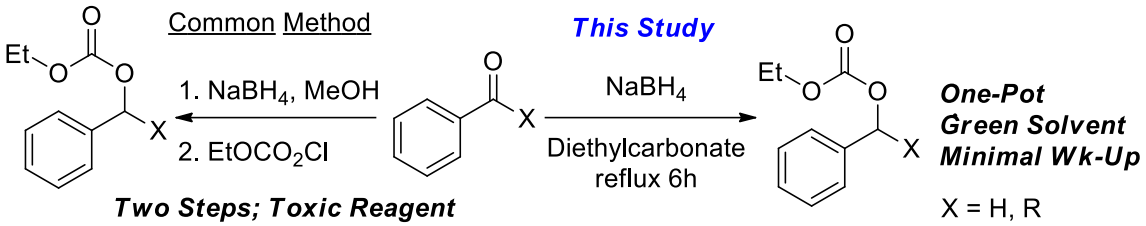

Figure 1. 1. The overall scheme of the study

1.2. Results

As illustrated in **Table 1.1**, the study began with the optimization of stoichiometry and temperature in the reduction of acetophenone **1-1** with $NaBH_4$ in diethyl carbonate. First, the use of one molar equivalent of $NaBH_4$ at room temperature gave only unreacted starting material and alcohol **1-2** after 24 h. Increasing the temperature to 90˚C gave a mixture of carbonate **1-3** and alcohol **1-2** after 6 h (entry 2). However, a complete conversion to the carbonate was observed after 17 h. Performing the reaction in refluxing diethyl carbonate (boiling point 128 ˚C) in the presence of air gave immaculate conversion to the mixed carbonate **1-3** in 6 h (entry 4) with an isolated product yield of 89 % on a 1 mmol scale. Unsurprisingly, a control reaction performed in the absence of $NaBH_4$ resulted in the recovery of unreacted starting material (entry 5), while 0.5 molar equivalents of $NaBH_4$ resulted in an inferior yield of the desired product (entry 6). When the amount of sodium borohydride was reduced further, carbonate product yield dropped, and the reaction took a longer time. Therefore, the reaction was evaluated at 1.0 equivalent of $NaBH_4$ under reflux conditions for 6 h. At completion, the content of the flask was cooled to room temperature, diluted with diethyl ether, filtered through Celite, and concentrated under reduced pressure to give carbonate products with a high degree of mass transfer and purity.

Table 1. 1. Optimization of direct conversion of acetophenone to carbonate 1-3.

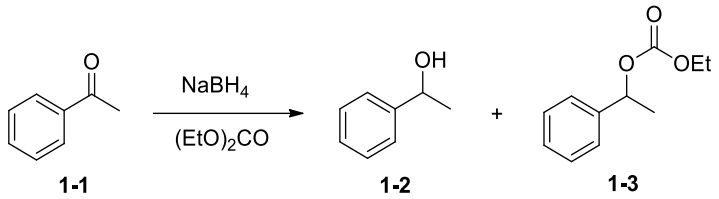

1-1 1-2 1-3

Entry	$NaBH_4$ (equiv)	Temp (°C)	Time (h)	1-1 (%)[1]	1-2 (%)[1]	1-3 (%)[1]
1	1.0	25	24	43	31	0
2	1.0	90	6	45	0	38
3	1.0	90	17	0	0	100
4	1.0	reflux	6	0	0	100 (89)[2]
5	0	reflux	6	100	0	0
6	0.5	reflux	6	5	0	84

[1] Yields determined via ^{1}H NMR with 1-methylnaphthalene as internal standard
[2] Isolated yield after chromatography

A variety of ketones and aldehydes were subjected to these optimized reaction conditions yielding carbonates **1-4** to **1-18** as shown in **Figure 1.2**. The reaction was repeated at least twice for each of the substrates. Dihydrocinnamaldehyde and naphthaldehyde gave good yields under the stoichiometric one-pot conditions (**1-13** and **1-14**). Aromatic aldehydes resulted in variable yields. For example, conversion of furfural to carbonate **1-15** in 43 % yield was in strict contrast to benzothiophene-3-carbaldehyde converting to carbonate **1-16** in 70% yield. Carbonates **1-17** and **1-18** were formed from the corresponding aliphatic ketone and aldehyde. The reaction was not compatible with substrates containing acidic protons such as phenols and carboxylic acids. Furthermore, α,β-unsaturated aldehydes gave mixtures of the corresponding alkyl carbonates and fully saturated carbonates formed via olefin reduction. Lastly, tetralone was unsuitable for these conditions yielding mixtures of carbonate and dihydronaphthalene elimination products.

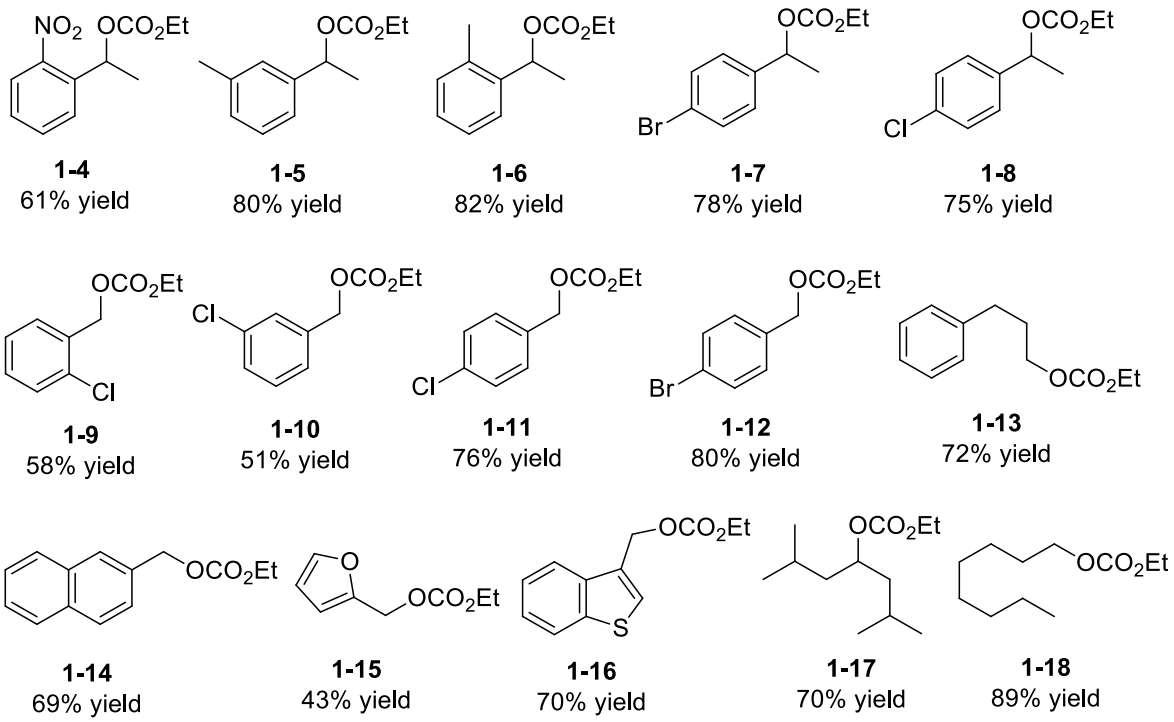

Figure 1. 2. Scope of representative examples of mixed carbonates formation from refluxing diethyl carbonate conditions.

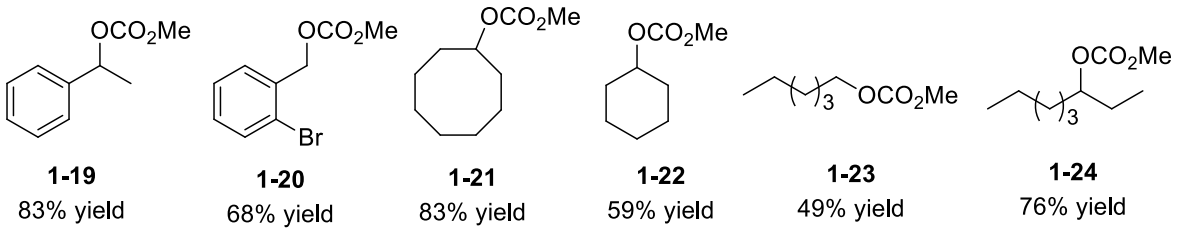

Figure 1. 3. Scope of mixed methyl carbonates from refluxing dimethyl carbonate conditions.

When the solvent was changed to dimethyl carbonate, as shown in **Figure 1.3** (reflux temperature at 90˚C), acetophenone was converted to the carbonate **1-19** in 83% yield over 6 h period. A variety of mixed methyl carbonates were formed from various ketones and aldehydes in 49 - 83% yield.

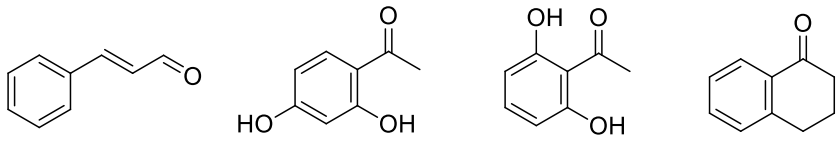

Figure 1. 4. Substrates that are unsuitable for the reaction condition.

The experimental protocols, ^{1}H NMR, and ^{13}C NMR data for these are included in the **Appendix to Chapter 1.**

Sodium borohydride is commercially produced from the reaction of borane with sodium hydride. Therefore, during one-pot reaction development, the formation of mixed carbonates from alcohols was investigated using catalytic amounts of sodium hydride. Benzyl alcohol (**1-25**) was treated with NaH (60% dispersion in oil) in dimethyl carbonate with varying temperatures to examine yields of carbonate product **1-26** as shown in **Table 1.2**. Complete consumption of starting material was observed in 6 hours under refluxing dimethyl carbonate conditions in the presence of 1, 0.5, and 0.1 equivalents of sodium hydride (entries 1-3). The isolated yield of the desired methyl carbonate was 89% on a 2 mmol scale and 84 % on a 10 mmol scale. Lowering the amount of NaH to 5 mol % gave a reduced yield (entry 5). Removal of NaH from the reaction, unsurprisingly, gave no product. The carbonate product from this reaction could also be obtained in high purity via ether filtration through a pad of Celite and silica, followed by evaporation of the solvent. Included in **Figure 1.4** is a wide range of alcohols converted to mixed carbonates providing decent to excellent yields.

Table 1. 2. Reaction scope for carbonate formation with NaH in Dimethyl carbonate.

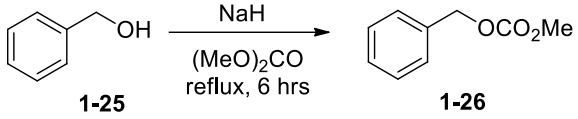

1-25 **1-26**

Entry	NaH (equiv)	NMR yield (%)[1]	Mass recovery (%)	Isolated yield (%)
1	1.0	78	100	62
2	0.5	82	100	79
3	0.1	92	100	89
4	0.1[2]	88	93	85
5	0.05	71	-	-
6	0	0	0	0

[1] Yields determined via ^{1}H NMR with 1-methyllnaphthalene as internal standard
[2] 10 mmol scale

Overall, many primary and secondary alcohols tolerated the reaction conditions, and the Celite/silica work-up yielding the carbonate as the sole product.

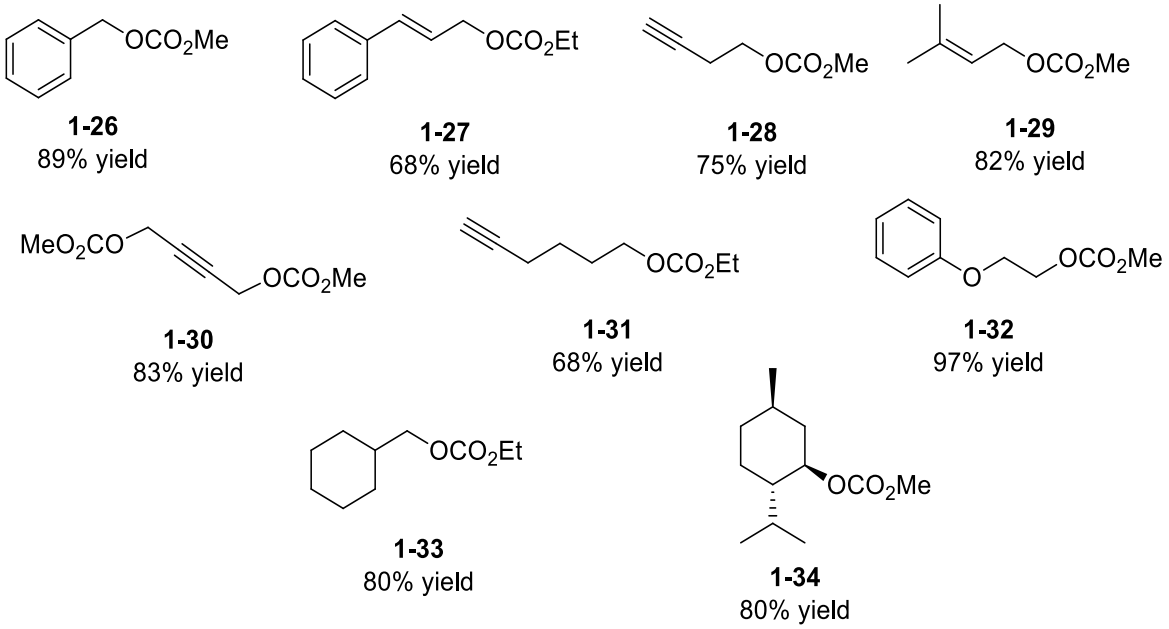

Figure 1. 5. Scope of mixed methyl carbonates formation from alcohols using NaH in refluxing dimethyl carbonate conditions.

Mechanistically, it is hypothesized that after the carbonyl reduction or formation of the alcohol, carbonate formation proceeds from the residual hydride abstracting a hydrogen from the alcohol (**Figure 1.5**). The resulting alkoxide attacks the dialkylcarbonate solvent to form the mixed carbonate. To test this theory, benzyl alcohol in diethyl carbonate was reacted with both sodium borohydride and borane (THF complex). While the former successfully facilitated the mixed carbonate formation, borane, although a powerful reductant, is less likely to act as a base, and thus the reaction did not proceed.

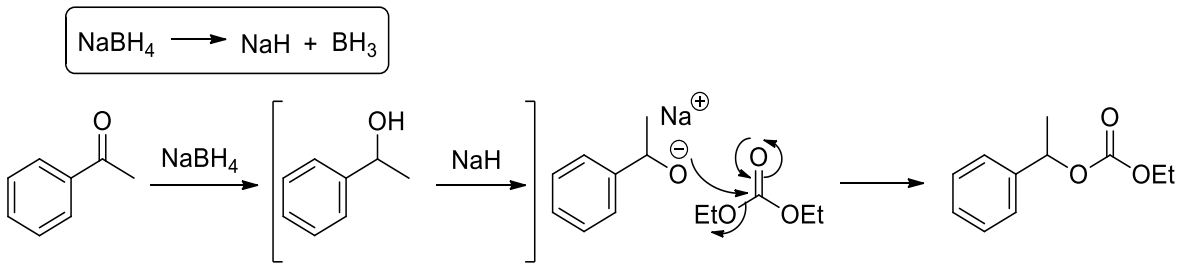

Figure 1. 6. The mechanistic hypothesis behind the reduction/carbonate formation strategy.

1.3. Conclusion

The one-pot reduction-protection strategy for carbonyl compounds directly to carbonates was well-tolerated for many ketones and aldehydes. It should be a welcomed protocol over the habit of reduction followed by alkyl chloroformate protection. The mass recovery, limited work-up procedures, and the overall ease of these reactions should lend well to the synthesis of mixed carbonates and the continued pursuit for facile conditions and fewer steps. Secondly, residual hydride and ultimately 10 mol % sodium hydride delivered good to excellent yields of unsymmetrical carbonates through refluxing DEC or DMC solvent/reagent and this reaction was very comparable to the other reported procedures. The green value of this reaction was delivered through the high mass recovery, good to excellent yields, and low loading amounts of hydride and open-to-air reaction conditions. With the continued use of carbonate solvents, there is high value in one-pot reactions where the solvent is ultimately a reagent.

1.4. Experimental

1.4.1. Materials and Methods

Sodium borohydride, dimethyl carbonate and diethyl carbonate were purchased from Acros Organics and used as received. Sodium hydride (60% immersion in oil) was purchased from Sigma Aldrich and used as received. All ketones, aldehydes, and alcohols were purchased from Sigma-Aldrich, Acros Organics, or AK Scientific and were used as received.

General procedure for the synthesis of carbonate from ketone/aldehyde: A 25 ml round bottom flask was charged with 1 mmol of the carbonyl compound, 1 mmol of $NaBH_4$ and 5 ml of diethyl carbonate. The mixture was refluxed and monitored by TLC until the reaction was complete over 6 h. The reaction was then cooled to room temperature, washed with 25 mL of

diethyl ether through a bed of Celite on silica in a fritted funnel and the solvent was removed at reduced pressure. The product was purified with column chromatography using EtOAc and hexanes.

General procedure for the synthesis of carbonates from alcohols: A 25 mL round bottom flask was charged with a stir bar, alcohol (1 mmol), NaH - 60% in oil dispersion (0.1 mmol) and diethyl carbonate (5 mL). The mixture is then refluxed for 6 hours while monitoring by TLC until the reaction is complete. The reaction was cooled to room temperature and washed with ~ 20 mL diethyl ether through a bed of Celite on silica in a fritted funnel. The solvent is then removed under reduced pressure to yield the pure product or a mixture that is purified by column chromatography using EtOAc and hexanes.

Characterization of carbonates 1-3 to 1-34

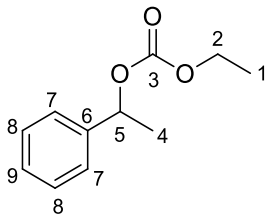

1-3

Ethyl (1-phenylethyl) carbonate 1-3: The general procedure for ketone/aldehyde was used and compound **1-3** was obtained (0.173 g, 89% yield) as a clear oil and matches previously reported spectra.[24] ^{1}H NMR (500 MHz, Chloroform-*d*) δ 7.40 – 7.28 (m, 5H, $\mathbf{H_{7\text{-}9}}$), 5.73 (q, *J* = 6.6 Hz, 1H, $\mathbf{H_5}$), 4.22 – 4.12 (m, 2H, $\mathbf{H_2}$), 1.60 (d, *J* = 6.6 Hz, 3H, $\mathbf{H_4}$), 1.29 (t, *J* = 7.1 Hz, 3H, $\mathbf{H_1}$). ^{13}C NMR (126 MHz, $CDCl_3$) δ 154.7 $\mathbf{C_3}$, 141.3 $\mathbf{C_6}$, 128.7 $\mathbf{C_8}$, 128.2 $\mathbf{C_9}$, 126.1 $\mathbf{C_7}$, 76.3 $\mathbf{C_5}$, 64.0 $\mathbf{C_2}$, 22.5 $\mathbf{C_4}$, 14.4 $\mathbf{C_1}$.

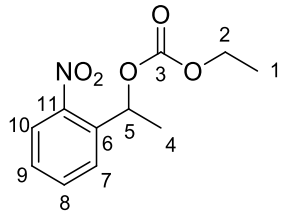

1-4

Ethyl (1-(2-nitrophenyl)ethyl) carbonate 1-4: The general procedure for ketone/aldehyde was used and compound **1-4** was obtained (0.146 g, 61% yield) as a clear oil. R_f(3:7 EtOAc/hexane): 0.43. ^{1}H NMR (500 MHz, Chloroform-*d*) δ 7.96 (ddd, *J* = 8.0, 1.4, 0.4 Hz, 1H, **H$_{10}$**), 7.70 (dd, *J* = 8.0, 1.4, 0.4 Hz, 1H, **H$_8$**), 7.65 (tdd, *J* = 8.0, 1.3, 0.5 Hz, 1H, **H$_9$**), 7.45 (ddd, *J* = 8.0, 7.3, 1.5 Hz, 1H, **H$_7$**), 6.26 – 6.22 (q, *J* = 6.5 Hz, 1H, **H$_5$**), 4.19 – 4.08 (m, 2H, **H$_2$**), 1.69 (d, *J* = 6.5 Hz, 3H, **H$_4$**), 1.27 (t, *J* = 7.1 Hz, 3H, **H$_1$**). ^{13}C NMR (126 MHz, $CDCl_3$) δ 154.2 **C$_3$**, 147.8 **C$_{11}$**, 137.9 **C$_6$**, 133.9 **C$_8$**, 128.7 **C$_9$**, 127.2 **C$_7$**, 124.6 **C$_{10}$**, 71.7 **C$_5$**, 64.4 **C$_2$**, 22.3 **C$_4$**, 14.3 **C$_1$**. IR (cm^{-1}): 2982, 1745, 1373, 1260, 1059, 863. MS (ES+) calcd. for $C_{10}H_{18}O_3$ *m/z* [MNa+]: 262.0691, found: 262.0683.

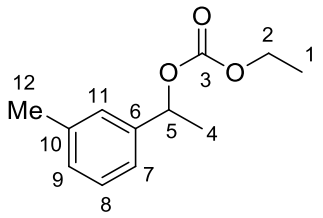

1-5

Ethyl (1-(m-tolyl)ethyl) carbonate 1-5: The general procedure for ketone/aldehyde was used and compound **1-5** was obtained (0.167g, 80% yield) as a clear oil. R_f (3:7 EtOAc/hexane): 0.71. ^{1}H NMR (500 MHz, Chloroform-*d*) δ 7.42 (ddd, *J* = 6.0, 2.0, 1.5 Hz, 1H, **H$_8$**), 7.21 (td, *J* =8.5, 2.0 Hz, 1H, **H$_{11}$**), 7.18 (dd, *J* = 7.3, 1.5 Hz, 1H, **H$_7$**), 7.14 (m, 1H, **H$_9$**), 5.94 (q, *J* = 6.6 Hz, 1H, **H$_5$**), 4.21 – 4.11 (m, 2H, **H$_2$**), 2.39 (s, 3H, **H$_{12}$**), 1.56 (d, *J* = 6.6 Hz, 3H, **H$_4$**), 1.29 (t, *J* = 7.1 Hz, 3H, **H$_1$**). ^{13}C NMR (126 MHz, $CDCl_3$) δ 154.7 **C$_3$**, 139.8 **C$_6$**, 134.6 **C$_{10}$**, 130.5 **C$_9$**,

127.9 **C11**, 126.5 **C7**, 125.3 **C8**, 73.2 **C5**, 64.0 **C2**, 21.7 **C4**, 19.1 **C12**, 14.4 **C1**. IR (cm^{-1}): 1739, 1262, 1057. MS (ES+) calcd. for $C_{10}H_{18}O_3$ *m/z* [MNa+]: 231.0997, found: 231.0993.

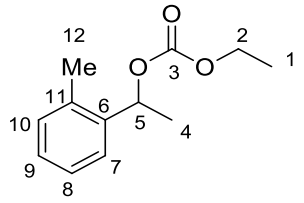

1-6

Ethyl (1-(o-tolyl)ethyl) carbonate 1-6: The general procedure for ketone/aldehyde was used and compound **1-6** was obtained (0.171 g, 82% yield) as a clear oil. R_f (3:7 EtOAc/hexane): 0.69. ^{1}H NMR (500 MHz, Chloroform-*d*) δ 7.43 – 7.41 (m, 1H, **H10**), 7.24 – 7.17 (m, 2H, **H9 H7**), 7.15 – 7.13 (m, 1H, **H8**), 5.96 – 5.92 (m, 1H, **H5**), 4.20 – 4.12 (m, 2H, **H2**), 2.39 (s, 3H, **H12**), 1.56 (d, *J* = 6.6 Hz, 3H, **H4**), 1.29 (t, *J* = 7.1 Hz, 3H, **H1**). ^{13}C NMR (126 MHz, $CDCl_3$) δ 154.7 **C3**, 139.8 **C6**, 134.6 **C11**, 130.5 **C10**, 127.9 **C9**, 126.5 **C8**, 125.3 **C7**, 73.2 **C5**, 64.0 **C2**, 21.7 **C4**, 19.1 **C12**, 14.4 **C1**. IR (cm^{-1}): 2981, 1739, 1456, 1261, 1049, 791. MS (ES+) calcd. for $C_{10}H_{18}O_3$ *m/z* [MNa+]: 231.0997, found: 231.0986.

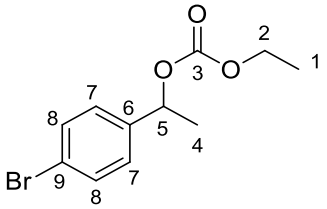

1-7

1-(4-bromophenyl)ethyl ethyl carbonate 1-7: The general procedure for ketone/aldehyde was used and compound **1-7** was obtained (0.213 g, 78% yield) as a clear oil. R_f (3:7 EtOAc/hexane): 0.65. ^{1}H NMR (500 MHz, Chloroform-d) δ 7.48 (d, *J* = 8.4 Hz, 2H, **H7**), 7.25 (d, *J* = 8.4 Hz, 2H, **H8**), 5.67 (q, *J* = 6.6 Hz, 1H, **H5**), 4.17 (m, 2H, **H2**), 1.56 (d, *J* = 6.7 Hz, 3H, **H4**), 1.29 (t, *J* = 7.1 Hz, 3H, **H1**) ^{13}C NMR (126 MHz, CDCl3) δ 154.5 **C3**, 140.3 **C6**, 131.8 **C8**, 127.9 **C7**,

122.1 **C9**, 75.5 **C5**, 64.1 **C2**, 22.4 **C4**, 14.3 **C1**. IR (cm^{-1}): 2984, 1740, 1490, 1372, 1260, 1032, 791. MS (ES+) calcd. for $C_{10}H_{18}O_3$ *m/z* [MNa+]: 294.9946, found: 294.9944.

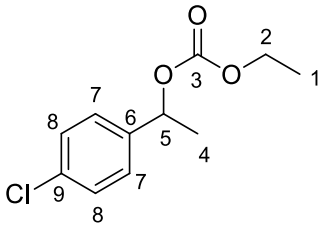

1-8

1-(4-chlorophenyl)ethyl ethyl carbonate 1-8: The general procedure for ketone/aldehyde was used and compound **1-8** was obtained (0.171 g, 75% yield) as a clear oil. Spectra matched that of known compound.[25] ^{1}H NMR (500 MHz, Chloroform-*d*) δ 7.34 – 7.30 (m, 4H, **H7-8**), 5.68 (q, *J* = 6.7 Hz, 1H, **H5**), 4.22 – 4.11 (m, 2H, **H2**), 1.57 (d, *J* = 6.6 Hz, 3H, **H4**), 1.29 (t, *J* = 7.1 Hz, 3H, **H1**). ^{13}C NMR (126 MHz, $CDCl_3$) δ 154.6 **C3**, 139.8 **C6**, 134.1 **C9**, 128.9 **C8**, 127.6 **C7**, 75.6 **C5**, 64.2 **C2**, 22.4 **C4**, 14.4 **C1**.

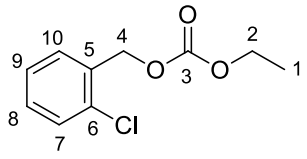

1-9

2-chlorobenzyl ethyl carbonate 1-9: The general procedure for ketone/aldehyde was used and compound **1-9** was obtained (0.124 g, 58% yield) as a clear oil. R_f (3:7 EtOAc/hexane): 0.67. ^{1}H NMR (500 MHz, Chloroform-*d*) δ 7.47 – 7.44 (m, 1H, **H7**), 7.40 – 7.38 (m, 1H, **H9**), 7.29 – 7.26 (m, 2H, **H8 H10**), 5.28 (s, 2H, **H4**), 4.24 (q, *J* = 7.1 Hz, 2H, **H2**), 1.33 (t, *J* = 7.1 Hz, 3H, **H1**). ^{13}C NMR (126 MHz, $CDCl_3$) δ 155.1 **C3**, 133.7 **C5**, 133.3 **C6**, 129.9 **C8**, 129.8 **C10**, 129.7

C7, 127.1 **C9**, 66.7 **C4**, 64.5 **C2**, 14.4 **C1**. FTIR (cm^{-1}): 2985, 1744, 1447, 1381, 1260, 1008. MS (ES+) calcd. for $C_{10}H_{18}O_3$ *m/z* [MNa+]: 237.0294, found: 237.0294.

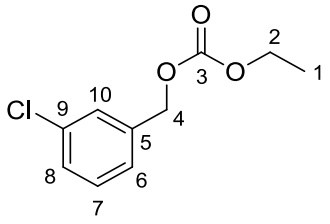

1-10

3-chlorobenzyl ethyl carbonate 1-10: The general procedure for ketone/aldehyde was used and compound **1-10** was obtained (0.109 g, 51% yield) as a clear oil. R_f (3:7 EtOAc/hexane): 0.61. ^{1}H NMR (500 MHz, Chloroform-d) δ 7.38 (m, *J* = 2.0, 0.6 Hz, 1H, **H10**), 7.32 – 7.26 (m, 3H, **H6-8**), 5.12 (s, 2H, **H4**), 4.22 (q, *J* = 7.1 Hz, 2H, **H2**), 1.32 (t, *J* = 7.1 Hz, 3H, **H3**). ^{13}C NMR (126 MHz, $CDCl_3$) δ 155.1 **C3**, 137.5 **C5**, 134.6 **C9**, 130.0 **C7**, 128.8 **C8**, 128.4 **C10**, 126.3 **C6**, 68.6 **C4**, 64.5 **C2**, 14.4 **C1**. FTIR (cm^{-1}): 2983, 1741, 1575, 1243, 1005, 784. MS (ES+) calcd. for $C_{10}H_{18}O_3$ *m/z* [MNa+]: 237.0294, found: 237.0284.

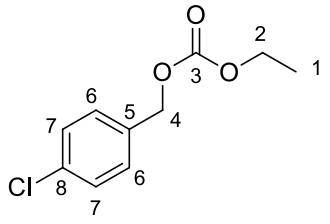

1-11

4-chlorobenzyl ethyl carbonate 1-11: The general procedure for ketone/aldehyde was used and compound **1-11** was obtained (0.163 g, 76% yield) as a clear oil. R_f (3:7 EtOAc/hexane): 0.61. ^{1}H NMR (500 MHz, Chloroform-*d*) δ 7.35 – 7.31 (m, 4H, **H6 H7**), 5.11 (s, 2H, **H4**), 4.21 (q, *J* = 7.1 Hz, 2H, **H2**), 1.31 (t, *J* = 7.1 Hz, 3H, **H1**). ^{13}C NMR (126 MHz, $CDCl_3$) δ 155.2 **C3**,

134.6 **C5**, 134.0 **C8**, 129.8 **C6**, 128.9 **C7**, 68.7 **C4**, 64.4 **C2**, 14.4 **C1**. FTIR (cm^{-1}): 2980, 1742, 1493, 1262, 1094, 845. MS (ES+) calcd. for $C_{10}H_{18}O_3$ *m/z* [MNa+]: 237.0294, found: 237.0283.

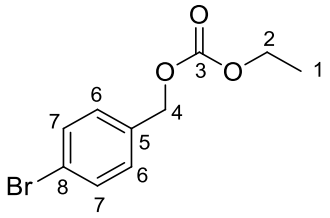

1-12

4-bromobenzyl ethyl carbonate 1-12: The general procedure for ketone/aldehyde was used and compound **1-12** was obtained (0.207 g, 80% yield) as a clear oil. R_f (3:7 EtOAc/hexane): 0.60. ^{1}H NMR (500 MHz, Chloroform-*d*) δ 7.50 (d, *J* = 8.5 Hz, 2H, **H7**), 7.27 (d, *J* = 8.3 Hz, 2H, **H6**), 5.10 (s, 2H, **H4**), 4.22 (q, *J* = 7.1 Hz, 2H, **H2**), 1.32 (t, *J* = 7.1 Hz, 3H, **H1**). ^{13}C NMR (126 MHz, CDCl3) δ 155.1 **C3**, 134.5 **C5**, 131.9 **C6**, 130.1 **C7**, 122.7 **C8**, 68.7 **C4**, 64.4 **C2**, 14.4 **C1**. FTIR (cm^{-1}): 2985, 1741, 1489, 1258, 1071, 799. MS (ES+) calcd. for $C_{10}H_{18}O_3$ *m/z* [MNa+]: 280.9789, found: 280.9800.

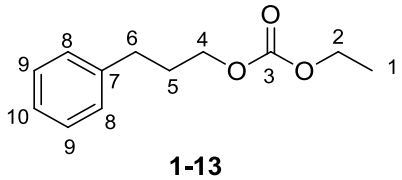

1-13

Ethyl (3-phenylpropyl) carbonate 1-13: The general procedure for ketone/aldehyde was used and compound **1-13** was obtained (0.150 g, 72% yield) as a clear oil. R_f (3:7 EtOAc/hexane): 0.54. ^{1}H NMR (500 MHz, Chloroform-*d*) δ 7.31 – 7.27 (m, 2H, **H9**), 7.22 – 7.18 (m, 3H, **H8 H10**), 4.21 (q, *J* = 7.1 Hz, 2H, **H2**), 4.16 (t, *J* = 6.5 Hz, 2H, **H4**), 2.74 – 2.70 (m, 2H, **H6**), 2.04 – 1.98 (m, 2H, **H5**), 1.32 (t, *J* = 7.1 Hz, 3H, **H1**). ^{13}C NMR (126 MHz, $CDCl_3$) δ 155.4 **C3**, 141.2

C7, 128.6 **C9**, 128.5 **C8**, 126.2 **C10**, 67.3 **C4**, 64.0 **C2**, 32.1 **C6**, 30.4 **C5**, 14.4 **C1**. FTIR (cm^{-1}): 1739, 1454, 1368, 1262, 1013. MS (ES+) calcd. for $C_{10}H_{18}O_3$ *m/z* [MNa+]: 231.0997; found: 231.0995.

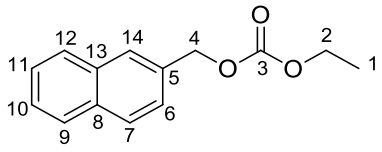

1-14

Ethyl (naphthalen-2-ylmethyl) carbonate 1-14: The general procedure for ketone/aldehyde was used and compound **1-14** was obtained (0.159 g, 69% yield) as a clear oil. R_f (3:7 EtOAc/hexane): 0.61. ^{1}H NMR (500 MHz, Chloroform-*d*) δ 7.87 – 7.83 (m, 4H, **H7 H9 H12 H14**), 7.52 – 7.48 (m, 3H, **H6 H10 H11**), 5.33 (s, 2H, **H4**), 4.24 (q, *J* = 7.1 Hz, 2H, **H2**), 1.33 (t, *J* = 7.1 Hz, 3H, **H1**). ^{13}C NMR (126 MHz, $CDCl_3$) δ 155.3 **C3**, 133.4 **C5**, 133.3 **C8**, 132.9 **C13**, 128.6 **C12**, 128.2 **C9**, 127.8 **C7**, 127.6 **C11**, 126.5 **C10**, 126.4 **C14**, 125.9 **C6**, 69.7 **C4**, 64.3 **C2**, 14.4 **C1**. FTIR (cm^{-1}): 1747, 1258, 998, 855. MS (ES+) calcd. for $C_{10}H_{18}O_3$ *m/z* [MNa+]: 253.0841, found: 253.0834.

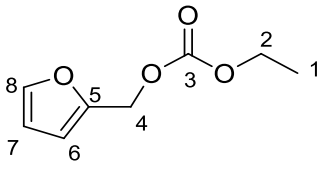

1-15

Ethyl (furan-2-ylmethyl) carbonate 1-15: The general procedure for ketone/aldehyde was used and compound **1-15** was obtained (0.073 g, 43% yield) as a clear oil. R_f (3:7 EtOAc/hexane): 0.61. ^{1}H NMR (500 MHz, Chloroform-*d*) δ 7.42 (dd, *J* = 1.8, 0.8 Hz, 1H, **H8**), 6.45 – 6.44 (dd, *J* = 3.3, 1.8 Hz 1H, **H7**), 6.36 (dd, *J* = 3.3, 0.8 Hz, 1H, **H6**), 5.11 (s, 2H, **H4**),

4.21 (q, *J* = 7.1 Hz, 2H, **H2**), 1.30 (t, *J* = 7.1 Hz, 3H, **H1**). ^{13}C NMR (126 MHz, $CDCl_3$) δ 155.1 **C3**, 149.0 **C5**, 143.6 **C8**, 111.3 **C7**, 110.7 **C6**, 64.4 **C4**, 61.2 **C2**, 14.4 **C1**. FTIR (cm^{-1}): 2981, 1743, 1377, 1256, 1054, 791. MS (ES+) calcd. for $C_{10}H_{18}O_3$ *m/z* [MNa+]: 193.0477; found: 193.0481.

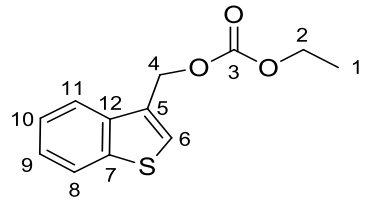

1-16

Benzo[b]thiophen-3-ylmethyl ethyl carbonate 1-16: The general procedure for ketone/aldehyde was used and compound **1-16** was obtained (0.165 g, 70% yield) as a pink oil. R_f (3:7 EtOAc/hexane): 0.61. ^{1}H NMR (500MHz, Chloroform-*d*) δ 7.89 – 7.85 (m, 2H, **H8 H11**), 7.54 (s, 1H, **H6**), 7.40 (m, 2H, **H9 H10**), 5.41 (d, *J* = 0.8 Hz, 2H, **H4**), 4.22 (q, *J* = 7.1 Hz, 2H, **H2**), 1.31 (t, *J* = 7.1 Hz, 3H, **H1**). ^{13}C NMR (126 MHz, $CDCl_3$) δ 155.3 **C3**, 140.6 **C12**, 137.9 **C7**, 130.5 **C5**, 127.2 **C10**, 124.8 **C9**, 124.6 **C11**, 123.0 **C8**, 122.0 **C6**, 64.4 **C4**, 63.4 **C2**, 14.4 **C1**. FTIR (cm^{-1}): 2981, 1740, 1462, 1257, 1032, 1008. MS (ES+) calcd. for $C_{10}H_{18}O_3$ *m/z* [MNa+]: 259.0405, found: 259.0398.

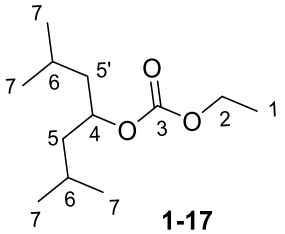

1-17

2,6-dimethylheptan-4-yl ethyl carbonate 1-17: The general procedure for ketone/aldehyde was used and compound **1-17** was obtained (0.151 g, 70% yield) as a colorless oil. R_f (3:7 EtOAc/hexane): 0.95. ^{1}H NMR (500MHz, Chloroform-*d*) δ 4.87 (td, *J* = 8.4, 4.3 Hz, 1H, **H4**),

4.17 (q, *J* = 7.2 Hz, 2H, **H$_2$**), 1.66 (dddd, *J* = 13.2, 12.2, 8.4, 6.5 Hz, 2H, **H$_5$/H$_5$'**), 1.59 – 1.53 (m, 2H, **H$_5$'/H$_5$**), 1.34 – 1.28 (m, 5H, **H$_1$ H$_6$**), 0.92 (t, *J* = 6.7 Hz, 12H, **H$_7$**). ^{13}C NMR (126 MHz, $CDCl_3$) δ. 155.3 **C$_3$**, 75.8 **C$_4$**, 63.8 **C$_2$**, 44.1 **C$_5$ C$_5$'**, 24.7 **C$_6$**, 23.2 **C$_7$**, 22.5 **C$_7$**, 14.4 **C$_1$**. FTIR (cm^{-1}): 2960, 1734, 1468, 1254, 1013. MS (ES+) calcd. for $C_{12}H_{24}O_3$ *m/z* [MNa+]: 239.1623; found: 239.1634.

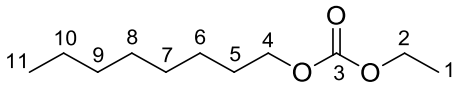

1-18

Ethyl octyl carbonate 1-18: The general procedure for ketone/aldehyde was used and compound **1-18** was obtained (0.180 g, 89% yield) as a colorless oil. Spectra matched that of the known compound.[26] ^{1}H NMR (500MHz, Chloroform-*d*) δ 4.19 (q, *J* = 7.1 Hz, 2H, **H$_2$**), 4.12 (t, *J* = 6.7 Hz, 2H, **H$_4$**), 1.66 (dq, *J* = 8.0, 6.7 Hz, 2H, **H$_5$**), 1.38 – 1.26 (m, 13H, **H$_6$ – H$_{10}$, H$_1$**), 0.87 (t, 3H, **H$_{11}$**). δ ^{13}C NMR (126 MHz, $CDCl_3$) δ 155.5 **C$_3$**, 68.2 **C$_4$**, 63.9 **C$_2$**, 31.9 **C$_9$**, 29.3 **C$_7$**, 29.3 **C$_8$**, 28.8 **C$_5$**, 25.9 **C$_6$**, 22.8 **C$_{10}$**, 14.4 **C$_1$**, 14.2 **C$_{11}$**.

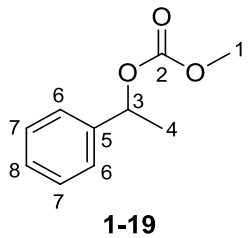

1-19

Methyl (1-phenylethyl) carbonate 1-19: The general procedure for ketone/aldehyde was used and compound **1-19** was obtained (0.150 g, 83**%** yield) as a clear oil. Spectra matched that of the known compound.[27] ^{1}H NMR (500 MHz, Chloroform-*d*) δ 7.29 – 7.39 (m, 5H, **H$_6$** – **H$_{10}$**),

5.73 (q, *J* = 6.6 Hz, 1H, **H$_3$**), 3.76 (s, 3H, **H$_1$**), 1.60 (d, *J* = 6.6 Hz, 3H, **H$_4$**). ^{13}C NMR (126 MHz, $CDCl_3$) δ 155.3 **C$_2$**, 141.2 **C$_5$**, 128.7 **C$_7$**, 128.3 **C$_8$**, 126.2 **C$_6$**, 76.6 **C$_3$**, 54.8 **C$_1$**, 22.5 **C$_4$**.

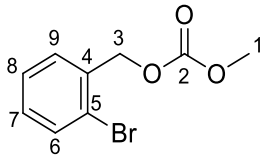

1-20

2-Bromobenzyl methyl carbonate 1-20: The general procedure for ketone/aldehyde was used and compound **1-20** was obtained (0.167 g, 68% yield) as a clear oil. R_f (3:7 EtOAc/hexane): 0.63. ^{1}H NMR (500 MHz, Chloroform-*d*) δ 7.57 (dt, *J* = 7.8, 1.5 Hz, 1H, **H$_6$**), 7.44 (dt, *J* = 7.6, 1.6 Hz, 1H, **H$_9$**), 7.32 (tt, *J* = 7.8, 1.5 Hz, 1H, **H$_7$**), 7.20 (t, *J* = 7.6, 1.6 Hz, 1H, **H$_8$**), 5.26 (d, *J* = 1.6 Hz, 2H, **H$_3$**), 3.82 (d, *J* = 1.6 Hz, 3H, **H$_1$**). ^{13}C NMR (126 MHz, $CDCl_3$) δ 155.6 **C$_2$**, 134.8 **C$_4$**, 133.0 **C$_6$**, 130.0 **C$_7$**, 129.9 **C$_9$**, 127.7 **C$_8$**, 123.4 **C$_5$**, 69.1 **C$_3$**, 55.1 **C$_1$**. FTIR (cm^{-1}): 2956, 1745, 1441, 1258, 1029, 943. MS (ES+) calcd for $C_9H_9BrO_3$ *m/z* [MNa^+]: 266.9633; found: 266.9634.

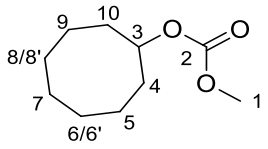

1-21

Cyclooctyl methyl carbonate 1-21: The general procedure for ketone/aldehyde was used and compound **1-21** was obtained (0.155 g, 83% yield) as a clear oil. R_f (3:7 EtOAc/hexane): 0.74. ^{1}H NMR (500 MHz, Chloroform-d) δ 4.79 (dt, J = 8.6, 4.4 Hz, 1H, **H$_3$**), 3.75 (s, 3H, **H$_1$**), 1.90 – 1.67 (m, 6H, **H$_4$ H$_{10}$ H$_{6/6'}$, H$_{8/8'}$**), 1.58 – 1.46 (m, 8H, **H$_5$ H$_7$ H$_{6/6'}$, H$_{8/8'}$, H$_9$**). ^{13}C NMR (126

MHz, CDCl3) δ 155.5 **C2**, 79.6 **C3**, 54.5 **C1**, 31.5 **C4 C10**, 27.2 **C6/6', C8/8'**, 25.5 **C7**, 22.9 **C5 C9**. FTIR (cm^{-1}): 2923, 2856, 1739, 1442, 1317, 1268, 1045. HRMS (ES+) calcd. for $C_{10}H_{18}O_3$ *m/z* [MNa+]: 209.1154; found: 209.1150.

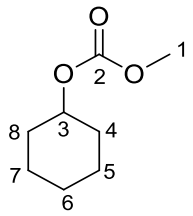

1-22

Cyclohexyl methyl carbonate 1-22: The general procedure for ketone/aldehyde was used and compound **1-22** was obtained (0.093 g, 59**%** yield) as a clear oil. Spectra matched that of the known compound.[28] ^{1}H NMR (500 MHz, Chloroform-*d*) δ 4.61 (m, 1H, **H3**), 3.76 (s, 3H, **H1**), 1.91 (dq, *J* = 13.2, 4.2 Hz, 2H, **H4/H8**), 1.74 (dp, *J* = 13.3, 4.5 Hz, 2H, **H8/H4**), 1.57 – 1.22 (m, 6H, **H5 H6 H7**). ^{13}C NMR (126 MHz, $CDCl_3$) δ 155.4 **C2**, 76.9 **C3**, 54.5 **C1**, 31.7 **C4 C8**, 25.4 **C5 C7**, 23.8 **C6**.

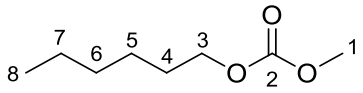

1-23

Hexanyl methyl carbonate 1-23: The general procedure for ketone/aldehyde was used and compound **1-23** was obtained (0.079 g, 49% yield) as a clear oil. Spectra matched that of the known compound.[29] ^{1}H NMR (500 MHz, Chloroform-*d*) δ 4.13 (t, *J* = 6.7 Hz, 2H, **H3**), 3.77 (s, 3H, **H1**), 1.69 – 1.63 (m, 2H, **H4**), 1.32 – 1.29 (m, 6H, **H5 - H7**), 0.89 (t, 3H, **H8**). ^{13}C NMR (126 MHz, $CDCl_3$) δ 156.1 **C2**, 68.4 **C3**, 54.7 **C1**, 31.5 **C6**, 28.8 **C4**, 25.5 **C5**, 22.7 **C7**, 14.1 **C8**.

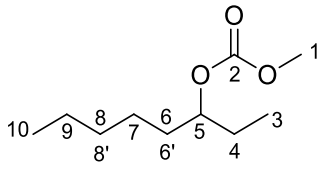

1-24

Methyl octan-3-yl carbonate 1-24: The general procedure for ketone/aldehyde was used and compound **1-24** was obtained (0.143 g, 76% yield) as a clear oil. R_f (3:7 EtOAc/hexane): 0.74. ^{1}H NMR (500 MHz, Chloroform-*d*) δ 4.66 – 4.60 (m, 1H, **H$_5$**), 3.76 (s, 3H, **H$_1$**), 1.64 – 1.57 (m, 3H, **H$_4$ H$_{6/6'}$**), 1.33 – 1.26 (m, 6H, **H$_{6/6'}$, H$_7$ H$_9$ H$_{8/8'}$**), 0.95 – 0.87 (m, 7H, **H$_{8/8'}$, H$_3$ H$_{10}$**). ^{13}C NMR (126 MHz, $CDCl_3$) δ 156.0 **C$_2$**, 80.4 **C$_5$**, 54.6 **C$_1$**, 33.6 **C$_{6/6'}$**, 31.8 **C$_{8/8'}$**, 27.0 **C$_4$**, 25.0 **C$_7$**, 22.7 **C$_9$**, 14.1 **C$_{10}$**, 9.6 **C$_3$**. FTIR (cm^{-1}): 2957, 1737, 1443, 1269. HRMS (ES+) calcd. for $C_{10}H_{20}O_3$ *m/z* [MNa+]: 211.1310; found: 211.1315.

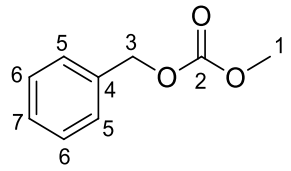

1-26

Benzyl methyl carbonate 1-26: The general procedure for alcohols was used, and compound **1-26** was obtained (0.141 g, 85% mass yield) as a clear oil. Spectra matched that of the known compound.[17] ^{1}H NMR (500 MHz, Chloroform-*d*) δ 7.40 – 7.33 (m, 5H, **H$_5$** – **H$_9$**), 5.17 (s, 2H, **H$_3$**), 3.80 (s, 3H, **H$_1$**). ^{13}C NMR (126 MHz, $CDCl_3$) δ 155.9 **C$_2$**, 135.4 **C$_4$**, 128.7 **C$_6$**, 128.7 **C$_7$**, 128.4 **C$_5$**, 69.8 **C$_3$**, 55.0 **C$_1$**.

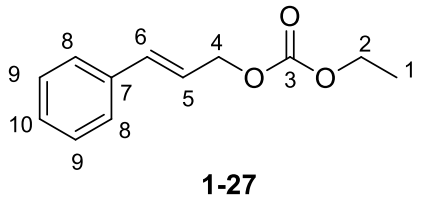

1-27

(E)-ethyl styryl carbonate 1-27: The general procedure for alcohols was used and compound **1-27** was obtained (0.196 g, 95% yield) as a clear oil after chromatography (3:7 EtOAc/hexane). Spectra matched that of the known compound.[30] ^{1}H NMR (500 MHz, Chloroform-*d*) δ 7.41 – 7.26 (m, 5H, $\mathbf{H_8}$ – $\mathbf{H_{10}}$), 6.69 (dt, *J* = 15.9, 1.4 Hz, 1H, $\mathbf{H_6}$), 6.30 (dt, *J* = 15.9, 6.4 Hz, 1H, $\mathbf{H_5}$), 4.79 (dd, *J* = 6.4, 1.4 Hz, 2H, $\mathbf{H_4}$), 4.23 (q, *J* = 7.1 Hz, 2H, $\mathbf{H_2}$), 1.33 (t, *J* = 7.1 Hz, 3H, $\mathbf{H_1}$). ^{13}C NMR (126 MHz, $CDCl_3$) δ 155.2 $\mathbf{C_3}$, 136.3 $\mathbf{C_7}$, 134.8 $\mathbf{C_6}$, 128.7 $\mathbf{C_9}$, 128.3 $\mathbf{C_{10}}$, 126.8 $\mathbf{C_8}$, 122.7 $\mathbf{C_5}$, 68.3 $\mathbf{C_4}$, 64.2 $\mathbf{C_2}$, 14.4 $\mathbf{C_1}$.

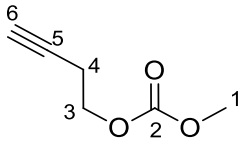

1-28

But-3-yn-1-yl methyl carbonate 1-28: The general procedure for alcohols was used and compound **1-28** was obtained (0.096 g, 75 % mass yield) as a clear oil. R_f (3:7 EtOAc/hexane): 0.56. ^{1}H NMR (500 MHz, Chloroform-*d*) δ 4.26 – 4.22 (m, 2H, $\mathbf{H_3}$), 3.79 (d, *J* = 1.7 Hz, 3H, $\mathbf{H_1}$), 2.57 (ddq, *J* = 7.1, 4.6, 2.3 Hz, 2H, $\mathbf{H_4}$), 2.03 – 1.99 (m, 1H, $\mathbf{H_6}$). ^{13}C NMR (126 MHz, $CDCl_3$) δ 155.6 $\mathbf{C_2}$, 79.5 $\mathbf{C_5}$, 70.4 $\mathbf{C_6}$, 65.6 $\mathbf{C_3}$, 55.0 $\mathbf{C_1}$, 19.2 $\mathbf{C_4}$. IR (cm^{-1}): 3294.25, 2959.63, 1744.78, 1442.54, 1386.04, 1255.11, 981.34. MS (ES+) calcd. for $C_6H_8O_3$ *m/z* [MNa^+]: 151.0371, found: 151.0368.

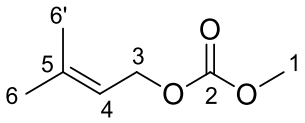

1-29

Methyl (3-methylbut-2-en-1-yl) carbonate 1-29: The general procedure for alcohols was used and compound **1-29** was obtained (0.118 g, 82% mass yield) as a colorless oil. Spectra matched that of the known compound.[31] ^{1}H NMR (500 MHz, Chloroform-*d*) δ 5.39 – 5.35 (m, 1H, **H$_4$**), 4.64 – 4.62 (m, 2H, **H$_3$**), 3.77 (s, 3H, **H$_1$**), 1.76 (s, 3H, **H$_{6/6'}$**), 1.72 (s, 3H, **H$_{6/6'}$**). ^{13}C NMR (126 MHz, $CDCl_3$) δ 156.0 **C$_2$**, 140.2 **C$_5$**, 118.2 **C$_4$**, 64.8 **C$_3$**, 54.8 **C$_1$**, 25.9 **C$_{6/6'}$**, 18.2 **C$_{6/6'}$**.

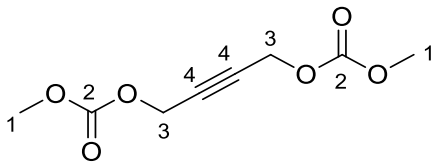

1-30

But-2-yne-1,4-diyl dimethyl carbonate 1-30: The general procedure for alcohols was used and compound **1-30** was obtained (0.168 g, 83 % mass yield) as a clear oil. R_f (3:7 EtOAc/hexane): 0.41. ^{1}H NMR (500 MHz, Chloroform-*d*) δ 4.77 (s, 4H, **H$_3$**), 3.81 (s, 6H, **H$_1$**). ^{13}C NMR (126 MHz, $CDCl_3$) δ 155.3 **C$_2$**, 81.1 **C$_4$**, 55.5 **C$_3$**, 55.3 **C$_1$**. IR (cm^{-1}): 2958.43, 1753.29, 1445.10, 1375.01, 1257.54. MS (ES+) calcd. for $C_8H_{10}O_6$ *m/z* [MNa^+]: 225.0375, found: 225.0377.

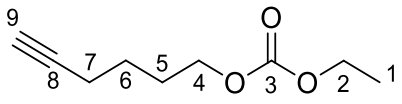

1-31

Ethyl hex-5-yn-1-yl carbonate 1-31: The general procedure for alcohols was used and compound **1-31** was obtained (0.119 g, 70 % yield) as a clear oil after chromatography (3:7 EtOAc/hexane). R_f (3:7 EtOAc/hexane): 0.68. ^{1}H NMR (500 MHz, Chloroform-*d*) δ 4.19 (q, *J* = 7.3 Hz, 2H, **H$_2$**), 4.15 (t, *J* = 6.4 Hz, 2H, **H$_4$**), 2.23 (td, *J* = 7.0, 2.7 Hz, 2H, **H$_7$**), 1.95 (t, *J* = 2.7 Hz, 1H, **H$_9$**), 1.83 – 1.77 (m, 2H, **H$_5$**), 1.66 – 1.59 (m, 2H, **H$_6$**), 1.30 (t, *J* = 7.1 Hz, 3H, **H$_1$**). ^{13}C NMR (126 MHz, $CDCl_3$) δ 155.4 **C$_3$**, 83.9 **C$_8$**, 68.9 **C$_4$**, 67.4 **C$_9$**, 64.0 **C$_2$**, 27.9 **C$_5$**, 24.8 **C$_6$**, 18.2 **C$_7$**, 14.4 **C$_1$**. IR (cm^{-1}): 3307.25, 2959.80, 1739.27, 1467.74, 1368.92, 1256.55, 1016.39. MS (ES+) calcd. for $C_9H_{14}O_3$ *m/z* [MNa^+]: 193.0841, found: 193.0844.

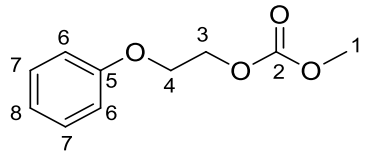

1-32

Methyl (2-phenoxyethyl) carbonate 1-32: The general procedure for alcohols was used and compound **1-32** was obtained (0.190 g, 97 % mass yield) as a clear oil. ^{1}H NMR (500 MHz, Chloroform-*d*) δ 7.26 – 7.30 (m, 2H, **H$_7$**), 6.97 (t, *J* = 7.4 Hz, 1H, **H$_8$**), 6.91 (d, *J* = 8.1 Hz, 2H, **H$_6$**), 4.49 (t, *J* = 5.5, 2H, **H$_3$**), 4.20 (t, *J*= 5.5, 2H, **H$_4$**), 3.81 (s, 3H, **H$_1$**). ^{13}C NMR (126 MHz, $CDCl_3$) δ 158.5 **C$_5$**, 155.8 **C$_2$**, 129.6 **C$_7$**, 121.4 **C$_8$**, 114.8 **C$_6$**, 66.3 **C$_4$**, 65.7 **C$_3$**, 55.1 **C$_1$**. MS (ES+) calcd. for $C_{10}H_{12}O_4$ *m/z* [MNa^+]: 219.0633, found: 219.0632.

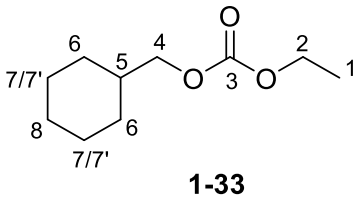

1-33

Cyclohexylmethyl ethyl carbonate 1-33: The general procedure for alcohols was used and compound **1-33** was obtained (0.149 g, 80% yield) as a clear oil after chromatography (3:7 EtOAc/hexane). R_f (3:7 EtOAc/hexane): 0.74. ^{1}H NMR (500 MHz, Chloroform-*d*) δ 4.18 (q, *J* = 7.1 Hz, 2H, **H$_2$**), 3.94 (d, *J* = 6.6 Hz, 2H, **H$_4$**), 1.78 – 1.63 (m, 6H, **H$_5$ H$_6$ H$_{7/7'}$**), 1.30 (t, *J* = 7.1 Hz, 3H, **H$_1$**), 1.27 – 1.14 (m, 3H, **H$_{7/7'}$**), 1.03 – 0.94 (m, 2H, **H$_8$**). ^{13}C NMR (126 MHz, $CDCl_3$) δ 155.5 **C$_3$**, 73.1 **C$_4$**, 63.9 **C$_2$**, 37.3 **C$_5$**, 29.6 **C$_6$**, 26.5 **C$_8$**, 25.8 **C$_{7/7'}$**, 14.4 **C$_1$**. IR (cm^{-1}): 2927.71, 2855.51, 1738.04, 1450.43, 1262.75, 1009.07. MS (ES+) calcd. for $C_{10}H_{18}O_3$ *m/z* [MNa^+]: 209.1154, found: 209.1150.

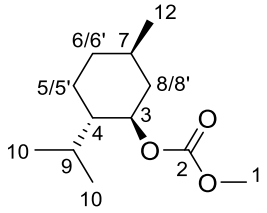

1-34

L-Menthylmethyl carbonate 1-34: The general procedure for alcohols was used and compound **1-34** was obtained (0.210 g, 98 % mass yield) as a clear oil. Spectra matched that of the known compound.[29] ^{1}H NMR (300 MHz, Chloroform-*d*) δ 4.51 (td, *J* = 10.9, 4.5 Hz, 1H, **H$_3$**), 3.77 (s, 3H, **H$_1$**), 2.12 – 2.04 (m, 2H, **H$_4$ H$_{8/8'}$**), 1.73 – 1.64 (m, 2H, **H$_7$ H$_{8/8'}$**), 1.54 – 1.35 (m, 2H, **H$_9$ H$_{5/5'}$**), 1.11 – 0.98 (m, 2H, **H$_{5/5'}$ H$_{6/6'}$**), 0.93 - 0.89 (m, 7H, **H$_{6/6'}$ H$_{10}$**), 0.79 (d, *J* = 7.0 Hz, 3H, **H$_{12}$**). ^{13}C NMR (126 MHz, $CDCl_3$) δ 155.7 **C$_2$**, 78.6 **C$_3$**, 54.6 **C$_1$**, 47.2 **C$_4$**, 40.9 **C$_{8/8'}$**, 34.3 **C$_{6/6'}$**, 31.6 **C$_7$**, 26.2 **C$_9$**, 23.5 **C$_{5/5'}$**, 22.1 **C$_{10}$**, 20.9 **C$_{10}$**, 16.4 **C$_{12}$**.

1.5. References

1. Newhouse, T.; Baran, P. S.; Hoffmann, R. W., The economies of synthesis. *Chem Soc Rev* **2009,** *38* (11), 3010-3021.

2. Wender, P. A., Toward the ideal synthesis and molecular function through synthesis-informed design. *Nat Prod Rep* **2014,** *31* (4), 433-440.

3. Nicolaou, K. C.; Montagnon, T.; Snyder, S. A., Tandem reactions, cascade sequences, and biomimetic strategies in total synthesis. *Chem Commun* **2003,** (5), 551-564.

4. Enders, D.; Huttl, M. R. M.; Grondal, C.; Raabe, G., Control of four stereocentres in a triple cascade organocatalytic reaction. *Nature* **2006,** *441* (7095), 861-863.

5. Li, Z.; Hu, B.; Wu, Y. W.; Fei, C.; Deng, L., Control of chemoselectivity in asymmetric tandem reactions: Direct synthesis of chiral amines bearing nonadjacent stereocenters. *P Natl Acad Sci USA* **2018,** *115* (8), 1730-1735.

6. Shaikh, A.-A. G.; Sivaram, S., Organic carbonates. *Chemical reviews* **1996,** *96* (3), 951-976.

7. Schaffner, B.; Schaffner, F.; Verevkin, S. P.; Borner, A., Organic carbonates as solvents in synthesis and catalysis. *Chemical reviews* **2010,** *110* (8), 4554-4581.

8. Aricò, F.; Tundo, P., Dimethyl carbonate as a modern green reagent and solvent. *Russian Chemical Reviews* **2010,** *79* (6), 479.

9. Aurbach, D.; Gamolsky, K.; Markovsky, B.; Gofer, Y.; Schmidt, M.; Heider, U., On the use of vinylene carbonate (VC) as an additive to electrolyte solutions for Li-ion batteries. *Electrochimica Acta* **2002,** *47* (9), 1423-1439.

10. Endo, A.; Danishefsky, S. J., Total synthesis of salinosporamide A. *Journal of the American Chemical Society* **2005,** *127* (23), 8298-8299.

11. Clive, D. L. J.; Yang, W.; MacDonald, A. C.; Wang, Z.; Cantin, M., Preparation of Polycyclic Systems by Sequential 5-E xo-D igonal Radical Cyclization, 1, 5-Hydrogen Transfer from Silicon, and 5-E ndo-T rigonal Cyclization. *The Journal of organic chemistry* **2001,** *66* (6), 1966-1983.

12. Nuñez, S. A.; Yeung, K.; Fox, N. S.; Phillips, S. T., A structurally simple self-immolative reagent that provides three distinct, simultaneous responses per detection event. *The Journal of organic chemistry* **2011,** *76* (24), 10099-10113.

13. Trost, B. M.; Czabaniuk, L. C., Palladium-Catalyzed Asymmetric Benzylation of Azlactones. *Chemistry–A European Journal* **2013,** *19* (45), 15210-15218.

14. Blakemore, D. C.; Marples, L. A., Palladium (0)-catalysed cross-coupling of 2-trimethylsilylpyridine with aryl halides. *Tetrahedron letters* **2011,** *52* (32), 4192-4195.

15. Ganton, M. D.; Kerr, M. A., A domino amidation route to indolines and indoles: Rapid syntheses of anhydrolycorinone, hippadine, oxoassoanine, and pratosine. *Organic letters* **2005,** *7* (21), 4777-4779.

16. am Ende, D.; Bronk, K. S.; Mustakis, J.; O'Connor, G.; Santa Maria, C. L.; Nosal, R.; Watson, T. J. N., API quality by design example from the torcetrapib manufacturing process. *Journal of Pharmaceutical Innovation* **2007,** *2* (3-4), 71-86.

17. Nakatake, D.; Yazaki, R.; Matsushima, Y.; Ohshima, T., Transesterification reactions catalyzed by a recyclable heterogeneous zinc/imidazole catalyst. *Advanced Synthesis & Catalysis* **2016,** *358* (15), 2569-2574.

18. Nakatake, D.; Yokote, Y.; Matsushima, Y.; Yazaki, R.; Ohshima, T., A highly stable but highly reactive zinc catalyst for transesterification supported by a bis (imidazole) ligand. *Green Chemistry* **2016,** *18* (6), 1524-1530.

19. Kumar, S.; Jain, S. L., An easy base-assisted synthesis of unsymmetrical carbonates from alcohols with dimethyl carbonate. *Monatshefte für Chemie-Chemical Monthly* **2014,** *145* (5), 791-795.

20. Hatano, M.; Kamiya, S.; Ishihara, K., In situ generated "lanthanum (III) nitrate alkoxide" as a highly active and nearly neutral transesterification catalyst. *Chemical Communications* **2012,** *48* (76), 9465-9467.

21. Hatano, M.; Kamiya, S.; Moriyama, K.; Ishihara, K., Lanthanum (III) isopropoxide catalyzed chemoselective transesterification of dimethyl carbonate and methyl carbamates. *Organic letters* **2011,** *13* (3), 430-433.

22. Selva, M.; Noè, M.; Perosa, A.; Gottardo, M., Carbonate, acetate and phenolate phosphonium salts as catalysts in transesterification reactions for the synthesis of non-symmetric dialkyl carbonates. *Organic & biomolecular chemistry* **2012,** *10* (32), 6569-6578.

23. Selva, M.; Perosa, A.; Fabris, M., Sequential coupling of the transesterification of cyclic carbonates with the selective N-methylation of anilines catalysed by faujasites. *Green Chemistry* **2008,** *10* (10), 1068-1077.

24. Kantam, M. L.; Pal, U.; Sreedhar, B.; Choudary, B. e. M., An efficient synthesis of organic carbonates using nanocrystalline magnesium oxide. *Advanced Synthesis & Catalysis* **2007,** *349* (10), 1671-1675.

25. Veldurthy, B.; Clacens, J. M.; Figueras, F., New highly active and selective heterogeneous catalytic system for the synthesis of unsymmetrical organic carbonates: A green protocol. *European journal of organic chemistry* **2005,** *2005* (10), 1972-1976.

26. Wu, L.; Tian, S., Immobilization of 1, 5, 7-Triazabicyclo [4.4. 0] dec-5-ene on Magnetic γ-Fe2O3 Nanoparticles: A Highly Recyclable and Efficient Nanocatalyst for the Synthesis of Organic Carbonates. *European Journal of Inorganic Chemistry* **2014,** *2014* (12), 2080-2087.

27. Verdecchia, M.; Feroci, M.; Palombi, L.; Rossi, L., A safe and mild synthesis of organic carbonates from alkyl halides and tetrabutylammonium alkyl carbonates. *The Journal of organic chemistry* **2002,** *67* (23), 8287-8289.

28. Hatano, M.; Kamiya, S.; Moriyama, K.; Ishihara, K., Lanthanum (III) isopropoxide catalyzed chemoselective transesterification of dimethyl carbonate and methyl carbamates. *Organic letters* **2010,** *13* (3), 430-433.

29. Zeng, R.; Sheng, H.; Zhang, Y.; Feng, Y.; Chen, Z.; Wang, J.; Chen, M.; Zhu, M.; Guo, Q., Heterobimetallic Dinuclear Lanthanide Alkoxide Complexes as Acid–Base Difunctional Catalysts for Transesterification. *The Journal of organic chemistry* **2014,** *79* (19), 9246-9252.

30. Vyas, D. J.; Oestreich, M., Expedient access to branched allylic silanes by copper-catalysed allylic substitution of linear allylic halides. *Chemical Communications* **2010,** *46* (4), 568-570.

31. Dai, Y.; Wu, F.; Zang, Z.; You, H.; Gong, H., Ni-catalyzed reductive allylation of unactivated alkyl halides with allylic carbonates. *Chemistry–A European Journal* **2012,** *18* (3), 808-812.

Chapter 2: Development of a Printable Calcium Ion Sensitive and Conductive Carbon Nanotube Ink for Additive Manufacturing

Chapter 2 is part of a NASA EPSCoR funded project entitled Space Grade Flexible Electronics with a current manuscript in preparation for submission.

Abstract

Additive manufacturing technologies are conducive for space travel (especially for extended missions) as needs can be met in real-time with the use of specially designed 2D and 3D printing technologies. Wearable sensors for monitoring health (glucose, Ca^{2+}), as well as potential hazards (UV, low O_2 levels) on such missions, are advantageous for further understanding of human health in space. Carbon materials represent a potential viable class of non-toxic and conductive materials for electrodes. For this study, a printable carbon nanotube (CNT) ink (Nink®, nanolab) was investigated for the development of flexible electrodes in the monitoring of calcium. CNT inks have been formulated with known calcium ion-sensitive compounds (calcium ionophore II, aka ETH129) and both drop-casted onto glass slides and ink-jet printed onto flexible Kapton polyimide materials. The printed materials were studied for their calcium sensitivity, selectivity, and durability to provide a realized example of this technology. The sensitivity was reported at 10^{-5} M^{-1}, reported as an Electromotive Force Test (EMF), providing a Nernstian slope of 29.58 mV/decade**,** and selectivity for calcium over other cations is comparable with other known systems. The printed layers gave similar selectivity and EMF tests when more than 30 layers of CNT ink were been printed. Electrochemical impedance spectroscopy supported this claim. Overall, the ionophore materials are compatible with jet-printing technologies.

Keywords: Calcium Ion Sensitive Electrode; ETH129, Carbon Nanotube; Contact Layer

2.1. Introduction

Electrodes act as transducers converting the activity of a specific ion in solution using the principles of molecular recognition chemistry, into electrical potential and are more commonly referred to as Ion-Selective Electrodes (ISE).[1] These chemical sensors can determine the concentration of specific ions by simple comparison to the magnitude of electrical potentials from a voltmeter.[2] The Nernst equation (**Equation 2.1**) is used to express the dependence of the voltage to the logarithm of the ionic activity.

$$E = E^0 + \frac{0.059\,\mathrm{V}}{n} log_{10} \frac{a_{Ox}}{a_{Red}} \tag{2.1}$$

Where E is the electromotive force; E^0 is the standard half-cell reduction potential; n is the number of electrons; a_{Ox} and a_{Red} are the activities of the oxidized and the reduced species respectively.

Ion-selective membranes (ISM) are defined as materials that sense ions and are the key sensing component(s) of an ISE. The first example of an ISE electrode dates to 1906, with Max Cremer's discovery of pH-sensitive glass.[3] Cremer observed with astonishment an increase in the potential difference of 360 mV on addition of sodium hydroxide to a 0.6% aqueous solution of sodium hydroxide in contact with a glass membrane.[4] This led to the availability of the commercial pH electrode in the 1930s by Arnold Beckman,[5, 6] and the introduction of sensing materials based on crystalline compounds like AgCl, As_2S, or LaF_3 in the early 1960s. These ISEs were extremely useful but subsequent development of these designs have limited selectivities,[7] and suffers from the poor ionic conductivity of most crystalline compounds. Further development of ISEs slowed down as their applications seemed promising for a finite chemical species of interest, which led to the introduction of ion-binding receptors (aka ion

carriers or ionophores), and a complete transformation of ISEs due to the significant impact on the host-guest chemistry of chemical sensors.[2]

Moore and Pressman inspired the early works on electrically neutral ionophores as ISEs. They observed that valinomycin **K^+-I** (Figure 1), effected the movement of K^+ into and that of H^+ out of mitochondria.[8] The first examples of the ISEs used the ammonium-selective receptors nonactin (**NH_4^+-I**) and monactin (**NH_4^+-II**), but the valinomycin based ISE that was reported later,[9] is one of the best known ISEs because of its high K^+ selectivity, enabling its use in the measurement of K^+ in biological samples.

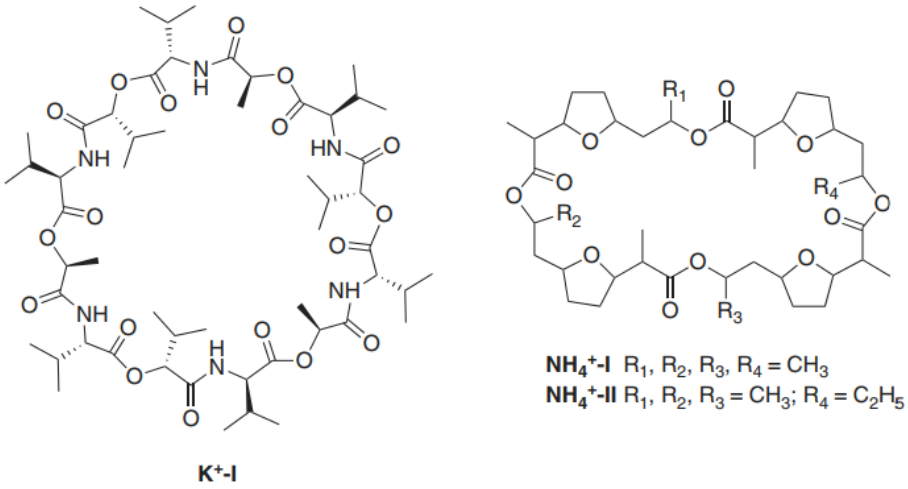

Figure 2. 1. Structures of valinomycin (K^+-I), nonactin (NH_4^+-I), and monactin (NH_4^+-II) that are early examples of ionophores used in ISE membranes.

Host-guest chemistry advanced significantly in the 1960s. Part of the successes was the Nobel prize awarded to Donald J. Cram, Jean-Marie Lehn and Charles J. Pedersen for the development of crown ethers and the budding science of supramolecular chemistry.[10] This encouraged an increase in the development of synthetic, ion-specific compounds, ionophores, and led to the switch from flame atomic emission spectroscopy to ion-selective potentiometry techniques for the measurement of blood and urine electrolyte ions in the 1980s. The subject

areas in which articles on ISEs were published increased greatly to and included fields such as medicine, environmental science, engineering, food science and technology, and more.[2]

Early designs of ISEs, in the form of liquid contact electrodes, resembled the glass electrodes but were followed by other types like microelectrodes,[11, 12] integrated enzyme layer ISEs, and ISEs modified with gas-permeable membranes for the detection of electrically neutral, volatile species like CO_2 and ammonia.[13] These designs were associated with experimental limitations because of the inner filling solution (storage vessel requirements) made up of an aqueous solution of chloride ions with commonly Ag/AgCl metal reference electrode and the ISM. The drawback to this design in the form of a wearable device is its bulkiness, poor diffusion of ions and molecules from the ISM into test solution and solvent evaporation.[2, 14] Alternatively, ISM-coated metals, as solid contact ISEs (SC-ISE) were then proposed and investigated.[1, 15-17]

Coated wire electrodes (CWE) were the first reported type of SC-ISEs.[18] The CWE is typically a metallic conductor coated with a sensing polymeric membrane. CWEs exhibited limited long-term stability and saw restricted use in areas like flow injection analysis[19] and capillary electrophoresis.[20] The flux in their measured potential was attributed to the "blocked" interface between the metallic conductor and the sensing membrane, which has poorly defined phase boundary potential which is dependent on oxygen and other redox-active components of the sample,[17, 21] and also the formation of a water layer at the metal-membrane interface.[2] This problem was not successfully solved as one of the attempts was the use of inner Ag/AgCl reference electrode, and the replacement of the inner electrolyte solution with a hydrogel-based electrolyte.[22, 23] However, ISEs based on/in hydrogels have water uptake/release and corresponding volume change limitations.[24] Improvements to the metal-ISM interface was

achieved by the use of electronically and ionically conducting polymers between the ISM membrane and the metal or graphite electrodes.[15, 25] Some benefits of this type of solid-contact ISEs are relative ease of preparation and their very low limits of detection, by the elimination of transmembrane fluxes resulting from the formation of a water layer at the metal-ISM membrane interface.

Presently, carbon materials with large surface area like three-dimensionally ordered microporous (3DOM) carbon[17] or carbon nanotubes (CNT)[16, 26, 27] shown in **Figure 2.2** are widely used in ISEs as ion-to-electron transducers. The ISM is coated directly onto the carbon material resulting in a high interfacial capacitance making it hard to polarize the interface because of the very large surface area between the two materials.[17] The chemical structure of CNTs confers exceptional properties which renders them very suitable for electrochemical sensing because of the mobile surface electrons, large surface area, and their ability to translocate electrons between heterogeneous phases.[16]

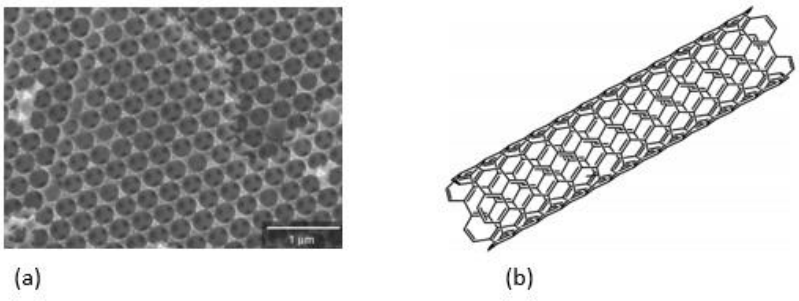

Figure 2. 2. (a) scanning electron microscope image of 3DOM carbon (b) schematic representation of carbon nanotube.

The use of carbon-based materials for ISE transduction continues to grow and has led to further devices and to new allotropes of carbon.[28, 29] That said, Cheng and coworkers at the University of Idaho have recently been exploring their own carbon-based material (GUITAR) for a variety of electrochemical processes.[30, 31]

2.2. Calcium ISEs

Calcium is one of the essential elements for human metabolism and is an abundant mineral in the body.[32] It is important for bone growth, nerve transmission, blood clotting, cardiac functions, and muscle contraction.[33] Some ailments linked to an excessive imbalance in calcium levels in the body biofluid are renal failure, cirrhosis, acid-base imbalance, normokalaemia and hyperparathyroidism.[32, 34, 35] Furthermore, bone loss or loss of skeletal mineral is a health issue known to astronauts on long-duration (>3 months) spaceflight. The human skeleton is adapted for strength and to support mechanical loads in human daily activities under the earth's gravity. In microgravity environments, weightlessness results in changes in the load support requirements and consequently, the spatial distribution of bone minerals, which results in bone degradation and a slight increase in the plasma level of calcium.[36] Recently, a study performed by NASA on twin astronauts Scott and Mark Kelly revealed the effects of an extended (340 day) space mission on numerous cellular and metabolic processes in addition to cognitive function.[37]

Measurement of free Ca^{2+} in the body is most often performed in laboratory settings on fluids such as urine, sweat or blood for disease diagnoses.[32, 35] While these fluids contain markers for various diseases, sweat analysis is of great interest to the wearable technologies as it involves a non-invasive method of sampling.[38] Electrochemical devices with sensors printed on flexible surfaces offer an approach to non-invasive on-body monitoring.[39, 40] In addition to electrochemical sensors, different types of calcium sensors have been reported, such as optical sensors,[41] and other calcium ion-selective sensor designs for biological applications and health assessment,[20, 32, 42-44] but a rapidly deployable jet-printable design has not yet been realized.

There are many commercially available calcium ion-sensitive materials on the market, including ionomycin, and other small molecules termed calcium ionophores. These compounds are sold commercially as calcium ionophore I, II, III, IV and others, as shown in **Figure 2.3**. For this study, calcium ionophore II was chosen for its high prevalence in the literature, its known ability to translocate Ca^{2+} across biological membranes[45, 46] and, as Chapter 3 involves the synthesis of an ionophore-inspired monomer, it is the most promising candidate to mimic.

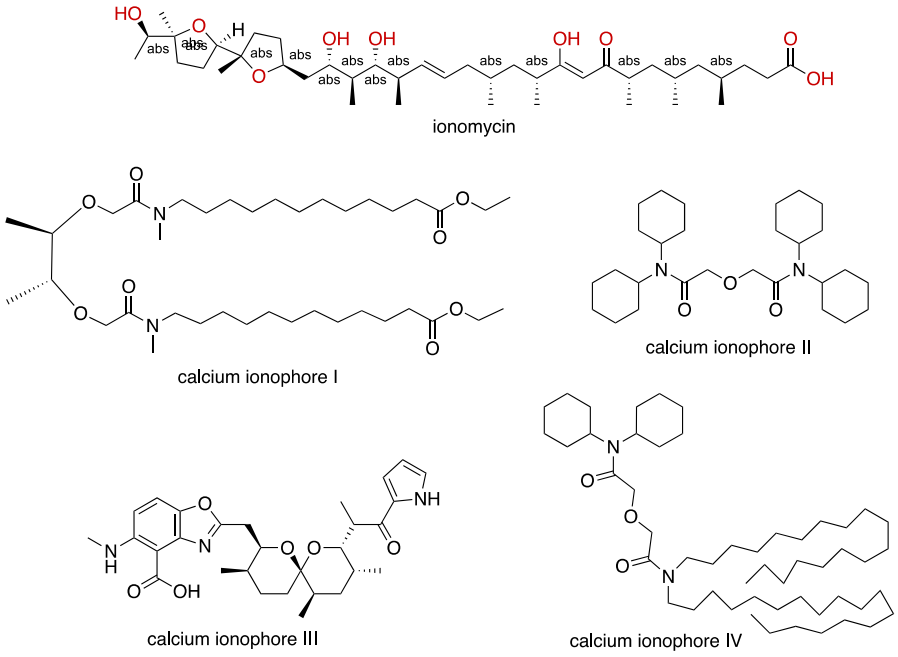

Figure 2. 3. Various structures of the small molecule ionophores commercially available towards calcium.

The main goal of this study was to investigate the compatibility of a known commercially available jet-printable CNT ink (Nink®, nanolab) to act as a transducing layer for a calcium ionophore sensing cocktail. The ionophore cocktails were prepared and tested with pre-printed CNT ink and with the cocktail mixed into the ink. By testing the jet printability of the pre-mixed ink-cocktail highlights the rapid accessibility of these ink-mix sensors as resultant printed layers were evaluated. As part of this project, calcium selectivity of the ionophore mix CNT ink was measured for both drop cast on glass slides and prints on Kapton

(polyimide). The research question in this investigation aimed to determine if ionophore based inks are reliable calcium ion-sensitive electrodes for incorporation into a flexible device. Jet-printed CNT inks show high potential for patterned conductive materials. Low toxicity of CNTs makes them suitable for use in wearable electrodes. To this end, there are numerous reports on the use of conductive CNT inks, and there are many commercially available CNT inks with varying aqueous dispersants. However, the use of a calcium ion-sensitive material formulated in a CNT ink could prove valuable as a printable electrode material for flexible and wearable devices to monitor micromolar quantities of calcium.

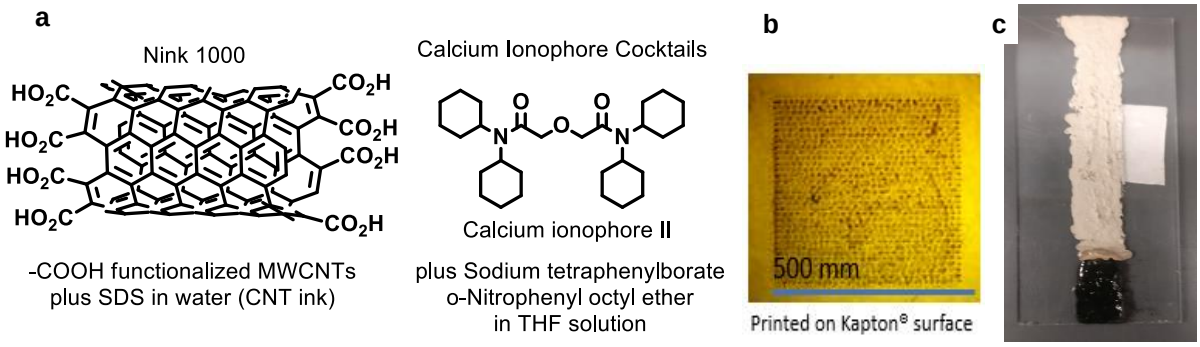

Figure 2. 4. a) Components of the calcium ISE electrode (b) actual print (c) drop cast on glass slide.

Herein is described a CNT ink formulation cast onto surfaces and printed to a flexible polyimide material that displays sensitivity to calcium and provides the possibility of an in-space manufactured calcium ion sensor.

2.3. Methods and Experimental Procedures

Preparation of the drop-cast solutions and slides: The calcium ion-selective membrane was prepared by mixing calcium ionophore II, *o*-nitrophenyl octyl ether (NPOE), sodium tetraphenylborate (NaTFB) and poly(vinyl chloride) (PVC) in the weight ratio 1 :65.8 :0.2 : 33, in THF solvent. The solvent fraction was measured to be approximately 85% (w/w) of the total

mixture. The membrane solution (100 µl) was drop cast on a layer of dried conductive CNT ink as the working electrode of the device. On a glass slide, a line was drawn with a silver conductive ink pen 2/3 down the slide lengthwise as the connector for the working electrode. The slide was transferred to a hot plate at 55 °C to cure for 15 minutes. Once the silver ink was cured, approximately 200 µL of NINK® solution was drop cast onto the glass slide in a line starting from the end of the silver ink to the end of the slide. The ink was allowed to dry before adding three more layers. When the ink layers are dry, 100 µL of calcium ionophore membrane was added to the top of the ink layer and let dry. The reference electrode is a standard Ag/AgCl electrode, and the working electrode is the line with NINK and the calcium ionophore membrane. The electrodes were conditioned in a 10^{-3} M solution of $CaCl_2$ for 3 hours for the emf step test. For water layer tests, the electrodes were conditioned in 10^{-2} M solution of $CaCl_2$ for 24 hours before use.

Preparation of ink-jet printed NINK®: The NINK was first drop tip sonicated for 30 minutes to break up carbon nanotube clusters present in the solution. The sonicated NINK was then centrifuged for 30 minutes so that the larger carbon nanotube materials settle to the bottom and the top colloidal part of the centrifuged solution is collected and transferred into the printer ink cartridge for printing on Kapton. Jet-printing was performed on a Fujifilm Dimatix 6800D printer using an average droplet size of 20 pL in multiple layers to make rectangular patterns of 1.2 cm^2 and 2.4 by 3.6 cm^2 on Kapton. The Kapton was heated at 155 °C for 30 minutes to cure the ink.

2.4. Results

Initially, the CNT ink calcium ionophore cocktails solutions were evaluated for sensitivity and compared against literature reports. Drop-casted CNT inks were coated with a solution of

calcium ionophore cocktail in THF as prepared above and allowed to dry. The screen cast electrodes were conditioned in 10^{-3} M $CaCl_2$ solution for 3 h and then were tested at different concentrations of calcium ions (as CaCl). **Figure 2.4** shows the Potential (in mV) vs. the Log Ca^{2+} activity. The concentration increases with a Nernstian slope of 29.58 mV/decade, an ideal slope for an ion with a valence of 2.

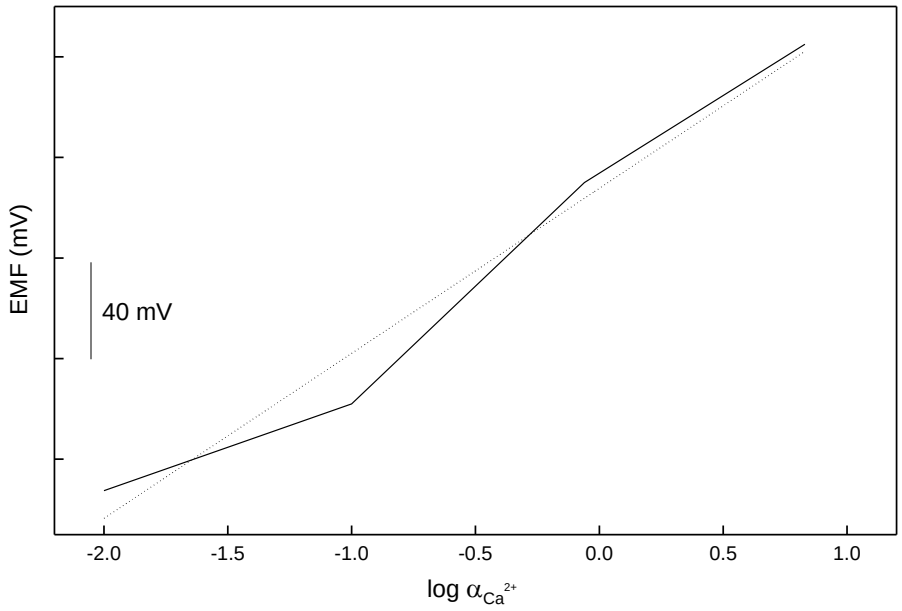

Figure 2. 5. The emf responses of the drop cast mix at different Ca^{2+} concentrations.

Figure 2.6 shows a typical curve for the electromotive force against time for the electrode. Normally, the serum calcium levels range from 0.5 to 3 mM.[35] The electromotive force response was measured for calcium ion concentration between $10^{-4.7}$ to $10^{-1.4}$ M which covers the biological range for the human body fluid calcium ion concentrations. Dynamic change in the electromotive force from the electrode with increase in calcium ion concentration shows that the electrode can respond to changes in calcium ion momentarily and can be used to monitor instantaneous change in calcium concentrations.

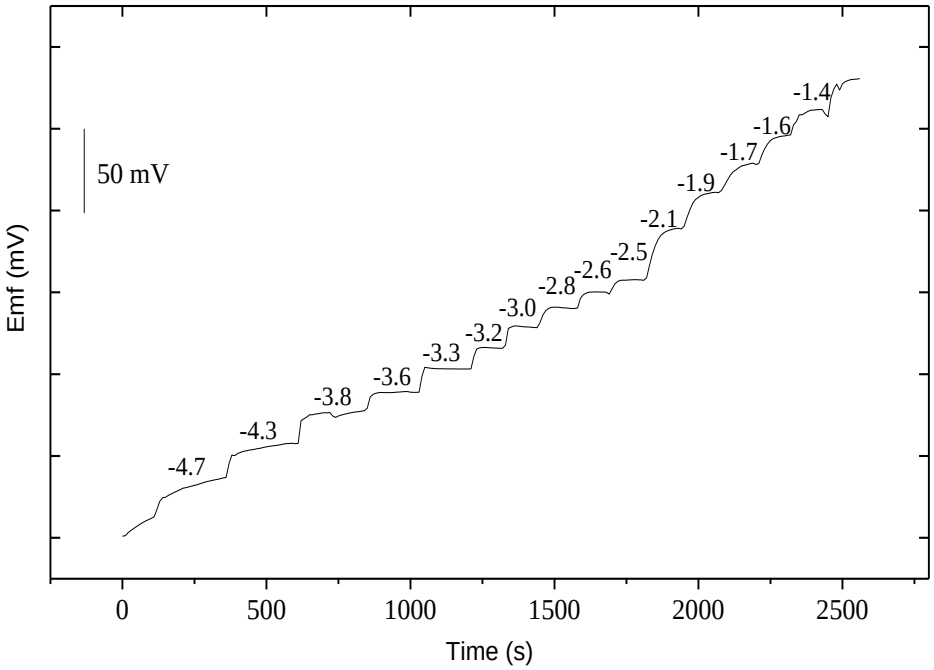

Figure 2. 6. Plot of the EMF response of the drop cast mix at different Ca^{2+} concentrations. The negative values are the logarithms of calcium ion activities of the solution.

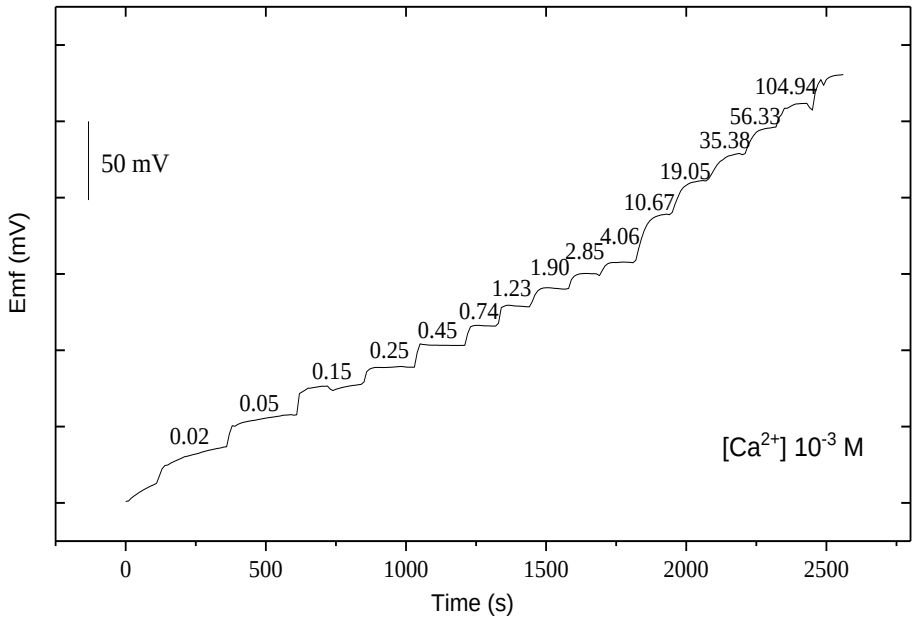

Figure 2. 7. EMF measurement with increasing Ca^{2+} concentration

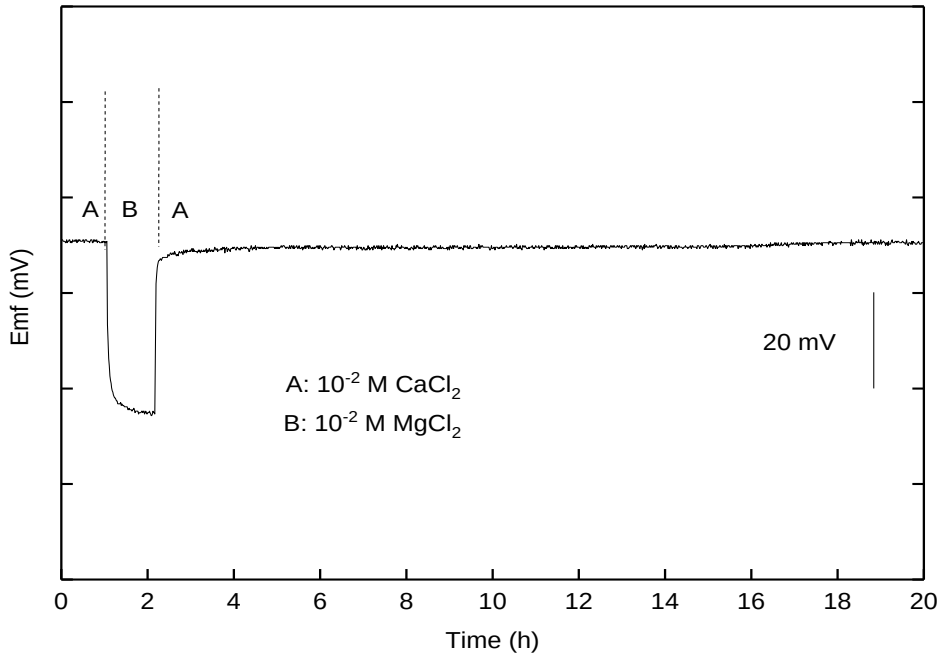

Figure 2. 8. Water layer tests for the Calcium ISE in 10^{-2} M $CaCl_2$ (A) and 10^{-2} M $MgCl_2$ (B)

Potentiometric water layer test was performed on the electrode drop cast on glass slide to determine if the formation of a thin water layer exists between the transducer layer and the membrane.[47] Equally, the water layer test can display selectivity for the ion. As shown in **Figure 2.8** the electrode is placed in a 10^{-2} M solution of $CaCl_2$ and registering a constant voltage, the electrode is then transferred into a similar solution of magnesium chloride and the response weakens by over 30 mV but returns once the electrode is replaced in the original calcium solution. As a result of the minimal drift observed on return to the original solution, it was determined that water layer did not form in between the ISM and the transducer layer. The selectivity test in **Figure 2.9** shows the sensitivity of the electrode to calcium ions in the presence of other counter ions. After addition of 32 mM of various counter ions to the 1 mM calcium solution, there was no significant change in the electromotive force, it dropped by 18 mV, compared to a change in calcium ion concentration of 0.49 mM that increased the emf by 12.6 mV (**Figure 2.7**). This shows that the electrode is selective for calcium ions.

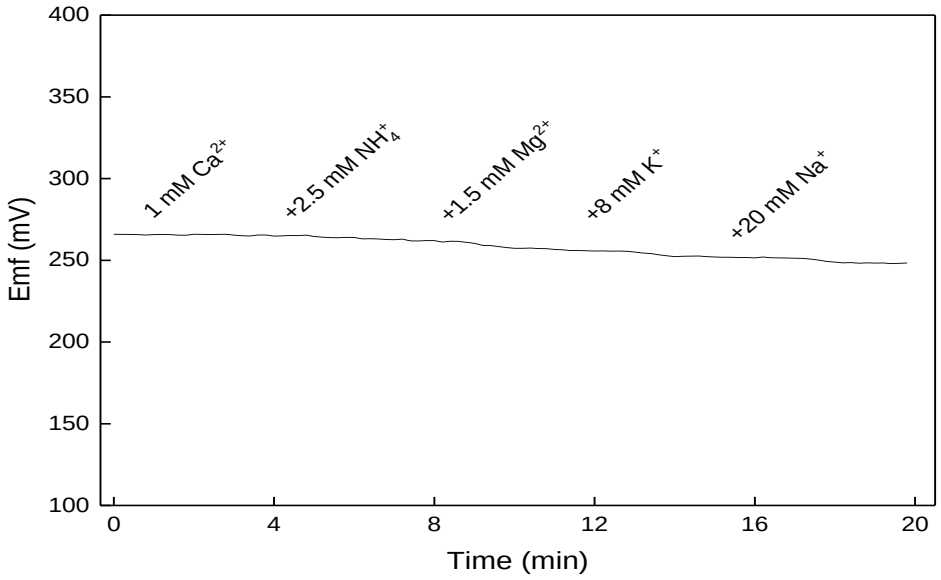

Figure 2. 9. Selectivity Test showing the response of the electrode to other counter ions.

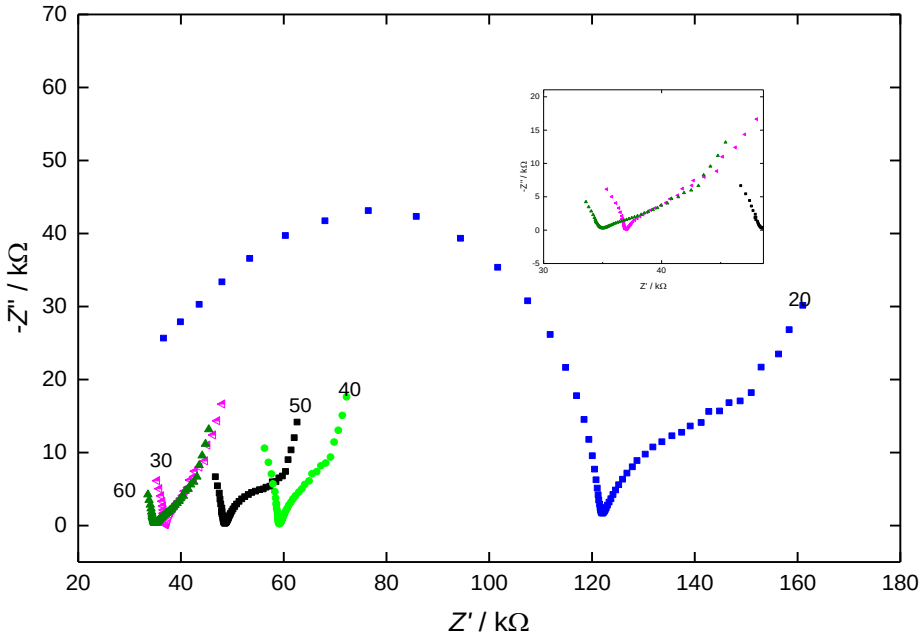

Figure 2. 10. EIS test for the various number of NINK layer prints in 10^{-3} M $CaCl_2$ solution.

To design the flexible electrodes, various number of layers of NINK were printed on Kapton, and evaluated with Electrochemical Impedance Spectroscopy (EIS) for calcium ion sensitivity. The EIS experiment of the various number of layers (**Figure 2.10**) shows that the 20-layer print exhibited the highest impedance to conductivity of the ionophore membrane in

solution. 30-layer print showed conductivity close to that of 60 layers, superior to that of 40- and 50-layers prints. The result shows that more than 20 layers of the CNT ink is necessary for good conductivity of the calcium ISM. Electromotive force test of the electrode printed on Kapton (**Figure 2.11**) over calcium ion concentration range of $10^{-5.5}$ to $10^{-0.63}$ M shows a dynamic change in electromotive force with increase in calcium ion concentration. The print displayed good sensitivity in the biological region (0.5 – 3 mM), with a limit of detection of 0.01 mM. After addition of higher concentrations of different counter ions to 1 mM Ca^{2+} solution in the presence of the electrode print (**Figure 2.12**), there was no significant change in the electromotive force of the electrode. The selectivity test shows that the print is selective for calcium ions.

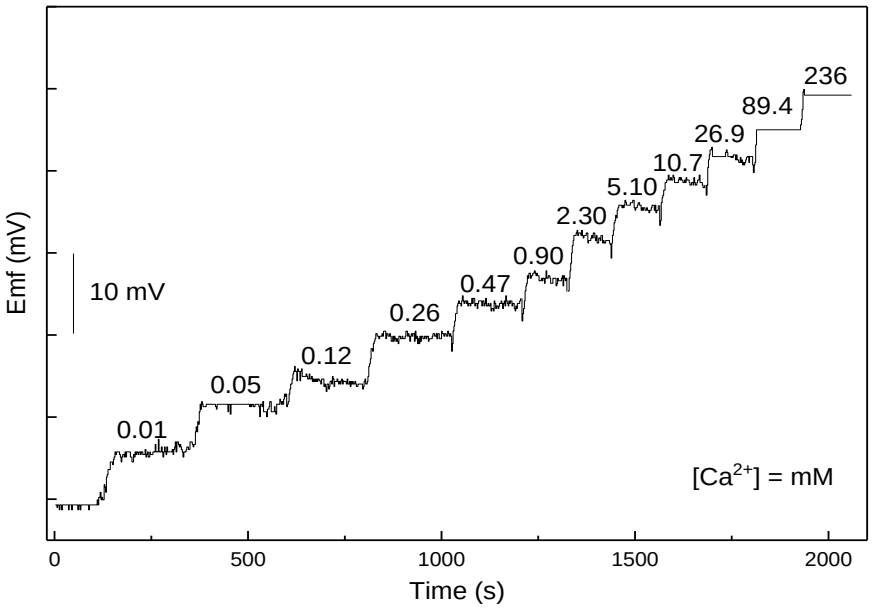

Figure 2. 11. EIS test for the various number of NINK layer prints in 10^{-3} M $CaCl_2$ solution.

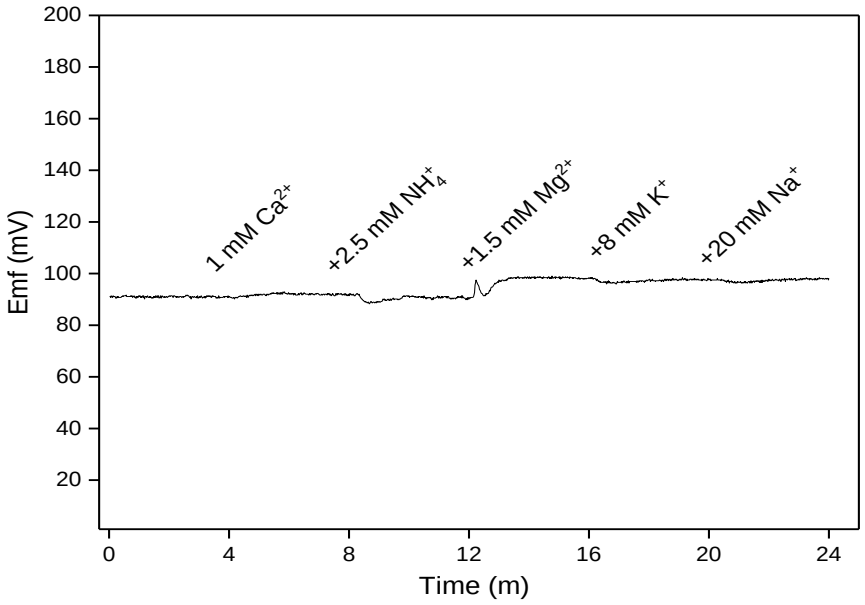

Figure 2. 12. Selectivity test of the print.

AFM image of the 30-layer print on Kapton (**Figure 2.13)** shows that 30 layers give a height of around 3 µm. Kapton surface is in the top right corner of the image and the CNT uniformity is in the far left of the image. 30 layers gave enough uniformity in the print to give a reliable conductance.

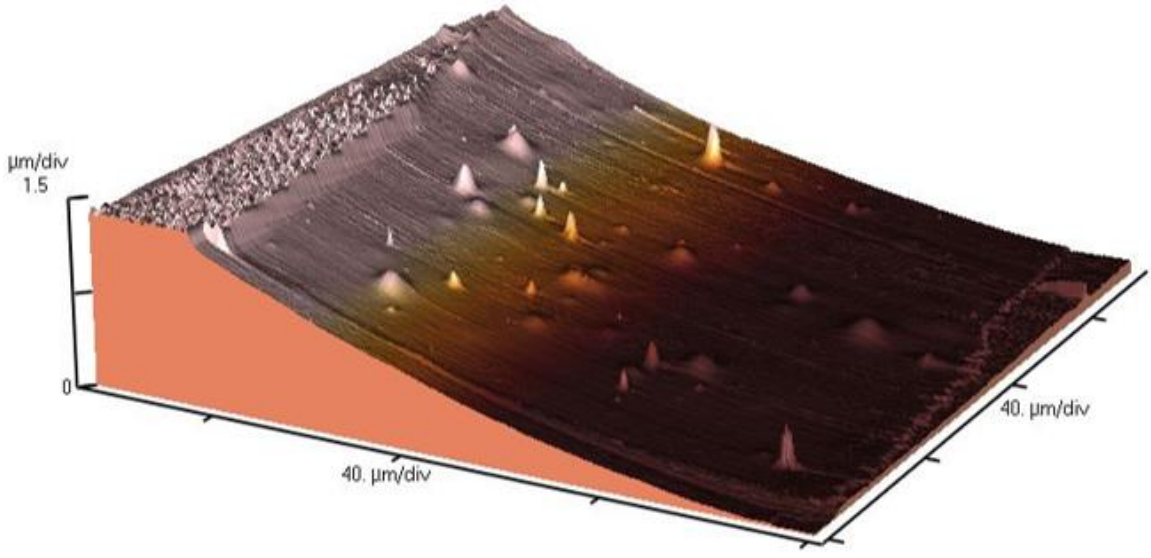

Figure 2. 13. AFM tapping mode of the edge of the CNT ink print.

2.5. Conclusions

The adaptation of CNT based printable inks with calcium ionophore cocktails were evaluated and deemed mostly compatible. Drop-casted CNT inks with added ionophore ink cocktails performed excellently on both glass slides and on Kapton polyimide. When the ink was mixed with ionophore cocktails, binding agents – for numerous reasons needed to be left out of the solution and therefore needed to be added back before testing. Printable ionophore CNT ink mixtures showed optimal performance after 30 layers ink (20 picoliter droplet sizes) of jet-printing.

2.6. References

1. Roy, S.; David-Pur, M.; Hanein, Y., Carbon Nanotube-Based Ion Selective Sensors for Wearable Applications. *ACS Applied Materials & Interfaces* **2017,** *9* (40), 35169-35177.

2. Bühlmann, P.; Chen, L. D., Ion-Selective Electrodes With Ionophore-Doped Sensing Membranes. In *Supramolecular Chemistry*, Gale, P. A.; Steed, J. W., Eds. John Wiley & Sons, Ltd: Chichester, UK, 2012.

3. Cremer, M., The cause of the electromotor properties of tissue, and a contribution to the science of polyphasic electrolytes. *Z Biol-Munich* **1906,** *29*, 562-608.

4. Dole, M., The early history of the development of the glass electrode for pH measurements. *Journal of Chemical Education* **1980,** *57* (2), 134.

5. Hines, W. G.; de Levie, R., The Early Development of Electronic pH Meters. *Journal of Chemical Education* **2010,** *87* (11), 1143-1153.

6. Beckman pH Meter - National Historic Chemical Landmark. https://www.acs.org/content/acs/en/education/whatischemistry/landmarks/beckman.html.

7. Philippe Bu¨hlmann, E. P. a. E. B., Carrier-Based Ion-Selective Electrodes and Bulk Optodes. 2. Ionophores for Potentiometric and Optical Sensors. *Chemical Reviews* **1998,** *98*, 1593-1687.

8. Moore, C.; Pressman, B. C., Mechanism of action of valinomycin on mitochondria. *Biochemical and Biophysical Research Communications* **1964,** *15* (6), 562-567.

9. Wipf, H. K.; Pioda, L. A.; Stefanac, Z.; Simon, W., Complexes of enniatins and other antibiotics with alkali metal ions. *Helvetica Chimica Acta* **1968,** *51* (2), 377-381.

10. The Nobel Prize in Chemistry 1987.

11. R. A. Steiner, M. O. D. A. a. W. S., Neutral Carrier Sodium Ion-Selective Microelectrode for Intracellular Studies. *Analytical Chemistry* **1979,** *51* (3), 351.

12. Rink, T. J.; Tsien, R. Y.; Warner, A. E., Free calcium in Xenopus embryos measured with ion-selective microelectrodes. *Nature* **1980,** *283* (5748), 658-660.

13. Radomska, A.; Bodenszac, E.; Głąb, S.; Koncki, R., Creatinine biosensor based on ammonium ion-selective electrode and its application in flow-injection analysis. *Talanta* **2004,** *64* (3), 603-608.

14. Eric Bakker, D. D. A. L. E. P., Ion sensors: current limits and new trends. *Analytica Chimica Acta* **1999,** *393*, 11-18.

15. Cadogan, A.; Gao, Z.; Lewenstam, A.; Ivaska, A.; Diamond, D., All-solid-state sodium-selective electrode based on a calixarene ionophore in a poly(vinyl chloride) membrane with a polypyrrole solid contact. *Analytical Chemistry* **1992,** *64* (21), 2496-2501.

16. Crespo, G. A.; Macho, S.; Rius, F. X., Ion-Selective Electrodes Using Carbon Nanotubes as Ion-to-Electron Transducers. *Analytical Chemistry* **2008,** *80* (4), 1316-1322.

17. Lai, C.-Z.; Fierke, M. A.; Stein, A.; Bühlmann, P., Ion-Selective Electrodes with Three-Dimensionally Ordered Macroporous Carbon as the Solid Contact. *Analytical Chemistry* **2007,** *79* (12), 4621-4626.

18. Cattrall, R. W.; Freiser, H., Coated wire ion-selective electrodes. 2.

19. Schnierle, P.; Kappes, T.; Hauser, P. C., Capillary Electrophoretic Determination of Different Classes of Organic Ions by Potentiometric Detection with Coated-Wire Ion-Selective Electrodes. *Analytical Chemistry* **1998,** *70* (17), 3585-3589.

20. Dimitrakopoulos, T.; Farrell, J. R.; Iles, P. J., A photo-cured calcium ion-selective electrode for use in flow injection potentiometry that tolerates high perchlorate levels. *Electroanalysis* **1996,** *8* (4), 391-395.

21. Freiser, H., *Ion-Selective Electrodes in Analytical Chemistry*. Springer Science & Business Media: 2012; p 448.

22. Lynch, A.; Diamond, D.; Leader, M., Point-of-need diagnosis of cystic fibrosis using a potentiometric ion-selective electrode array. *Analyst* **2000,** *125* (12), 2264-2267.

23. Cosofret, V. V.; Erdosy, M.; Johnson, T. A.; Buck, R. P.; Ash, R. B.; Neuman, M. R., Microfabricated Sensor Arrays Sensitive to pH and K+ for Ionic Distribution Measurements in the Beating Heart. *Analytical Chemistry* **1995,** *67* (10), 1647-1653.

24. Bobacka, J., Conducting Polymer-Based Solid-State Ion-Selective Electrodes. *Electroanalysis* **2006,** *18* (1), 7-18.

25. Bobacka, J.; Ivaska, A.; Lewenstam, A., Potentiometric Ion Sensors Based on Conducting Polymers. *Electroanalysis* **2003,** *15* (5-6), 366-374.

26. Bandodkar, A. J.; Molinnus, D.; Mirza, O.; Guinovart, T.; Windmiller, J. R.; Valdés-Ramírez, G.; Andrade, F. J.; Schöning, M. J.; Wang, J., Epidermal tattoo potentiometric sodium sensors with wireless signal transduction for continuous non-invasive sweat monitoring. *Biosensors and Bioelectronics* **2014,** *54*, 603-609.

27. Guinovart, T.; J. Bandodkar, A.; R. Windmiller, J.; J. Andrade, F.; Wang, J., A potentiometric tattoo sensor for monitoring ammonium in sweat. *Analyst* **2013,** *138* (22), 7031-7038.

28. Diederich, F., Carbon scaffolding: building acetylenic all-carbon and carbon-rich compounds. *Nature* **1994,** *369* (6477), 199-207.

29. Zhao, Z.; Tian, F.; Dong, X.; Li, Q.; Wang, Q.; Wang, H.; Zhong, X.; Xu, B.; Yu, D.; He, J., Tetragonal allotrope of group 14 elements. *Journal of the American Chemical Society* **2012,** *134* (30), 12362-12365.

30. Gyan, I. O.; Cheng, I. F., Electrochemical study of biologically relevant molecules at electrodes constructed from GUITAR, a new carbon allotrope. *Microchem J* **2015,** *122*, 39-44.

31. Kabir, H.; Ma, P. Y.; Renn, N.; Nicholas, N. W.; Cheng, I. F., Electrochemical determination of free chlorine on pseudo-graphite electrode. *Talanta* **2019,** *205*, 120101.

32. Nyein, H. Y. Y.; Gao, W.; Shahpar, Z.; Emaminejad, S.; Challa, S.; Chen, K.; Fahad, H. M.; Tai, L.-C.; Ota, H.; Davis, R. W.; Javey, A., A Wearable Electrochemical Platform for Noninvasive Simultaneous Monitoring of Ca ²⁺ and pH. *ACS Nano* **2016,** *10* (7), 7216-7224.

33. Cáceres, E.; García, M. L.; Selgas, M. D., Design of a new cooked meat sausage enriched with calcium. *Meat Science* **2006,** *73* (2), 368-377.

34. Arnold, S. R., Metabolic consequences of acid-base disorders | Elsevier Enhanced Reader. *Kidney International* **1972,** *1*, 347-359.

35. Robertson, W. G.; Marshall, R. W.; Bowers, G. N., Ionized Calcium in Body Fluids. *CRC Critical Reviews in Clinical Laboratory Sciences* **1981,** *15* (2), 85-125.

36. Lang, T.; LeBlanc, A.; Evans, H.; Lu, Y.; Genant, H.; Yu, A., Cortical and Trabecular Bone Mineral Loss From the Spine and Hip in Long-Duration Spaceflight. *Journal of Bone and Mineral Research* **2004,** *19* (6), 1006-1012.

37. Garrett-Bakelman, F. E.; Darshi, M.; Green, S. J.; Gur, R. C.; Lin, L.; Macias, B. R.; McKenna, M. J.; Meydan, C.; Mishra, T.; Nasrini, J.; Piening, B. D.; Rizzardi, L. F.; Sharma, K.; Siamwala, J. H.; Taylor, L.; Vitaterna, M. H.; Afkarian, M.; Afshinnekoo, E.; Ahadi, S.; Ambati, A.; Arya, M.; Bezdan, D.; Callahan, C. M.; Chen, S.; Choi, A. M. K.; Chlipala, G. E.; Contrepois, K.; Covington, M.; Crucian, B. E.; De Vivo, I.; Dinges, D. F.; Ebert, D. J.; Feinberg, J. I.; Gandara, J. A.; George, K. A.; Goutsias, J.; Grills, G. S.; Hargens, A. R.; Heer, M.; Hillary, R. P.; Hoofnagle, A. N.; Hook, V. Y. H.; Jenkinson, G.; Jiang, P.; Keshavarzian, A.; Laurie, S. S.; Lee-McMullen, B.; Lumpkins, S. B.; MacKay, M.; Maienschein-Cline, M. G.; Melnick, A. M.; Moore, T. M.; Nakahira, K.; Patel, H. H.; Pietrzyk, R.; Rao, V.; Saito, R.; Salins, D. N.; Schilling, J. M.; Sears, D. D.; Sheridan, C. K.; Stenger, M. B.; Tryggvadottir, R.; Urban, A. E.; Vaisar, T.; Van Espen, B.; Zhang, J.; Ziegler, M. G.; Zwart, S. R.; Charles, J. B.; Kundrot, C. E.; Scott, G. B. I.; Bailey, S. M.; Basner, M.; Feinberg, A. P.; Lee, S. M. C.; Mason, C. E.; Mignot, E.; Rana, B. K.; Smith,

S. M.; Snyder, M. P.; Turek, F. W., The NASA Twins Study: A multidimensional analysis of a year-long human spaceflight. *Science* **2019,** *364* (6436), eaau8650.

38. Bandodkar, A. J.; Jeang, W. J.; Ghaffari, R.; Rogers, J. A., Wearable Sensors for Biochemical Sweat Analysis. *Annu Rev Anal Chem (Palo Alto Calif)* **2019,** *12* (1), 1-22.

39. Windmiller, J. R.; Wang, J., Wearable electrochemical sensors and biosensors: a review. *Electroanalysis* **2013,** *25* (1), 29-46.

40. Windmiller, J. R.; Bandodkar, A. J.; Valdés-Ramírez, G.; Parkhomovsky, S.; Martinez, A. G.; Wang, J., Electrochemical sensing based on printable temporary transfer tattoos. *Chemical Communications* **2012,** *48* (54), 6794-6796.

41. Shalom, S.; Strinkovski, A.; Peleg, G.; Druckmann, S.; Krauss, A.; Lewis, A.; Linial, M.; Ottolenghi, M., An optical submicrometer calcium sensor with conductance sensing capability. *Analytical biochemistry* **1997,** *244* (2), 256-259.

42. Ping, J. F.; Wu, J.; Ying, Y. B., Screen-Printed Potentiometric Strip for Calcium Ion Determination in Water and Milk. *Transactions of the ASABE* **2013,** *56* (2), 13.

43. Bedlechowicz, I.; Sokalski, T.; Lewenstam, A.; Maj-zurawska, M., Calcium ion-selective electrodes under galvanostatic current control. *Sensors and Actuators B: Chemical* **2005,** *108* (1-2), 836-839.

44. Lindfors, T.; Ivaska, A., Calcium-selective electrode based on polyaniline functionalized with bis [4-(1, 1, 3, 3-tetramethylbutyl) phenyl] phosphate. *Analytica Chimica Acta* **2001,** *437* (2), 171-182.

45. Prestipino, G.; Falugi, C.; Falchetto, R.; Gazzotti, P., The ionophore ETH 129 as Ca2+ translocator in artificial and natural membranes. *Analytical biochemistry* **1993,** *210* (1), 119-122.

46. Brown, H. M.; Marron, S. K., Fabrication method to enhance stability of N,N,N',N'-tetracyclohexyl-3-oxapentanediamide calcium microelectrodes. *Analytical Chemistry* **1990,** *62* (19), 2153-2155.

47. Fibbioli, M.; Morf, W. E.; Badertscher, M.; Rooij, N. F. d.; Pretsch, E., Potential Drifts of Solid-Contacted Ion-Selective Electrodes Due to Zero-Current Ion Fluxes Through the Sensor Membrane. *Electroanalysis* **2000,** *12* (16), 1286-1292.

Chapter 3: Development of a Calcium Ionophore Inspired Monomer from Binding Studies to Polymerizations and Structural Properties

Chapter 3 is part of a NASA EPSCoR funded project entitled Space Grade Flexible Electronics with a current manuscript in preparation for submission.

Abstract:

Ionophores, ion sensing compounds, are critical components to ion-sensitive electrodes (ISEs), providing high sensitivity and good selectivity for analytes of interest. As electrodes have evolved from solution-based to solid contact, the lipophilic ionophore and resultant formulations have proved more rugged and portable while affording sensitivity. These formulations usually require a polymeric binding agent that keeps the system intact for testing. Based on known calcium ionophore ETH129, (2,2'-oxybis(*N*,*N*-dicyclohexylacetamide), a nitrogen analog was synthesized and evaluated for sensitivity. The nitrogen analog was selected as it allows for conjugation to a polymerizable 3-bromopropyl methacrylate appendage. Following the synthesis of the monomer, crystallization studies, potentiometric evaluations of calcium sensitivity and selectivity, and polymerizations were performed. Both the *N*-analog and monomer bind calcium in a 2:1 stoichiometry with similar bond distances, as seen with the known ETH129. Co-polymerizations with various concentrations of methyl methacrylate through free radical techniques gave polymer blends in high yields. These polymers gave low average molecular weights (M_n, 2447 – 2864), polydispersities of 1.03 – 1.05, and glass transition temperatures of 62 – 91 $^{\circ}$C. Polymer blends were evaluated as potential binding agents and ionophore/binding agent combinations for solid contact electrodes. Lastly, homo-polymerization of ionophore inspired monomers via ARGET ATRP was accomplished to grow ion-sensitive molecules directly onto carbon nanotubes (CNTs). Functionalized CNTs were

characterized via TEM and FT-IR and then incorporated into commercially available CNT inks to evaluate as potential jet printable solutions for advanced manufacturing of smart inks. Ultimately, the stoichiometric limitations of the ionophore inspired monomer dictated a lower sensitivity and selectivity to calcium.

Keywords: ionophore, ionophore-inspired monomer, co-polymerization, CNT inks

3.1. Introduction

Ion sensitive electrodes (ISEs) have become commonplace in potentiometric chemical analysis.[1] Many ion-sensitive compounds, termed ionophores, are either found in nature or have been discovered to be selective for various ions.[2, 3] For example crown ethers have been found to be compatible molecular recognition compounds with various cations (18-Crown-6 fits potassium cations preferentially; 15-crown-5 fits sodium selectively)[4]. Similarly, boronic acids have shown affinity in binding sugars such as glucose through covalent bonds of the boronic acids to the sugar alcohols.[5] These recognition phenomena have been built into polymeric units such as those shown in **Scheme 3.1** using a polymeric styrene derivative of benzo-18-crown-6, **3-4** for the detection of potassium and the commercially available acrylamide derivative (4-methacrylamidophenyl)boronic acid, **3-5** for the detection of glucose.[6] Sequel to our investigations of the incompatibility of the calcium ionophore II, **3-3** (ETH129) formulations with printable CNT inks (Chapter 2) a study was proposed to probe the possibility of creating a polymeric calcium ion sensor that mimics a key known molecular recognition event.

The simple structure of the known calcium ionophore (**3-3**), ETH129, and its prevalence in calcium sensing materials serves as an excellent substrate to emulate, especially as many of the calcium ionophores are quite complex (i.e. valinomycin) and arduous to synthesize.[7] Furthermore, the crystal structure of ETH129 bound to calcium is known and can be compared

easily if crystals of analogs pre-polymerization can be prepared.[8] Yet overall, the ionophore has to interact with both the analyte of interest and the conductive material if a reliable sensor is to be built. While there have been known examples of polymeric membranes,[9] the envisioned application of a polymeric derivative of ionophore **3-3** would be to: 1) incorporate the polymer as both binding agent and ionophore in formulations for solid contact layers of ISEs; 2) incorporate the polymers into the commercially available printable CNT based inks to add the ISE to a fully compatible system.

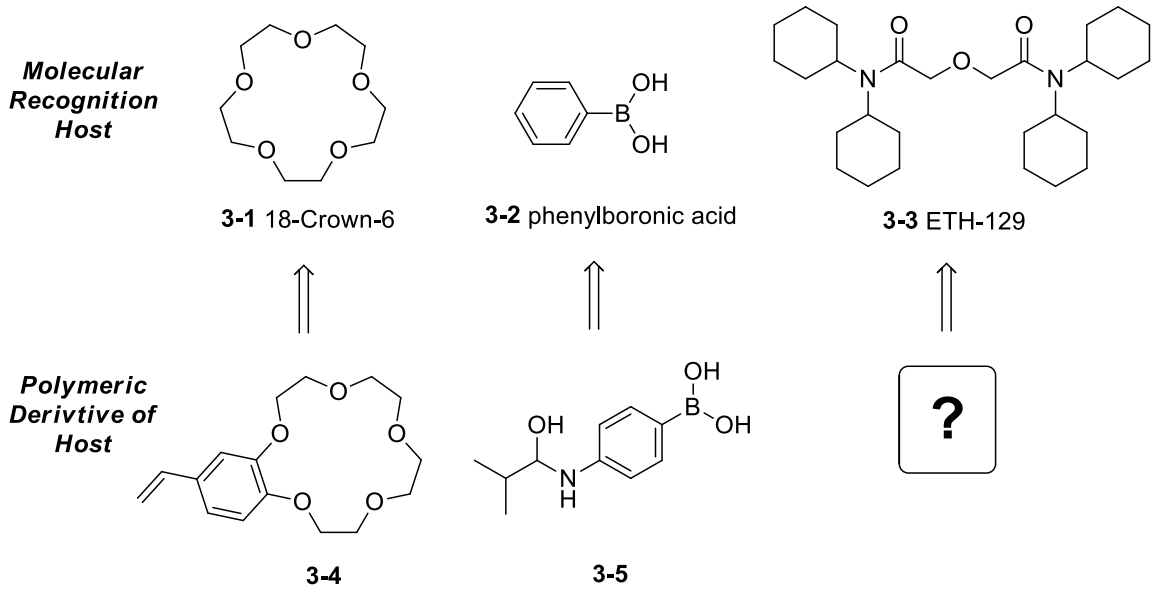

Scheme 3. 1. Representative examples of analyte sensitive materials that have been built into polymeric derivatives and the goal of this chapter; to synthesize a polymeric ion-sensitive derivative to ETH129.

Incorporation of the polymers into the inks can be accomplished via multiple pathways, including simple addition of the polymer to the mixture yet as solubility of lipophilic polymers in aqueous printed inks may be an issue, we wondered if the polymer could be incorporated directly onto the conductive surfaces. For example, a variety of methods have been reported for preparing CNTs surfaces for modification with a wide range of chemical/biological molecules. These include covalent approaches by amidation or esterification of oxidized CNTs with

functionalized hydroxyl groups or amines and by addition chemistry (1,3-dipolar cycloaddition, carbene addition, diazonium coupling etc.).[16] Many of these methods result in non-uniform functionalization and their harsh conditions tarnish the surface framework of the CNTs. Another method to functionalize CNTs is through encapsulation with organic polymers via in-situ polymerization of monomers and wrapping of the CNTs.[17] This theory was encouraged by a recent report from the Matyjaszewski group in which uranium ions were trapped and sensed from seawater utilizing a methacrylate-based polymer grown directly from a CNT as shown below in **Figure 3.1**.[18, 19]

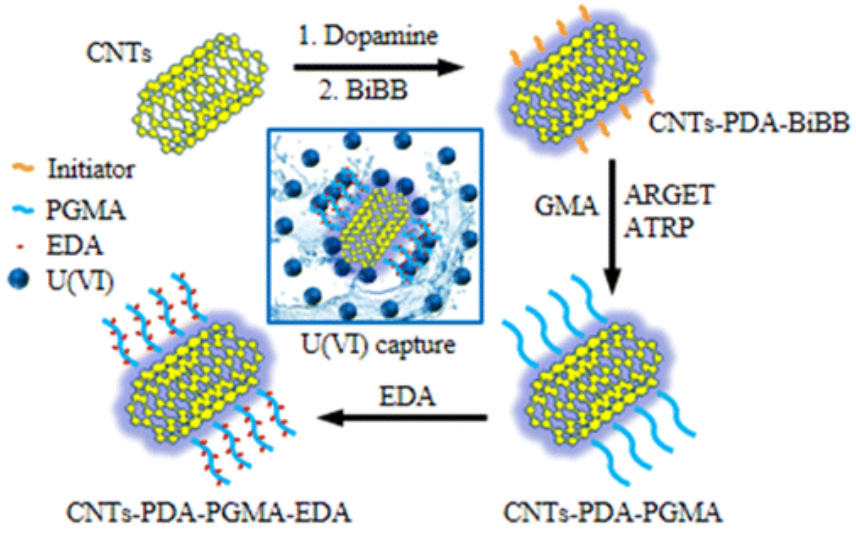

Figure 3. 1. CNTs platform for U(VI) capture via anchoring ATRP initiations and PGMA functionalization.

Encapsulation with polydopamine (PDA) has been found to be desirable due to mild dconditions, biocompatibility, and hydrophilicity of PDA.[19] It is formed from the oxidative polymerization of dopamine under alkaline conditions.[20] It is a hydrophilic adhesive layer that can be formed on the surface of nanomaterials.[21] It is proposed that following cyclization of dopamine to indole-5,6-diol, polymerization occurs through the aromatic rings as shown in **Scheme 3.2**.

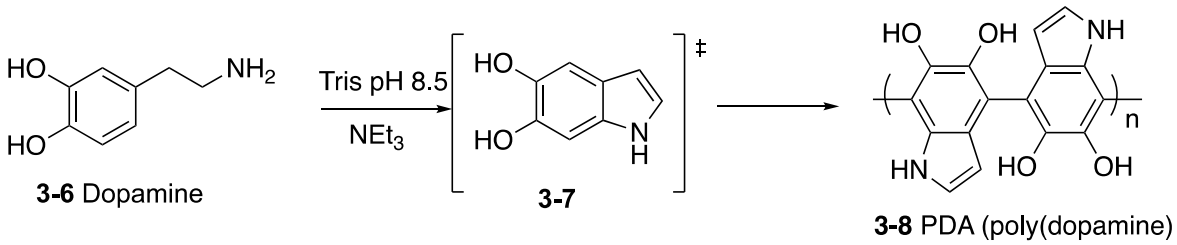

Scheme 3. 2. A proposed schematic pathway in the formation of polydopamine

While the mechanism of the self-polymerization of dopamine and the 3D structure of PDA is not fully known, the presence of the phenolic hydroxyl groups allows for functionalization. Polymerization initiators can be anchored to the catechol groups of the PDA layer for further functionalization of the coated nanomaterials. Towards the application of calcium ion sensing through a conductive and printable ink material, a hypothesis of growing calcium ion sensing polymers onto PDA wrapped CNTs was proposed. While the ability to functionalize CNTs directly and provide -OH, -NH_2, and -COOH groups on the CNTs, the integrity of the sp^2 structure of the CNT is compromised.[22] Our hypothesis was to coat the CNTs with PDA as to leave the CNT sp^2 structures unaffected and then functionalize the CNTs with a polymerization initiator. By varying the time of PDA coating provides a tunable feature in that thinner or thicker coatings could be established.[23] Furthermore, formulating ion sensing CNTs with printable CNT based inks then allows for an ink-jet printable medium towards the additive manufacturing of ion sensitive electrodes and lab-on-chip devices. To evaluate this hypothesis, a series of steps were undertaken 1) synthesis of a calcium ion-sensitive monomer; 2) evaluation of the monomer and monomer analog's sensitivity to calcium; 3) the polymerization of the monomer in radical polymerization strategies; 4) the growth of polymer

onto the PDA-wrapped CNTs and/or surfaces. Lastly, the optimized polymer-wrapped CNTs can then be formulated and tested for calcium sensitivity.

Towards mimicking the calcium ionophore II as a potential monomer it was proposed that the ether "O" bridge of the ionophore **3-3** could be replaced with isosteric atom to build an analog with a polymerizable moiety such as a methacrylate. This option, (replacing the oxygen) was chosen over breaking the symmetry of the compound (leaving the ether intact and building a functionalizable unit into one of the amides. As for a similarly sized (isostere) atom that allows for further attachment, the most direct choices are CH_2 or NH. As shown in **Scheme 3.3**, a nitrogen atom was chosen to replace the ether "O" with a secondary amine that can then easily undergo an S_N2 reaction to afford a monomer. The nitrogen atom, with a coordinating lone pair was thought to be more beneficial over a carbon atom (methylene) isostere as the crystal structure reported of ETH129 and calcium ion displayed coordination from all 9 oxygen atoms of 3 ETH129 molecules and thus the benefit of the added electron density. Similarly, 3-bromopropyl methacrylate (3-BPM) was selected as the primary alkyl halide of choice to provide the S_N2 reaction's coupling partner. 3-BPM was chosen as the 3-carbon length was hypothesized to provide reasonable space for methacrylate polymerization.[24] The retrosynthesis and ionophore comparison are shown in **Scheme 3.3**. Monomer **3-12** could be formed by an *N*-alkylation with 3-bromopropyl methacrylate, **3-9**, and the deprotected diamide **3-11**, which will be obtained from the protection and amide formation of readily available iminodiacetic acid **3-8** (based on 12/2019 pricing iminodiacetic acid is $0.09/g when 500 g was purchased). 3-bromopropyl methacrylate, **3-9**, can be derived from DCC coupling of methacrylic acid and 3-bromopropanol. Following the synthesis of the monomer, a series of polymer blends with poly(methyl methacrylate) were undertaken under radical polymerization conditions. These

blends were then tested as replacements for the binding agent polymer in CISE as to provide a more robust and selective ISM. PMMA was chosen as the co-polymer due to the numerous examples of 10:1 PMMA/n-BA binding agents in the literature.[25]

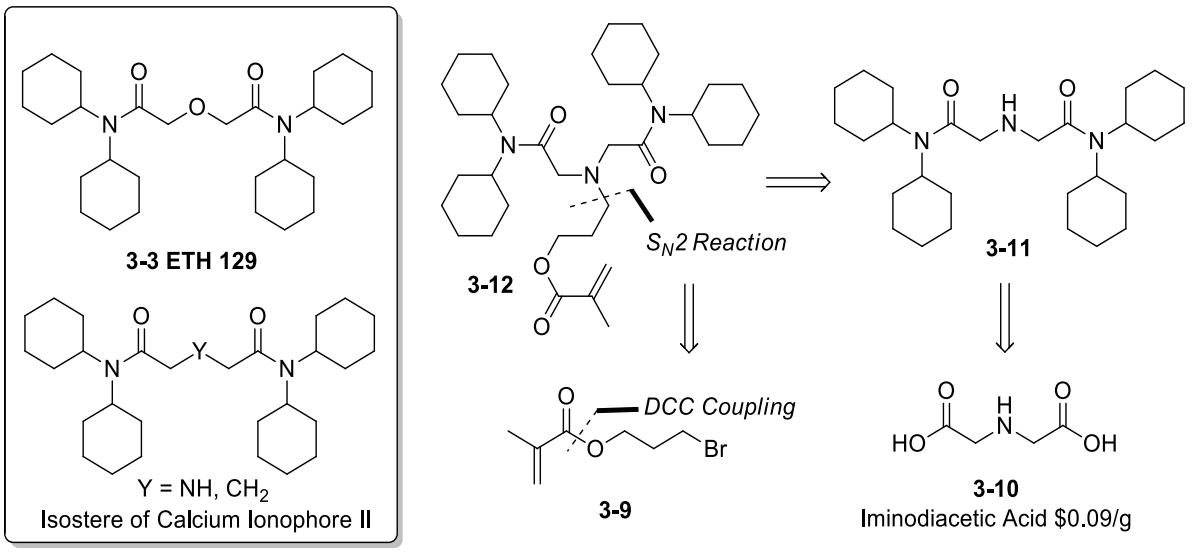

Scheme 3. 3. Comparison of the ETH129 and the potential isosteres; Retrosynthesis of the Ionophore-inspired monomer 3-12 from commercially available iminodiacetic acid 3-10.

The development of compatible CNT ink ionophore technologies that can be printed either in an additive manufacturing technique or co-printed simultaneously with conductive ink, either an organic soluble polymeric calcium ionophore will need to be created for ISE electrode formulations or a covalently attached ionophore to the CNT. Our hypothesis is that a calcium ionophore methacrylate-based polymer will have a stimulus response in the presence of calcium that will induce a change in resistance to the CNT ink and give a detectable and quantitative signal. This hypothesis was explored in two ways; through creation of an organic soluble ionophore-inspired monomer for incorporation as a conductive layer on top of multiple prints / drop casts of CNT inks and; grown from multi-wall CNTs (MWCNTs) after PDA and initiator coating. To probe these hypotheses, we have synthesized a calcium ionophore mimic methacrylate monomer, have probed its selectivity as an analog, as a polymer, and covalently

linked this polymer to the PDA that coats the CNT through ATRP controlled living polymerization techniques. These technologies could then be extended towards other analytes of interest for a multi-sensor system. Chapter 3.2 results will be discussed in 3 parts – 1) synthesis of monomer and comparison to known ETH129 ionophore; 2) development of copolymers of ionophore-inspired monomer and the electrochemical testing with calcium; 3) the development of ionophore-inspired monomer coated MWCNTs for potential incorporation as inks in jet printing additive manufacturing.

3.2. Results and Discussion

3.2.1 Synthesis of Monomer

The initial synthesis commenced with the carboxy benzoyl protection of the nitrogen of iminodiacetic acid **3-10** through reaction with benzyl chloroformate in alkaline conditions to give **3-13** in excellent yield **(Scheme 3.4)**. Attempts to make the amide bond via the acid chloride intermediate of the protected diacid were unsuccessful, however the diacid was effectively converted to the succinimide diester **3-14** which was subsequently converted to the bis(dicyclohexyl)acetamide with N,N'-dicyclohexylamine in 1,4-dioxane under reflux. Deprotection of the Cbz group gave the ionophore analog **3-11**, which could then be pushed forward to the ionophore inspired monomer **3-12** on reflux with 3-bromopropyl methacrylate. This initial strategy took five steps and proceeded with a low overall yield. Through synthetic route optimization, it was discovered that the succinimide step was unnecessary. **Scheme 3.4** illustrates the shorter and more economical sequence beginning from similar protected diacid **3-13** underwent DCC coupling but was sensitive to the order of addition of the reagents.

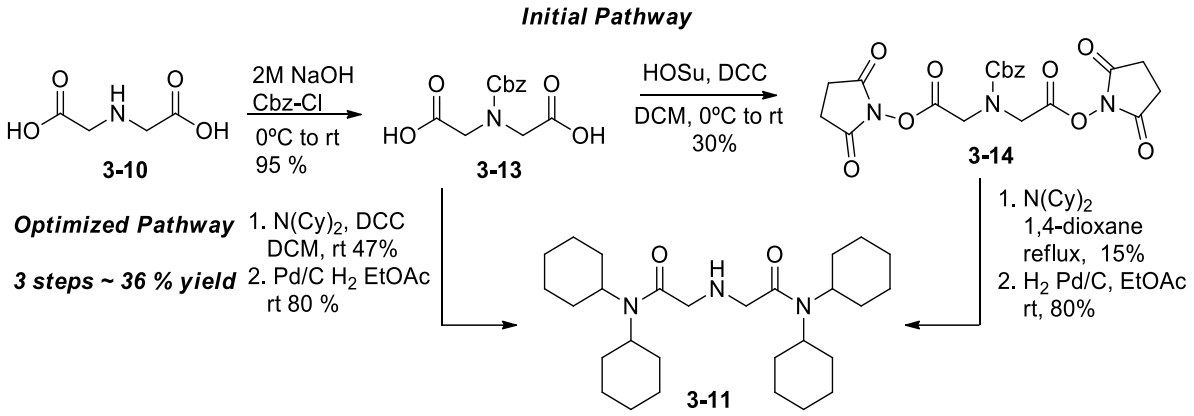

Scheme 3. 4. Initial and optimized synthetic schemes for Nitrogen analog 3-11 of the calcium Ionophore.

Overall, this reduced the sequence to four steps and an overall 36% yield to obtain *N*-analog **3-11** of ETH129. At this juncture, **3-11** was compared for calcium ion sensitivity and selectivity against known ionophore ETH129 (**3-3**). Stoichiometry of **3-11** with calcium was examined through a crystallization experiment of **3-11** with $Ca(ClO_4)_2 \cdot 4H_2O$ in MeOH. Slow evaporation of methanol gave monoclinic crystals of a 2:1 stoichiometry of **3-11** with calcium as shown in X-Ray crystal structure **Figure 3.2** (Full crystal structure data can be found in **Appendix to Chapter 3**). A key difference between the known calcium ionophore ETH129 and the NH analog crystallization studies with calcium found that the latter binds in a 2:1 stoichiometry contrary to the 3:1 stoichiometry of the former, as observed by Neupert-Laves and Dopler.[8] The report also studied ETH129 with magnesium and found a 2:1 stoichiometry, yet only 5 coordination sites between the 2 ligands as the central ether O did not give a particularly close bond distance (3.01(3) Å). This may suggest why ETH129 is more selective for calcium. For synthesized nitrogen analog, while a 2:1 stoichiometry was found, the bond distances from both nitrogen atoms to the calcium were on the same order as the oxygen carbonyls and most likely contributed to the coordination. Secondly, as the two water molecules

did bind to the calcium in a *cis* fashion, this suggests that potentially in solution, the ionphore could bind in a 3:1 fashion as seen in some Zn:phen species.[26]

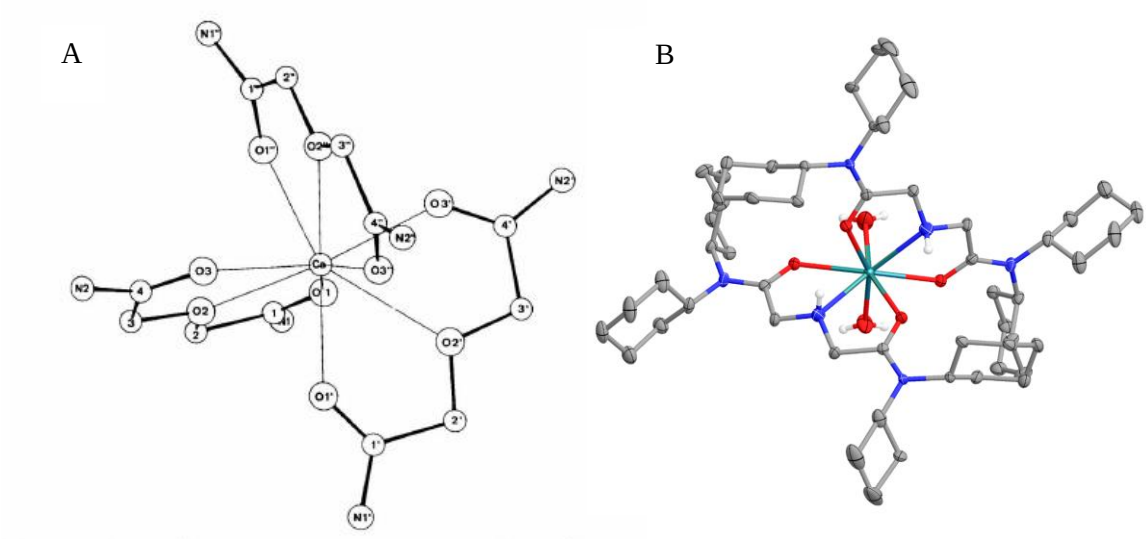

Figure 3. 2. X-ray crystal structure of A) ETH129 with calcium as reported by Neubert-Laves and Dobler in a 3:1 stoichiometry and B) the Nitrogen analog **3-11** in a 2:1 stoichiometry with calcium.

Coordination bond lengths obtained from the crystal structure of **3-11**, **3-12**, and ETH129 (taken from Neupert-Laves and Dobler)[8] to calcium (taken from Neupert-Laves and Dobler) are shown in **Table 3.1**. Coordination to **3-11** appears to utilize both the amide carbonyls and the central amine of the ligand while pushing the hydrogen of the NH away from the coordination sphere and, therefore amenable to functionalization with a moiety for polymerization yet still reliably provide binding. Two water molecules were found trans to each other in the coordination sphere. When the *N*-analog, **3-11** with $Ca(ClO_4)_2 \bullet 4H_2O$, was analyzed, it was found that the average bond length from carbonyl oxygen to calcium was 2.4623 Å, and slightly shorter than the average Ca-O bond length in ETH129 at 2.470 Å. The average nitrogen to calcium bonds in **3-11** were slightly shorter (2.5182 Å) than the average ethereal Ca-O (O2, O2', O2") bonds in ETH129 (2.578 Å). Overall, the percentage difference in bond lengths to

Ca for the *N*-analog vs. ETH129 was less than 0.5 percent (calculated to 0.34%) yet the marked difference in crystal structure stoichiometry may hinder the ligand's selectivity to calcium.

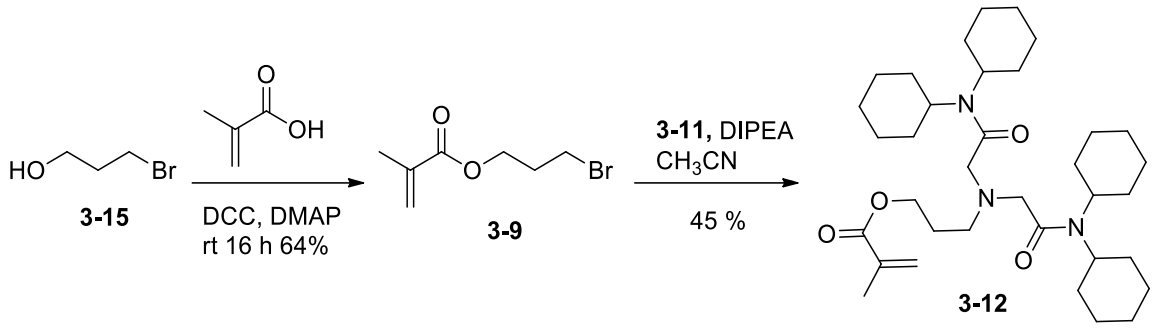

Scheme 3. 5. Synthesis of 3-bromopropyl methacrylate and completion of Ionophore-inspired monomer.

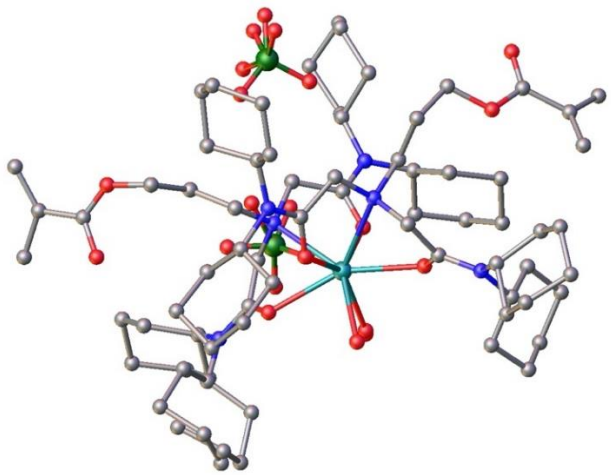

Figure 3. 3. X-Ray crystal structure of monomer 3-12 with calcium**.**

As highlighted in the retrosynthesis, synthesis of monomer **3-12** begins with the synthesis of 3-bromopropyl methacrylate, **3-9**, by DCC coupling of methacrylic acid and 3-bromopropan-1-ol **3-15** as shown in **Scheme 3.5**. This methacrylate was purified, fully characterized, and then coupled to the nitrogen analog **3-11** through an S_N2 reaction in acetonitrile in the presence of Hünig's base. The monomer **3-12** was then purified through

chromatography and fully characterized. Characterization data (NMRs) of all compounds can be found in Appendix to Chapter 3.

The monomer **3-12** crystallized with $Ca(ClO_4)_2 \cdot 4H_2O$ in methanol as orthorhombic crystals to give a 2:1 stoichiometric ratio of the monomer to calcium as shown in **Figure 3.3**, with two water molecules *cis* to each other in the coordination sphere. Bond distances were compared to the precursor analog **3-11** and ETH129 as shown in **Table 3.1**. Average Ca-O bond lengths (excluding water molecules), were found to be shorter than ETH129 at 2.4058 Å and the Ca-N average bond lengths however were longer at 2.6662 Å. The percent difference was calculated at 2.5% when compared to ETH129 bond distances.

Table 3. 1. X-Ray Diffraction Bond Lengths of Analog 3-11, Monomer 3-12, and ETH 129 with Calcium

Analog 3-11		**Monomer 3-12**		**ETH129**	
Bond	**Length (Å)**	**Bond**	**Length (Å)**	**Bond**	**Length (Å)**
Ca1-O1	2.4904(18)	**Ca1-O1**	2.409(5)	**Ca1-O1**	2.389(6)
Ca1-O1'	2.4903(18)	**Ca1-O2**	2.403(6)	**Ca1-O2**	2.550(5)
Ca1-O2	2.4325(17)	**Ca1-O3**	2.353(5)	**Ca1-O3**	2.469(6)
Ca1-O2'	2.4325(17)	**Ca1-O4**	2.456(6)	**Ca1-O1'**	2.383(5)
Ca1-O3	2.408(2)[a]	**Ca1-O9**	2.471[a]	**Cal-O2'**	2.627(5)
Ca1-O3'	2.408(2)[a]	**Ca1-O10**	2.446(6)[a]	**Ca1-O3'**	2.405(5)
Ca1-N1	2.518(2)	**Ca1-N2**	2.638(7)	**Ca1-O1"**	2.434(5)
Ca1-N1'	2.518(2)	**Ca1-N5**	2.693(7)	**Ca1-O2"**	2.557(6)
[a]Water molecules				**Ca1-O3"**	2.417(5)

While there was some disorder in the crystal on the cyclohexyl groups and in the methacrylate (methylene/methyl groups were found in both positions and therefore difficult to resolve), the overall stoichiometry in the crystal structure held to 2:1. Multiple attempts at recrystallizing these mixtures in various solvent systems resulted in similar crystal structures.

An evaluation of the bond angles between the amide oxygens to the calcium atoms to the central isosteric atom (O, N) gave more insight as shown in **Table 3.2**. The angles between the ETH129 and Calcium are slightly smaller than those with the nitrogen analogs which may describe why these structures exhibit a 2:1 stoichiometry over the 3:1. At this juncture the *N*-analog was deemed an excellent candidate to evaluate as a potential ion selective ionophore as the bond distances to calcium were very similar to those in ETH129 and selectivity studies proceeded. Similarly, with the monomer now synthesized, a series of polymerizations and materials testing could be accomplished.

Table 3. 2. Bond Angles of Amide Oxygen to Calcium to Central Isosteric Atoms

ETH129 with Ca				Analog **3-11**			Monomer **3-12**		
	Lig 1	Lig 2	Lig 3		Lig 1	Lig 2		Lig 1	Lig 2
O1-Ca-O2	61.1˚	59.6˚	60.9˚	O1-Ca-N1	63.3˚	63.3˚	N2-Ca-O1	63.4˚	62.7˚
O3-Ca-O2	60.9˚	59.4˚	61.1˚	O3-Ca-N1	65.1˚	65.1˚	N2-Ca-O2	62.9˚	61.5˚

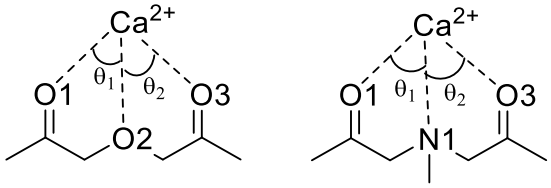

Figure 3. 4. Schematics of the bond angles in the molecules.

3.2.2. Evaluation of *N*-analog 3-11 as Ion-sensitive Ionophore

Initial calcium sensitivity tests of **3-11** were prepared in a similar fashion as ETH129 (in Chapter 2) yet replacing ETH129 for **3-11** in the same ratio. As described, a typical ion sensitive formulation for a solid contact sensor consists of ionophore, plasticizer, ionic salt**,** and binding polymer which can be administered in an organic solvent onto a pre-printed conductive electrode. When such a formulation was prepared and tested, ion selective membrane (ISM) mix of **3-11** produced an emf measurement that was less sensitive to calcium and with a higher

limit of detection (**Figure 3.5**) compared to the ETH129 mix. This was justified as the stoichiometric ratio of **3-11** to calcium is a third less and therefore should be less sensitive to changes in calcium. It is hypothesized that the nitrogen atom being less electronegative and larger in size, and bite angle cannot conform to the 3:1 stoichiometry and give optimal selectivity of calcium.

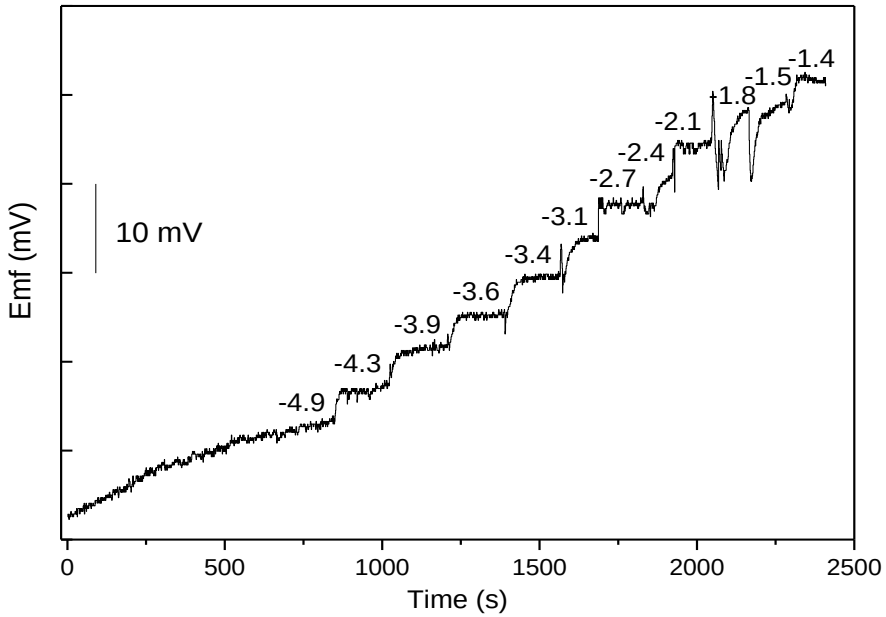

Figure 3. 5. EMF experiment with increasing Ca^{2+} concentration. Initial test of the calcium ionophore analog substituting it for CI2 in the drop cast mix.

Selectivity tests (**Figure 3.6**). were then performed utilizing a starting concentration of 1 mM Ca^{2+} and sequentially adding potentially interfering cations such as NH_4^+, Mg^{2+}, K^+, and Zn^{2+}. An addition of NH_4^+ gave only a slight rise in drift (18 mV**)** indicating a slight drop in selectivity. However, the addition of Mg^{2+}, NH_4^+, and Zn^{2+} unfortunately caused further rise in signal indicating that the *N*-analog is not as selective to calcium as ETH129.

3.3. Development of Polymer blends of IIM for potentiometric investigations

Following the synthesis of ionophore inspired monomer **3-12**, a series of random block copolymer blends were synthesized using methyl methacrylate (MMA) as copolymer using

AIBN initiated free radical polymerization (full experimental procedures are found at the end of this chapter). **Table 3.3** displays the various percentages and physical properties of the polymers synthesized. Polymers were characterized to their amount of ionophore monomer using ^{1}H NMR (integrating methoxy peak of MMA against the broad singlet for the CH_2 groups in the acetamide against each other) to provide a ratio as shown in **Figure 3.7.** These ratios were confirmed using CHN analysis as the only nitrogen component of each blend came from the ionophore inspired monomer. Each blend was synthesized in triplicate to give an accurate account of polymerization yields and percentages.

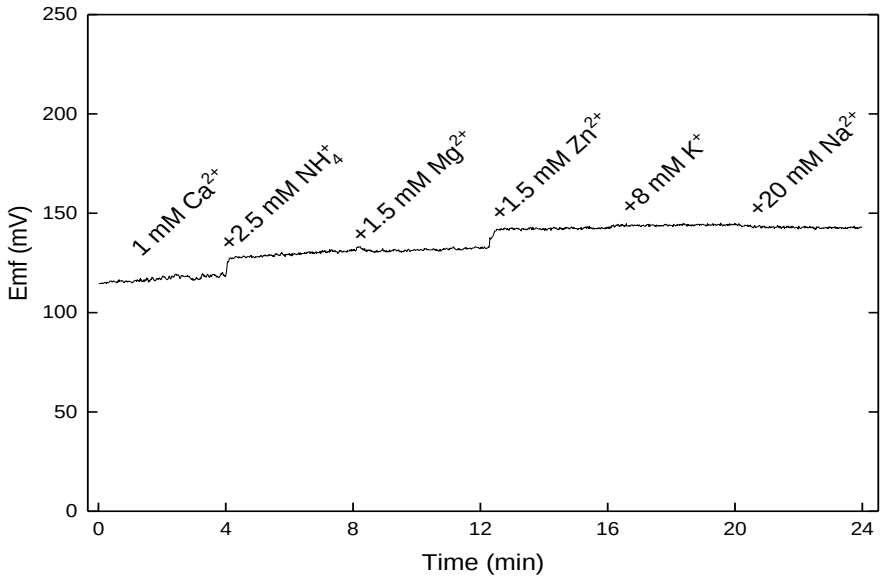

Figure 3. 6. Selectivity Test for *N*-analog **3-11.**

Table 3. 3 Copolymer blend percentages of **3-12** and physical properties of polymers

Sample	x_1 feed	yield	x_1 NMR	x_1 CHN	M_n	T_g °C
AP0	0	99	0	0	38800	100
AP7, 9	0.05	99	0.04	0.03	2447	82.9
AP4,10	0.09	85	0.07	0.06	2854	77.8
AP8,11	0.12	83	0.1		2739	65.3
AP6,12	0.2	83	0.25	0.21	2668	61.7

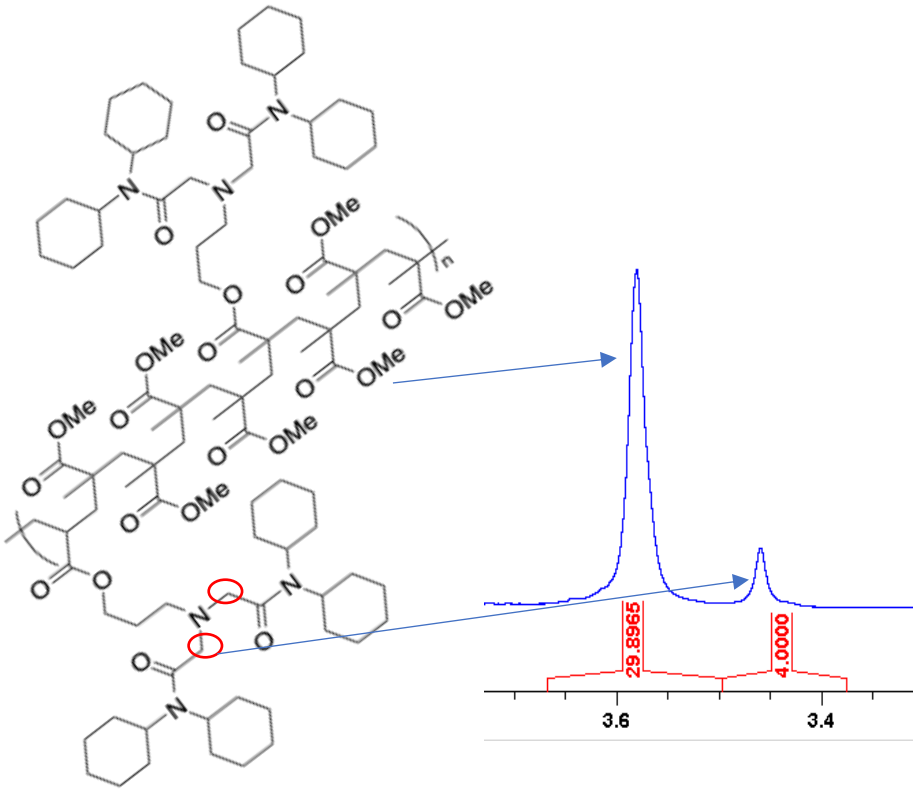

Figure 3. 7. Schematic representation of poly(methyl methacrylate-co-2-(bis(2-(dicyclohexylamino)-2-oxoethyl)amino)propyl methacrylate showing the integration of PMMA methyl peak at 3.57 ppm vs that of the IIM -CH_2- peaks 3.46 ppm used to calculate percentages of each monomer in the copolymer**.**

As all polymerizations were run for equal times, the average molecular weights (M_n), and weight average molecular weights are relatively the same over the blends. Interestingly, GPC (to determine M_n) was unreliable and gave poor elution times. M_n was therefore determined based on ESI-MS. The polydispersity was quite good for a free radical polymerization especially compared to that of PMMA. The glass transition temperatures (T_g) decreased with increase in the amount of ionophore inspired monomer in the blend, an indication that the addition of the bulky lipophilic unit adds less rigidity to the polymer. These low molecular weight polymers could also be investigated as potential gelating agents.

The polymer blends were then tested as potential binding agents in calcium ionophore mixtures. Similar to the drop-cast experiments in Chapter 2, poly(methyl methacrylate-co-2-

(bis(2-(dicyclohexylamino)-2-oxoethyl)amino)propyl methacrylate (from now referred to as co-pMMA/IIM), were added to ionophore mixtures as potential binding agents and binding agents/ionophores, and applied to commercially available electrodes (Pine Instruments) as shown in **Figure 3.7** for testing in Electrochemical impedance spectroscopy (EIS) for sensitivity to Ca^{2+} ions (**Figure 3.8**). From EIS of the various electrode mixtures, the blend of 17% was chosen for selectivity testing due to weak EIS signal and indicating low resistance.

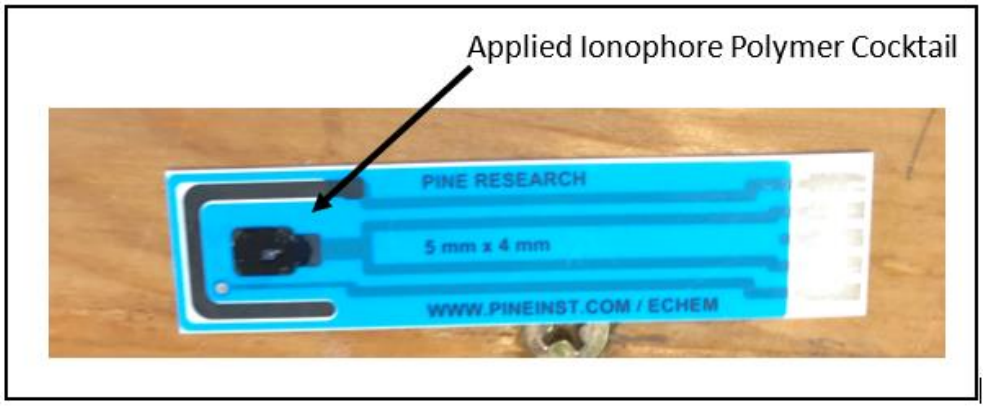

Figure 3. 8. Picture of commercially available screen-printed electrode with added copolymer cocktail to test for calcium sensitivity using EIS**.**

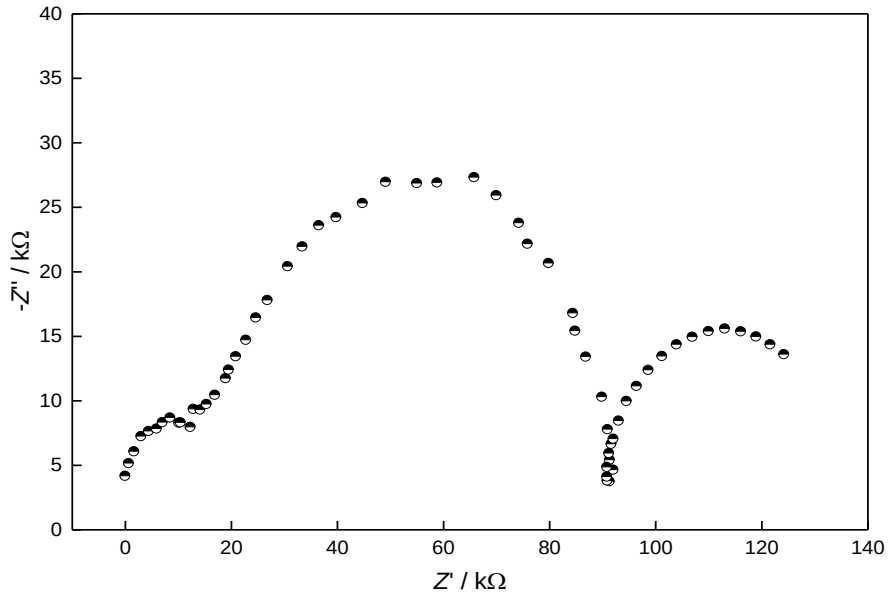

Figure 3. 9. A representative EIS for the copolymer cocktail (12% IIM in copolymer blend) on pine electrode in 10^{-3} M calcium solution.

3.2.3 - Development of Polymer-coated CNTs for ink-jet printing

Lastly, as part of the NASA EPSCoR Flexible Hybrid Electronics project, ion-sensitive polymer-coated CNTs were attempted as proposed for potential materials to be added to conductive CNT inks for direct jet printing of sensors in an additive manufacturing concept for flexible hybrid electronics. To achieve this goal, the non-covalent poly(dopamine) wrapping of MWCNTs was chosen. Wrapped CNTs could then undergo addition of ATRP initiator bromo-isobutyryl bromide through attachment at the catecholic end groups on the polydopamine and finally ARGET ATRP polymerization of monomer **3-12** as the ultimate concept figure as shown in **Scheme 3.6**.

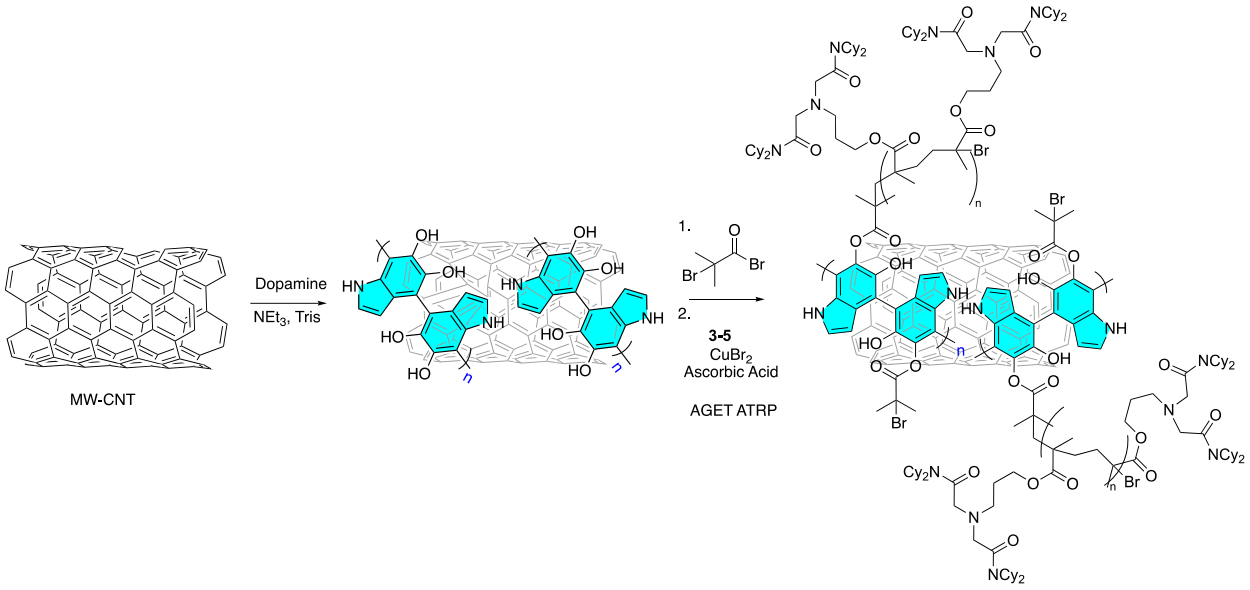

Scheme 3. 6. Conceptual figure for the synthesis of ion sensitive polymer coated CNTs

Optimal methods for coating MWCNTs with PDA, initiator addition, and methacrylate polymerization needed to be determined. Starting with commercially available MWCNTs (nanolabs), dopamine solutions in Tris buffer were explored over various time intervals to attempt to explore the thickness of coating of PDA on the tubes. TEM images of our CNTs bare compared to variable time lengths of exposure to dopamine solutions indicated that average

CNT width increased from ~35 nm bare to around 50 nm when coated with PDA and then average 90 nm following an ARGET ATRP polymerization with 2-hydroxyethyl methacrylate for 6 h as shown in **Figure 3.10.** Poly(2-hydroxyethyl) methacrylate (PHEMA) was chosen as a representative monomer to test ARGET ATRP conditions on PDA coated CNTs while synthesis of monomer **3-12** was in progress. Analysis of the CNTs with transmission electron microscopy (TEM) showed a progressive increase in thickness after each stage of the process from wrapping it in PDA to polymerization of hydroxyethyl methacrylate on the CNTs. FTIR comparison as shown in **Figure 3.11** indicated that pHEMA successfully grew on the MWCNTs.

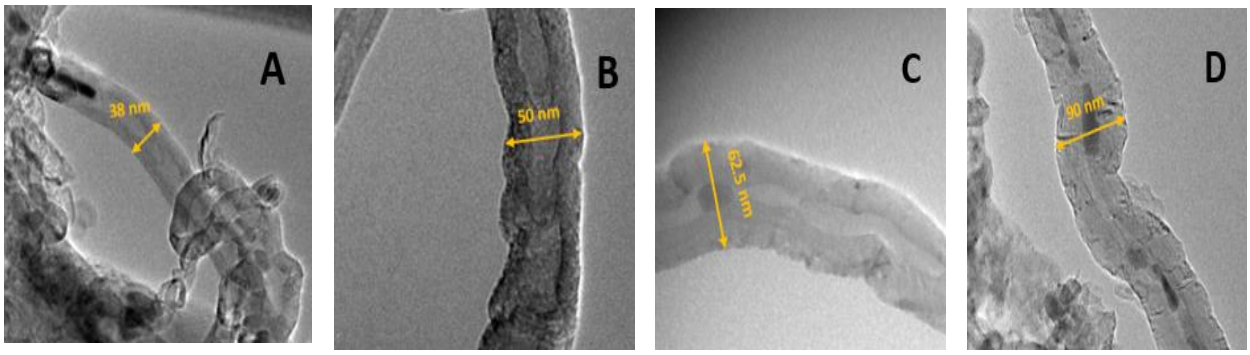

Figure 3. 10. TEM Images of; (A) MWCNTs; (B) MWCNTs-PDA; (C) MWCNTs-PDA-BiBB; (D) CNTs-PDA-PHEMA

With confidence of ARGET ATRP polymerization method following successful pHEMA growth on PDA wrapped CNTs, monomer **3-12** was substituted for HEMA and polymerization of ion-sensitive monomers on CNTs was explored. At this juncture, both MWCNTs and COOH-end group MWCNTs were both wrapped with PDA, esterified with 2-bromoisobutyrate and subjected to ARGET ATRP conditions. The -COOH-end group MWCNTs were also chosen as they are known to disperse more readily in water.

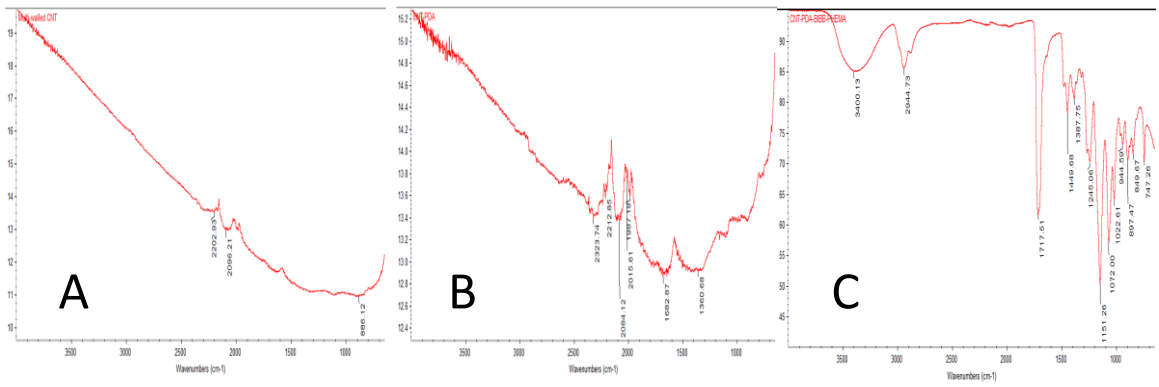

Figure 3. 11. FT-IR spectrum of (A) MWCNT (B) MWCNT-PDA (C) MWCNT-PDA-PHEMA.

3.3. Experimental Procedures.

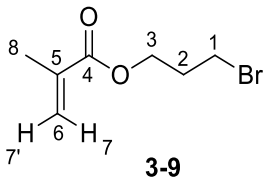

3-9

Synthesis of 3-bromopropyl methacrylate (3-9). To a solution of the acid (5 g, 58.08 mmol) and bromoalcohol (8.07 g, 58.08 mmol) in 150 mL of anhydrous dichloromethane DCM, a solution of 1,3-dicyclohexylcarbodiimide DCC (11.98 g, 58.08 mmol) in DCM (50 mL) was slowly added followed by addition of a catalytic amount of DMAP (0.709 g, 0.58 mmol). The resulting mixture was stirred at room temperature for 16 h. After filtration, the filtrate was washed with 5% $NaHCO_3$ (100 mL), brine and dried over $MgSO_4$. After removing the solvent, chromatography (10% EtOAc: hexane) gave a pure compound 6.43 g, 53% yield. ^{1}H NMR (500 MHz, Chloroform-*d*) δ 6.11 (dq, *J* = 2.0, 1.0 Hz, 1H, **H**$_{7'}$), 5.58 (q, *J* = 1.6 Hz, 1H, **H**$_7$), 4.29 (t, *J* = 6.0 Hz, 2H, **H**$_3$), 3.48 (t, *J* = 6.5 Hz, 2H, **H**$_1$), 2.23 (tt, *J* = 6.5, 6.0 Hz, 2H, **H**$_2$), 1.95 (dd, *J* = 2.0, 1.0 Hz, 3H, **H**$_8$). ^{13}C NMR (126 MHz, CDCl3) δ 167.3 **C**$_4$, 136.3 **C**$_5$, 125.8 **C**$_6$, 62.6 **C**$_3$, 31.9 **C**$_1$, 29.5 **C**$_2$, 18.4 **C**$_8$.

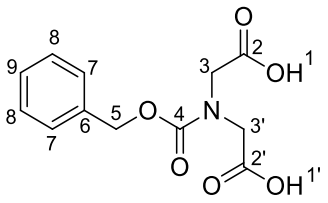

3-13

Synthesis of 2,2'-(((benzyloxy)carbonyl)azanediyl)diacetic acid (3-13). Using an established procedure,[27] iminodiacetic acid (5 g, 0.0375 mol) was dissolved in 2 M NaOH (37.5 mL) and the resulting solution was cooled in an ice bath. Benzyl chloroformate (7 g, 5.86 mL, 0.041 mol) and 2 M NaOH (22.5 mL) were subsequently added to the stirred solution, the reaction mixture was stirred at room temperature for 6 h. The reaction mixture was transferred to a separatory funnel and washed with Et_2O (2 × 25 mL). The aqueous phase was acidified with conc. HCl to pH 1–2 and extracted with Et_2O (3 × 40 mL). The organic extract was dried over Na_2SO_4 and evaporated. The product 9.74 g was used in the subsequent reactions without further purification (colorless oil). ^{1}H NMR (500 MHz, Chloroform-*d*) δ 7.37 – 7.29 (m, 5H, **H$_{7\text{-}9}$**), 5.17 (s, 2H, **H$_5$**), 4.21 (s, 2H, **H$_{3/3'}$**), 4.15 (s, 2H, **H$_{3/3'}$**). ^{13}C NMR (126 MHz, $CDCl_3$) δ 175.1 **C$_{2/2'}$**, 173.4 **C$_{2/2'}$**, 156.2 **C$_4$**, 136.8 **C$_6$**, 128.8 **C$_8$**, 128.5 **C$_9$**, 128.1 **C$_7$**, 68.8 **C$_5$**, 50.1 **C$_{3/3'}$**, 50.0 **C$_{3/3'}$**.

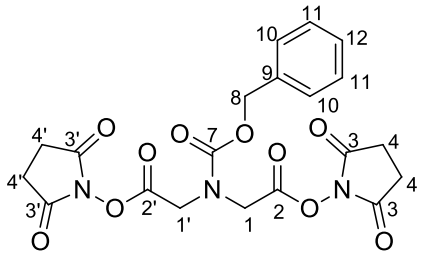

3-14

bis(2,5-dioxopyrrolidin-1-yl) 2,2'-(((benzyloxy)carbonyl)azanediyl)diacetate (3-14). To a solution of the diacid (9.74 g) and *N*-hydroxysuccinimide (72.86 mmol) in 120 mL of anhydrous

dichloromethane DCM, a solution of 1,3-dicyclohexylcarbodiimide DCC (72.86 mmol) in DCM was slowly added followed by addition of a catalytic amount of DMAP (7.29 mmol). The resulting mixture was stirred at room temperature for 16 h. After filtration, the filtrate was washed with 5% $NaHCO_3$ and dried over $MgSO_4$. After removing the solvent, the product was purified by column chromatography using EtOAc and hexane (white solid) 5.04 g, yield 30% over 2 steps. ^{1}H NMR (500 MHz, Chloroform-*d*) δ 7.40 – 7.30 (m, 5H, **H$_{10\text{-}12}$**), 5.22 (s, 2H, **H$_8$**), 4.59 (s, 2H, **H$_{1/1'}$**), 4.48 (s, 2H, **H$_{1/1'}$**), 2.85 (d, *J* = 4.4 Hz, 8H, **H$_{4/4'}$**). ^{13}C NMR (126 MHz, $CDCl_3$) δ 168.5 **C$_{2/2'}$**, 165.1 **C$_{3/3'}$**, 164.9 **C$_{3/3'}$**, 155.3 **C$_7$**, 135.5 **C$_9$**, 128.7 **C$_{11}$**, 128.5 **C$_{12}$**, 128.4 **C$_{10}$**, 69.1 **C$_8$**, 47.4 **C$_{1/1'}$**, 47.2 **C$_{1/1'}$**, 25.7 **C$_{4/4'}$**.

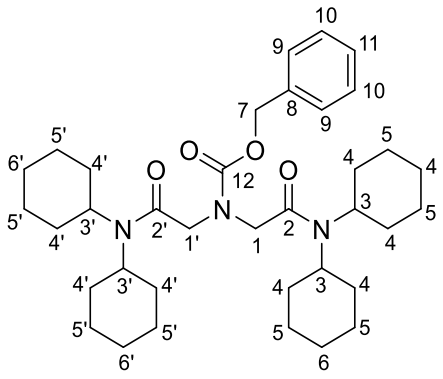

benzyl bis(2-(dicyclohexylamino)-2-oxoethyl)carbamate. To a solution of the diacid (8.24 g) and dicyclohexyl amine (11.18 g, 61.68 mmol) in 120 mL of anhydrous dichloromethane DCM, a solution of 1,3-dicyclohexylcarbodiimide DCC (12.73 g, 61.68 mmol) in DCM was slowly added followed by addition of a catalytic amount of DMAP (1.50 g, 12.34 mmol). The resulting mixture was stirred at room temperature for 16 h. After filtration, the filtrate was washed with 5% $NaHCO_3$ and dried over $MgSO_4$. After removing the solvent, the product was recrystallized in 20% EtOAc and hexane to give the pure compound 8.69 g, 39% yield over 2 steps. ^{1}H NMR (500 MHz, Chloroform-*d*) δ 7.31 – 7.28 (m, 5H, **H$_{8\text{-}11}$**), 5.10 (s, 2H, **H$_7$**), 4.30 (s, 2H, **H$_{1/1'}$**),

4.16 (s, 2H, **H1/1'**), 3.50 – 3.20 (m, 2H, **H3/3'**), 2.39 (s, 2H, **H3/3'**), 1.84 – 1.15 (m, 40H, **H4/4'** – **H6/6'**). ^{13}C NMR (126 MHz, $CDCl_3$) δ 167.9 **C2**, 156.0 **C12**, 136.7 **C8**, 128.4 **C10**, 128.1 **C11**, 127.9 **C9**, 67.7 **C7**, 56.9 **C2/2'**, 56.3 **C2/2'**, 50.8 **C1/1'**, 50.1 **C1/1'**, 31.4 **C4/4'**, 30.3 **C4/4'**, 30.2 **C4/4'**, 26.7 **C5/5'**, 26.0 **C5/5'**, 25.9 **C5/5'**, 25.6 **C6/6'**, 25.5 **C6/6'**, 25.4 **C6/6'**, 25.3 **C6/6'**. $C_{36}H_{65}N_3O_4$ (593.85): requires C, 72.81; H, 9.34; N, 7.08; found C, 72.51; H, 9.; N, 6.97.

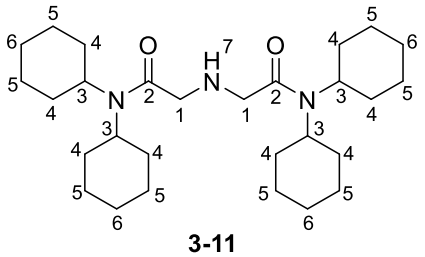

3-11

2,2'-azanediylbis(N,N-dicyclohexylacetamide) (3-11). To solution of the protected diamide (4 g, 6.74 mmol) in EtOH (50 mL) was added slowly Pd/C 5% (1.30 g) under an N_2 atmosphere at room temperature. The vessel was evacuated, filled with H_2, evacuated a second time and filled with H_2, and left to stir overnight. After this period, the H_2 was expelled, the solution filtered through a celite pad with EtOH, and the solvent removed under reduced pressure to yield pure product as a white solid (2.78 g, 90%). ^{1}H NMR (500 MHz, Chloroform-*d*) δ 3.49 (s, 4H, **H1**), 3.37 – 2.85 (m, 5H, **H1 H3 H7**), 2.51 – 2.34 (m, 4H, **H4**), 1.91 – 0.94 (m, 36H, **H4-6**). ^{13}C NMR (126 MHz, $CDCl_3$) δ 168.9 **C2**, 56.8 **C3**, 56.2 **C3**, 51.3 **C1**, 34.1 **C4**, 31.4 **C4**, 31.1 **C4**, 30.2 **C4**, 26.8 **C5**, 26.1 **C5**, 25.5 **C6**, 25.4 **C6**.

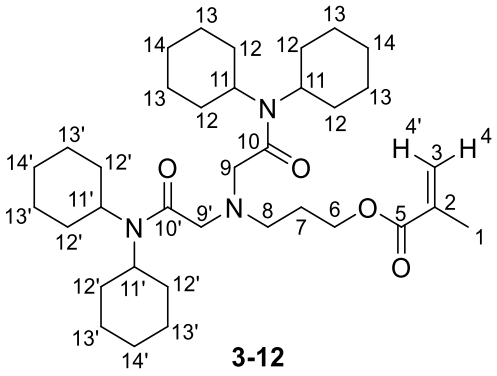

3-12

3-(bis(2-(dicyclohexylamino)-2-oxoethyl)amino)propyl methacrylate (3-12). To a solution of the amine (0.82 g, 1.79 mmol) and 3-bromopropyl methacrylate (0.37 g, 1.79 mmol) in acetonitrile (150 mL), was added diisopropylethylamine (0.311 mL, 1.79 mmol). The solution was stirred at reflux overnight. The reaction was stopped when TLC showed no sign of the starting material. The reaction was evaporated to dryness, the residue dissolved in water, extracted with EtOAc (3 x 30 mL) and dried over $MgSO_4$. The product was purified with column chromatography using EtOAc and hexane to get the pure product as a white solid (0.46 mg, 43% yield). ^{1}H NMR (300 MHz, Chloroform-*d*) δ 6.07 (s, 1H, **H$_4$**), 5.52 (s, 1H, **H$_4$'**), 4.19 (t, *J* = 6.5 Hz, 2H, **H$_6$**), 3.47 (s, 4H, **H$_{9/9'}$**), 2.90 (t, *J* = 7.4 Hz, 2H, **H$_8$**), 2.50 – s2.37 (m, 4H, **H$_{11/11'}$**), 1.92 (s, 3H, **H$_1$**), 1.89 – 0.98 (m, 42H, **H$_7$ H$_{12/12'}$ - H$_{14/14'}$**). ^{13}C NMR (75 MHz, $CDCl_3$) δ 169.9 **C$_5$**, 167.6 **C$_{10/10'}$**, 136.7 **C$_2$**, 125.3 **C$_3$**, 63.4 **C$_6$**, 57.0 **C$_{11/11'}$**, 56.7 **C$_{11/11'}$**, 56.1 **C$_{11/11'}$**, 52.0 **C$_7$**, 34.1 **C$_{12/12'}$**, 31.5 **C$_{12/12'}$**, 30.3 **C$_{13/13'}$**, 27.7 **C$_{13/13'}$**, 26.8 **C$_{14/14'}$**, 26.1 **C$_{14/14'}$**, 25.5 **C$_{13}$**, 25.1 **C$_{13}$**, 18.4 **C$_1$**.

Polymerizations

As blends with PMMA: AIBN (0.0041 g, 24.9 μmol), 2-(bis(2-(dicyclohexylamino)-2-oxoethyl)amino)propyl methacrylate (292. 5 mg, 0.50 mmol), methyl methacrylate (0.451 g, 4.5 mmol) and 1,2-dichloroethane (5.5 mL) was added to an oven dried 30 mL glass pressure

vessel. The reaction vessel was sealed and degassed via three freeze-pump-thaw cycles and brought to room temperature. The solution was heated to 70 °C for 12 hours and then cooled to room temperature. Polymerization was stopped by exposure to air. Precipitation into tenfold excess hexanes yielded white polymer precipitate, which was isolated via filtration and dried to constant weight under reduced pressure at room temperature.

Preparation of Polydopamine (PDA) coated CNTs: CNTs (100 mg) was added to a solution of ethanol (40 mL) in water (30 mL) and sonicated for 10 minutes. Dopamine (80 mg) was under to the CNT solution under magnetic stirring. After 5 minutes, 20 ml of 25 mM Tris buffer solution was added dropwise. The reaction was stirred at room temperature for 24 hours. The product was washed with ethanol 3 times, separated by centrifugation, and dried in a vacuum oven at 60 °C for 24 hours to give a black powder.

Preparation of CNTs-PDA-BiBB macroinitiator: CNTs-PDA (40 mg) was suspended in DMF (40 ml) and sonicated for 12 minutes. Triethylamine (2.0 ml, 14.4 mmol) was added dropwise with stirring under N_2 atmosphere. After 10 minutes, a solution of BiBB (1.80 mL, 14.4 mmol) in DMF (20 mL) was added dropwise. The reaction was stirred under N2 atmosphere for 24 hours at room temperature. The product was washed repeatedly with acetone, ethanol and water respectively and dried in a vacuum oven at 60 °C for 24 hours.

ARGET ATRP growth of PHEMA brushes: CNTs-PDA-BiBB (60 mg, 0.09 mol initiator) was suspended in ethanol (10 mL) and sonicated for 30 minutes. HEMA (8.73 ml, 72 mmol), $CuBr_2$ (0.00132 g, 0.006 mmol) and HMTETA (0.00822 mL, 0.03 mmol) were added sequentially under stirring. The vial was sealed and purged with N_2. After 10 minutes, a solution of Ascorbic acid sodium salt (0.04752 g, 0.24 mmol) in ethanol (1 mL) was added via syringe. The molar ratio of monomer: macroinitiator: catalyst: ligand: reducing agent = 12000: 1: 5: 40.

The reaction was stirred at room temperature for 6 h. The product was successively washed with dichloromethane, ethanol and water, and dried in a vacuum oven at 60 ℃ for 24 hours.

3.4. Materials and Methods

1,2-dichloroethane was purchased from Fischer Chemical and used as received. 2,2'-Azobis(2-methylpropionitrile) AIBN was obtained from Sigma-Aldrich and used as received. Methyl methacrylate was purchased from Sigma-Aldrich. Inhibitor was removed by distillation under vacuum at room temperature immediately before use. 2-hydroxyethyl methacrylate (HEMA) was purchased from Sigma-Aldrich.

3.5. Conclusions

This multifaceted project began with the successful synthesis and crystallization study of a novel monomer designed to mimic a known ionophore of calcium to test for potential polymeric systems for calcium sensing. The synthesis was readily accomplished in 5 steps and this compound is now synthesized on the multi-gram scale (>50 g) starting from a readily available iminodiacetic acid ($0.09/g). The crystallization studies with calcium provided a mixed response as the stoichiometric ratio of both the monomer and the NH-analog precursor to the monomer gave a undesirable 2:1 stoichiometry yet favorable bond distances that mimicked known calcium ionophore ETH129. Moving forward, this part of the project could diverge in two separate directions: 1) using the 2:1 calcium: monomer **3-12** stoichiometry to an advantage and the possible incorporation of this salt as a cross-linker for degradable polymers as seen in various drug delivery hydrogels or; 2) as the stoichiometry was unfavorable, perhaps a non-symmetric diglycolic acid derivative may be more advantageous to synthesize although potentially more complex of a synthesis. As for potential cross-linking agents, the *N*-analog **3-11** could be utilized directly with longer chain primary alkyl halide methacrylates/acrylates to

explore the structure/function relationships of potential cross-linked polymers as shown as a future direction of this work in **Figure 3.12**. The synthesis of more complex non-symmetric.

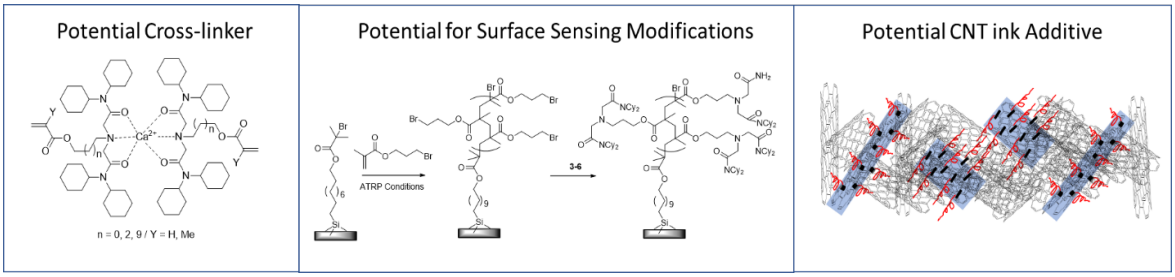

Figure 3.12: Future directions of this project leading to (a) cross-linkers (b) surface modifications and (c) mixed CNT compatible inks.

Secondly, the monomer readily polymerized when mixed with poly(methyl methacrylate) in excellent yields at various percentages. These copolymers were then evaluated as potential binding agents for calcium ion sensitivity. MMA copolymers over 7% of ionophore inspired monomer gave good sensitivity to calcium as measured by EIS experiments and were selected as potential candidates for further developments for devices. What is more, this highlights how a thin layer of ionophore inspired monomer can affect the physical properties of the system. Moving forward, this technology could be advanced to thin-film polymer brushes as the 3-BPM monomer can be grown from the surface and then undergo the S_N2 reaction with **3-11** to create the monomer on the surface of these brushes in a post-polymerization modification as shown in the middle section of **Figure 3.12**.

Finally, the synthesized monomer was polymerized on PDA coated MWCNTs as to evaluate the potential for polymer coated CNT compatibility with conductive CNT inks for additive manufacturing technologies. These polymer coated CNTs can now move forward for testing in printable CNT devices. Results here indicate that CNT coating is possible and next steps could evaluate the many variables that will realize coated ionophore CNTs with printable CNTs.

3.6. References

1. Bobacka, J.; Ivaska, A.; Lewenstam, A., Potentiometric ion sensors. *Chem Rev* **2008,** *108* (2), 329-51.

2. Bakker, E.; Pretsch, E.; Buhlmann, P., Selectivity of potentiometric ion sensors. *Anal Chem* **2000,** *72* (6), 1127-33.

3. Bakker, E.; Qin, Y., Electrochemical sensors. *Anal Chem* **2006,** *78* (12), 3965-84.

4. Pedersen, C. J., Cyclic Polyethers and Their Complexes with Metal Salts. *Journal of the American Chemical Society* **1967,** *89* (26), 7017-&.

5. Springsteen, G.; Wang, B. H., A detailed examination of boronic acid-diol complexation. *Tetrahedron* **2002,** *58* (26), 5291-5300.

6. Brooks, W. L.; Sumerlin, B. S., Synthesis and Applications of Boronic Acid-Containing Polymers: From Materials to Medicine. *Chem Rev* **2016,** *116* (3), 1375-97.

7. Wang, E.; Erdahl, W. L.; Hamidinia, S. A.; Chapman, C. J.; Taylor, R. W.; Pfeiffer, D. R., Transport properties of the calcium ionophore ETH-129. *Biophys J* **2001,** *81* (6), 3275-3284.

8. Neupertlaves, K.; Dobler, M., Crystal-Structure Analyses of Divalent Metal Cation Complexes with Neutral Non-Cyclic Ionophores .2. Mg-2+ and Ca-2+ Complexes of N,N,N',N'-Tetracyclohexyl-3-Oxapentanediamide. *J Cryst Spectrosc* **1982,** *12* (3), 287-299.

9. Bakker, E.; Meruva, R. K.; Pretsch, E.; Meyerhoff, M. E., Selectivity of polymer membrane-based ion-selective electrodes: self-consistent model describing the potentiometric response in mixed ion solutions of different charge. *Anal Chem* **1994,** *66* (19), 3021-30.

10. Kong, J.; Chapline, M. G.; Dai, H. J., Functionalized carbon nanotubes for molecular hydrogen sensors. *Adv Mater* **2001,** *13* (18), 1384-1386.

11. Pengfei, Q. F.; Vermesh, O.; Grecu, M.; Javey, A.; Wang, O.; Dai, H. J.; Peng, S.; Cho, K. J., Toward large arrays of multiplex functionalized carbon nanotube sensors for highly sensitive and selective molecular detection. *Nano Lett* **2003,** *3* (3), 347-351.

12. Li, C.; Thostenson, E. T.; Chou, T. W., Sensors and actuators based on carbon nanotubes and their composites: A review. *Compos Sci Technol* **2008,** *68* (6), 1227-1249.

13. Bekyarova, E.; Davis, M.; Burch, T.; Itkis, M. E.; Zhao, B.; Sunshine, S.; Haddon, R. C., Chemically functionalized single-walled carbon nanotubes as ammonia sensors. *J Phys Chem B* **2004,** *108* (51), 19717-19720.

14. Gao, C.; Guo, Z.; Liu, J. H.; Huang, X. J., The new age of carbon nanotubes: An updated review of functionalized carbon nanotubes in electrochemical sensors. *Nanoscale* **2012,** *4* (6), 1948-1963.

15. Shearer, C. J.; Cherevan, A.; Eder, D., Application and Future Challenges of Functional Nanocarbon Hybrids. *Adv Mater* **2014,** *26* (15), 2295-2318.

16. Singh, P.; Campidelli, S.; Giordani, S.; Bonifazi, D.; Bianco, A.; Prato, M., Organic functionalisation and characterisation of single-walled carbon nanotubes. *Chem Soc Rev* **2009,** *38* (8), 2214-2230.

17. Yue, Q.; Wang, M. H.; Sun, Z. K.; Wang, C.; Wang, C.; Deng, Y. H.; Zhao, D. Y., A versatile ethanol-mediated polymerization of dopamine for efficient surface modification and the construction of functional core-shell nanostructures. *J Mater Chem B* **2013,** *1* (44), 6085-6093.

18. Song, Y.; Ye, G.; Lu, Y. X.; Chen, J.; Wang, J. C.; Matyjaszewski, K., Surface-Initiated ARGET ATRP of Poly(Glycidyl Methacrylate) from Carbon Nanotubes via Bioinspired Catechol Chemistry for Efficient Adsorption of Uranium Ions. *Acs Macro Lett* **2016,** *5* (3), 382-386.

19. Lee, H.; Dellatore, S. M.; Miller, W. M.; Messersmith, P. B., Mussel-inspired surface chemistry for multifunctional coatings. *Science* **2007,** *318* (5849), 426-430.

20. Fei, B.; Qian, B. T.; Yang, Z. Y.; Wang, R. H.; Liu, W. C.; Mak, C. L.; Xin, J. H., Coating carbon nanotubes by spontaneous oxidative polymerization of dopamine. *Carbon* **2008,** *46* (13), 1795-1797.

21. Liu, Y. L.; Ai, K. L.; Lu, L. H., Polydopamine and Its Derivative Materials: Synthesis and Promising Applications in Energy, Environmental, and Biomedical Fields. *Chem Rev* **2014,** *114* (9), 5057-5115.

22. Liu, C. M.; Cao, H. B.; Li, Y. P.; Xu, H. B.; Zhang, Y., The effect of electrolytic oxidation on the electrochemical properties of multi-walled carbon nanotubes. *Carbon* **2006,** *44* (14), 2919-2924.

23. Ling, Y.; Li, W. Z.; Wang, B. Y.; Gan, W. J.; Zhu, C. H.; Brady, M. A.; Wang, C., Epoxy resin reinforced with nanothin polydopamine-coated carbon nanotubes: a study of the interfacial polymer layer thickness. *Rsc Adv* **2016,** *6* (37), 31037-31045.

24. Zeng, W. Z.; He, J. W.; Liu, F., Preparation and properties of antibacterial ABS plastics based on polymeric quaternary phosphonium salts antibacterial agents. *Polym Advan Technol* **2019,** *30* (10), 2515-2522.

25. Hernandez, R.; Riu, J.; Rius, F. X., Determination of calcium ion in sap using carbon nanotube-based ion-selective electrodes. *Analyst* **2010,** *135* (8), 1979-1985.

26. Das, D.; Nag, S.; Datta, D., Chemistry of the binary mixture of 1,10-phenanthroline and zinc perchlorate hexahydrate in methanol and gas phase. Monohydroxo species and tricoordination of zinc and water clusters. *Inorg Chim Acta* **2009,** *362* (8), 2890-2894.

27. Roh, J.; Karabanovich, G.; Novakova, V.; Šimůnek, T.; Vávrová, K., Large-scale synthesis of piperazine-2, 6-dione and its use in the synthesis of dexrazoxane analogues. *Synthesis* **2016,** *48* (24), 4580-4588.

AFTERWORD

This dissertation included both a novel method for a one-pot green transformation of carbonyls to mixed carbonates and the beginning of a polymer-derived supramolecular coordination research program and the potential applications.

Carbonates represent a commonly utilized protecting group and essential building block in organic synthesis. While the investigated transformation required reflux temperatures to reach substantial amounts of product at a reasonable time (6h), the celerity of the functionalization and the simplicity of the work-up allowed for numerous substrates to be sampled. Further investigations of these reactions may include other methods, including solid-supported borohydrides or microwave assistance, other carbonate solvents, and different functional groups (i.e., imines). Perhaps the development of green Lewis acids may help lower the activation energy needed for the carbonates to react and allow for lower temperatures and more delicate substrates.

The second 2/3 of this dissertation was dedicated to a NASA funded project on the integration of polymer-based calcium ion sensors for potential incorporation with conductive ink technologies to make an array of electrode sensors on a flexible substrate. For this project, we chose commercially available CNT ink as our inkjet printing collaborators were very familiar with this product. We found that the ink was very compatible with calcium ion membranes when added directly to the CNT ink drop cast. The print design, when printed with over 30 layers of CNT ink on Kapton, gave reliable impedance measurements and were compatible with the ionophore membranes yet with less sensitivity. This was most likely due to the non-uniformity in the jet printing process. In the future, hopefully, a variety of inks or

larger droplet sizes of ink cartridges will be recommended as the 60 layers of ink still showed inconsistencies in the prints.

In the original proposal to NASA, we suggested the use of polymer brushes as potential calcium ion sensors, grown from the surface of the flexible electrode. There were two instances where this proposed idea seemed less feasible. Firstly, attempts to oxidize the Kapton surface as easily as we oxidized the silicon wafer and glass slide for attachment of the initiators were unsuccessful. Secondly, the calcium ionophore cocktail, needing a quantitative amount of plasticizer to allow for the binding agent to hold onto the solid contact ISE for it to be functional, was not compatible with the aqueous conductive inks. Therefore the option to build our calcium ion-sensitive monomer, test its selectivity and sensitivity to calcium, and then either attach the monomer directly to the conductive ink or mix with the ion-selective membrane as a copolymer was much more attractive. By switching iminodiacetic acid for diglycolic acid, we quickly created our nitrogen analog, and, with the addition of 3-bromopropyl methacrylate, our monomer. Crystallization with calcium produced coordinating complexes, and the sensitivity in an electrochemical cell was agreeable. Unfortunately, the iminobis(acetamide) was not as selective for calcium; it is sensitive to Zn^{2+} and NH_4^+ as well. While this was not as favorable a result as we expected, we were still able to characterize the calcium sensitivity and grow a copolymer of our monomer with poly(methyl methacrylate) at various concentrations. The polymers created are low molecular weight blends yet represent a potential substitute for the non-compatible PVC and PMMA:PtBMA mixes that serve as binding agents in ISEs. The research group will continue to explore these polymers for further applications such as metal coordination studies for water purification or further sensing entities.

Appendix I

^{1}H and ^{13}C NMR Spectra

Chapter 1

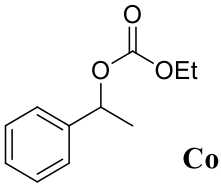

Compound 1-3

^{1}H NMR spectrum ($CDCl_3$, 500 MHz)

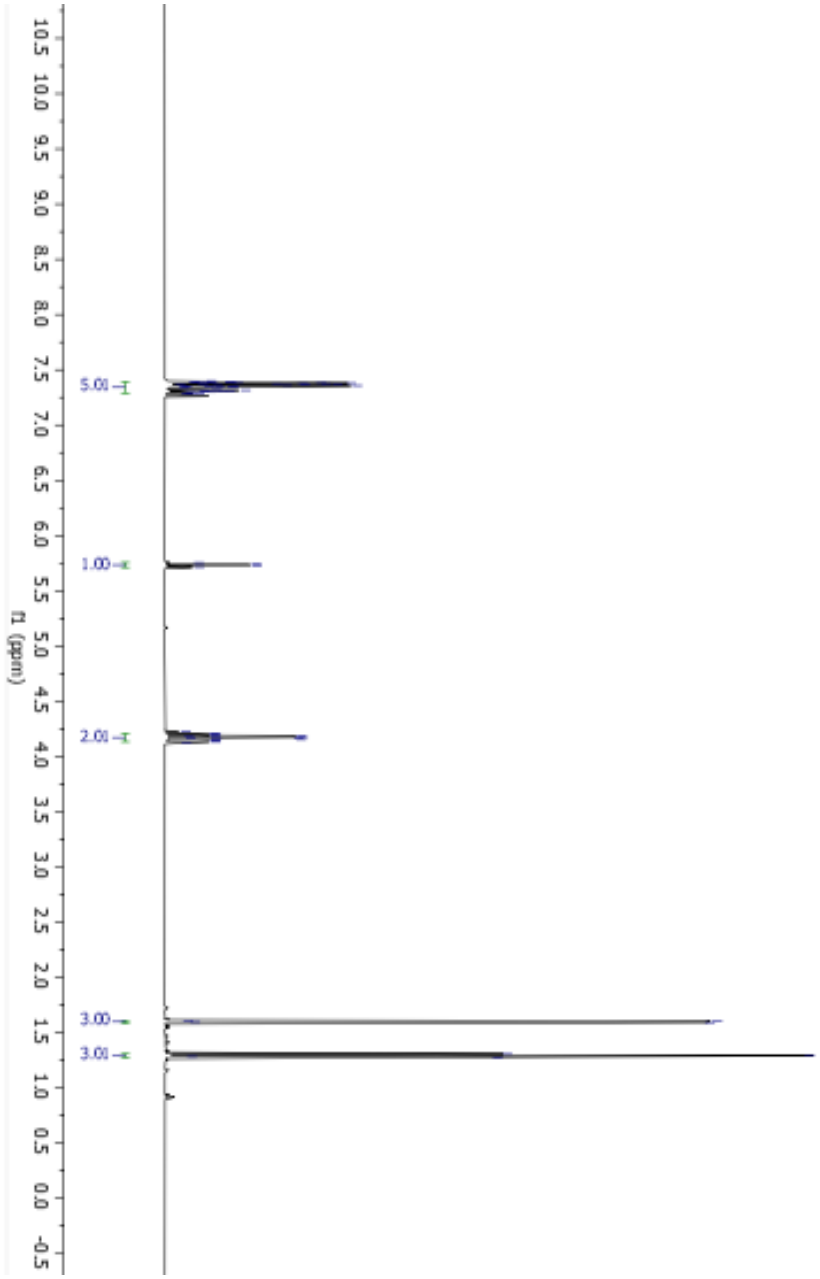

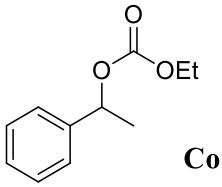

Compound 1-3

^{13}C NMR spectrum ($CDCl_3$, 500 MHz)

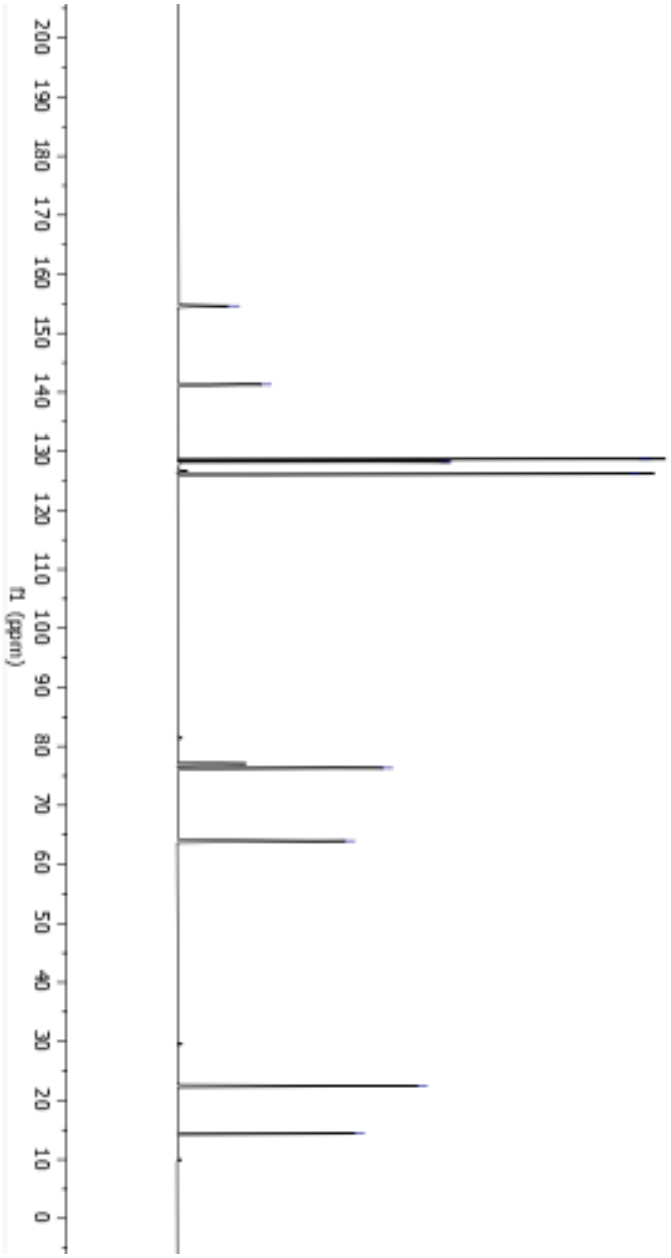

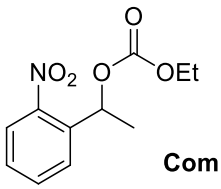

Compound 1-4

^{1}H NMR spectrum ($CDCl_3$, 500 MHz)

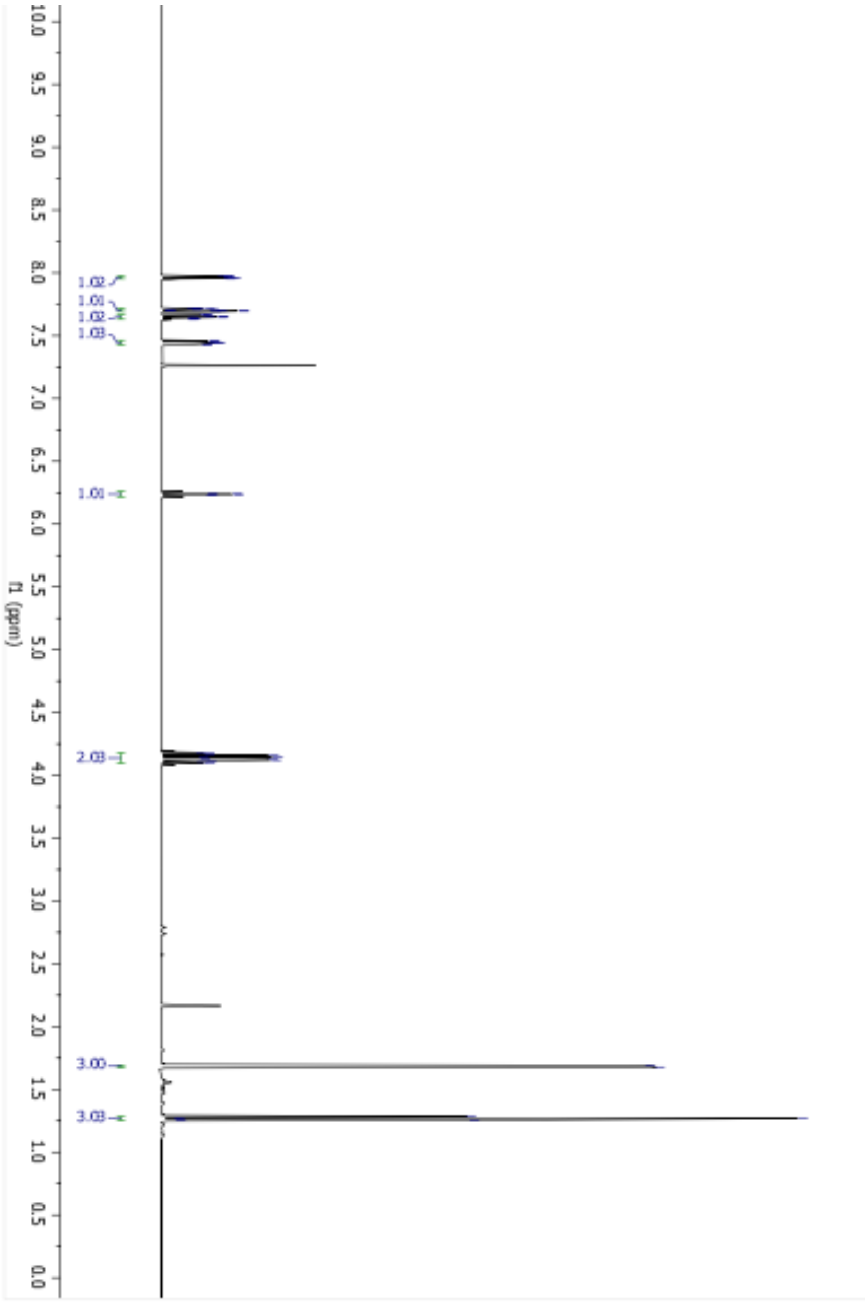

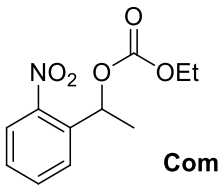

Compound 1-4

^{13}C NMR spectrum ($CDCl_3$, 500 MHz)

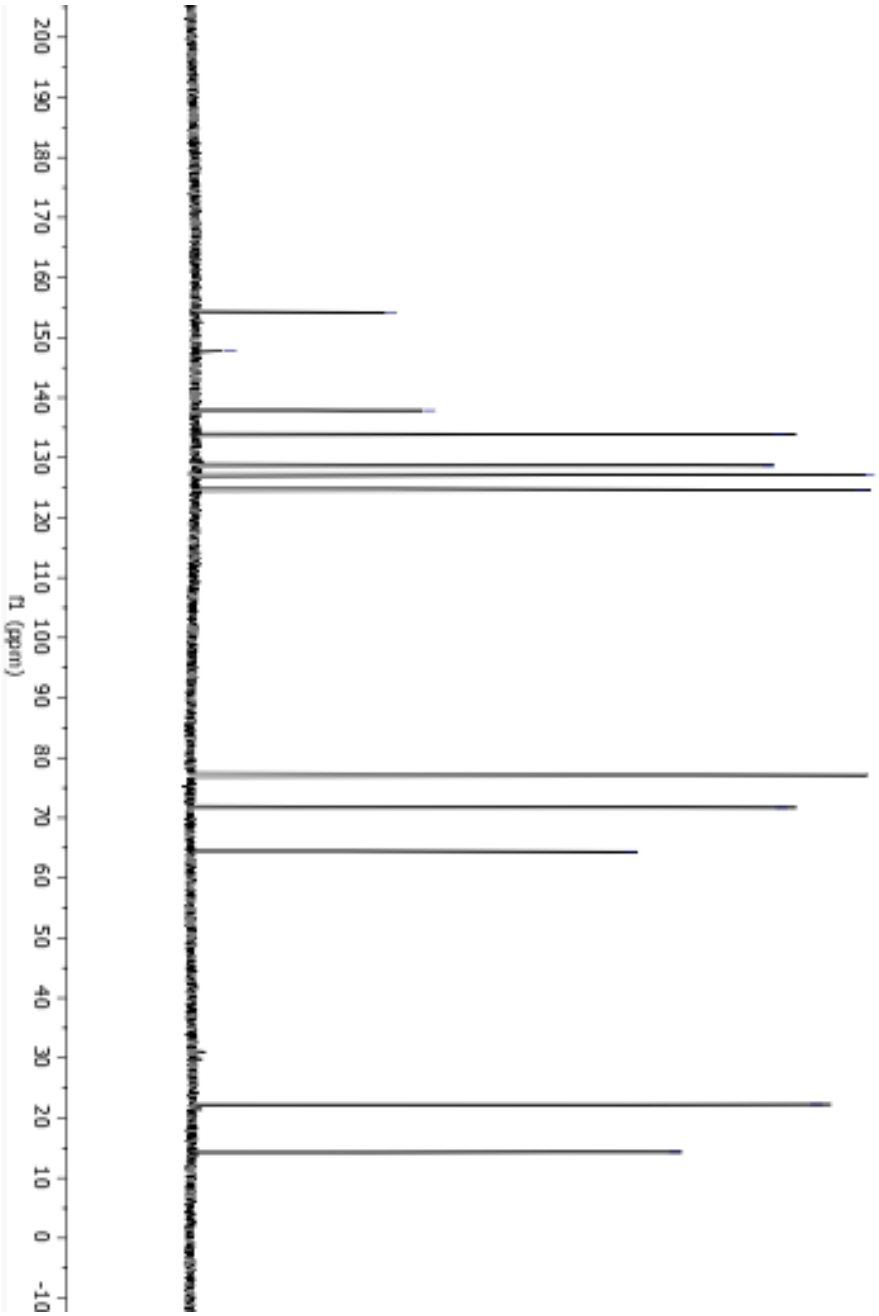

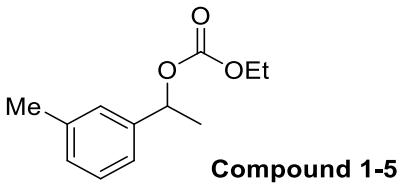

Compound 1-5

^{1}H NMR spectrum ($CDCl_3$, 500 MHz)

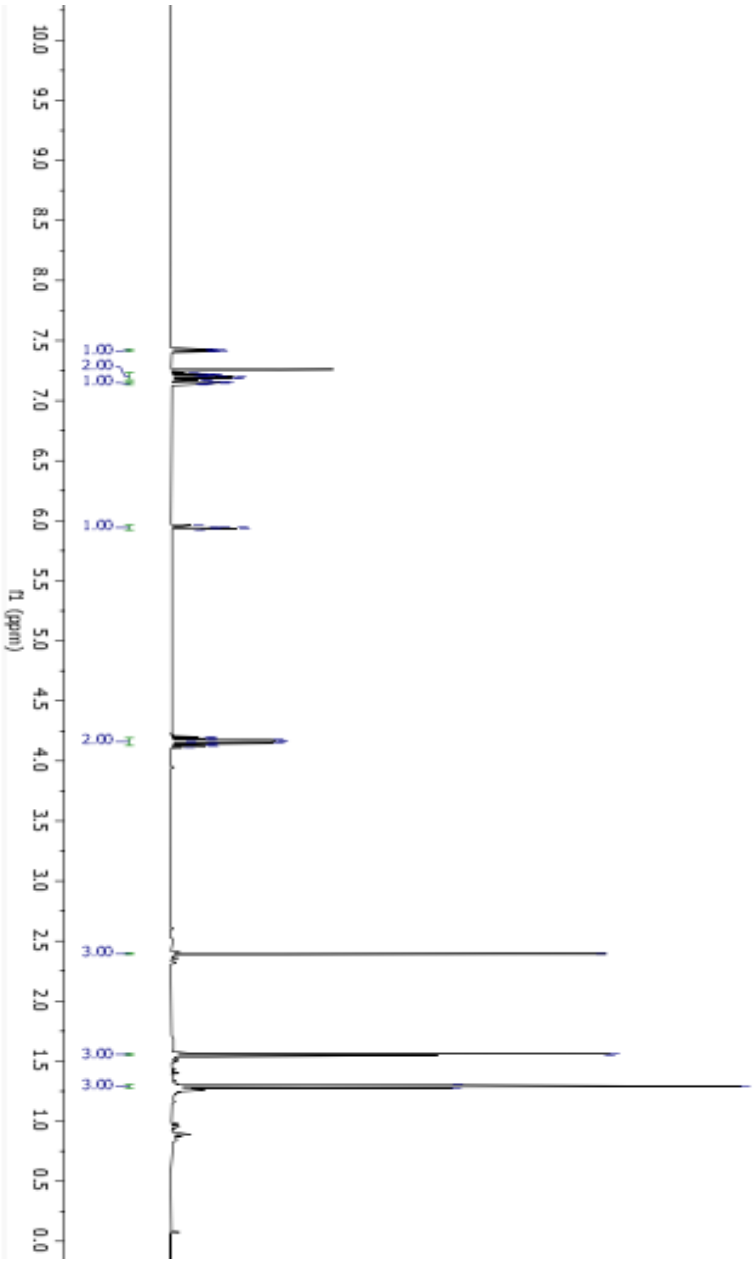

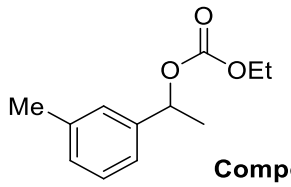

Compound 1-5

^{13}C NMR spectrum ($CDCl_3$, 500 MHz)

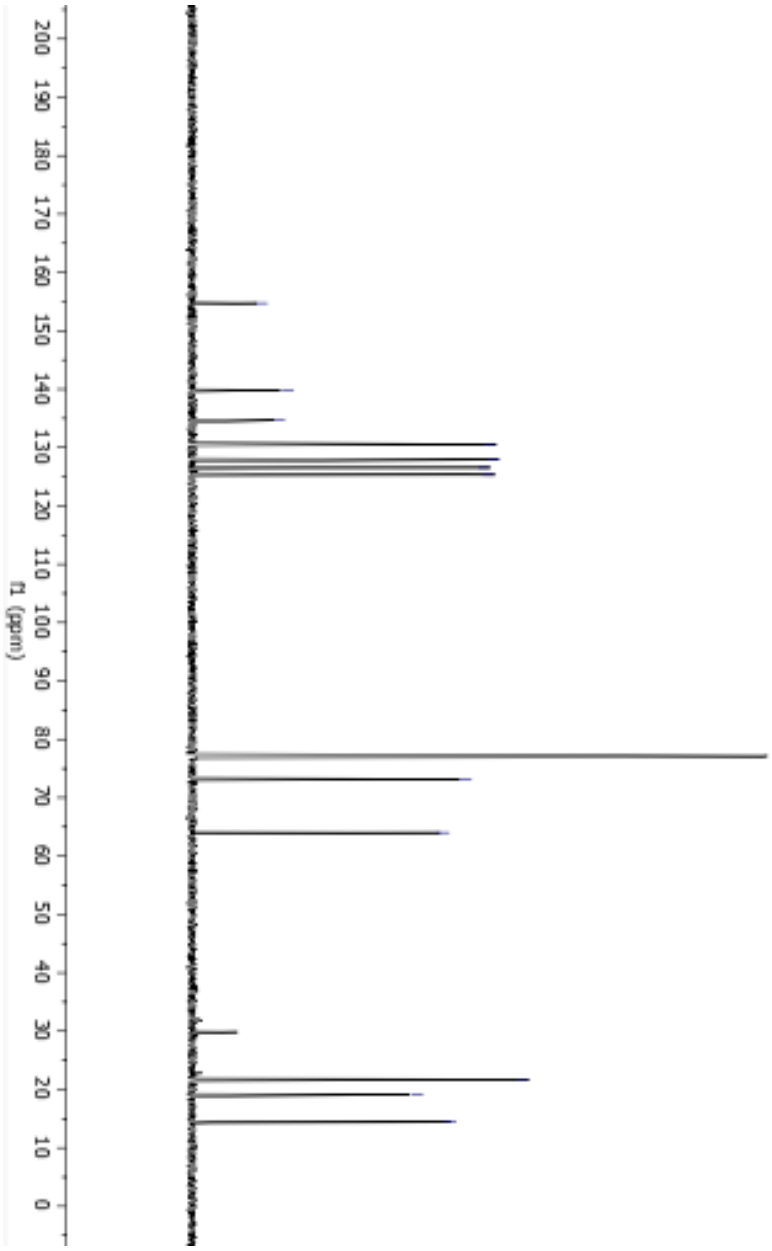

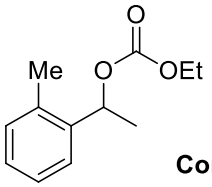

Compound 1-6

^{1}H NMR spectrum ($CDCl_3$, 500 MHz)

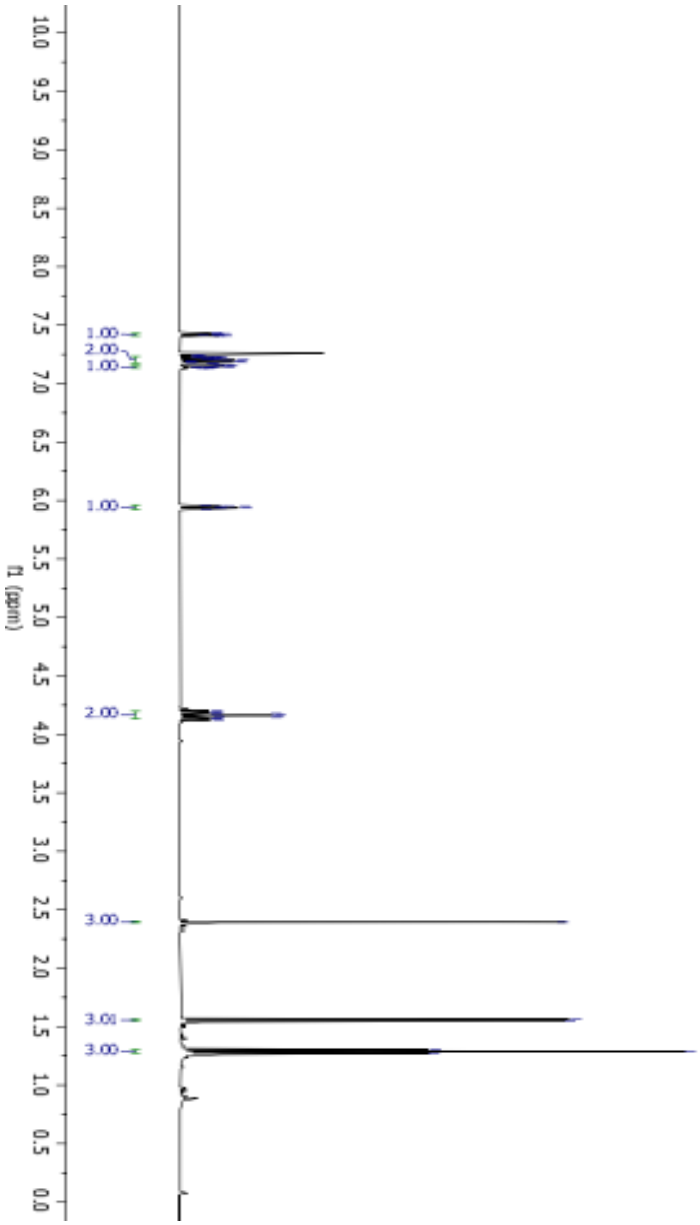

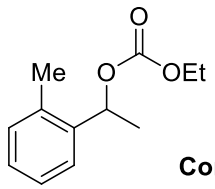

Compound 1-6

^{13}C NMR spectrum ($CDCl_3$, 500 MHz)

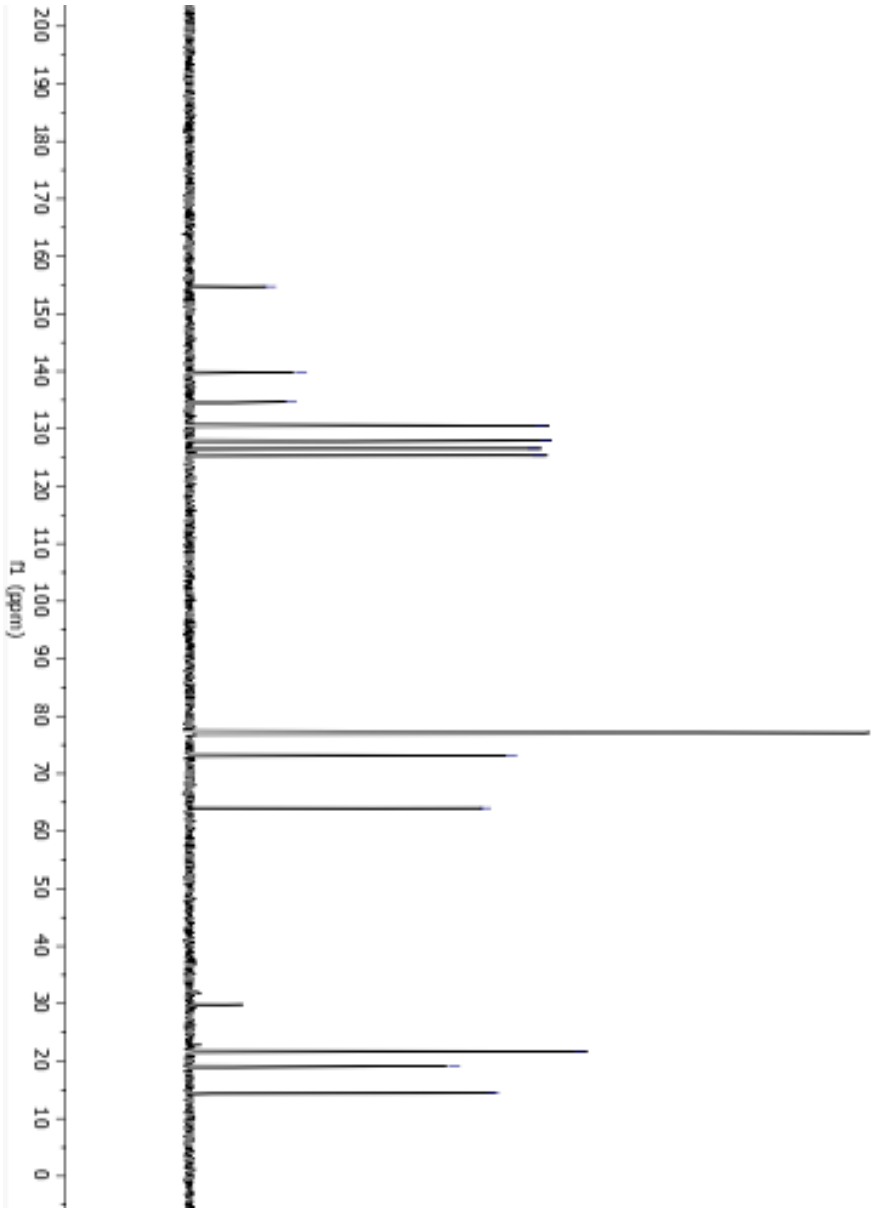

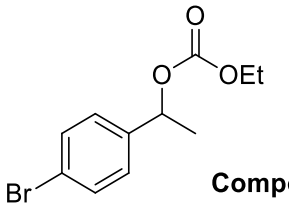

Compound 1-7

^{1}H NMR spectrum ($CDCl_3$, 500 MHz)

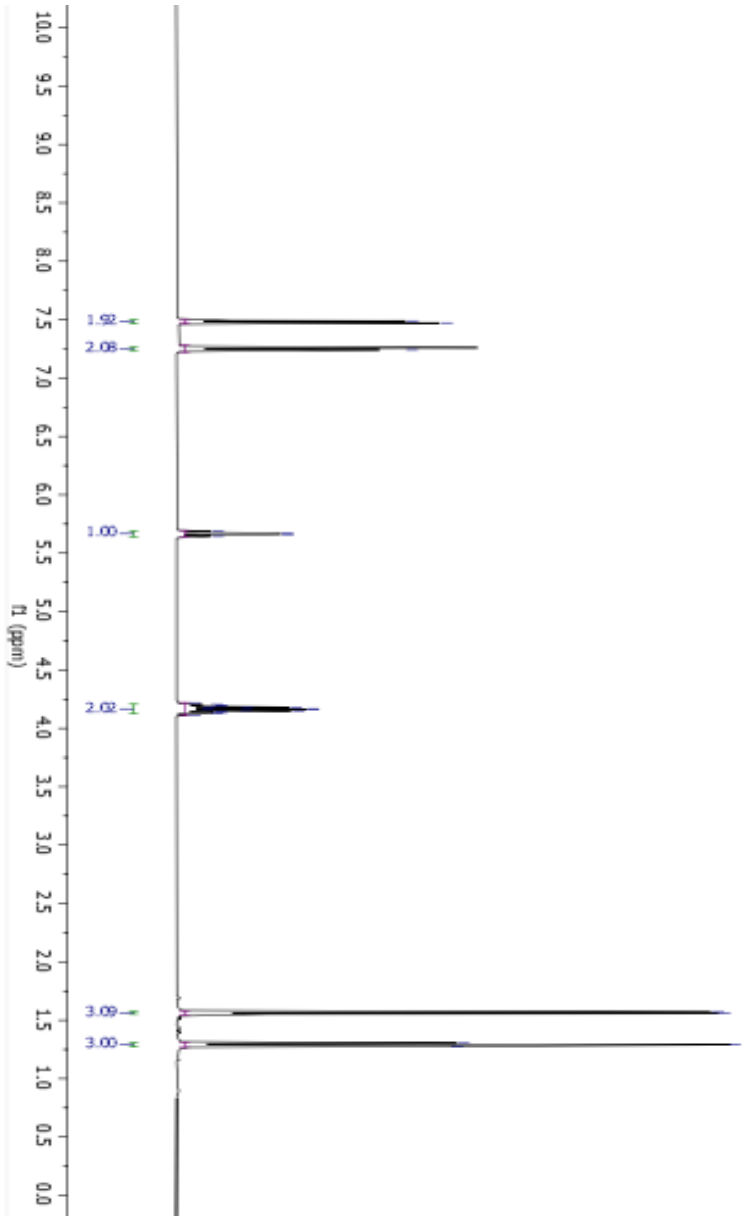

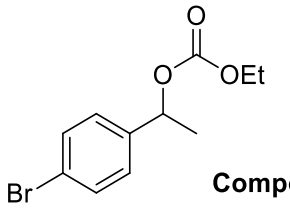

Compound 1-7

^{13}C NMR spectrum ($CDCl_3$, 500 MHz)

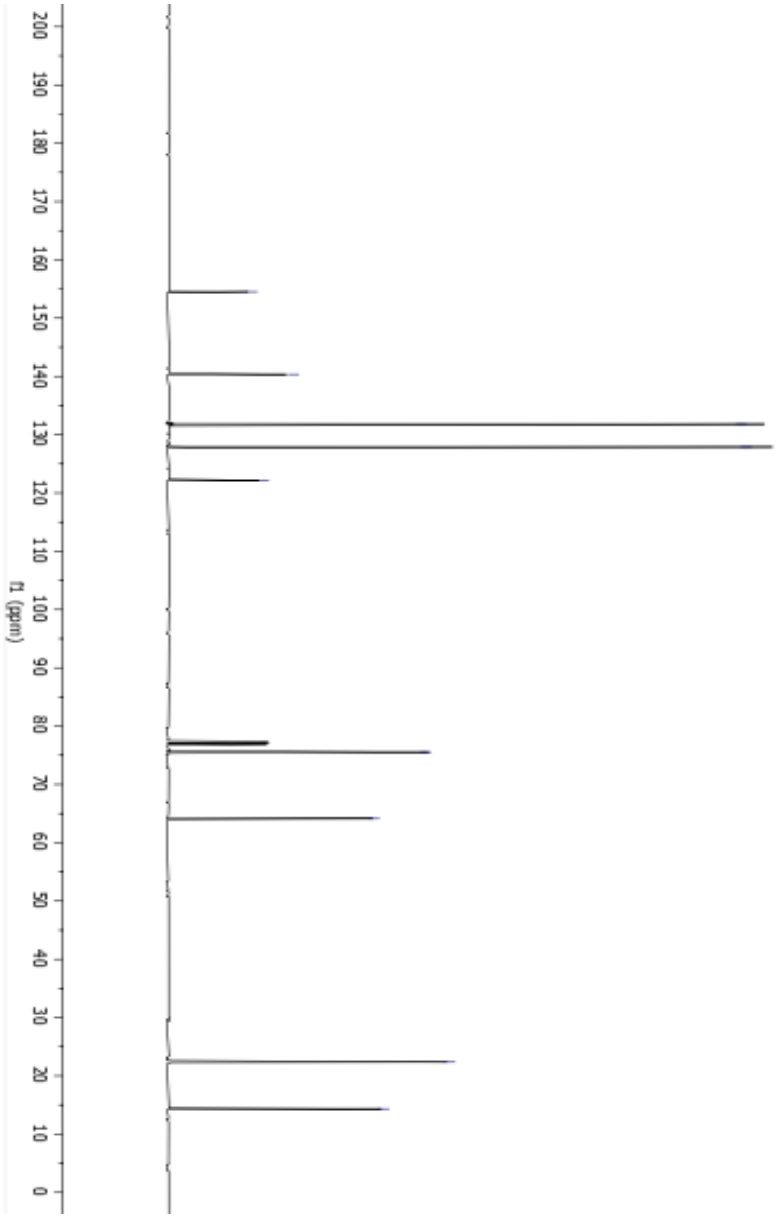

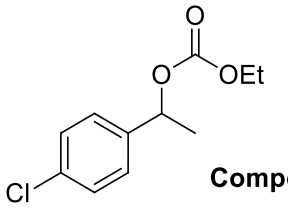

Compound 1-8

^{1}H NMR spectrum ($CDCl_3$, 500 MHz)

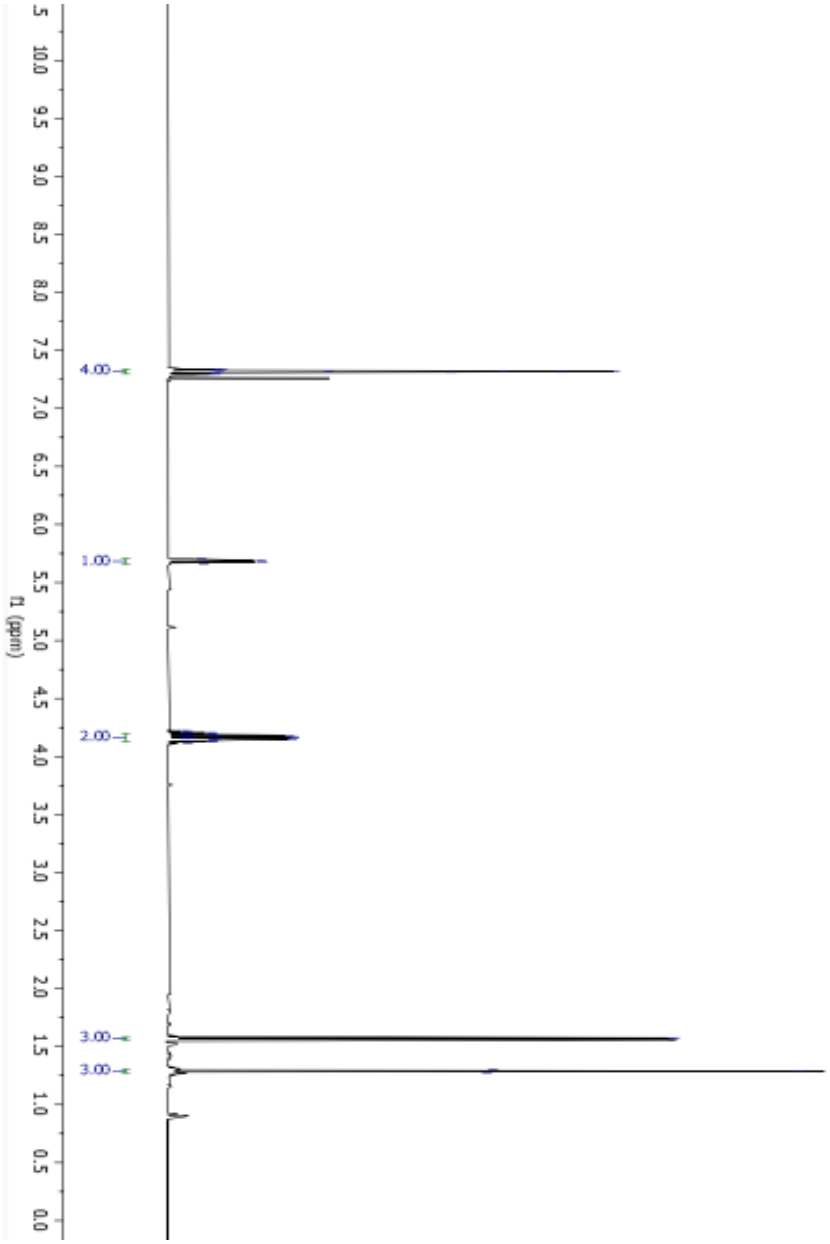

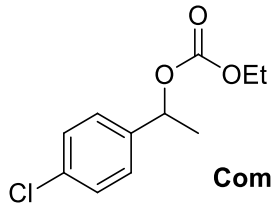

Compound 1-8

^{13}C NMR spectrum ($CDCl_3$, 500 MHz)

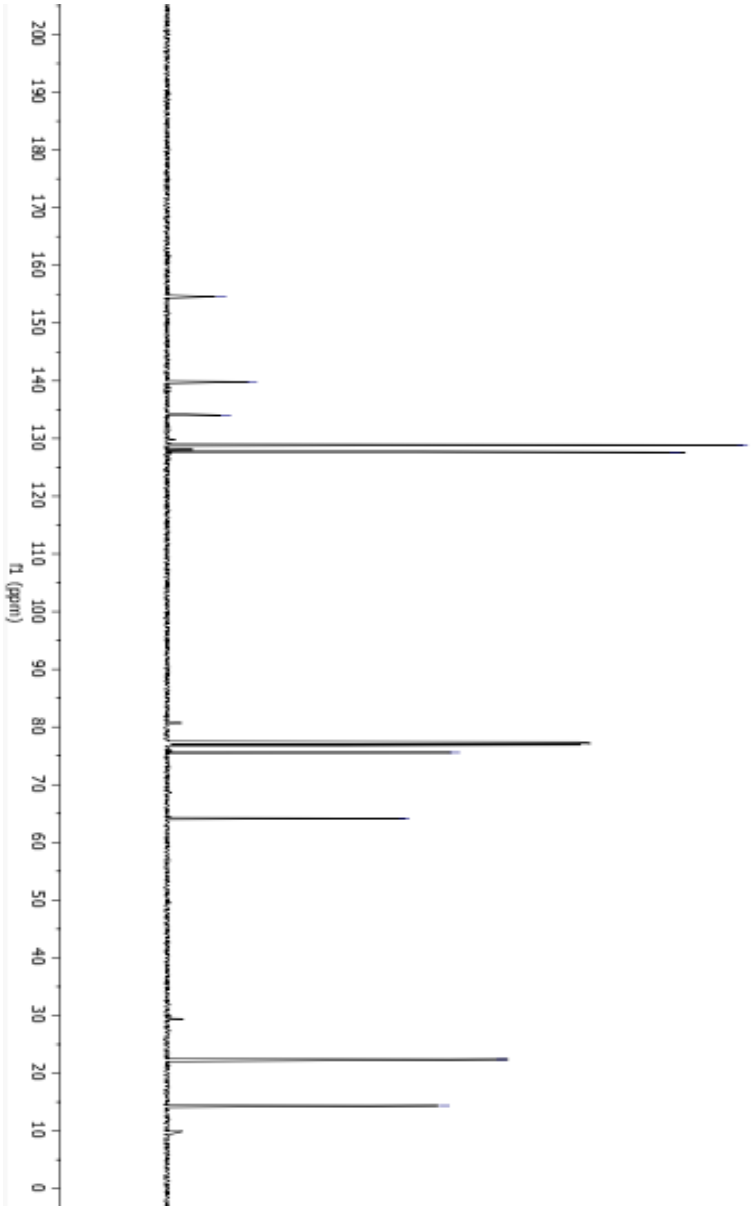

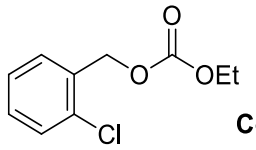

Compound 1-9

^{1}H NMR spectrum ($CDCl_3$, 500 MHz)

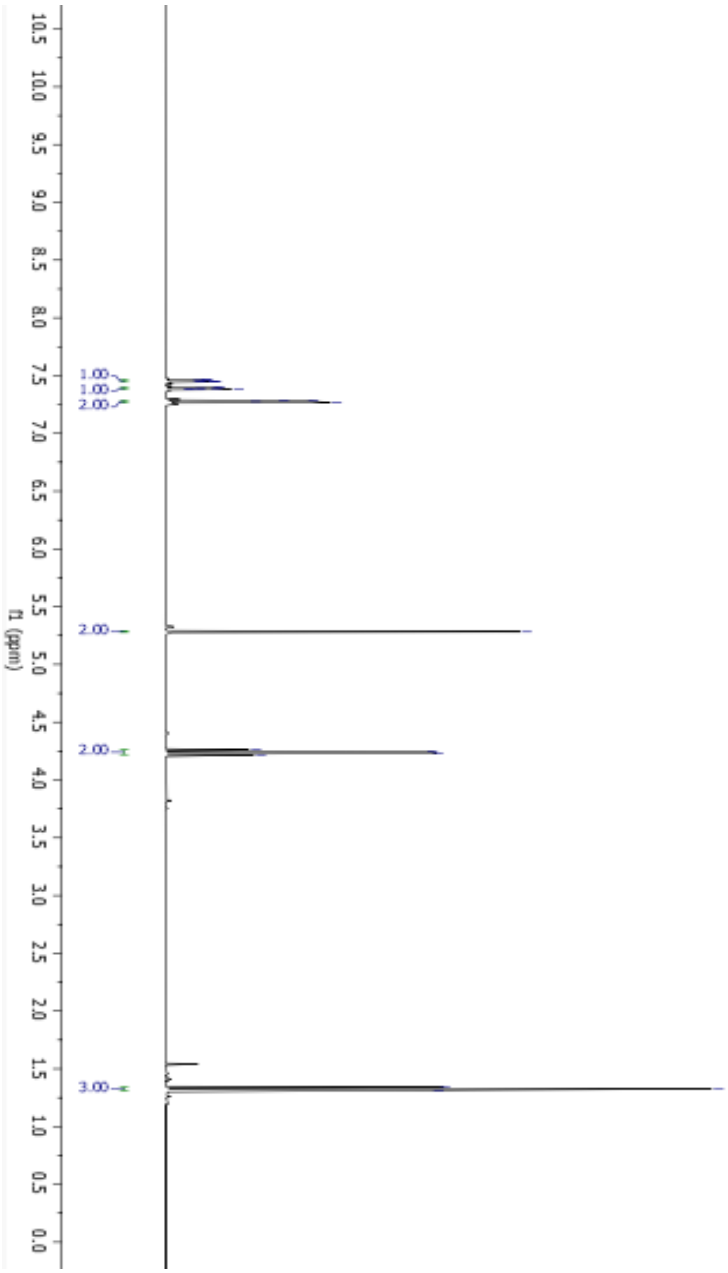

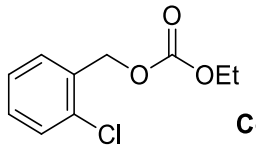

Compound 1-9

^{13}C NMR spectrum ($CDCl_3$, 500 MHz)

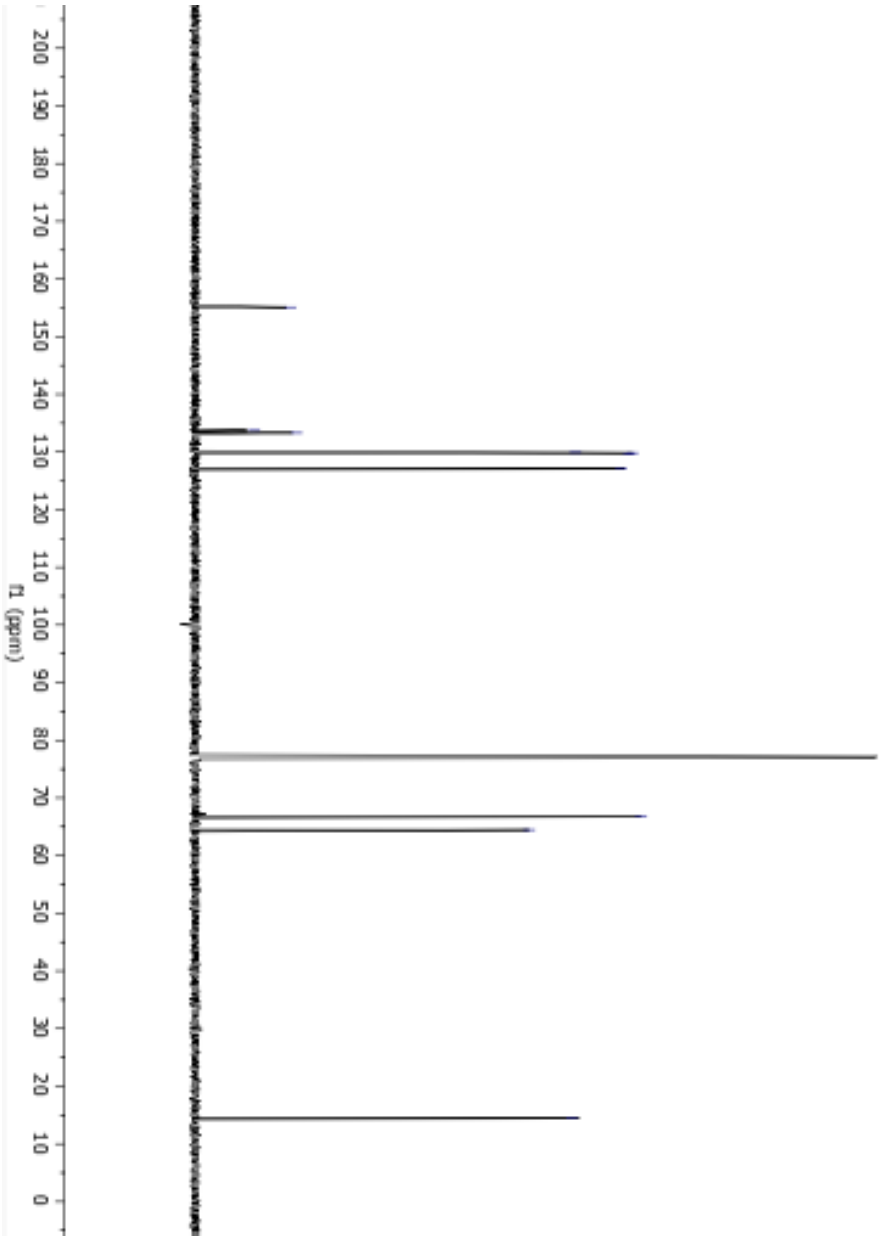

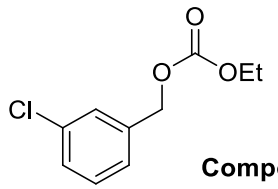

Compound 1-10

^{1}H NMR spectrum ($CDCl_3$, 500 MHz)

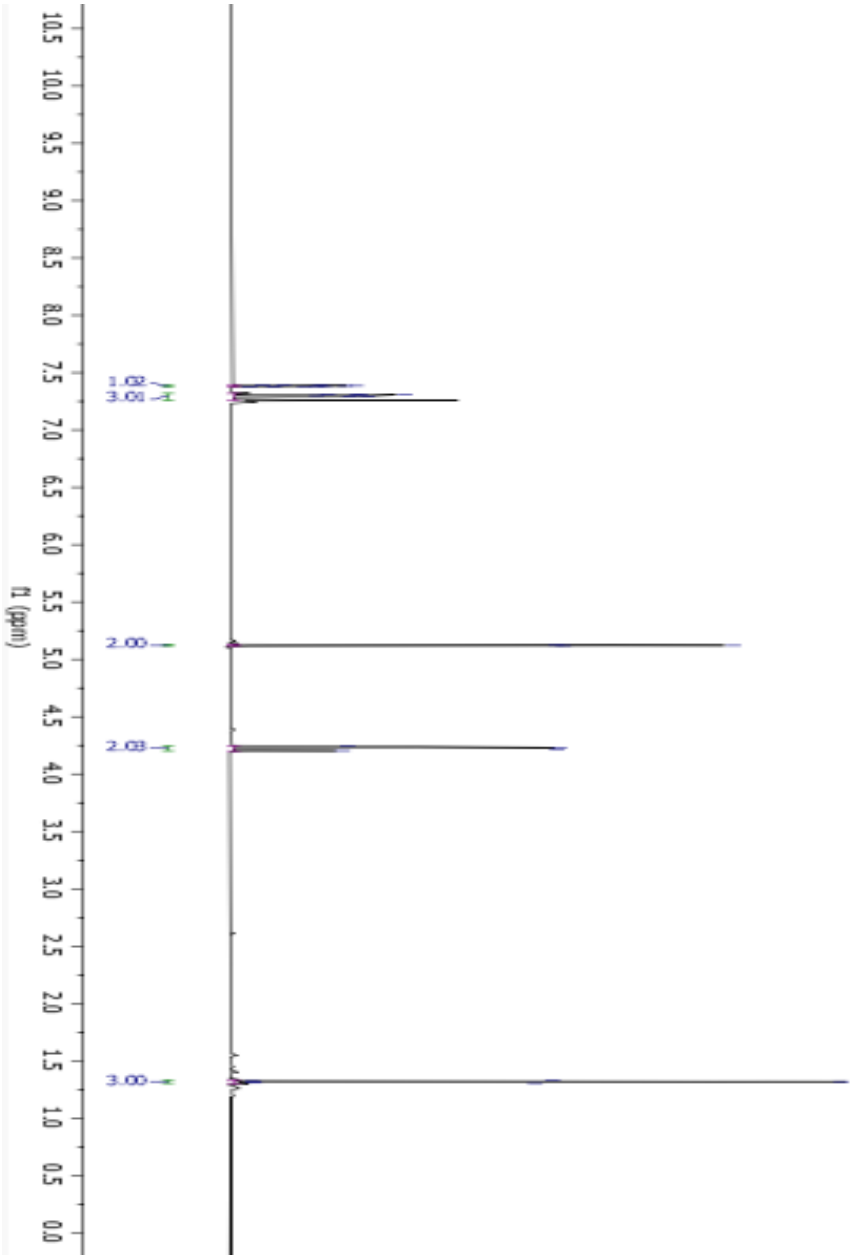

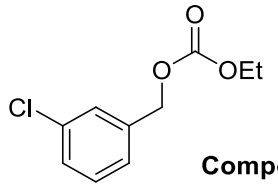

Compound 1-10

^{13}C NMR spectrum ($CDCl_3$, 500 MHz)

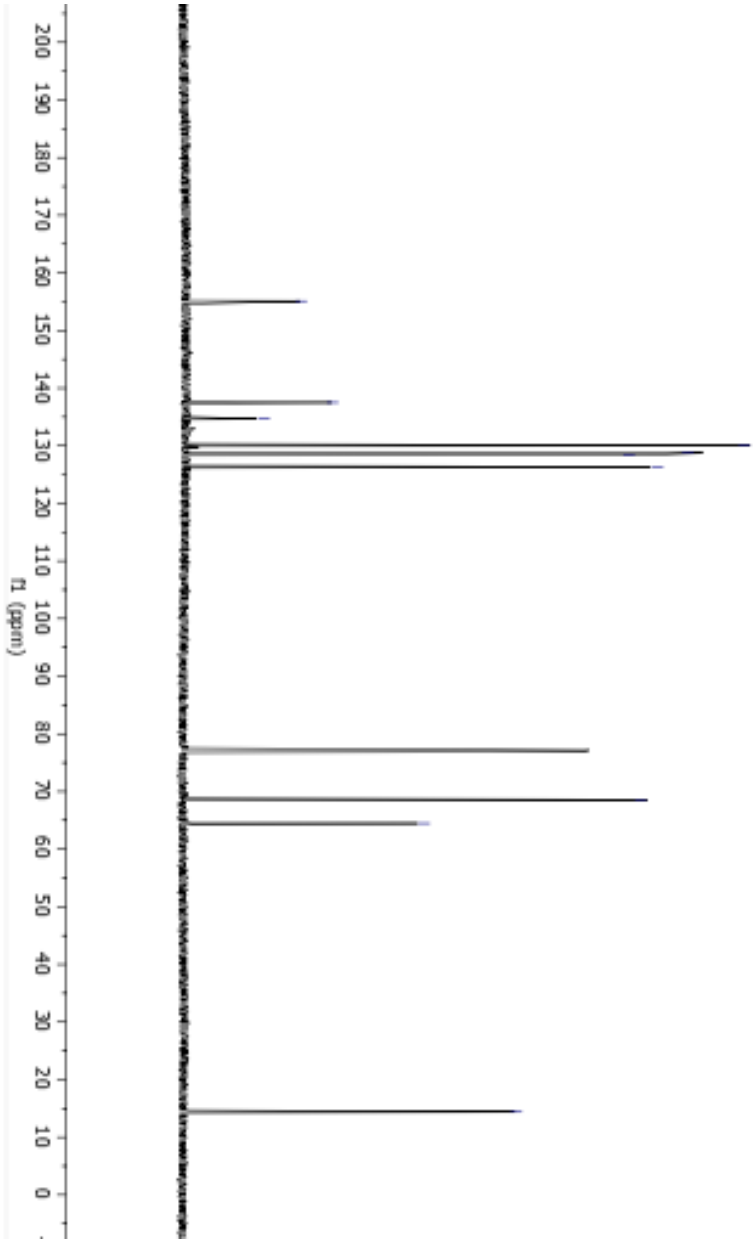

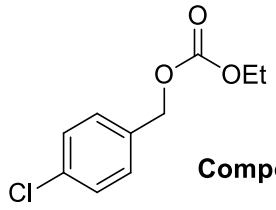

Compound 1-11

^{1}H NMR spectrum ($CDCl_3$, 500 MHz)

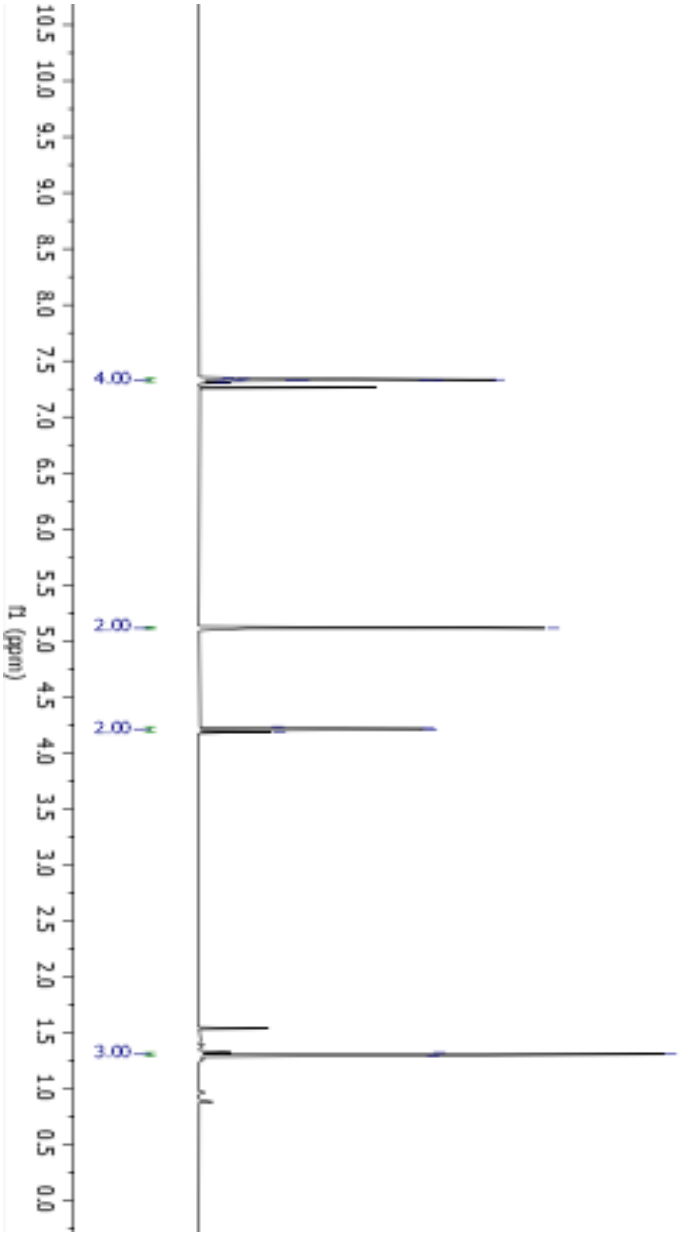

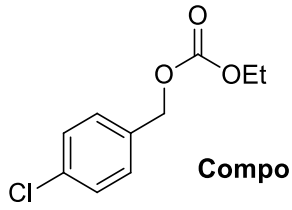

Compound 1-11

^{13}C NMR spectrum ($CDCl_3$, 500 MHz)

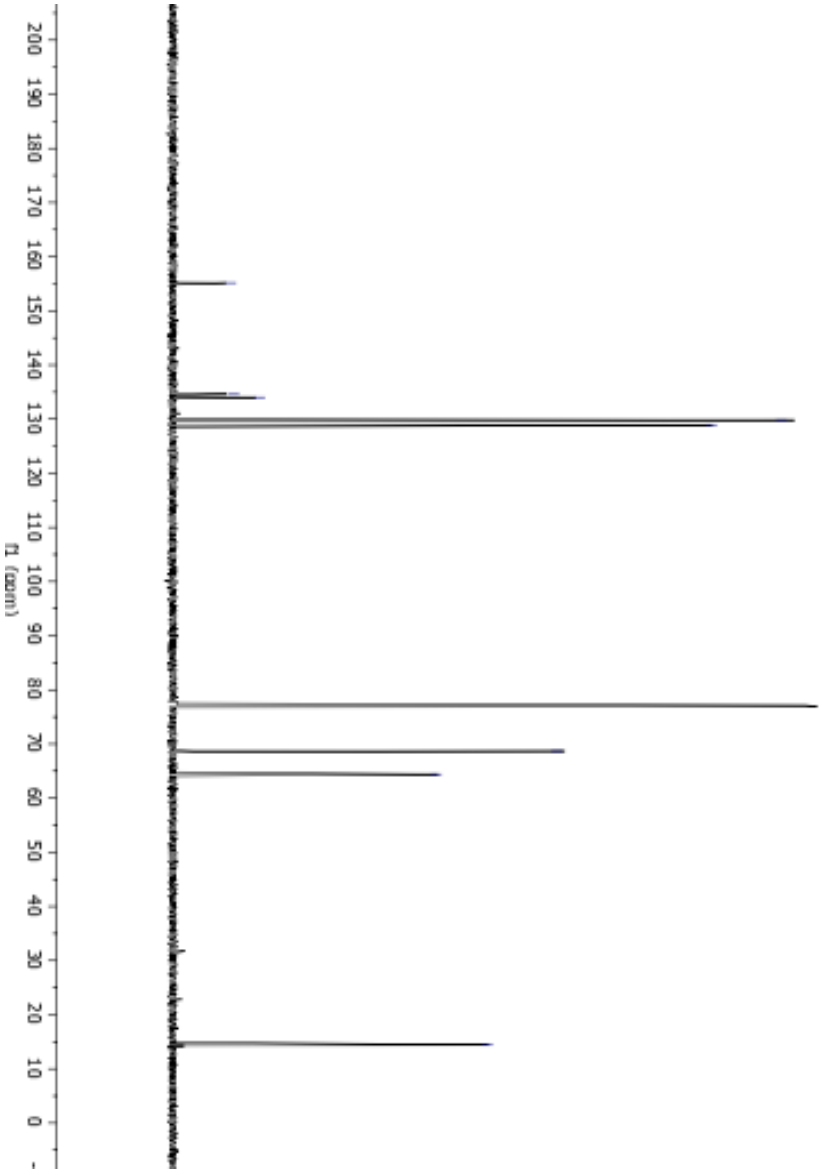

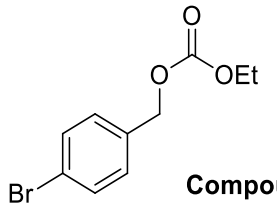

Compound 1-12

^{1}H NMR spectrum ($CDCl_3$, 500 MHz)

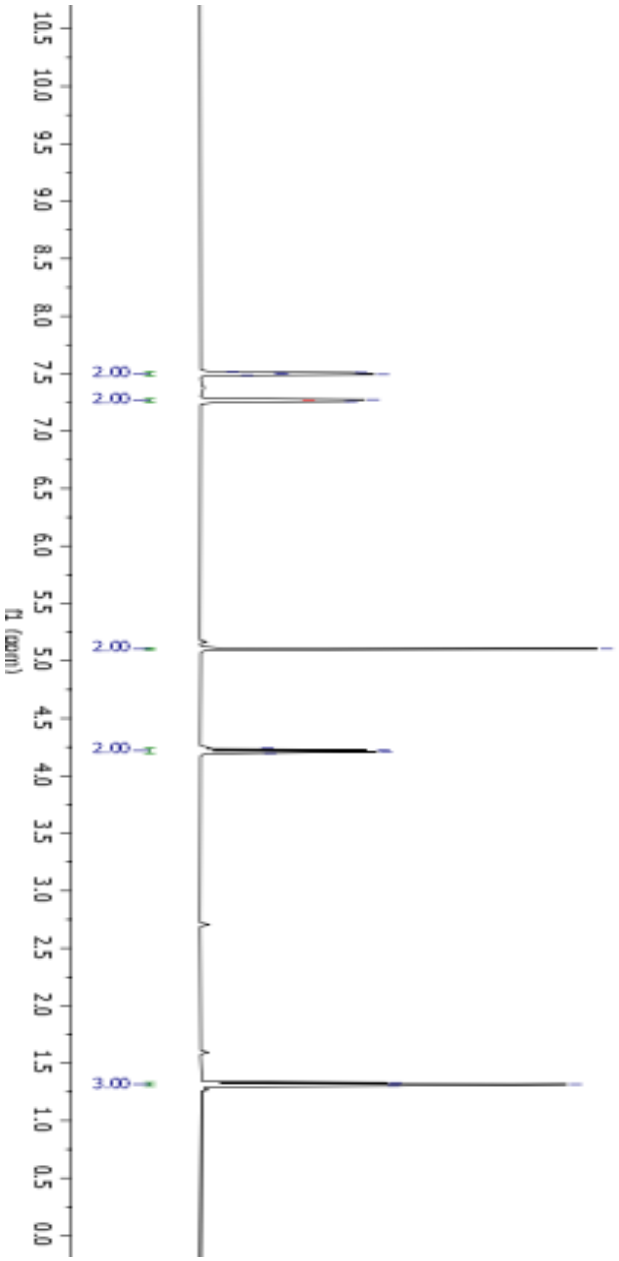

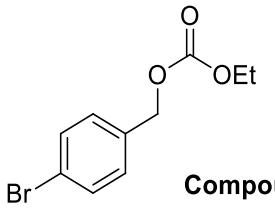

Compound 1-12

^{13}C NMR spectrum ($CDCl_3$, 500 MHz)

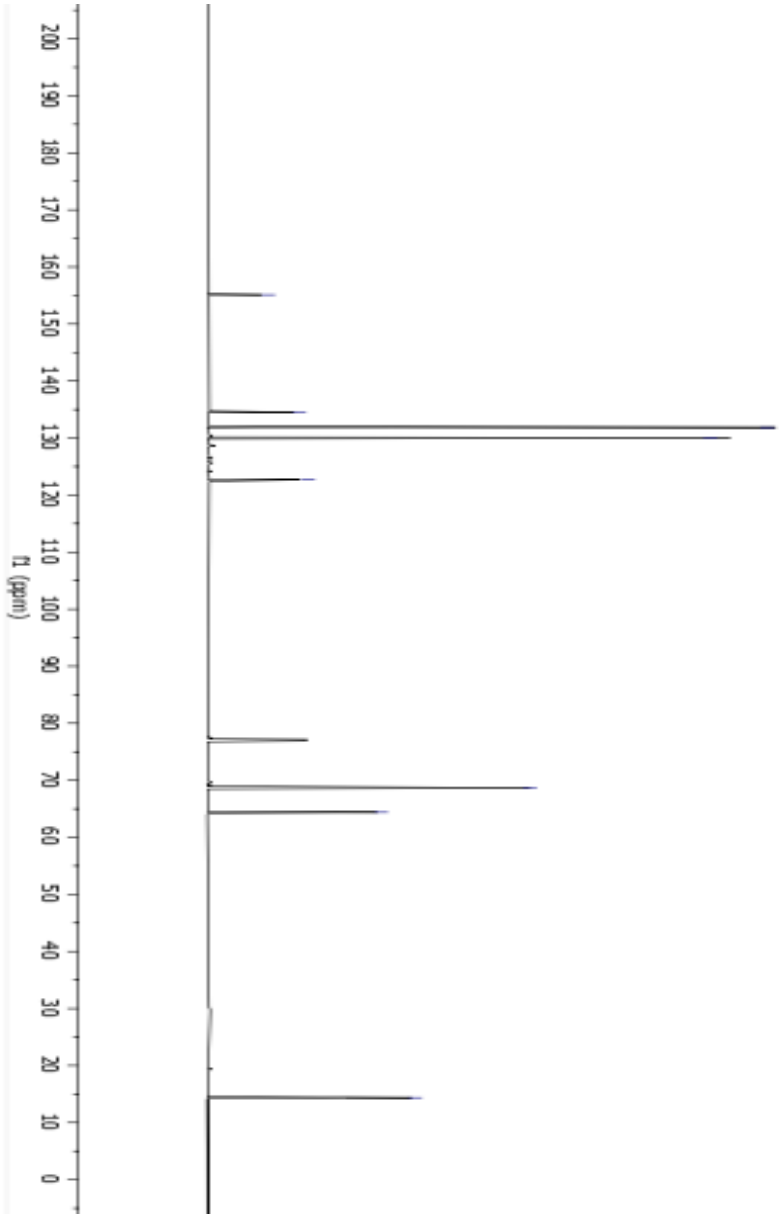

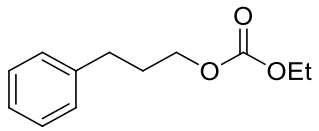

Compound 1-13

^{1}H NMR spectrum ($CDCl_3$, 500 MHz)

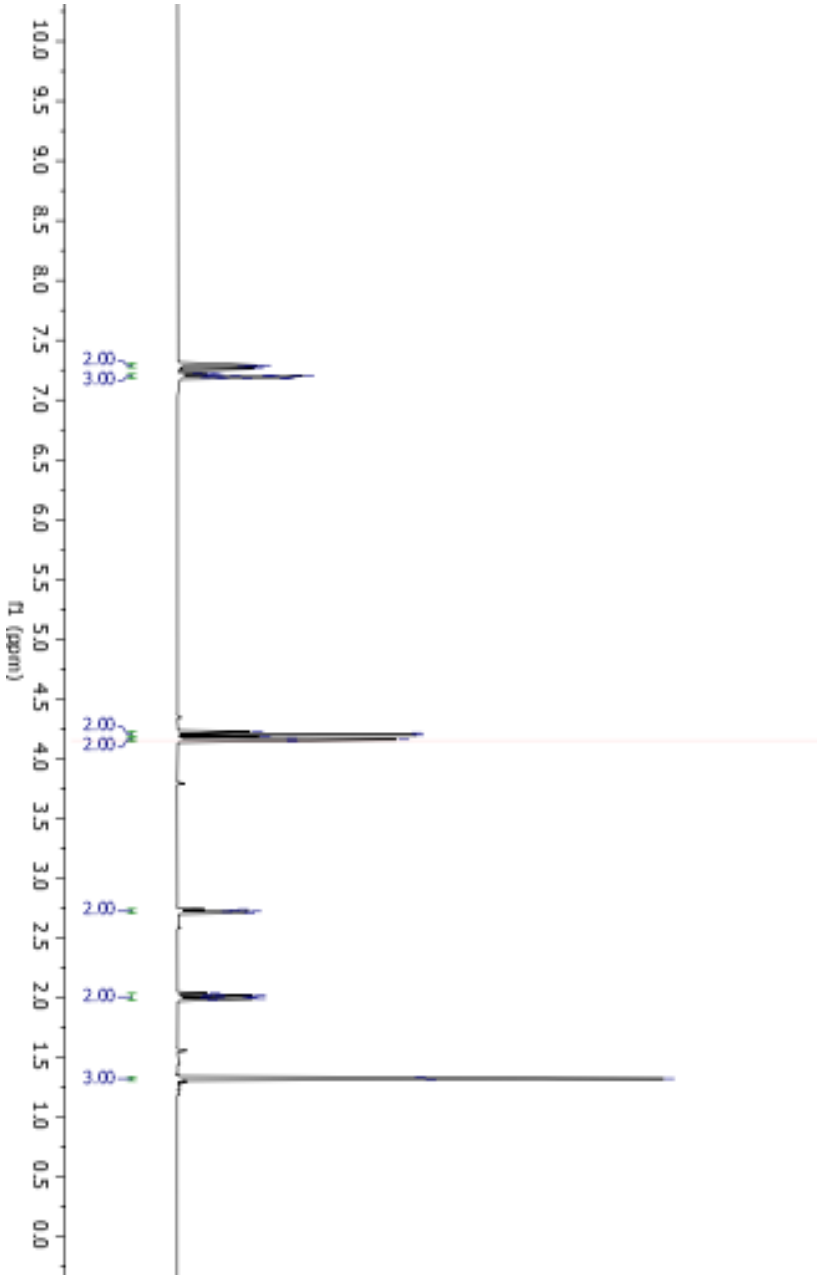

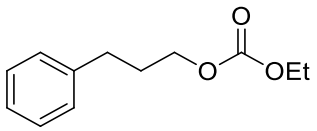

Compound 1-13

^{13}C NMR spectrum ($CDCl_3$, 500 MHz)

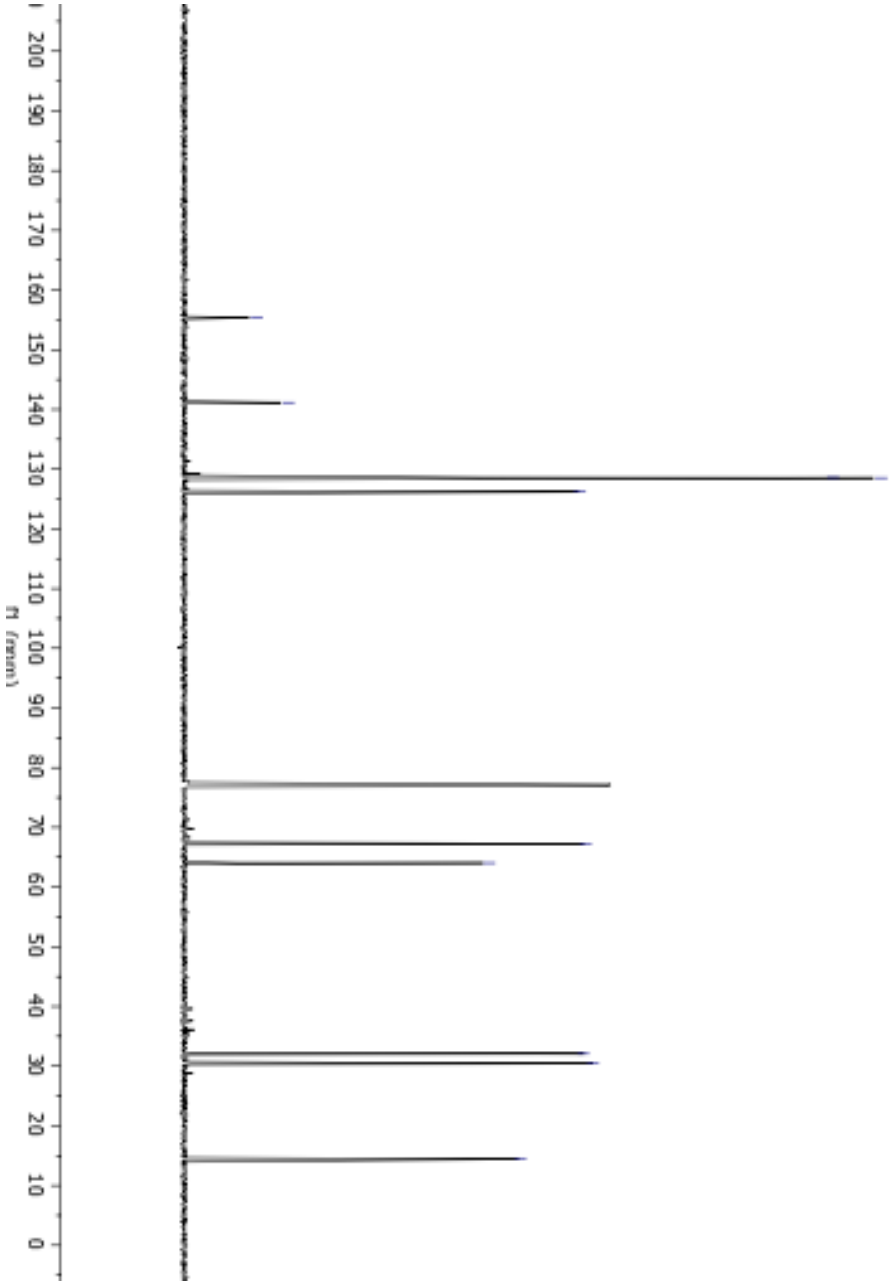

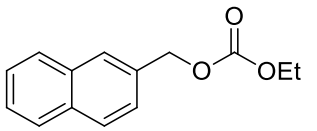

Compound 1-14

^{1}H NMR spectrum ($CDCl_3$, 500 MHz)

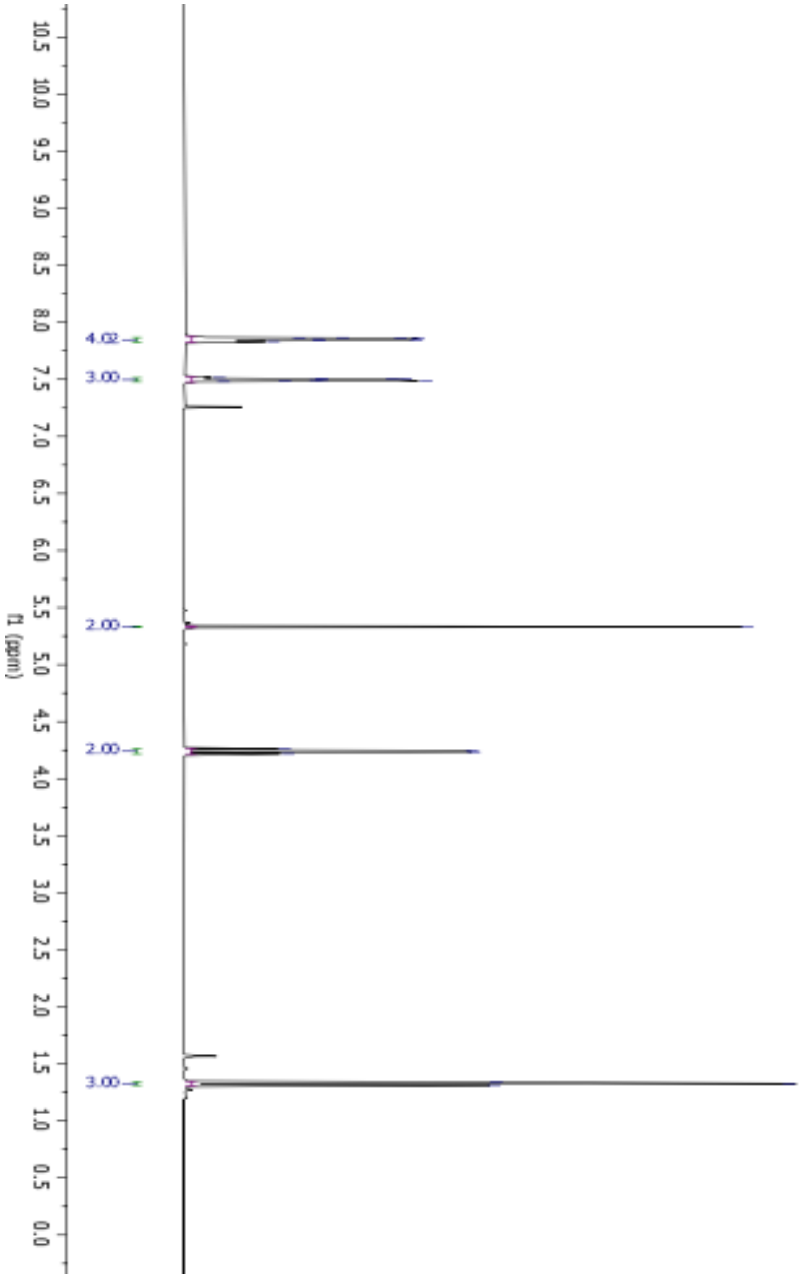

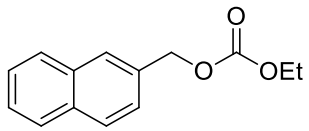

Compound 1-14

^{13}C NMR spectrum ($CDCl_3$, 500 MHz)

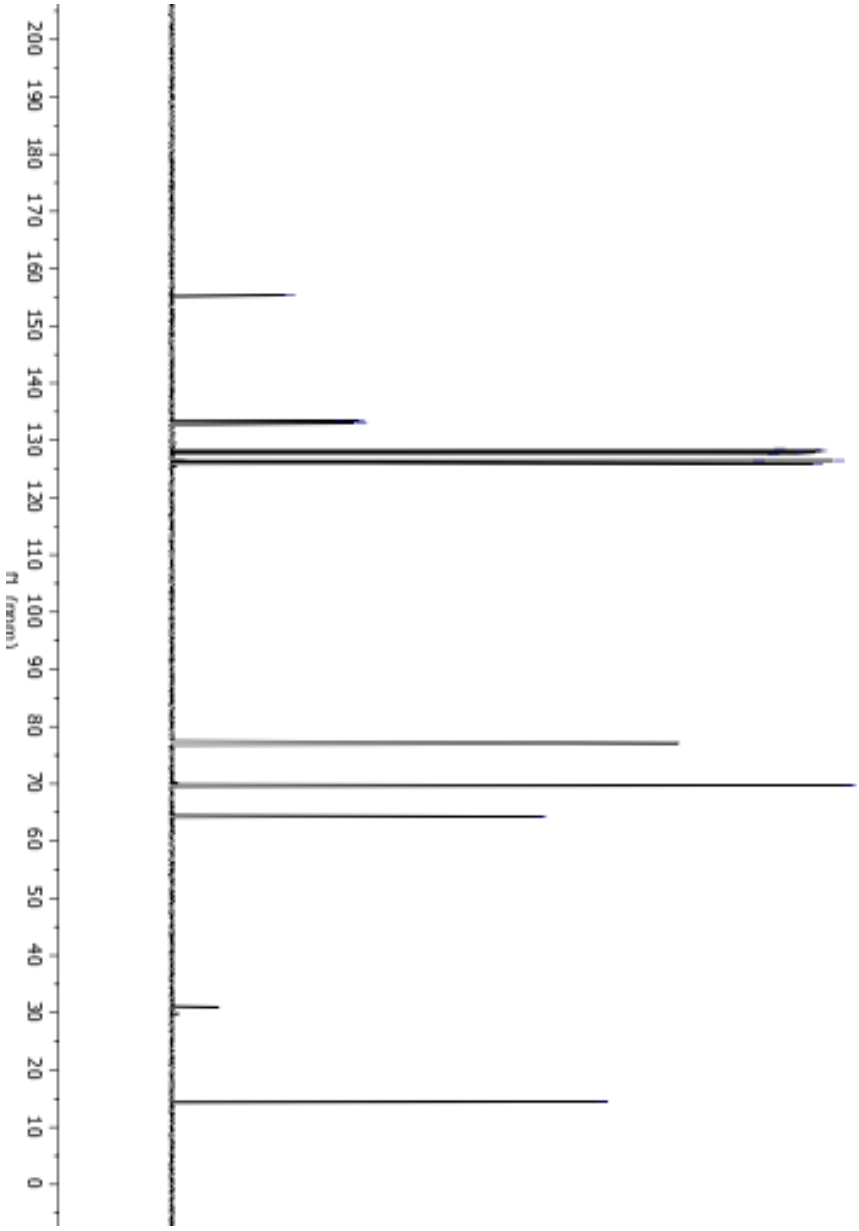

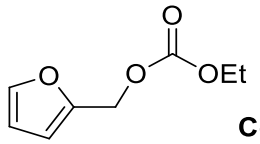

Comound 1-15

^{1}H NMR spectrum ($CDCl_3$, 500 MHz)

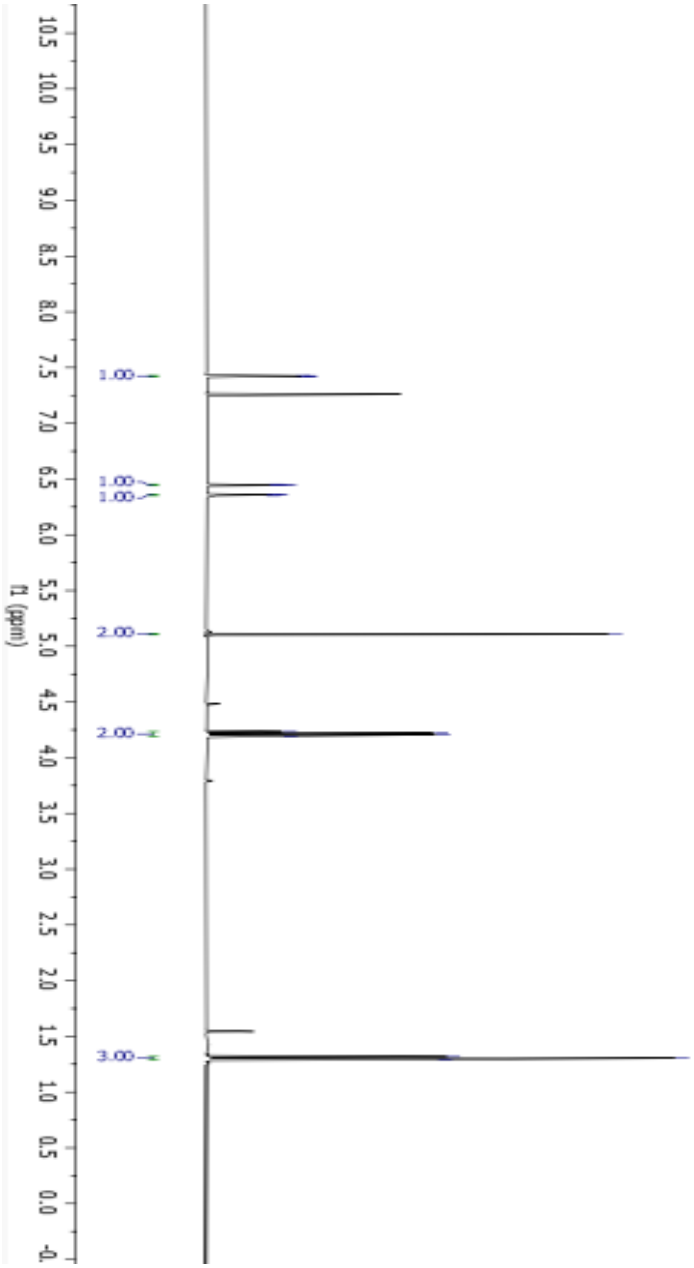

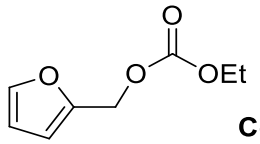

Comound 1-15

^{13}C NMR spectrum ($CDCl_3$, 500 MHz)

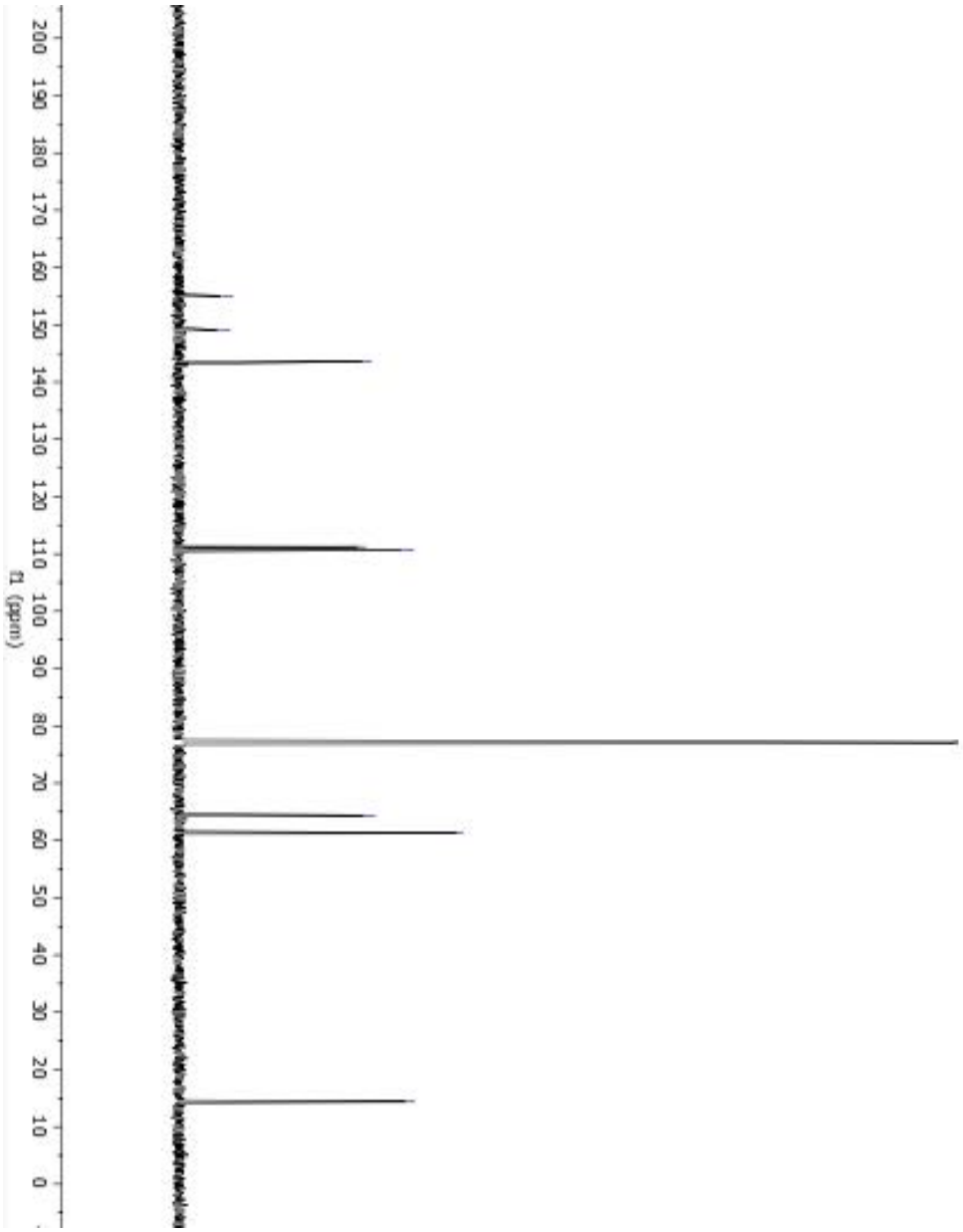

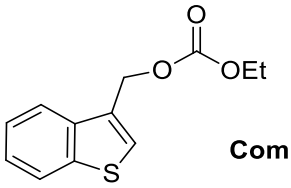

Compound 1-16

^{1}H NMR spectrum ($CDCl_3$, 500 MHz)

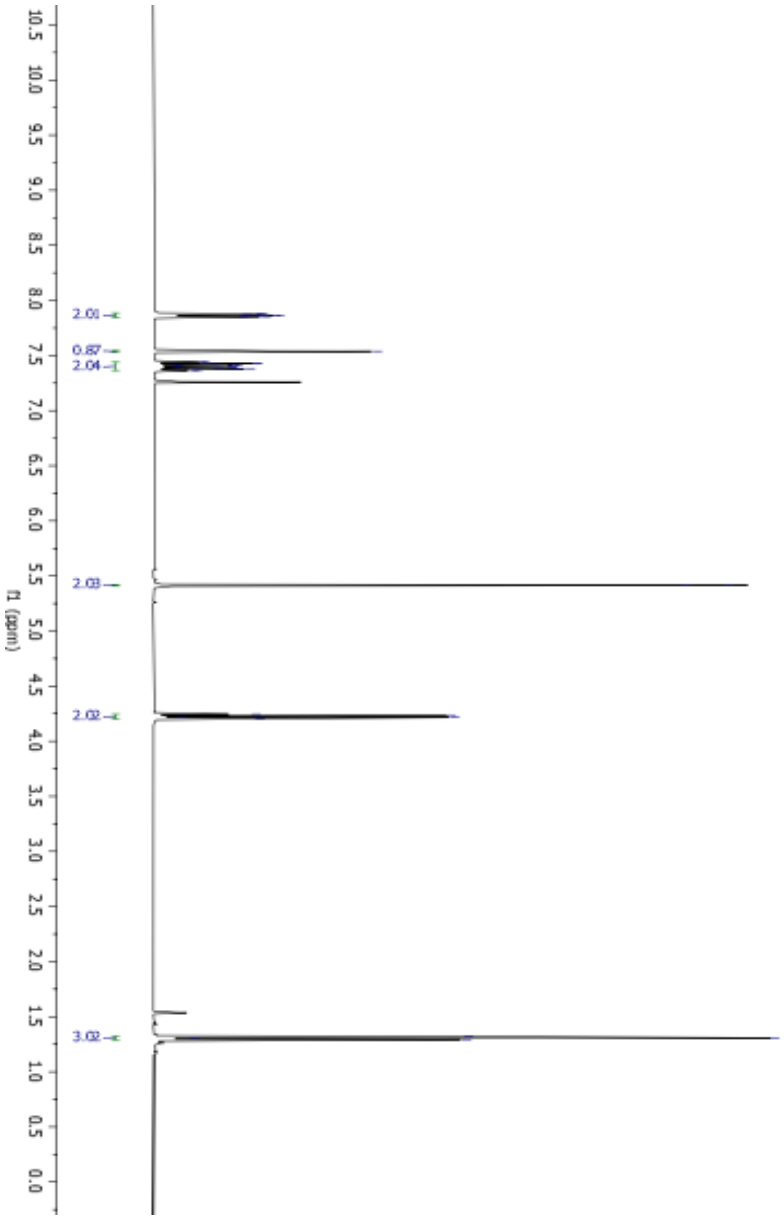

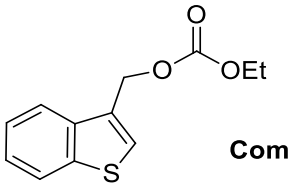

Compound 1-16

^{13}C NMR spectrum ($CDCl_3$, 500 MHz)

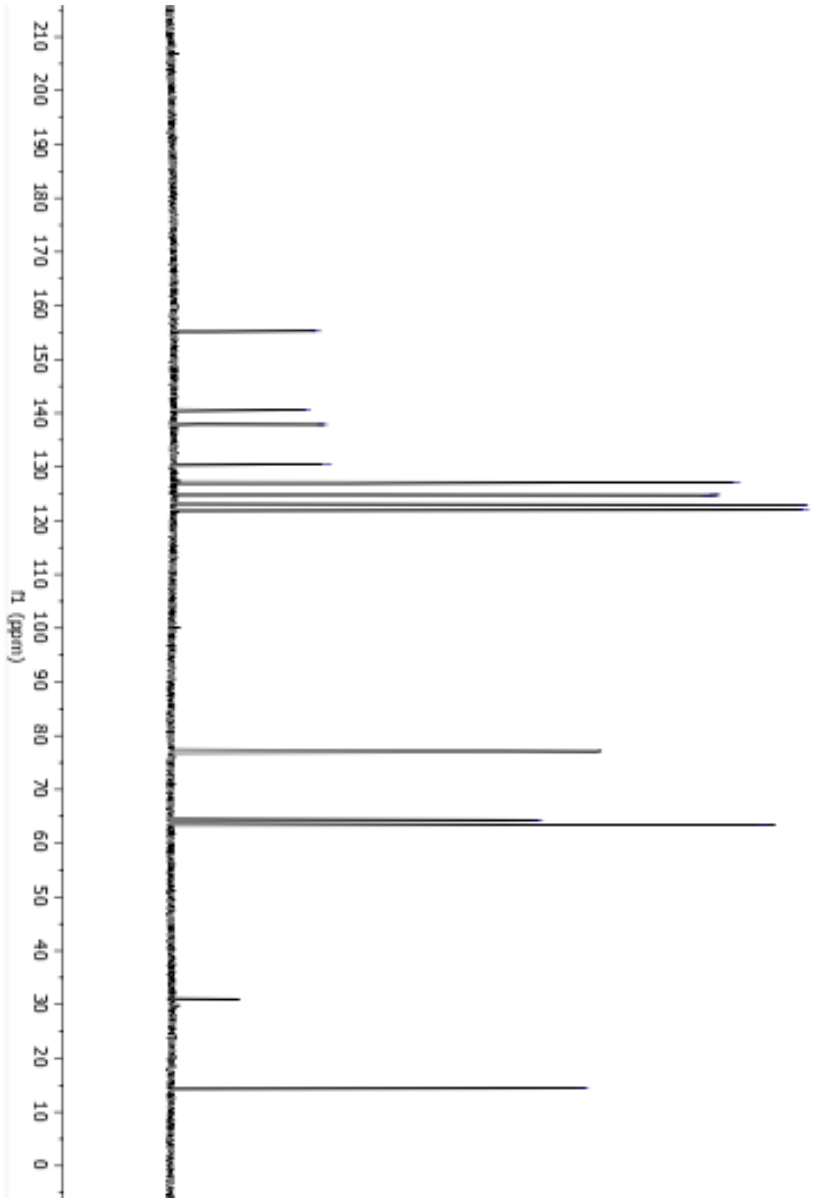

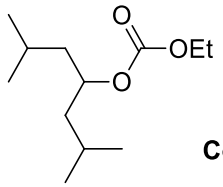

Compound 1-17

^{1}H NMR spectrum ($CDCl_3$, 500 MHz)

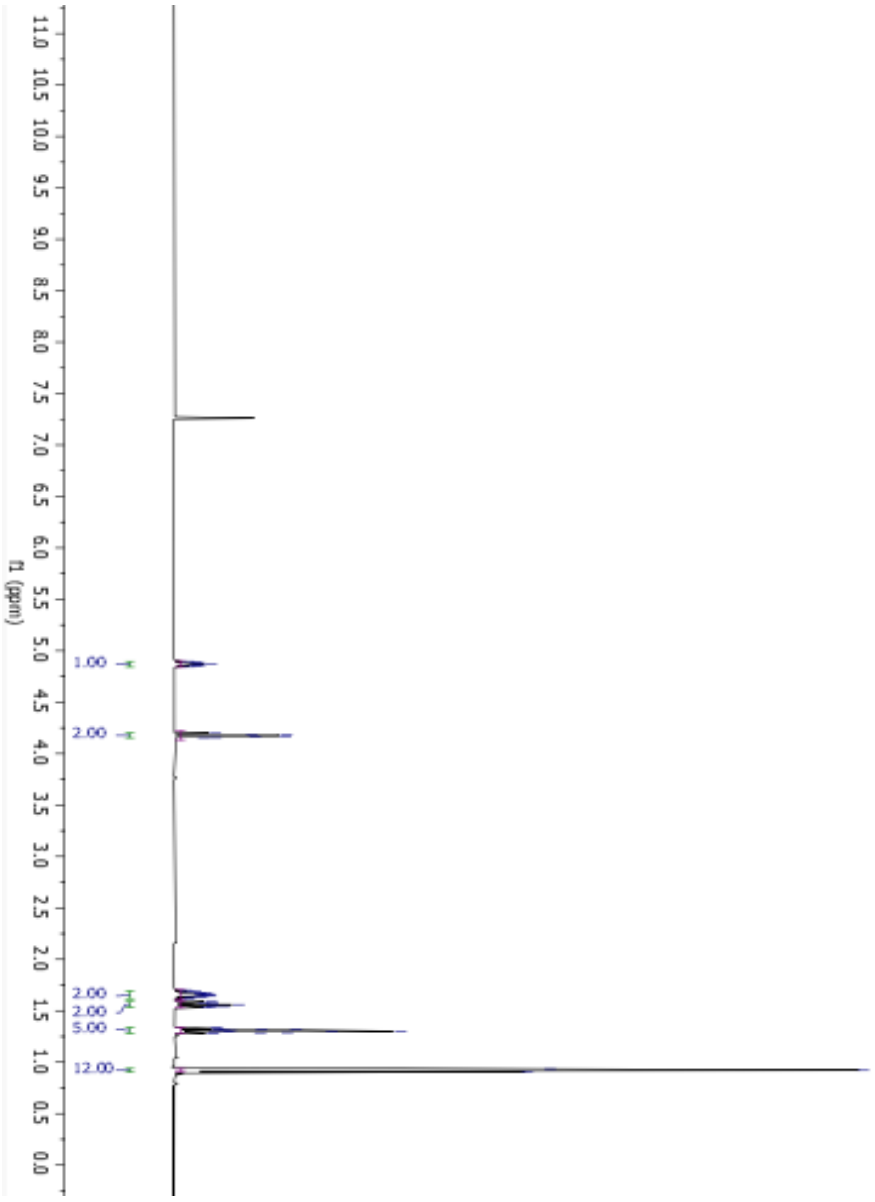

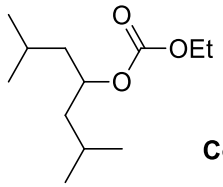

Compound 1-17

^{13}C NMR spectrum ($CDCl_3$, 500 MHz)

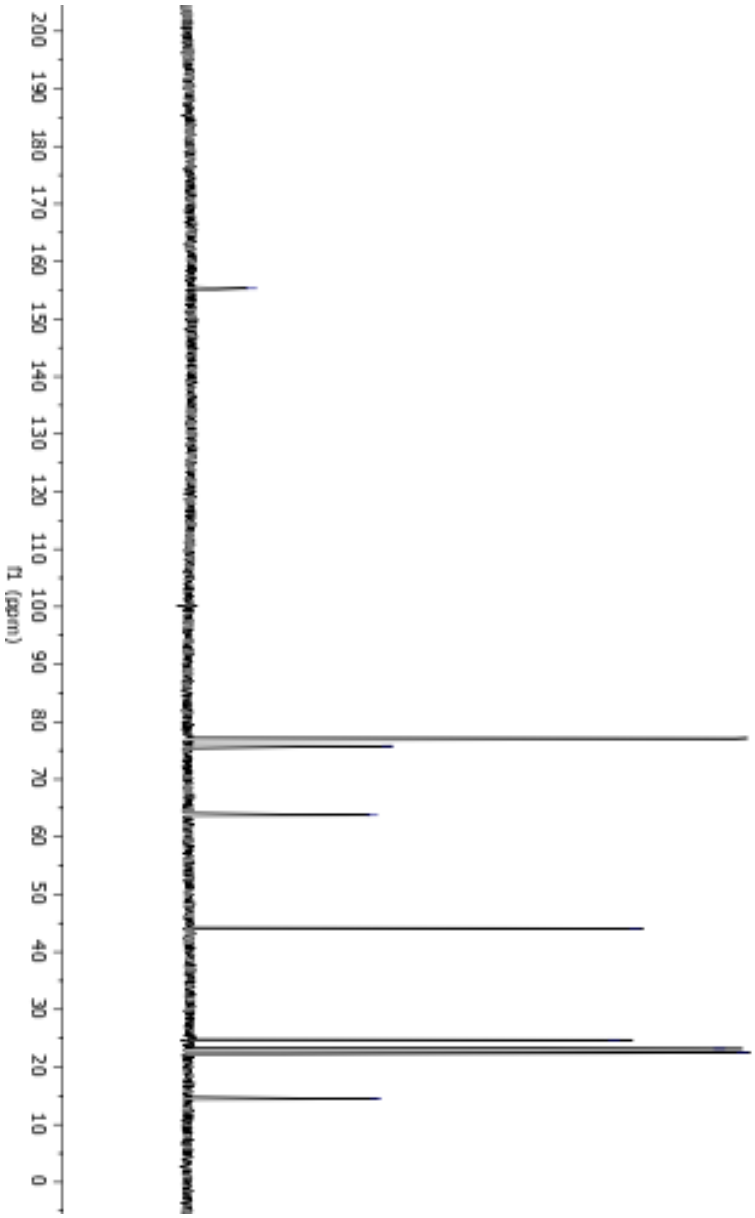

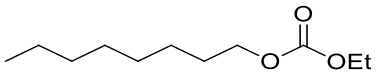

Compound 1-18

^{1}H NMR spectrum ($CDCl_3$, 500 MHz)

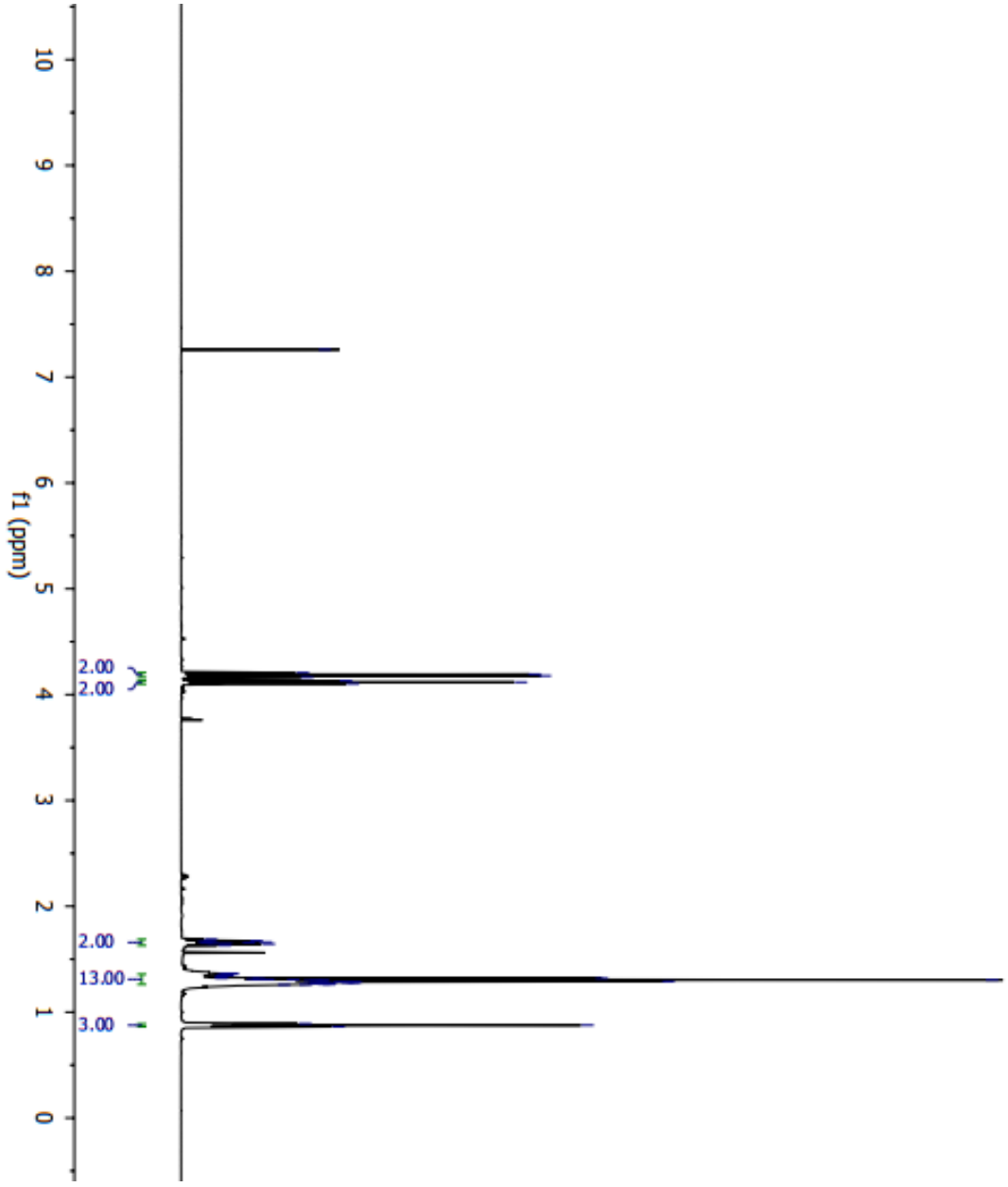

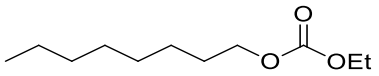

Compound 1-18

^{13}C NMR spectrum ($CDCl_3$, 500 MHz)

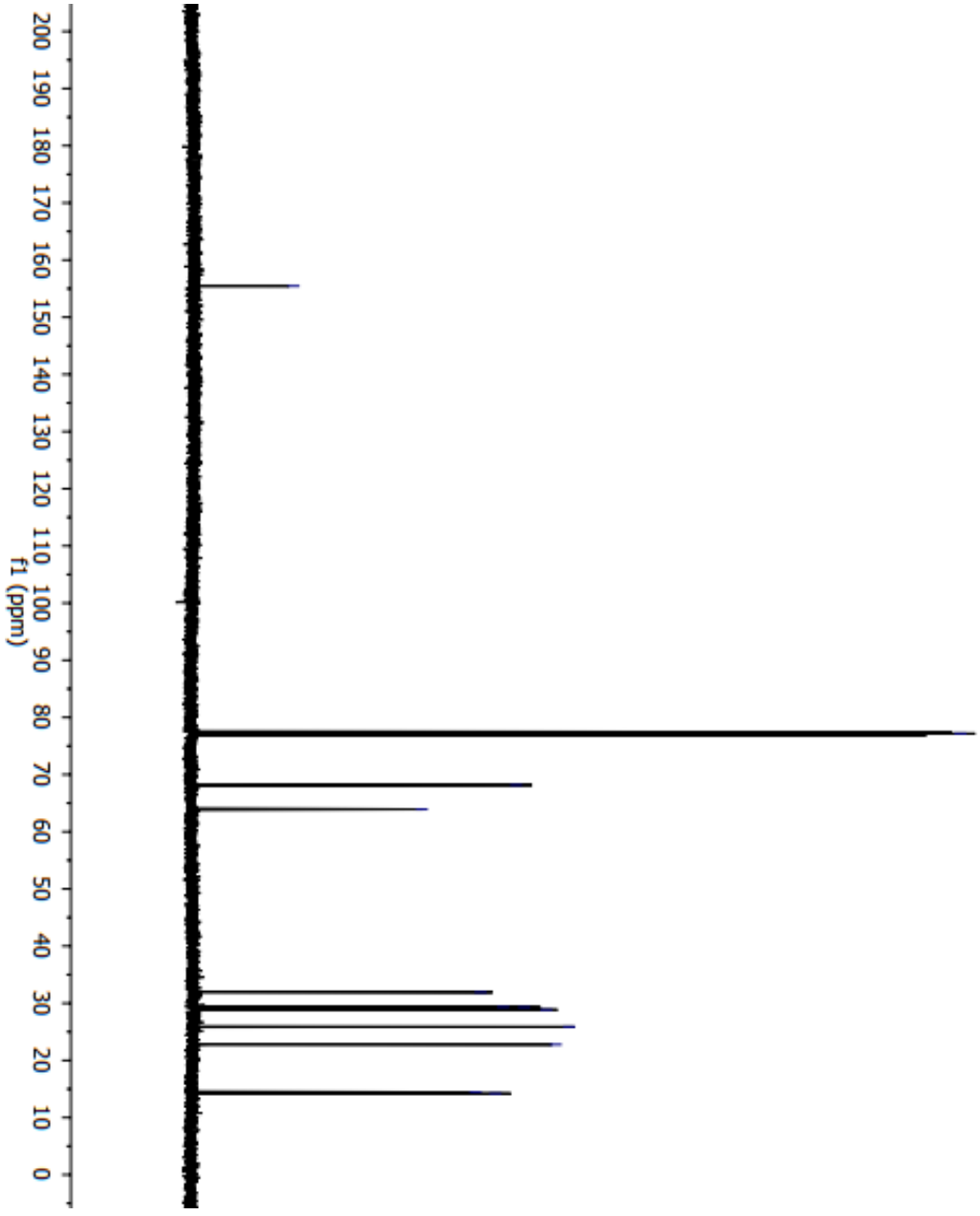

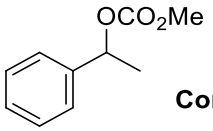

Compound 1-19

^{1}H NMR spectrum ($CDCl_3$, 500 MHz)

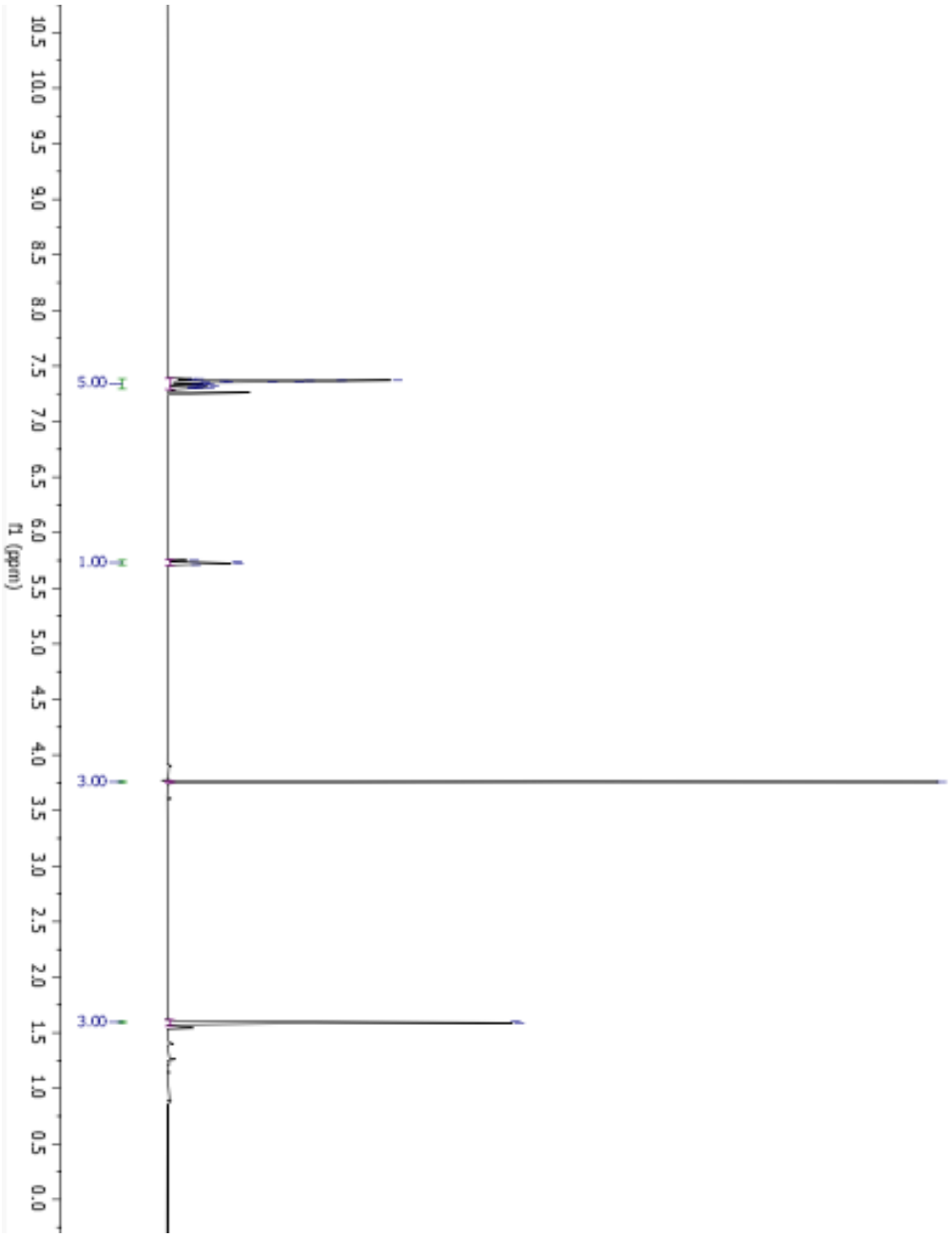

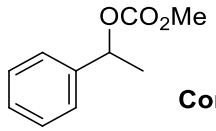

Compound 1-19

^{13}C NMR spectrum ($CDCl_3$, 500 MHz)

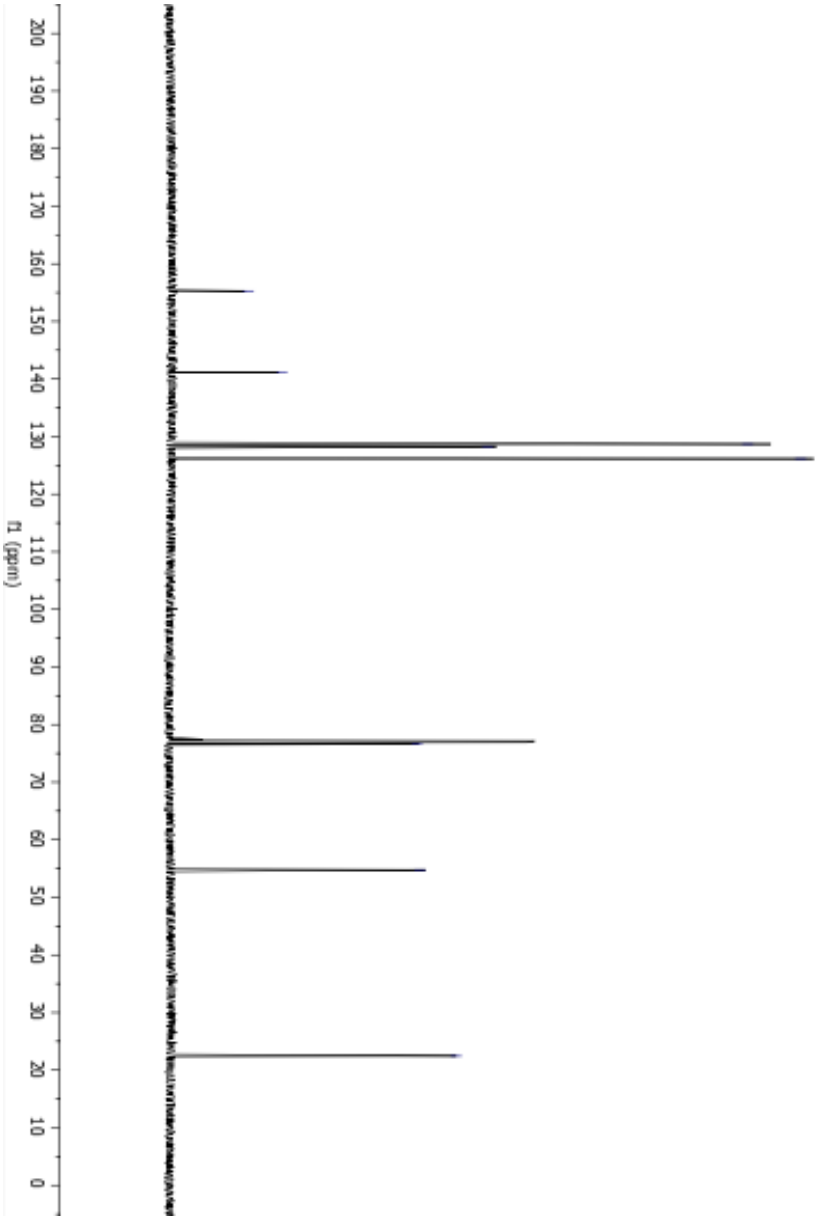

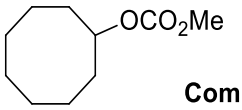

Compound 1-21

^{1}H NMR spectrum ($CDCl_3$, 500 MHz)

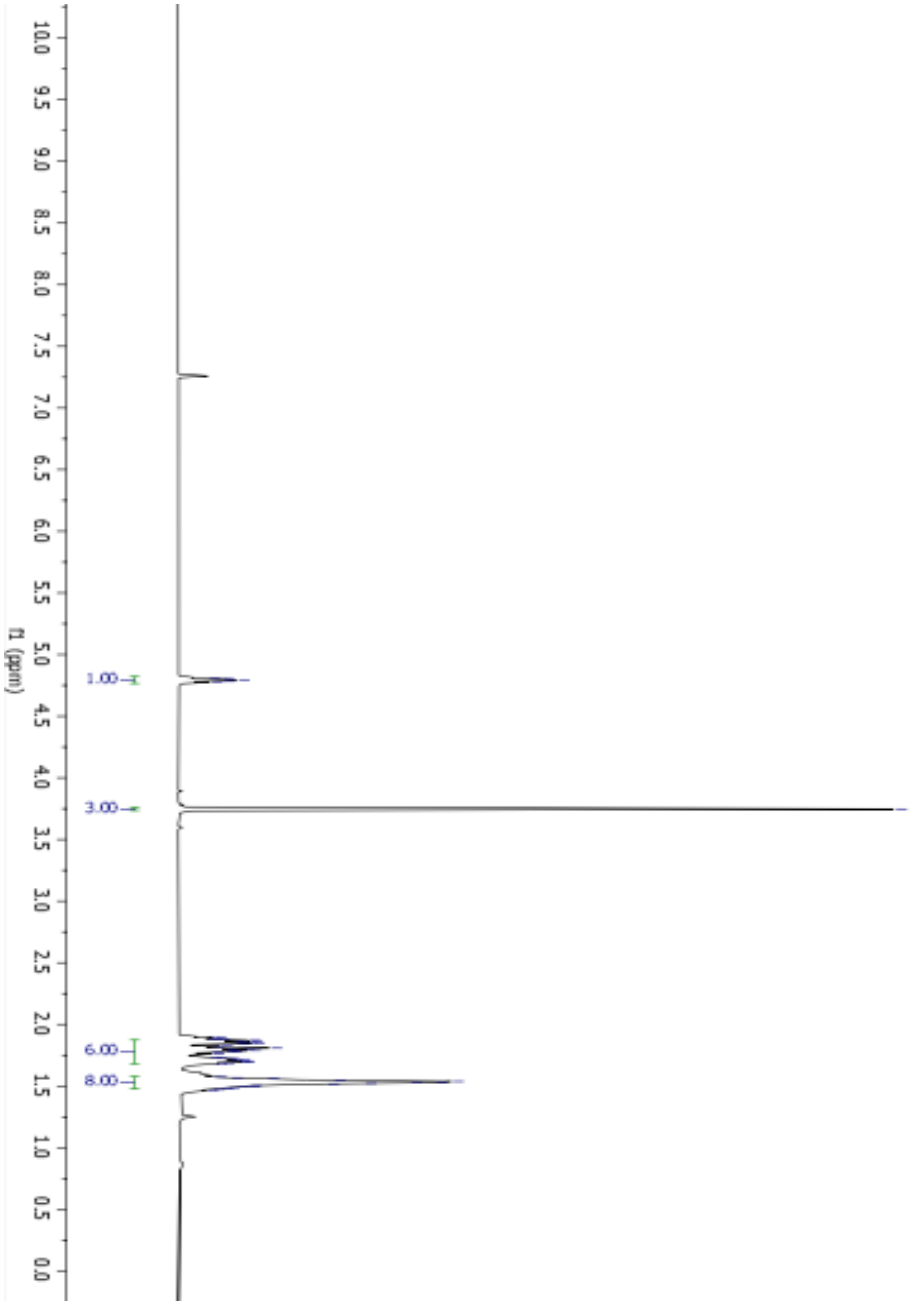

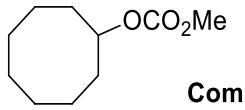

Compound 1-21

^{13}C NMR spectrum ($CDCl_3$, 500 MHz)

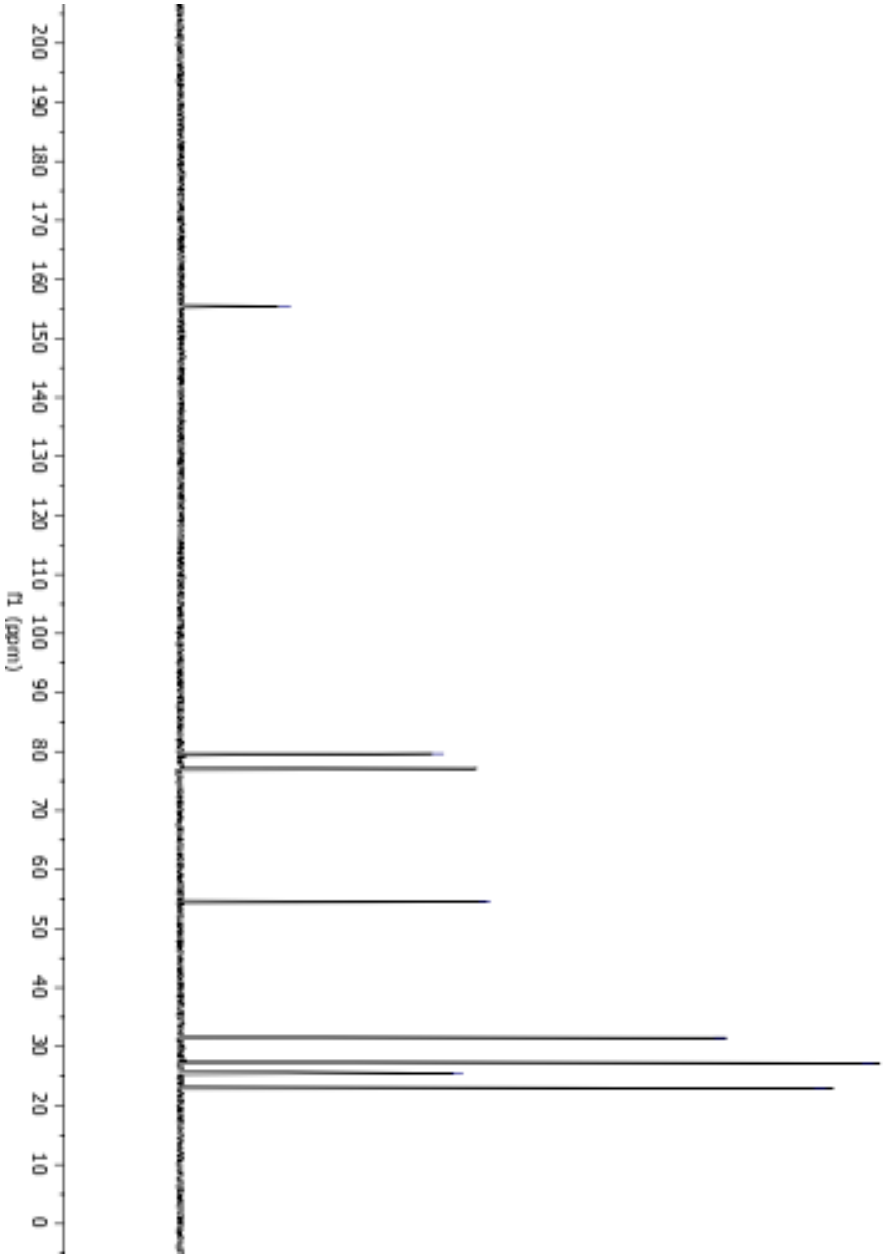

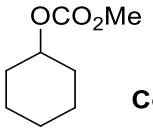

Compound 1-22

^{1}H NMR spectrum ($CDCl_3$, 500 MHz)

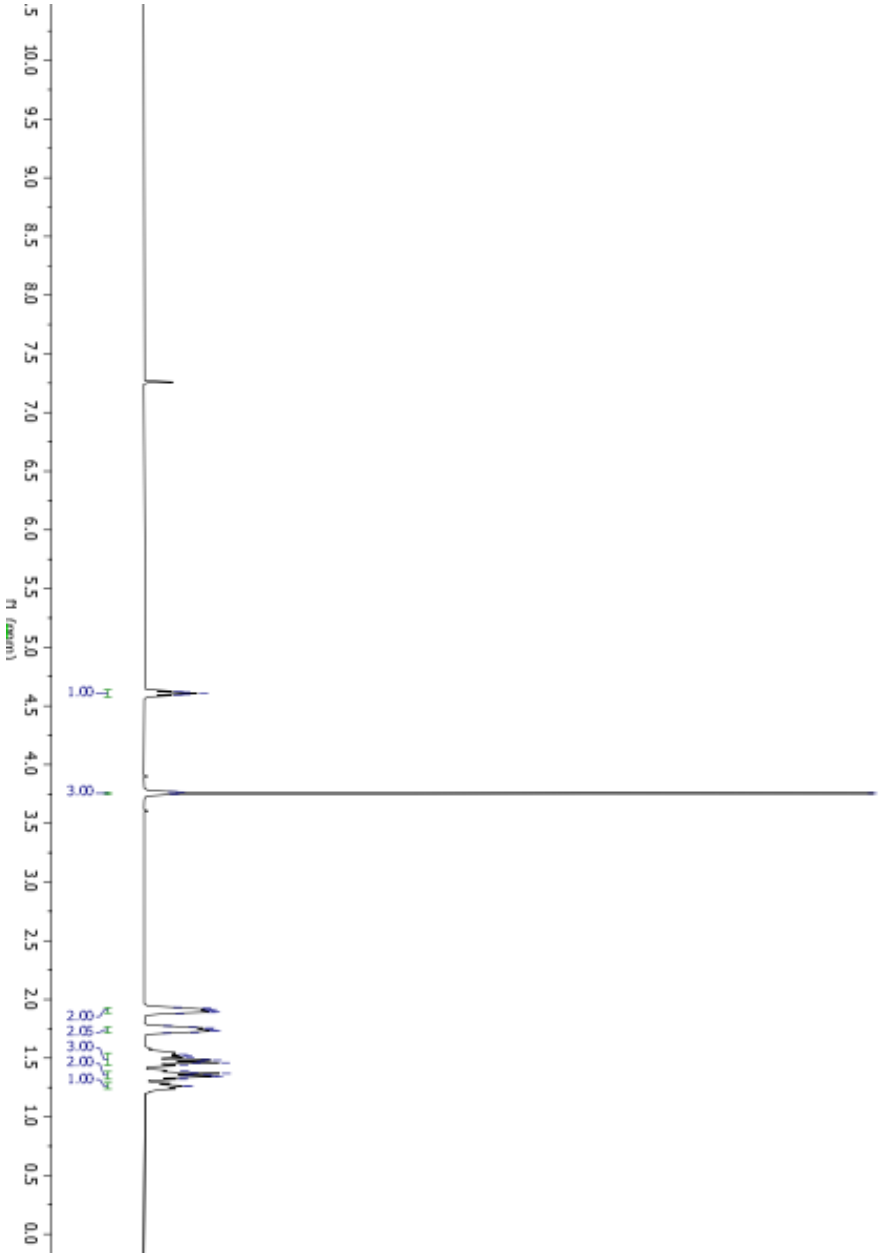

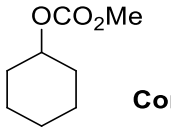

Compound 1-22

^{13}C NMR spectrum ($CDCl_3$, 500 MHz)

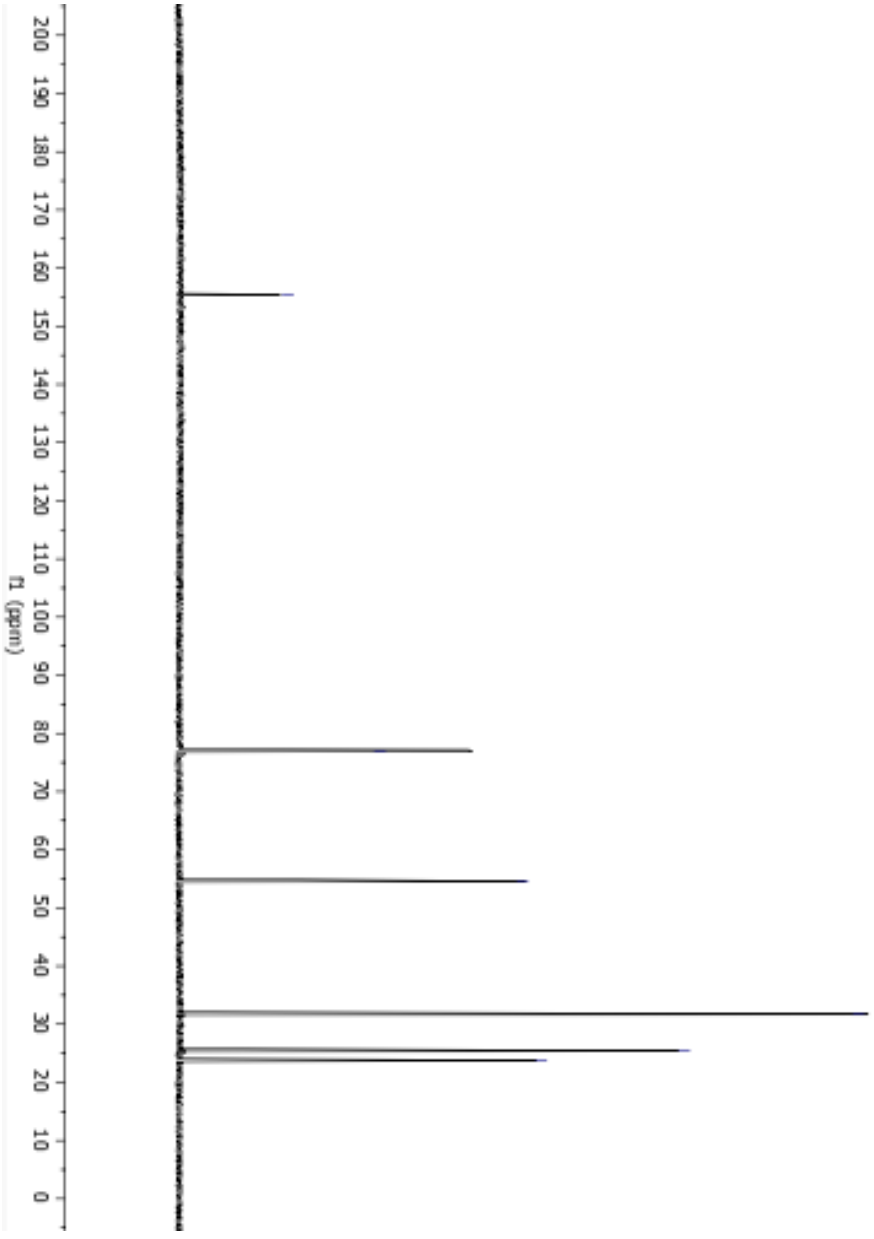

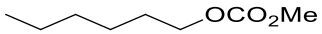

Compound 1-23

^{1}H NMR spectrum ($CDCl_3$, 500 MHz)

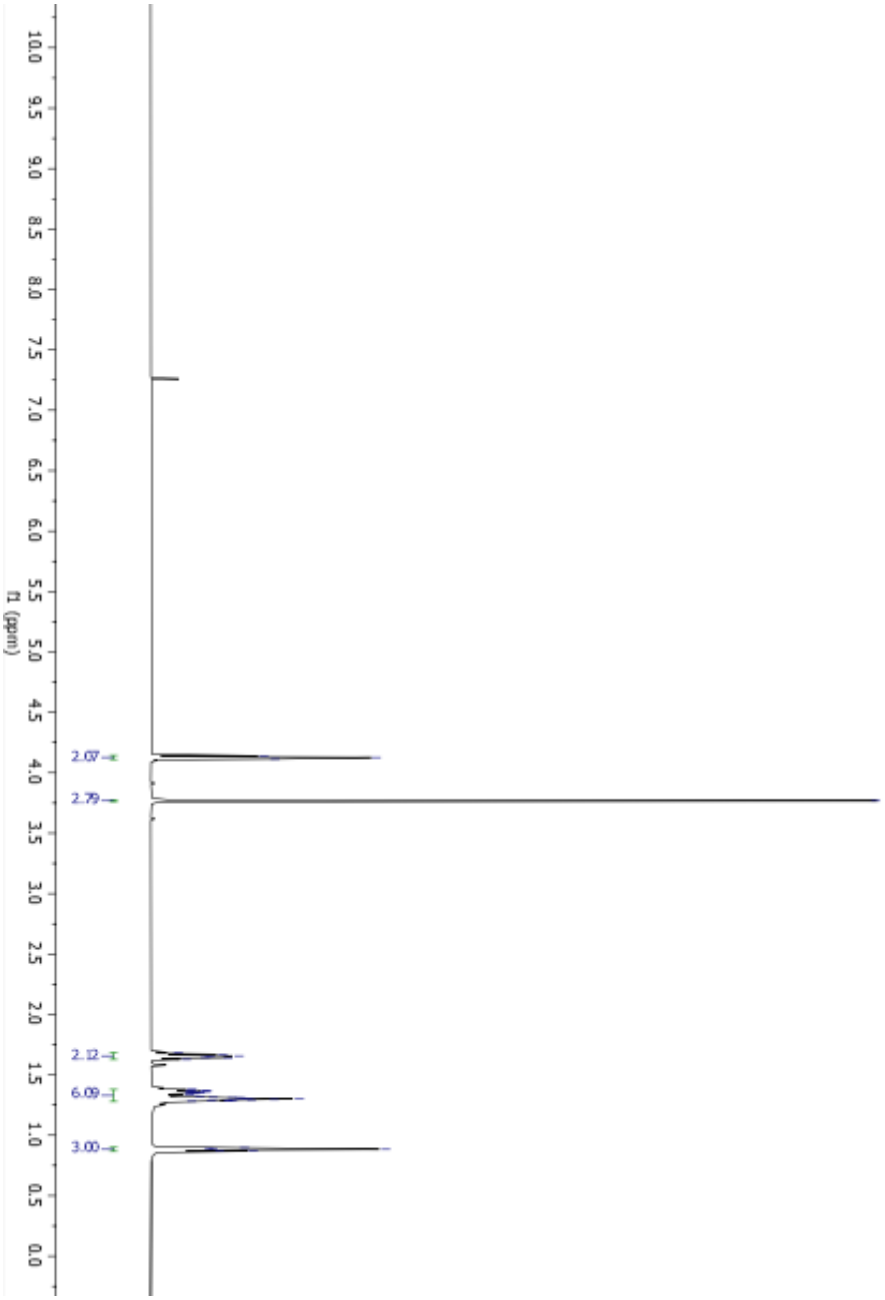

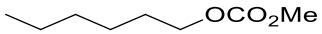

Compound 1-23

^{13}C NMR spectrum ($CDCl_3$, 500 MHz)

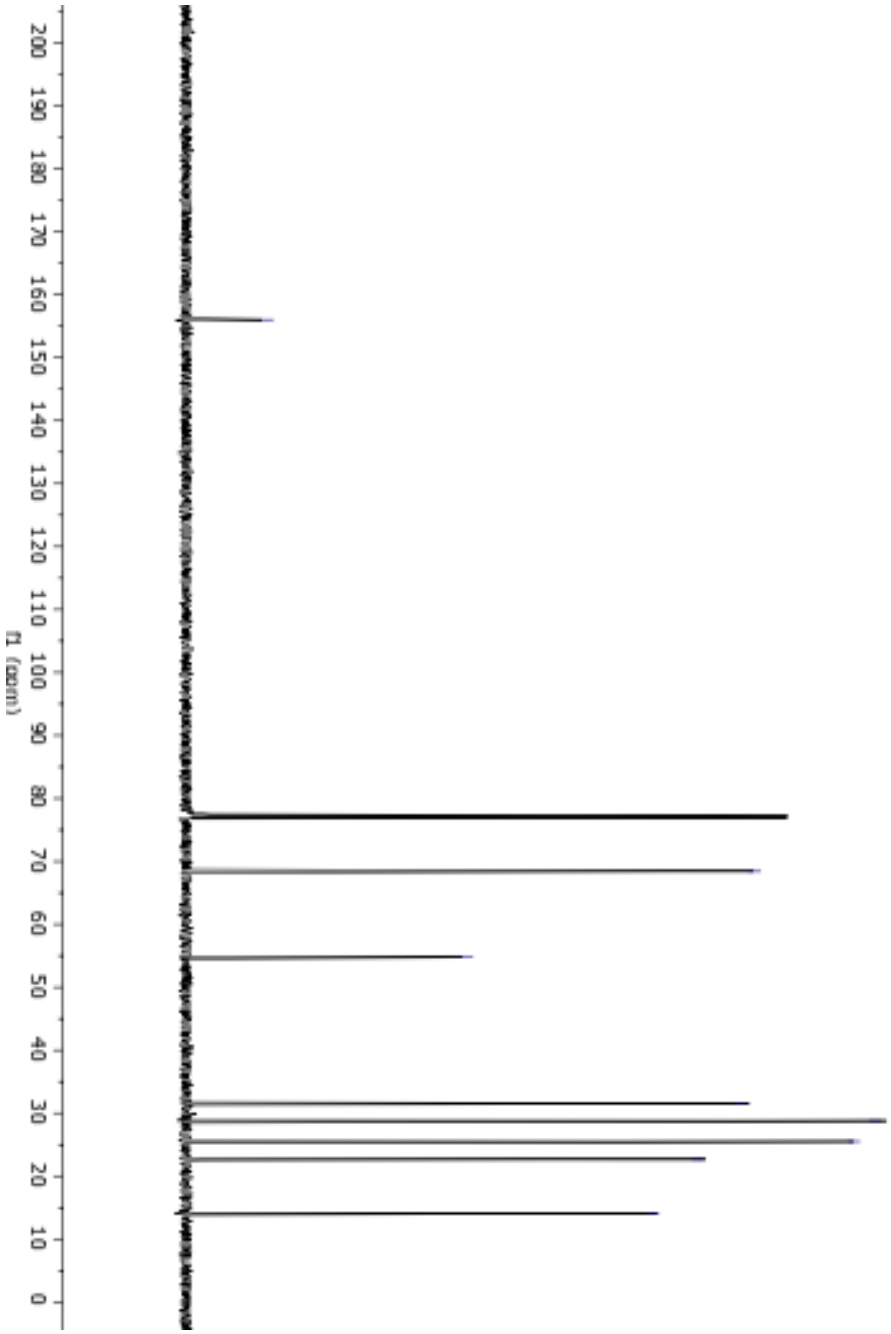

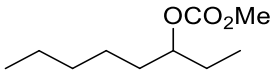

Compound 1-24

^{1}H NMR spectrum ($CDCl_3$, 500 MHz)

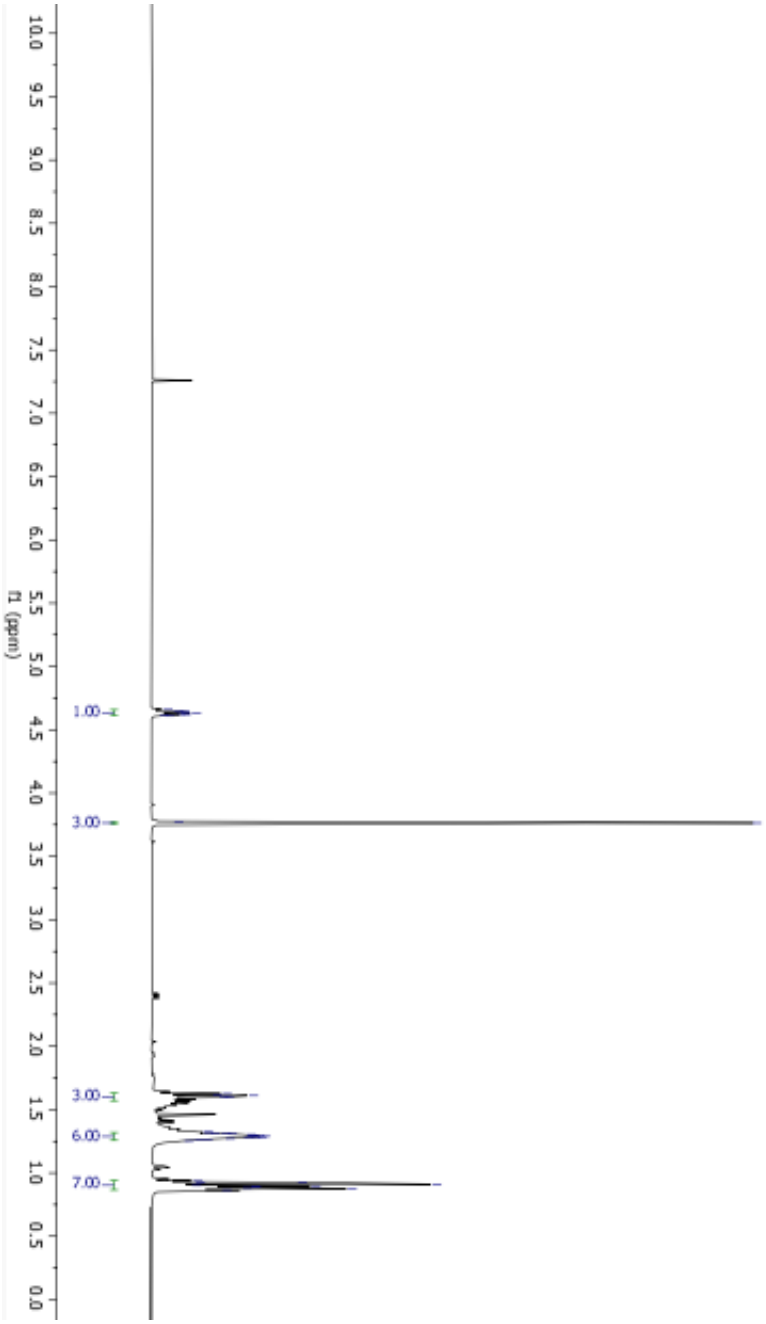

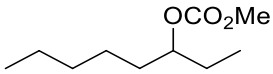

Compound 1-24

^{13}C NMR spectrum ($CDCl_3$, 500 MHz)

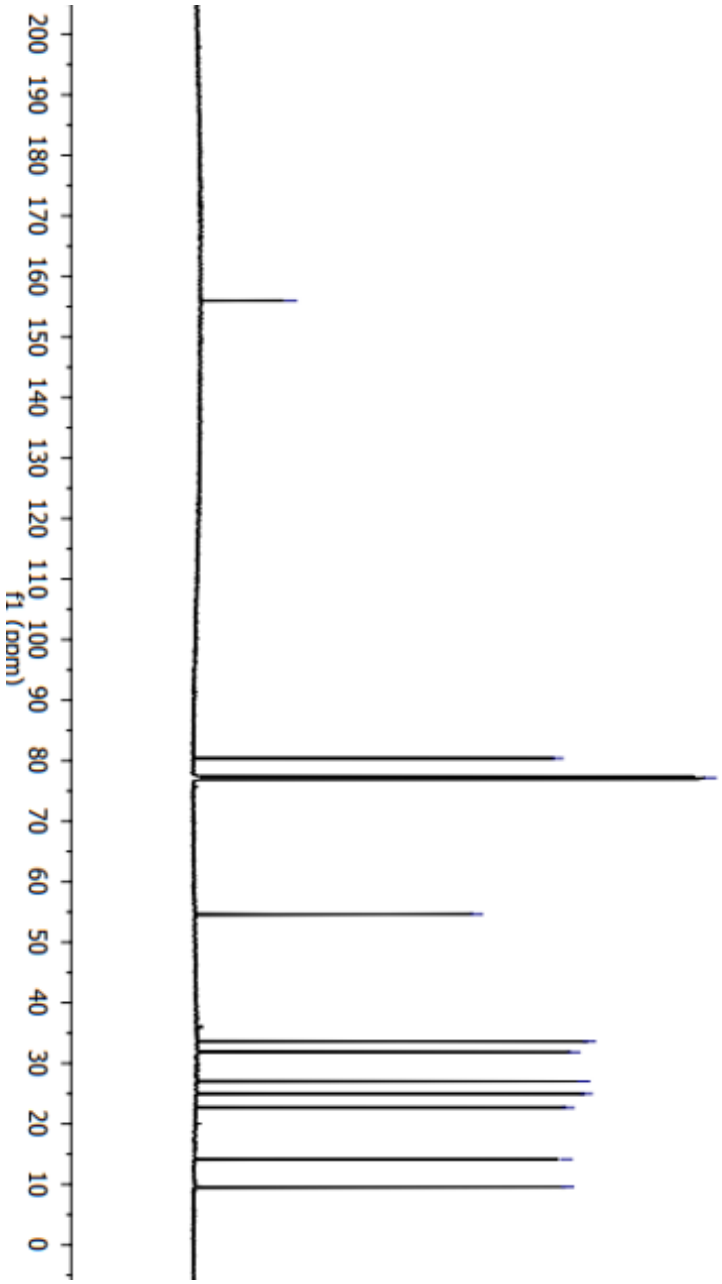

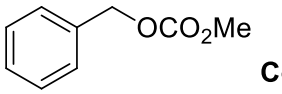

Compound 1-26

^{1}H NMR spectrum ($CDCl_3$, 500 MHz)

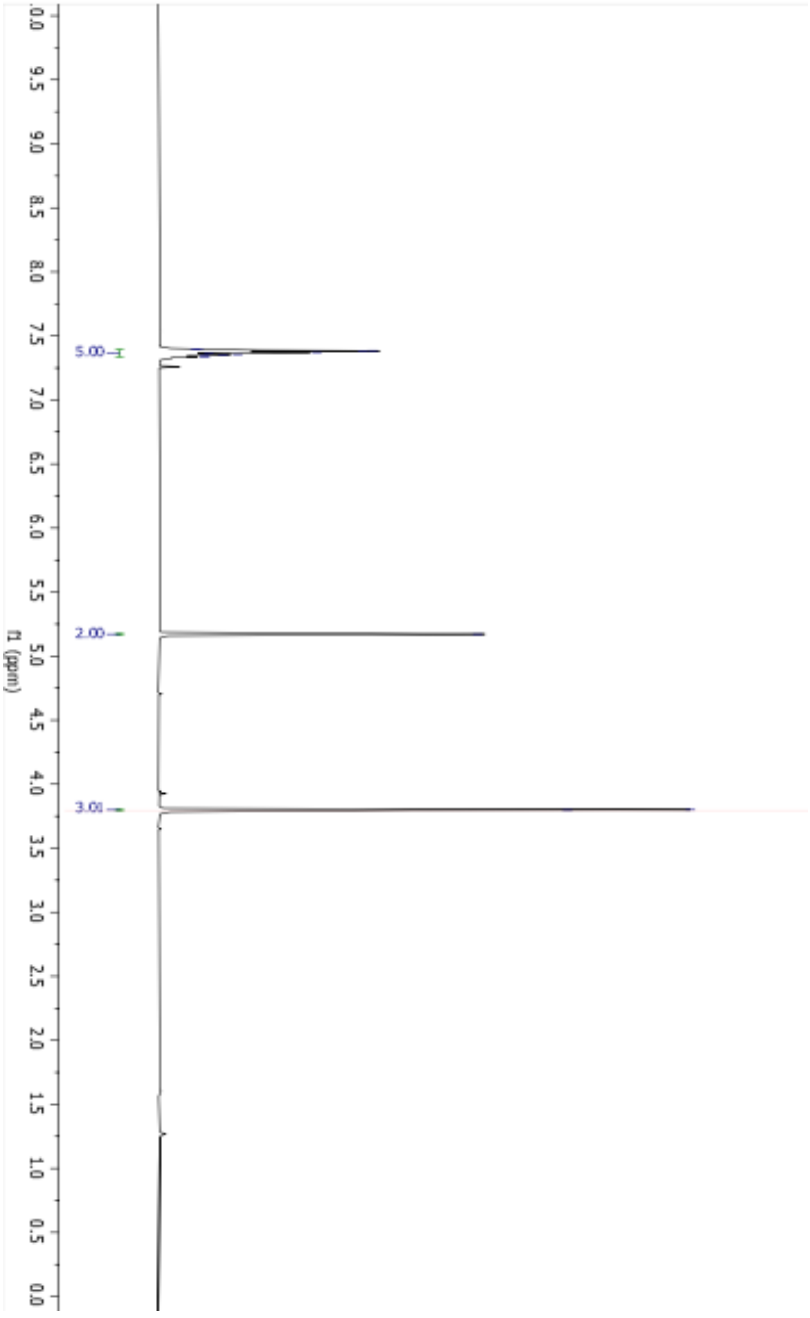

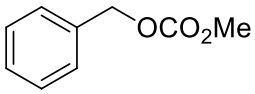

Compound 1-26

^{13}C NMR spectrum ($CDCl_3$, 500 MHz)

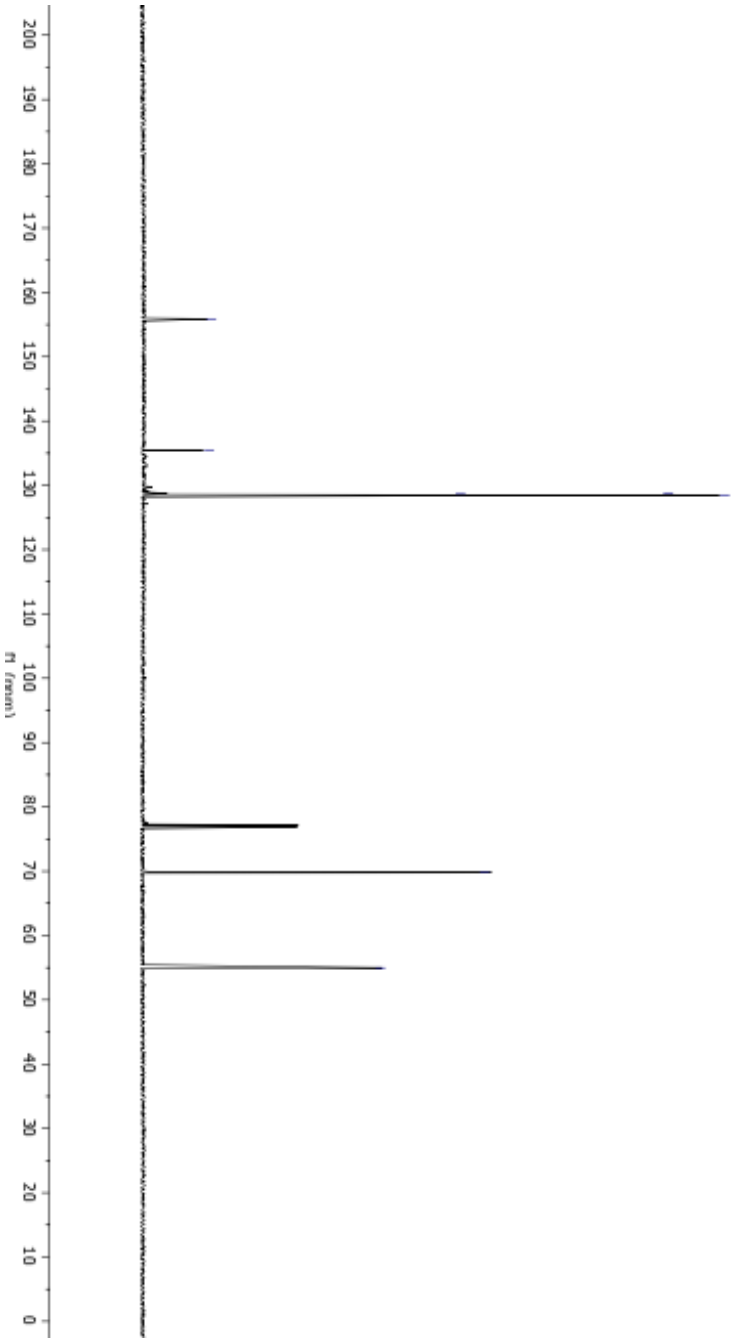

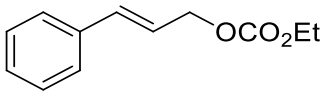

Compound 1-27

^{1}H NMR spectrum ($CDCl_3$, 500 MHz)

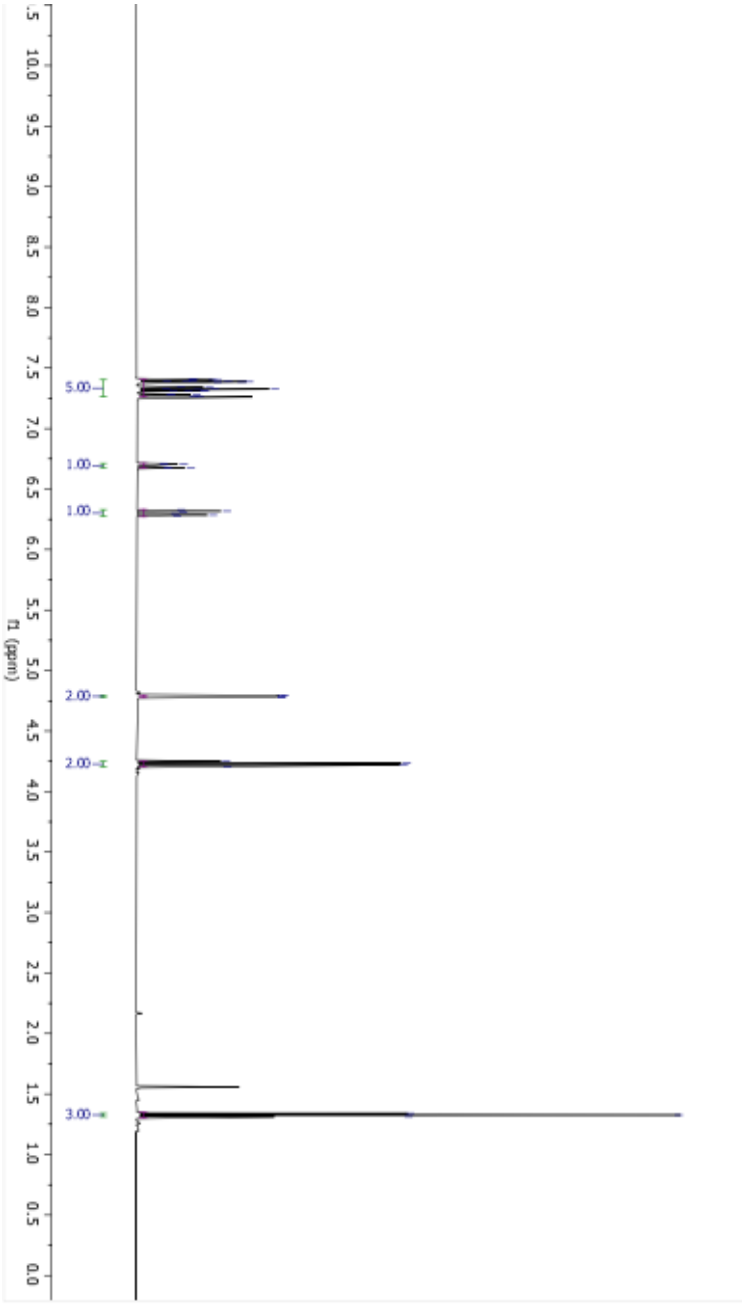

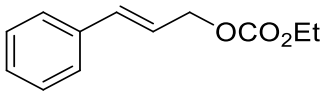

Compound 1-27

^{13}C NMR spectrum ($CDCl_3$, 500 MHz)

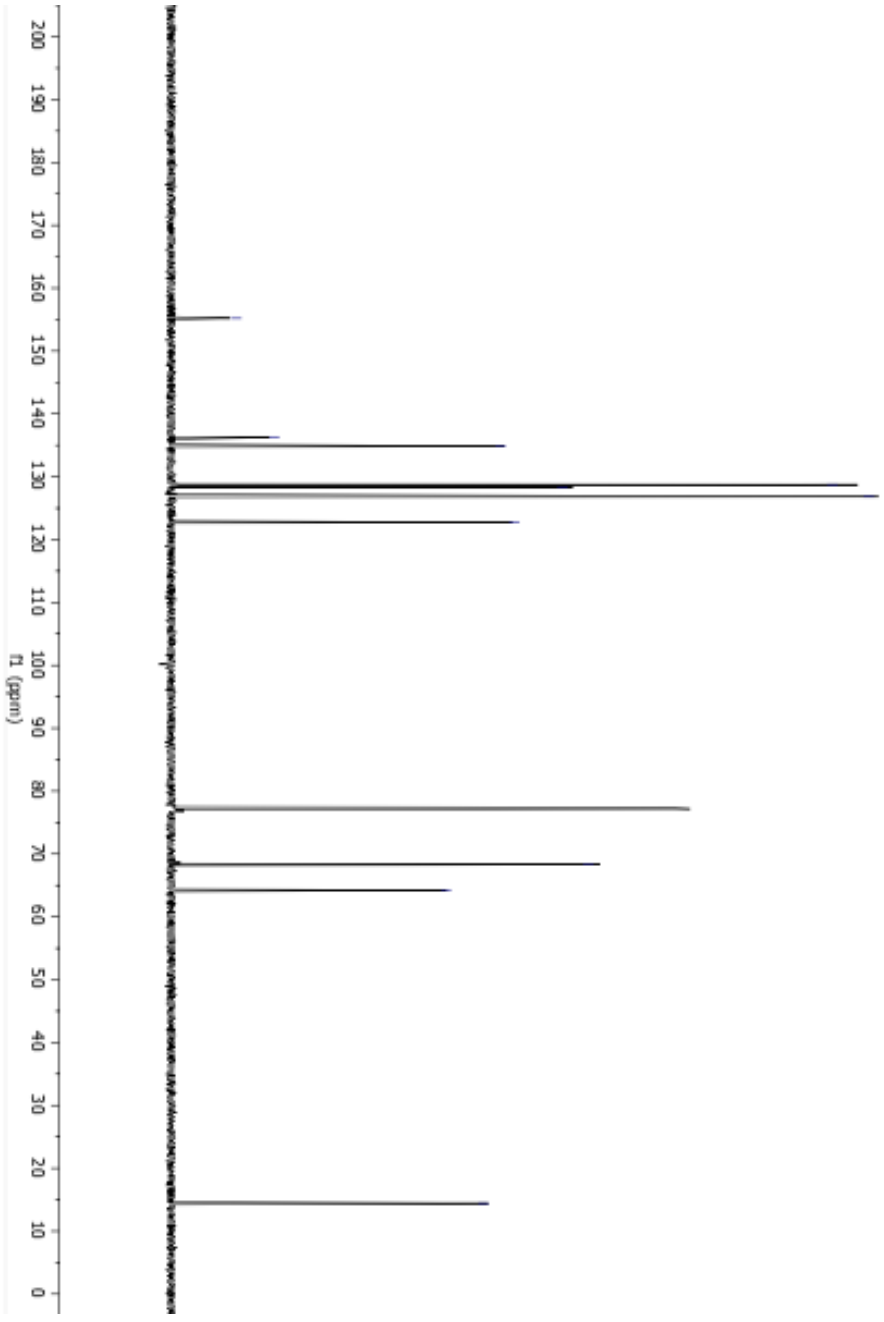

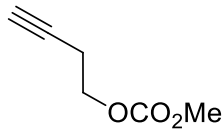

Compound 1-28

^{1}H NMR spectrum ($CDCl_3$, 500 MHz)

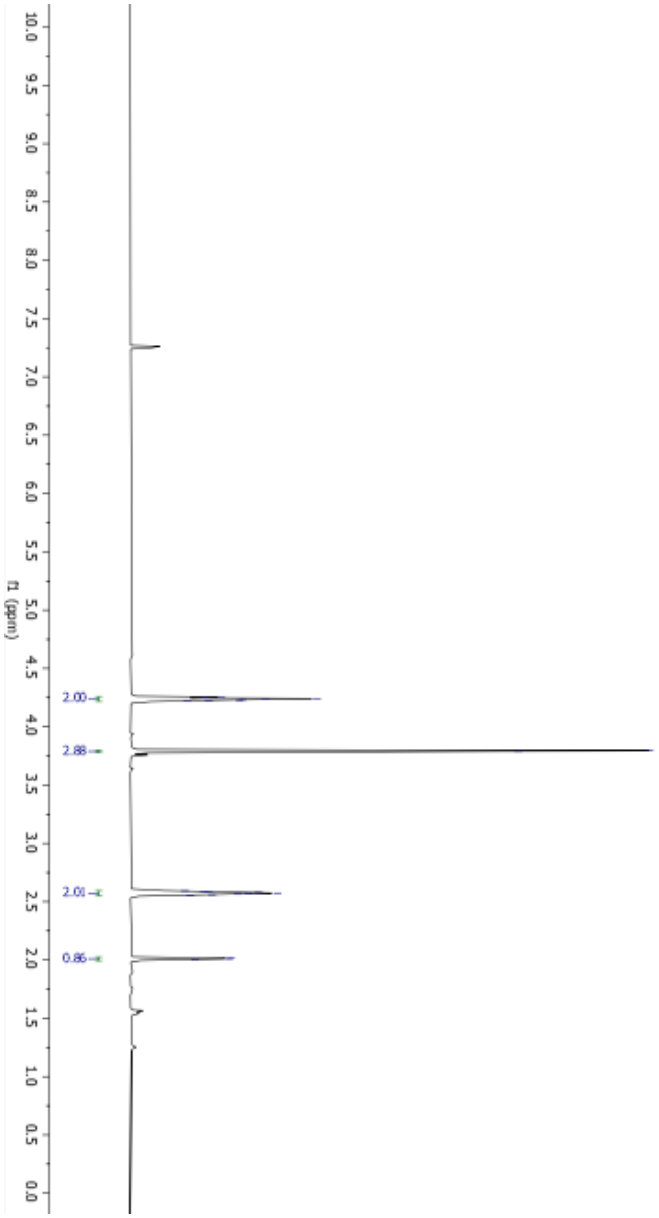

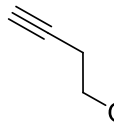

Compound 1-28

^{13}C NMR spectrum ($CDCl_3$, 500 MHz)

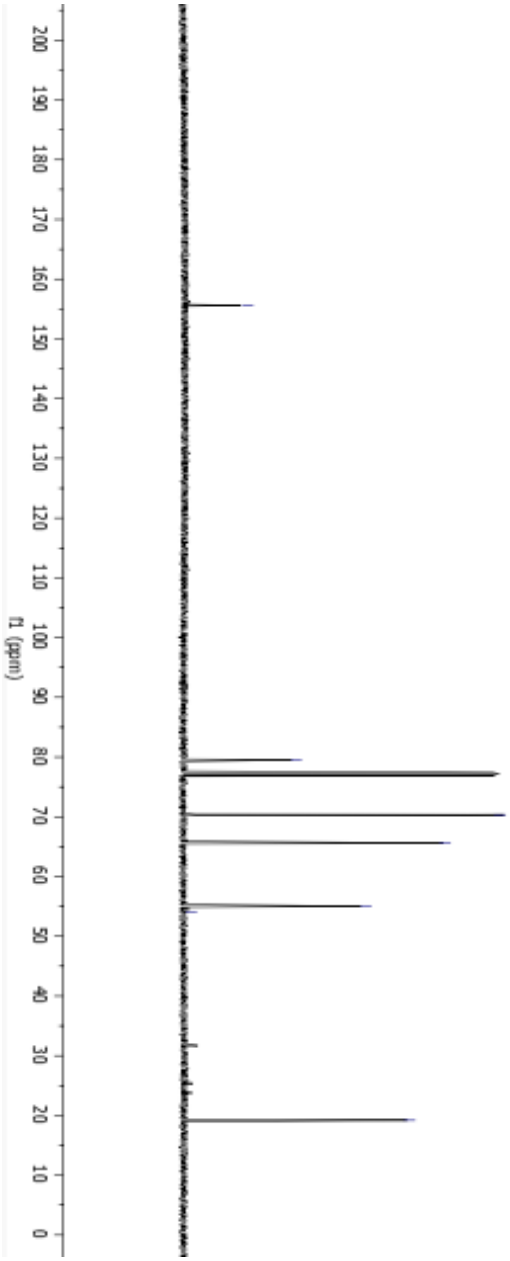

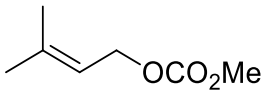

Compound 1-29

^{1}H NMR spectrum ($CDCl_3$, 500 MHz)

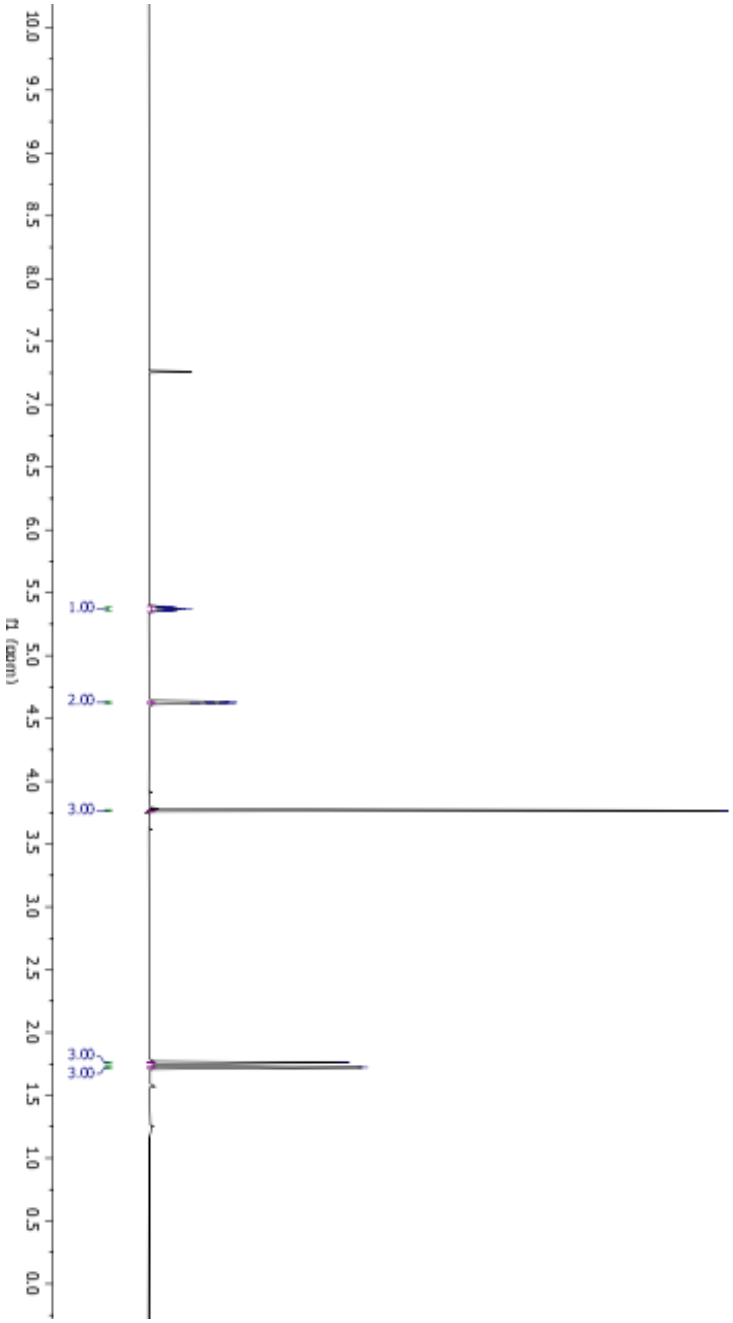

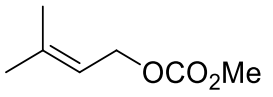

Compound 1-29

^{13}C NMR spectrum ($CDCl_3$, 500 MHz)

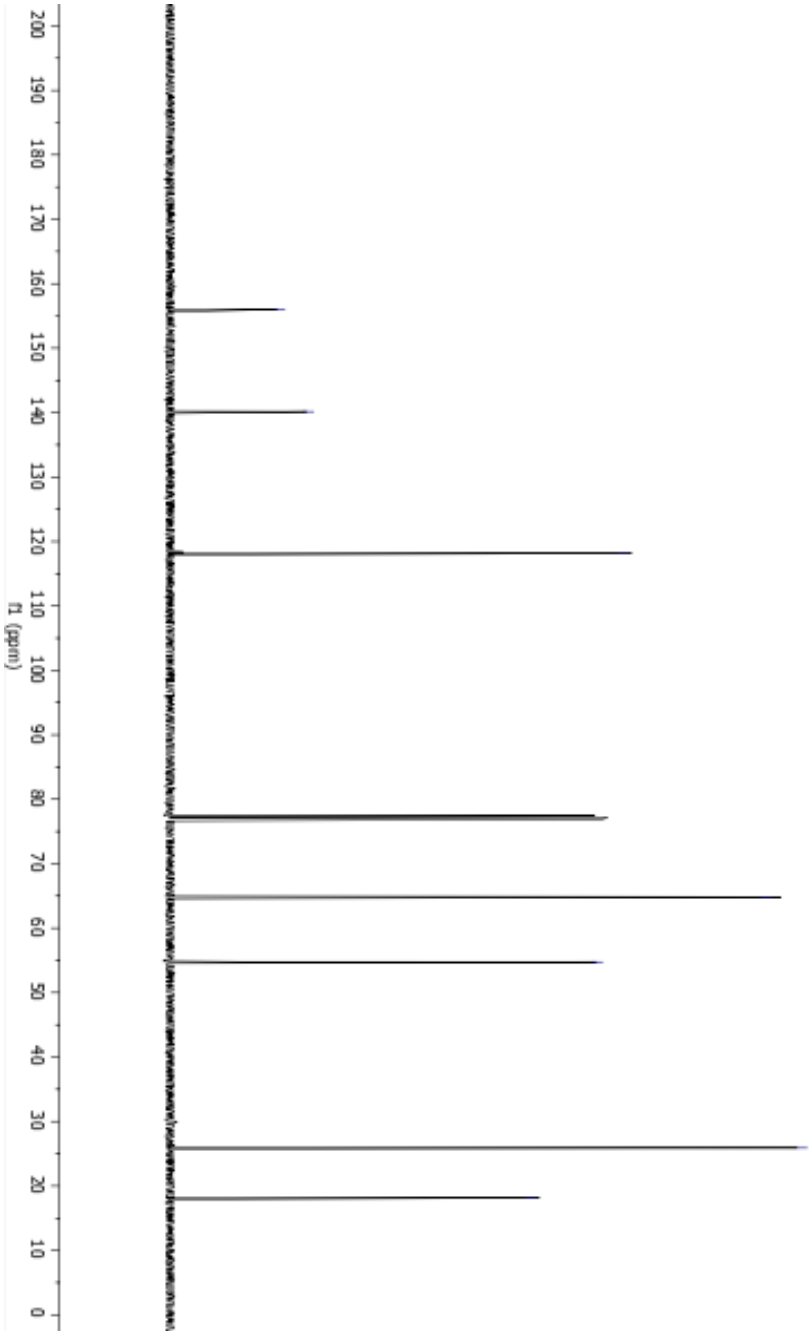

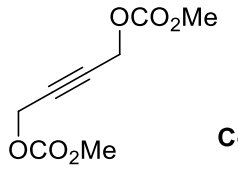

Compound 1-30

^{1}H NMR spectrum ($CDCl_3$, 500 MHz)

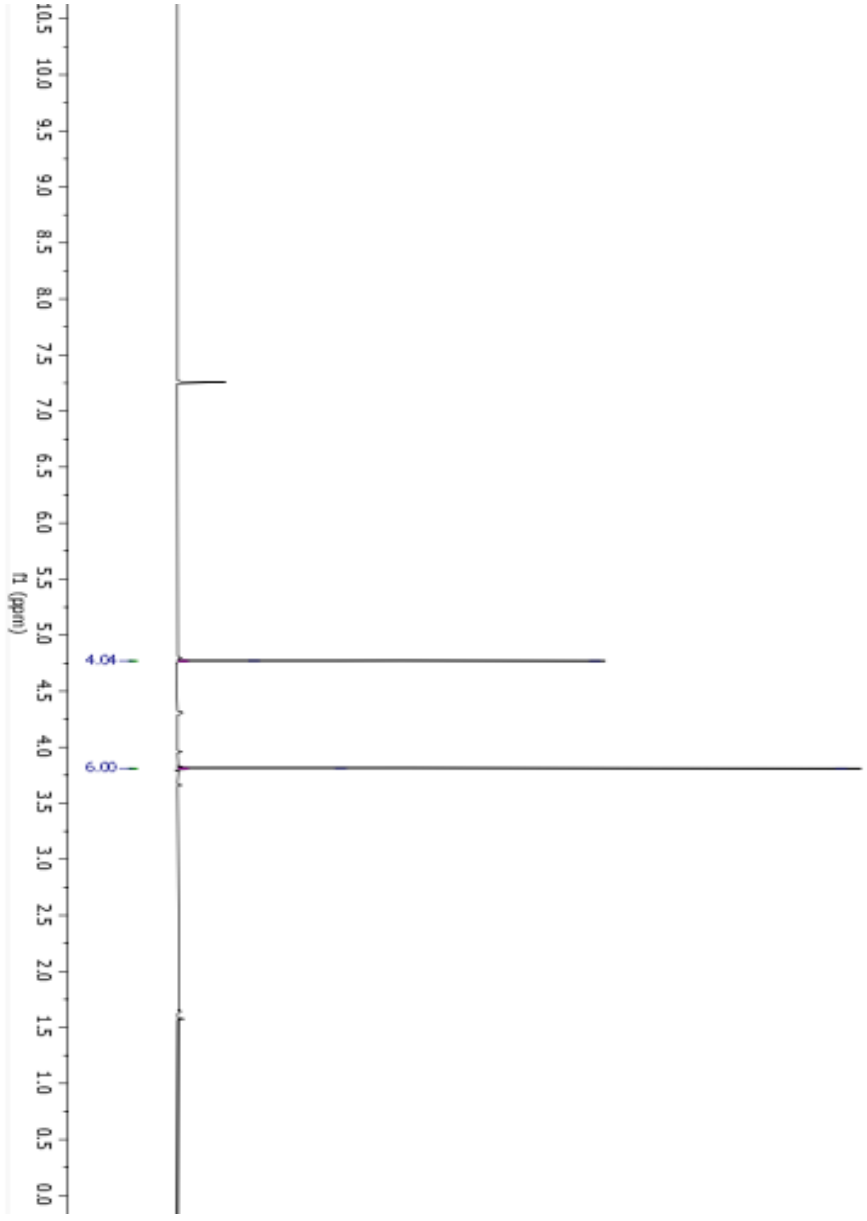

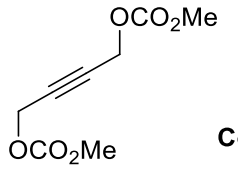

Compound 1-30

^{13}C NMR spectrum ($CDCl_3$, 500 MHz)

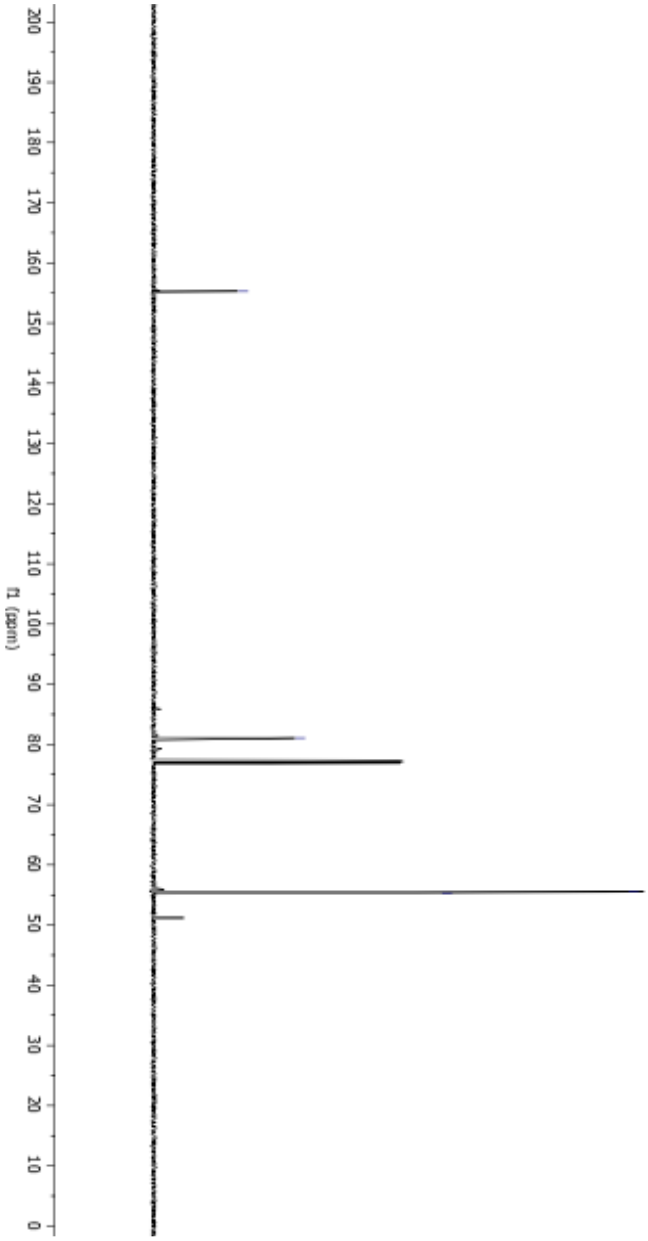

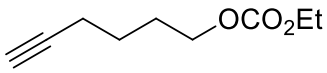

Compound 1-31

^{1}H NMR spectrum ($CDCl_3$, 500 MHz)

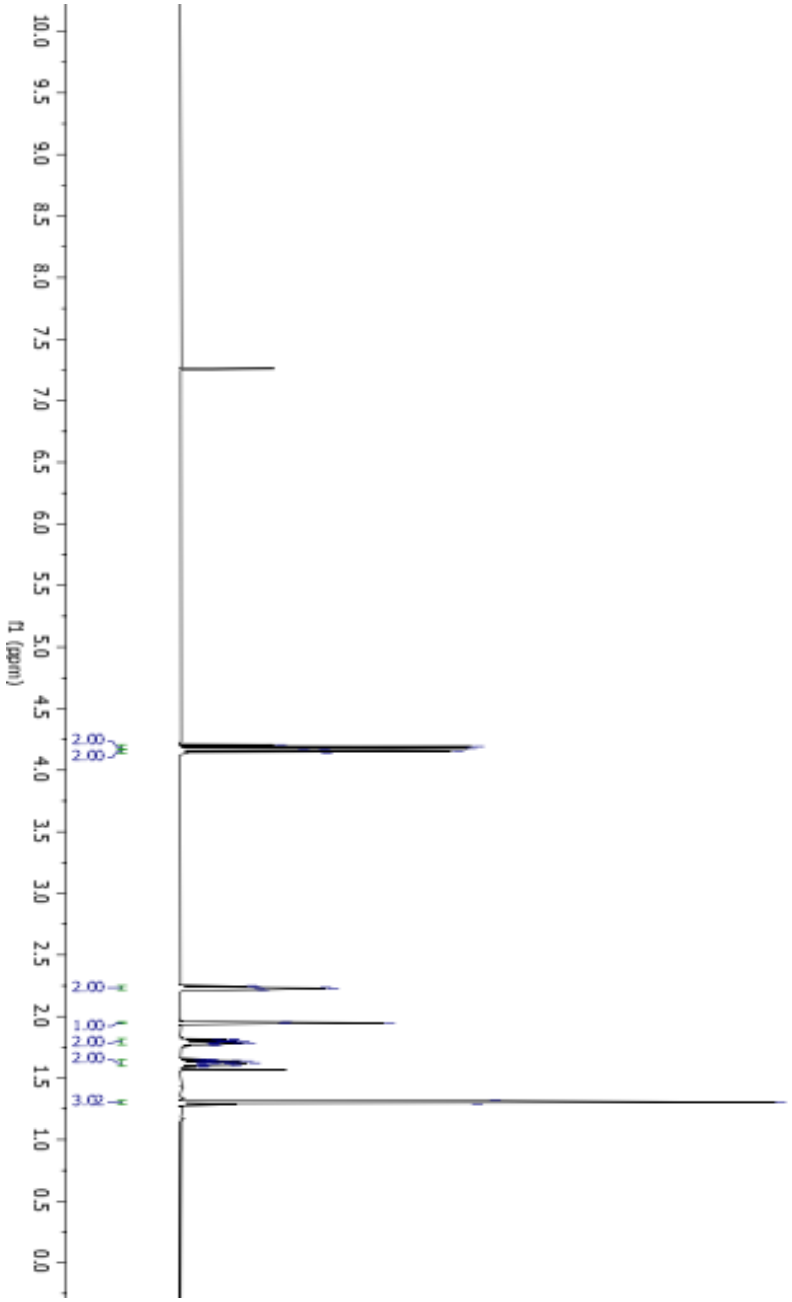

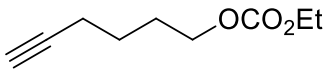

Compound 1-31

^{13}C NMR spectrum ($CDCl_3$, 500 MHz)

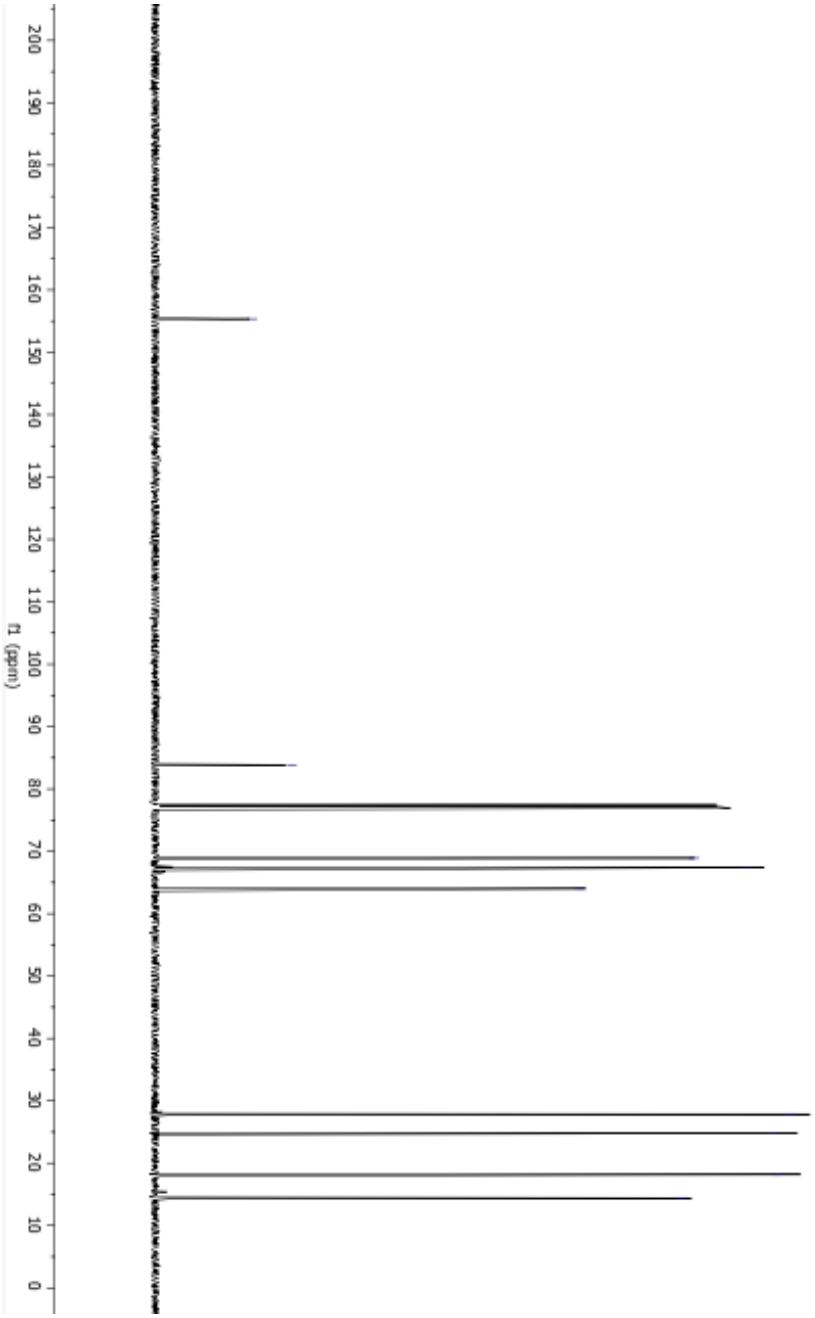

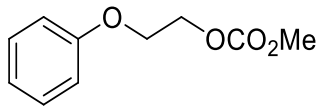

Compound 1-32

^{1}H NMR spectrum ($CDCl_3$, 500 MHz)

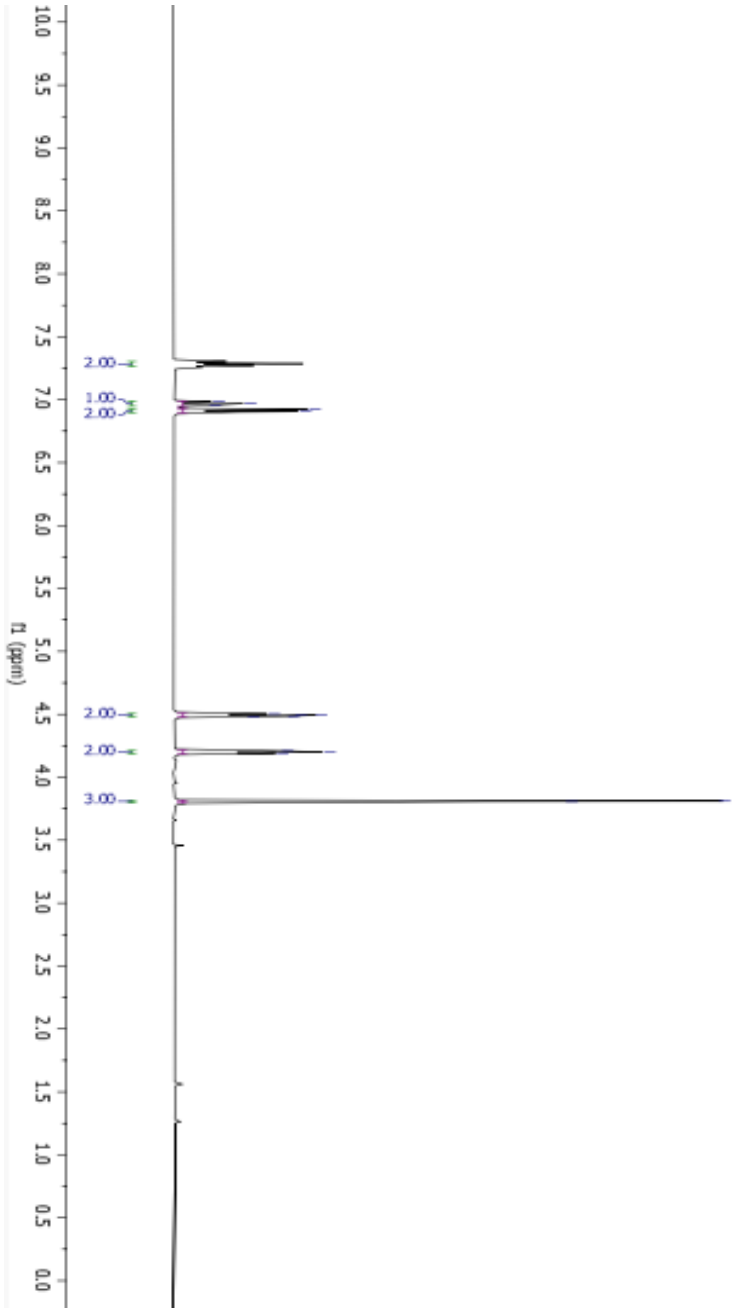

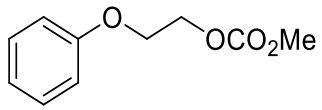

Compound 1-32

^{13}C NMR spectrum ($CDCl_3$, 500 MHz)

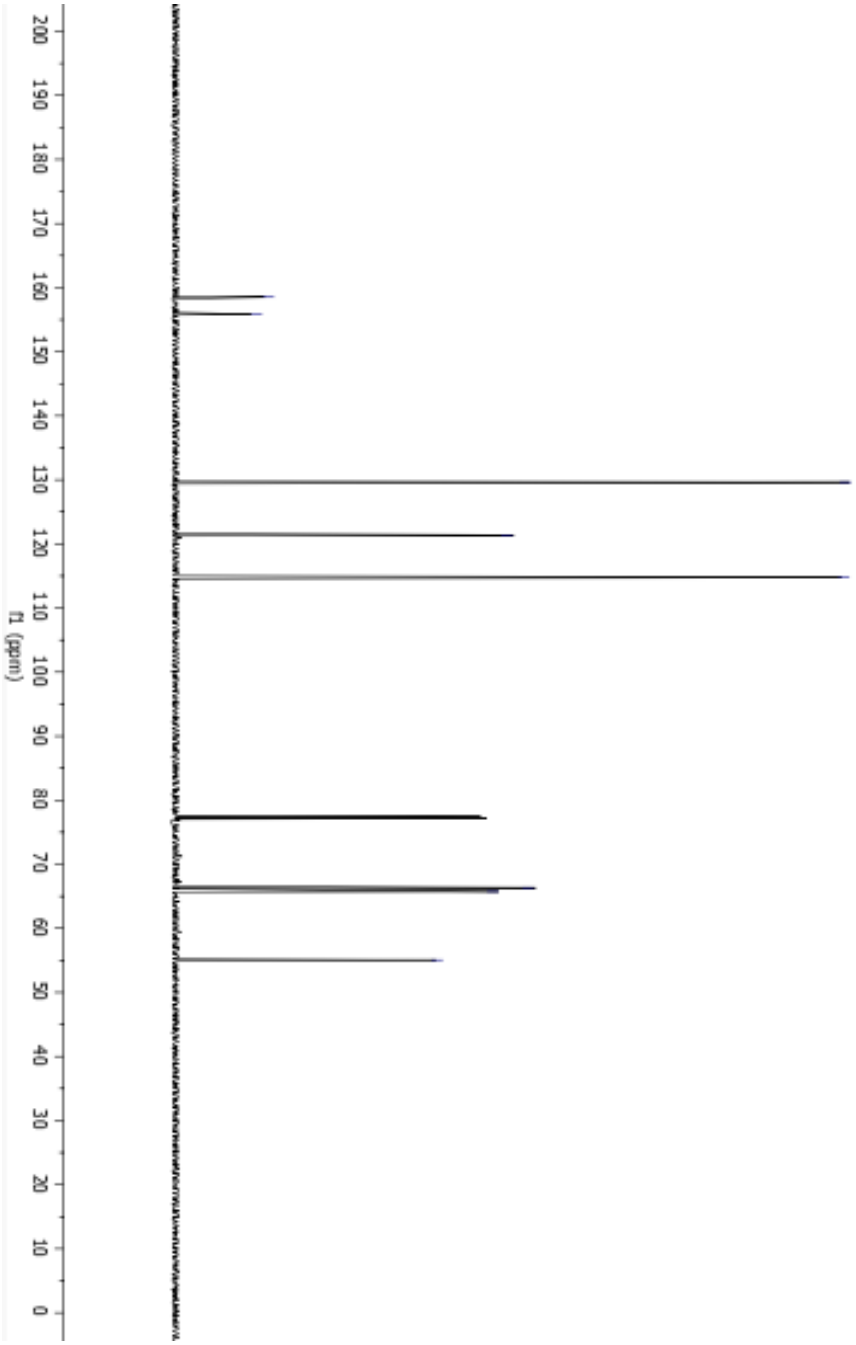

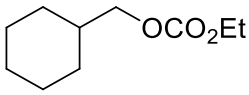

Compound 1-33

^{1}H NMR spectrum ($CDCl_3$, 500 MHz)

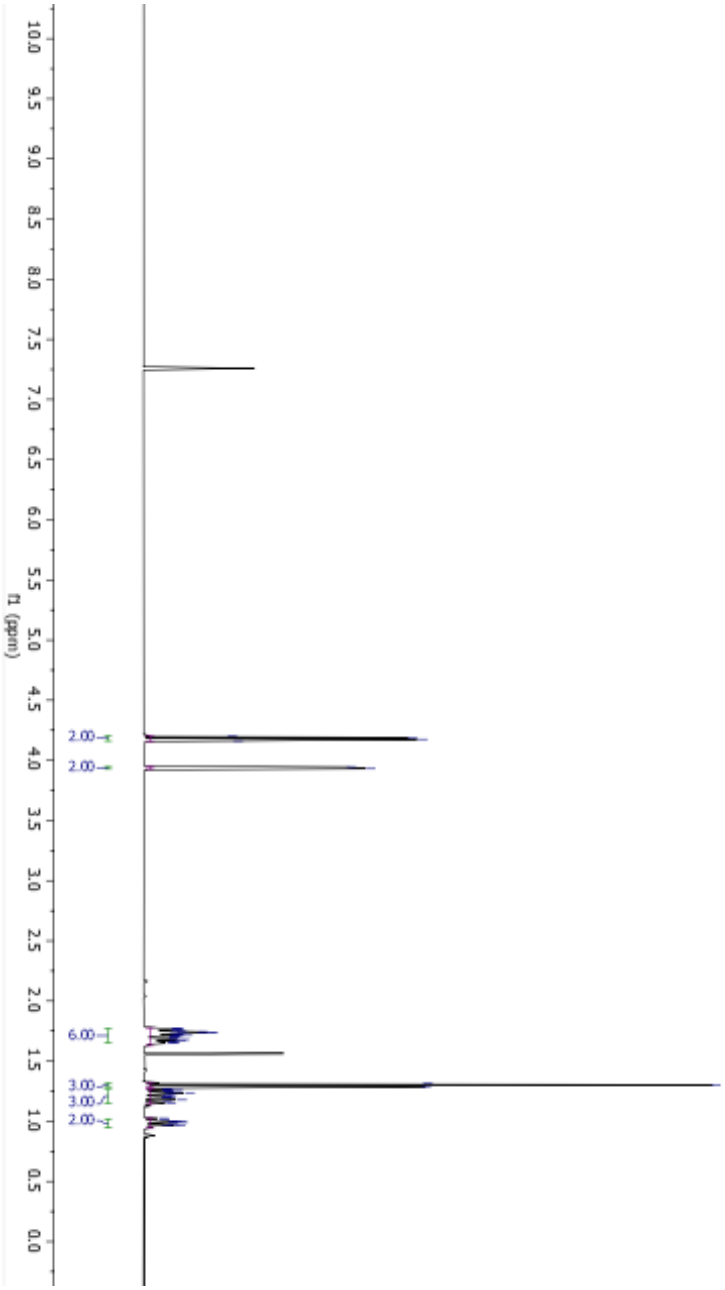

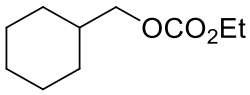

Compound 1-33

^{13}C NMR spectrum ($CDCl_3$, 500 MHz)

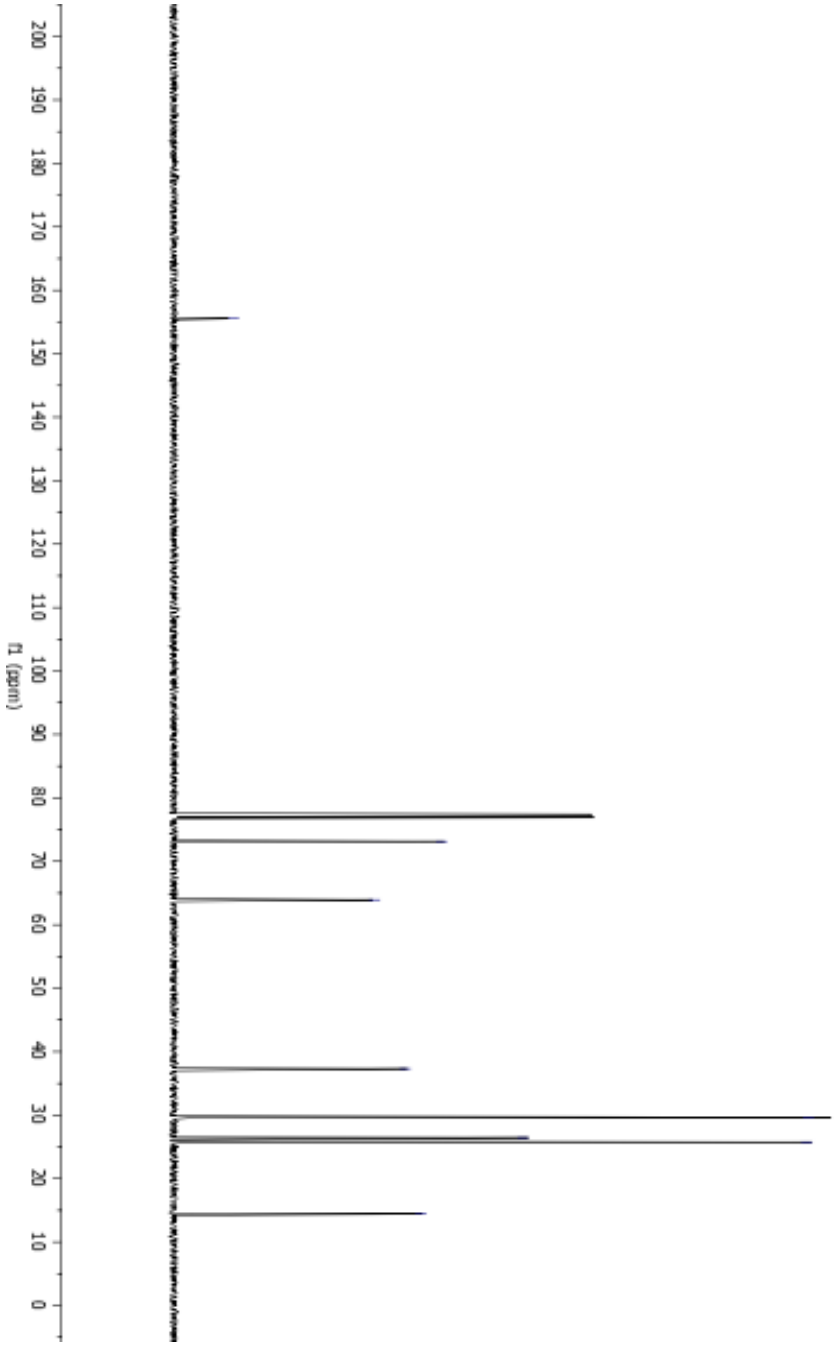

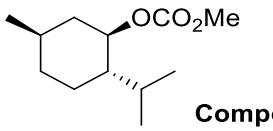

Compound 1-34

^{1}H NMR spectrum ($CDCl_3$, 500 MHz)

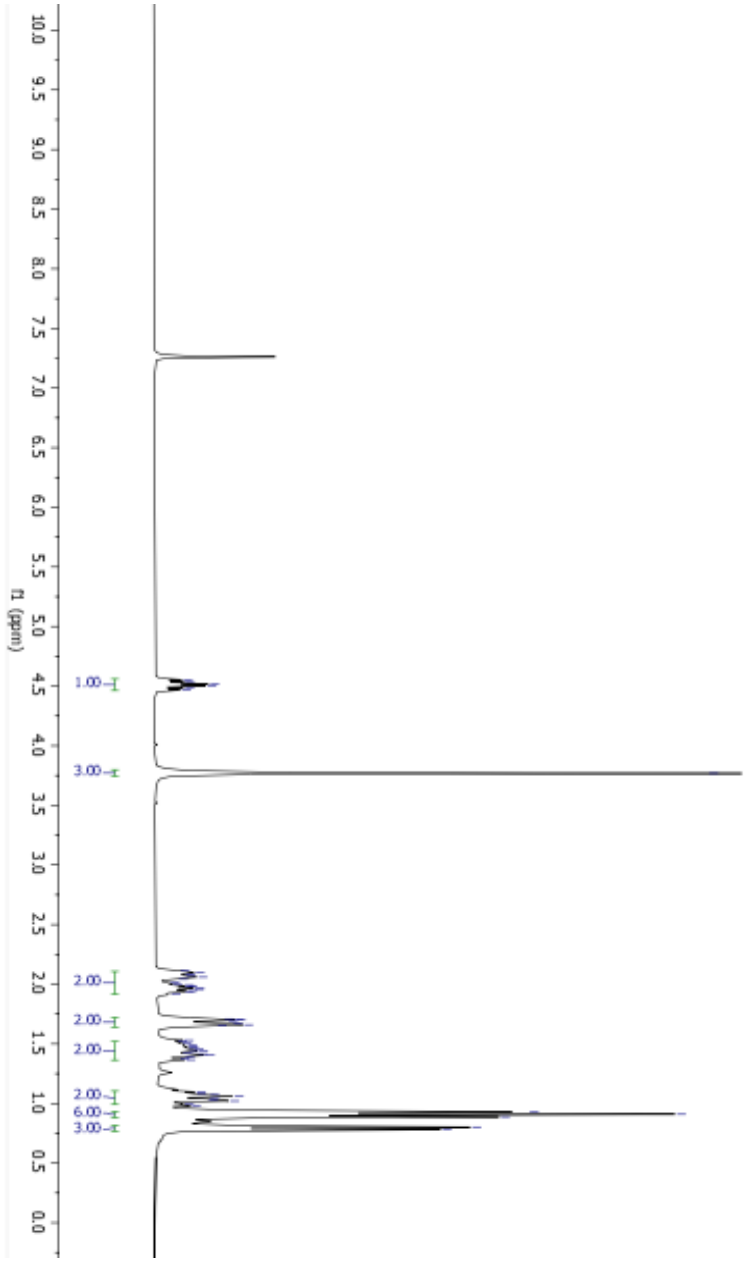

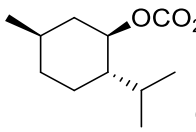

Compound 1-34

^{13}C NMR spectrum ($CDCl_3$, 500 MHz)

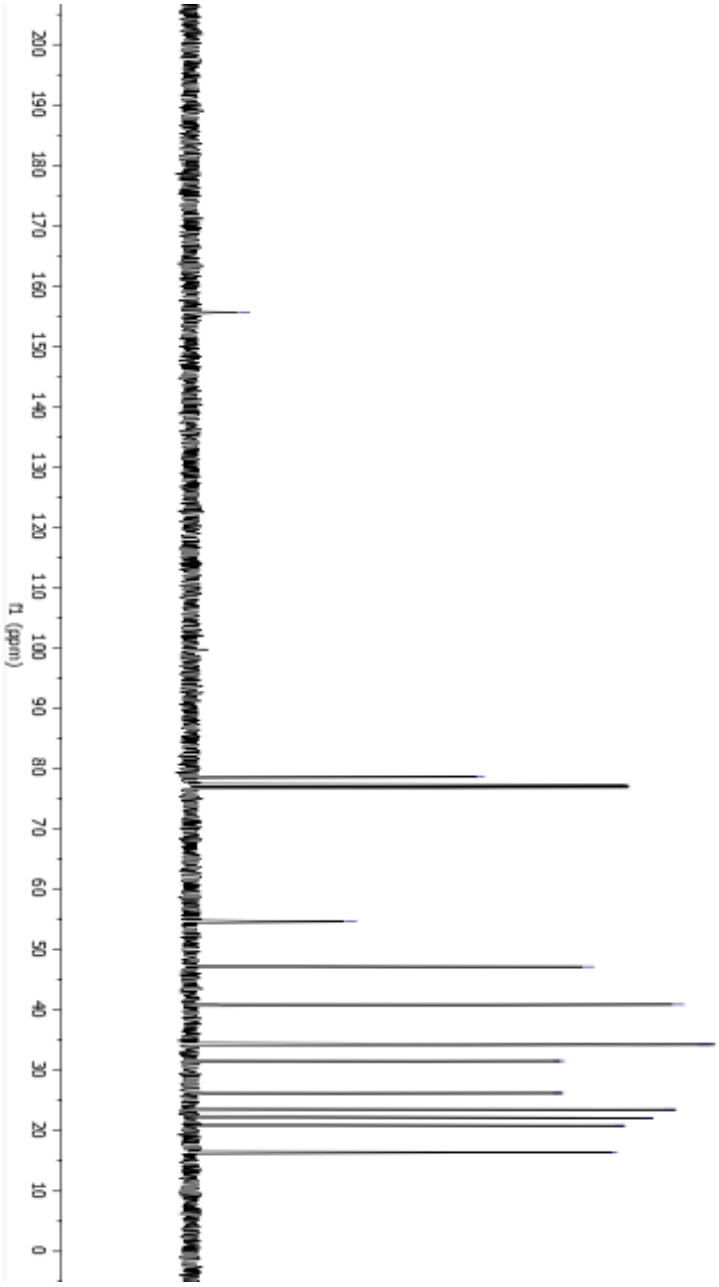

Appendix III

^{1}H and ^{13}C NMR Spectra

Chapter 3

EXPERIMENTAL: X-ray diffraction data for **3-6** were collected at 100 K on a Bruker D8 Venture using MoKα-radiation (λ=0.71073 Å). Data have been corrected for absorption using SADABS[1] area detector absorption correction program. Using Olex2[2], the structure was solved with the SHELXT[3] structure solution program using Direct Methods and refined with the SHELXL[4] refinement package using least squares minimization. All non-hydrogen atoms were refined with anisotropic thermal parameters. Hydrogen atoms attached to heteroatoms were found from the residual density maps, placed, and refined with isotropic thermal parameters. The hydrogen atom of the amine required a N—H distance restraint (DFIX 0.87 0.02) due to unreasonable lengthening of the N—H bond upon initial refinement. The rest of the hydrogen atoms of the investigated structure were located from difference Fourier maps but finally their positions were placed in geometrically calculated positions and refined using a riding model. Isotropic thermal parameters of the placed hydrogen atoms were fixed to 1.2 times the *U* value of the atoms they are linked to. Calculations and refinement of structures were carried out using APEX3[5], SHELXTL[6], and Olex2 software.

Crystallographic Data for **3-6** $C_{56}H_{102}CaCl_2N_6O_{14}$ (*M* =1194.41 g/mol): monoclinic, space group C2/c (no. 15), *a* = 18.3034(10) Å, *b* = 21.5957(12) Å, *c* = 16.3153(10) Å, *β* = 101.582(2)°, *V* = 6317.7(6) Å^3, *Z* = 4, *T* = 100 K, μ(MoKα) = 0.249 mm^{-1}, *Dcalc* = 1.256 g/cm^3, 2Θmax =50.12°, 91044 reflections measured, 5589 unique (R_{int} = 0.0920, R_{sigma} = 0.0353), R_1 was 0.0487 (I > 2σ(I)), wR_2 = 0.1257 (all data).

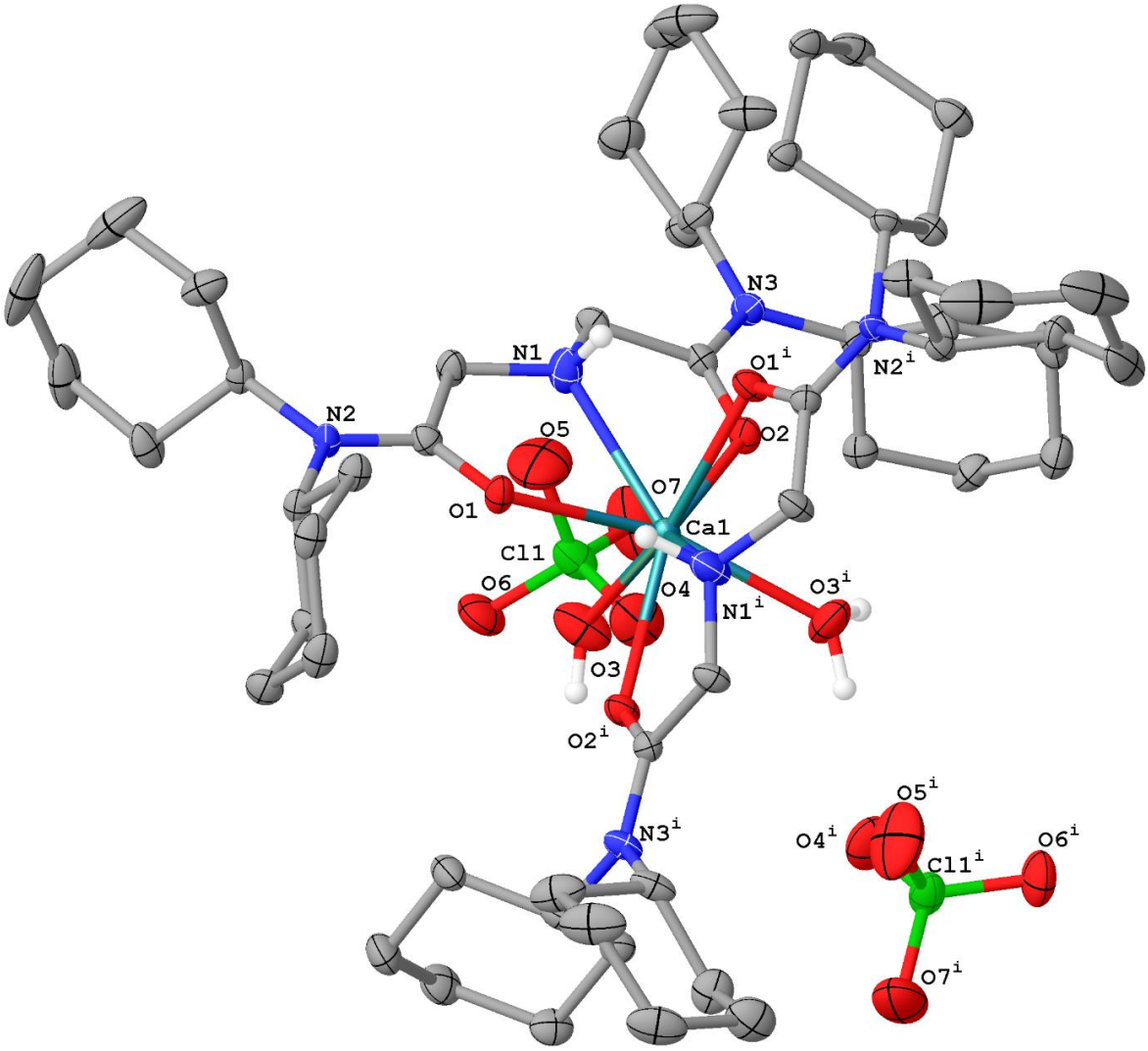

X-Ray Crystal Structure of Analogue **3-6** with Calcium perchlorate

Acknowledgement

X-ray crystallographic data were collected at the University of Montana X-ray diffraction core facility supported by the Center for Biomolecular Structure and Dynamics CoBRE (National Institutes of Health, CoBRE NIGMS P20GM103546). Single crystal X-ray diffraction data were collected using a Bruker D8 Venture, principally supported by NSF MRI CHE-1337908.

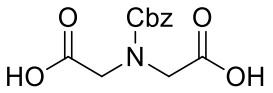

Compound 3-13

^{1}H NMR spectrum ($CDCl_3$, 500 MHz)

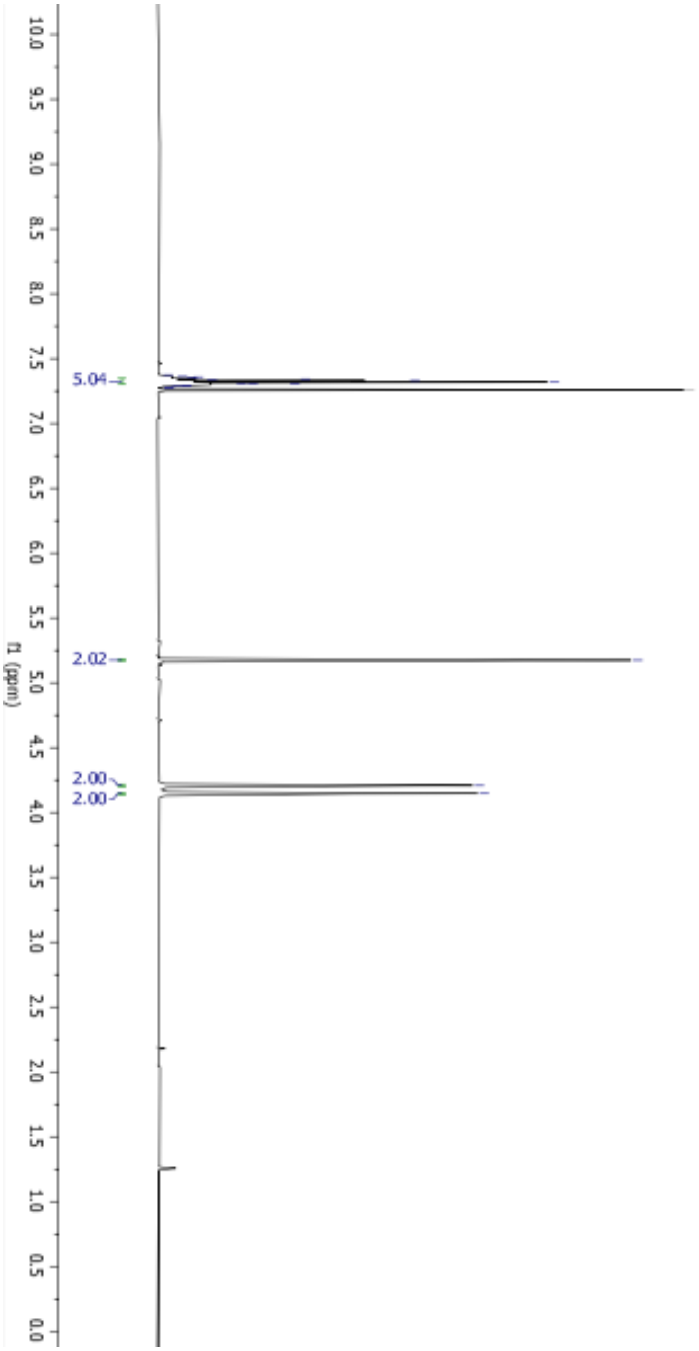

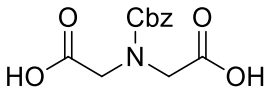

Compound 3-13

^{13}C NMR spectrum ($CDCl_3$, 500 MHz)

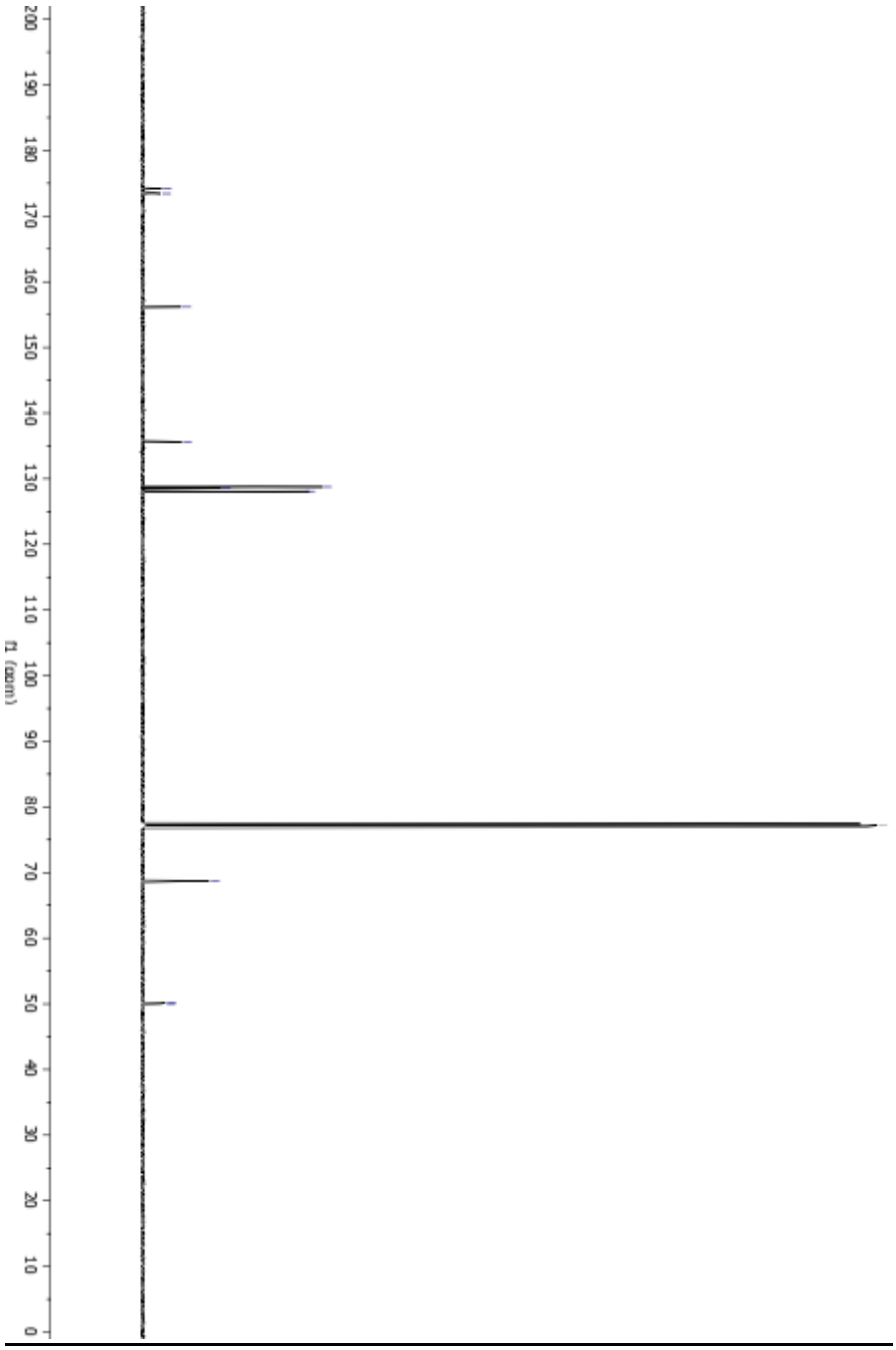

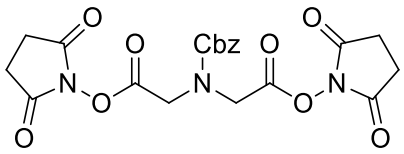

Compound 3-14

^{1}H NMR spectrum ($CDCl_3$, 500 MHz)

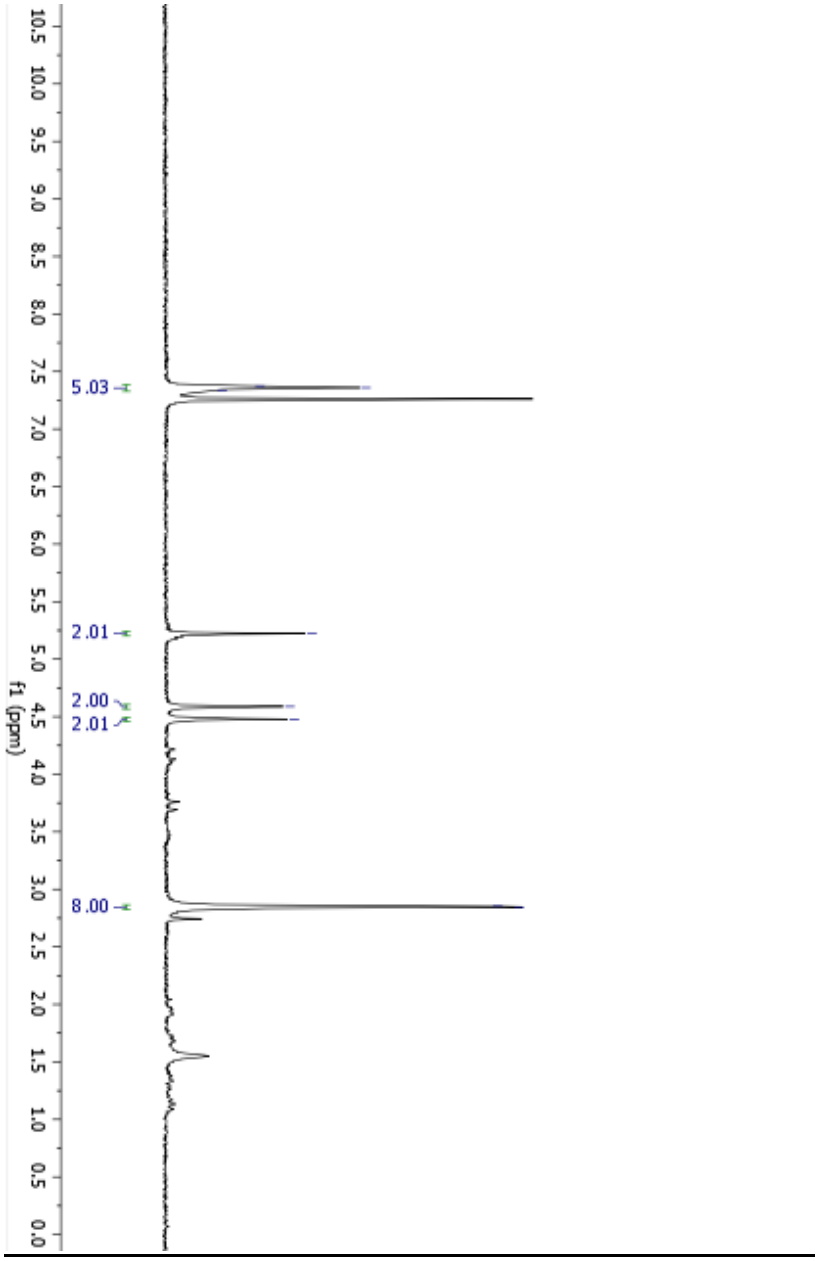

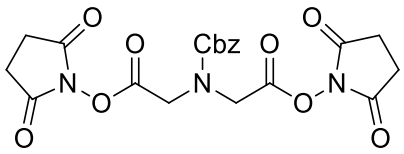

Compound 3-14

^{13}C NMR spectrum ($CDCl_3$, 500 MHz)

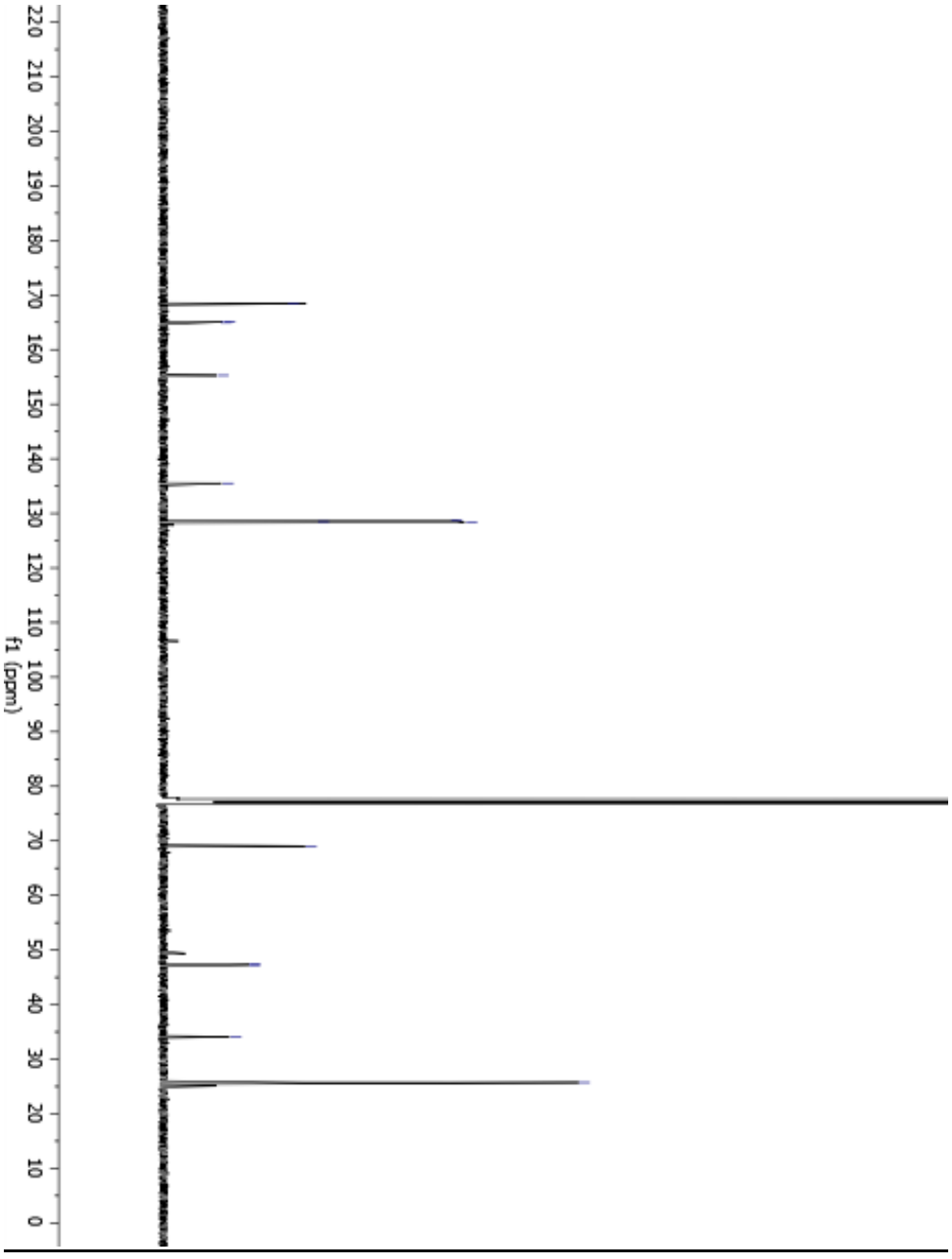

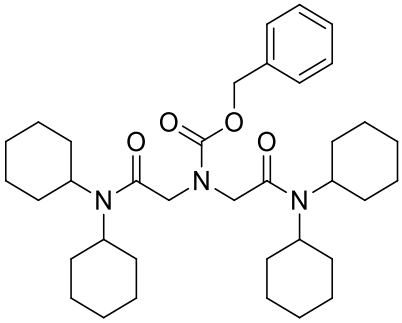

^{1}H NMR spectrum ($CDCl_3$, 500 MHz)

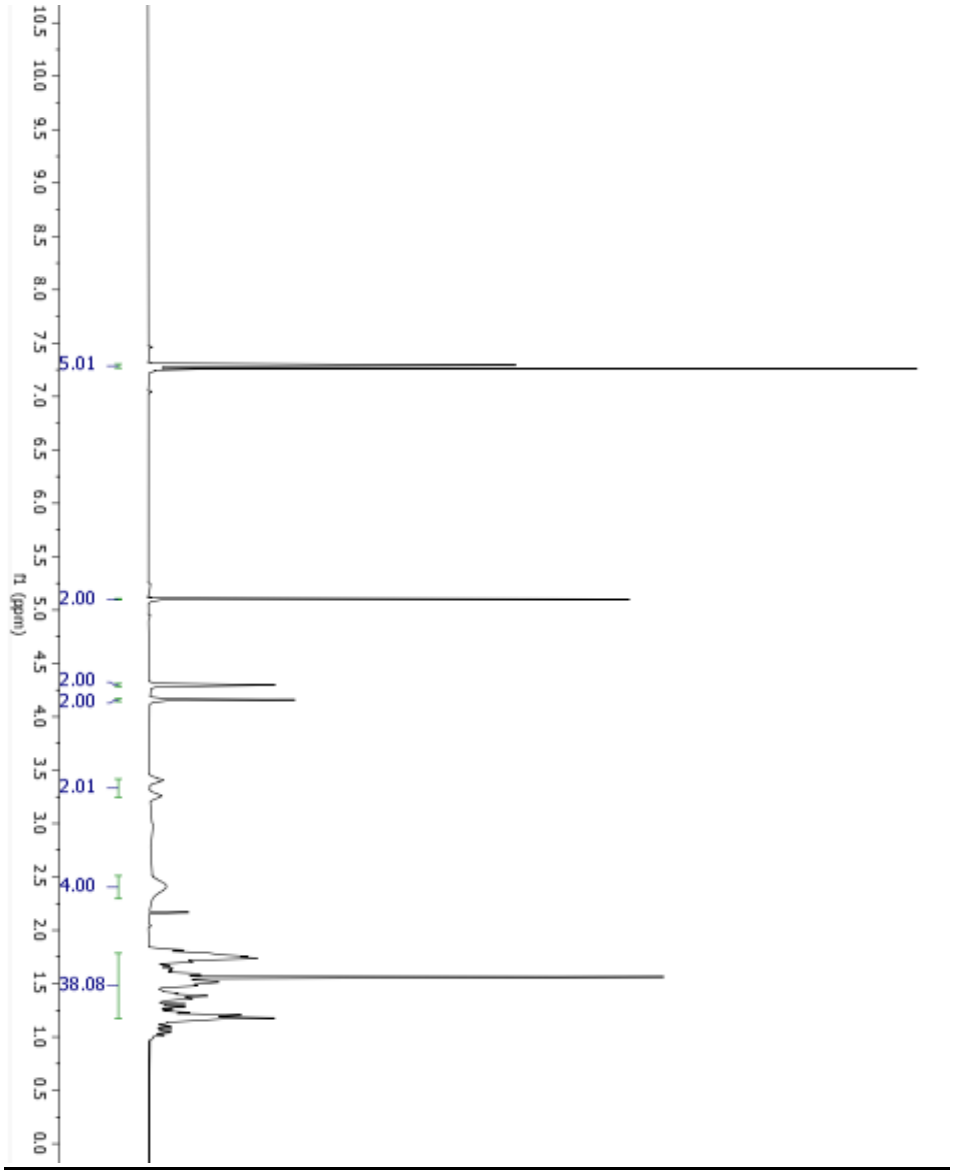

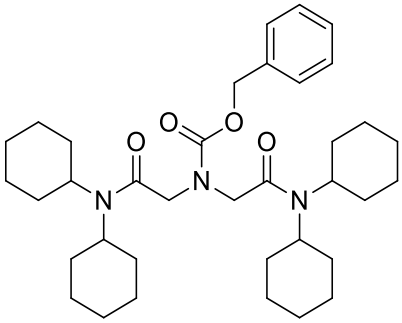

^{13}C NMR spectrum ($CDCl_3$, 500 MHz)

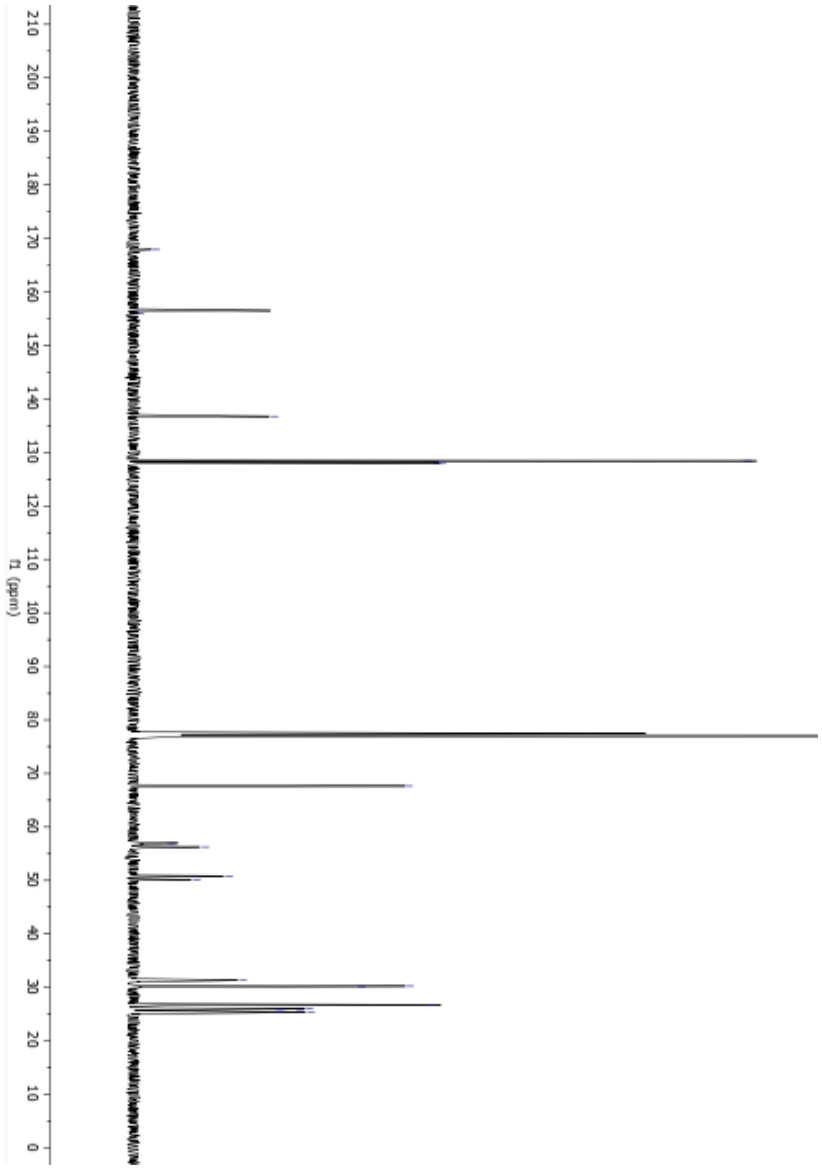

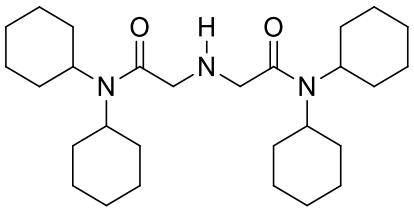

Compound 3-11

^{1}H NMR spectrum ($CDCl_3$, 500 MHz)

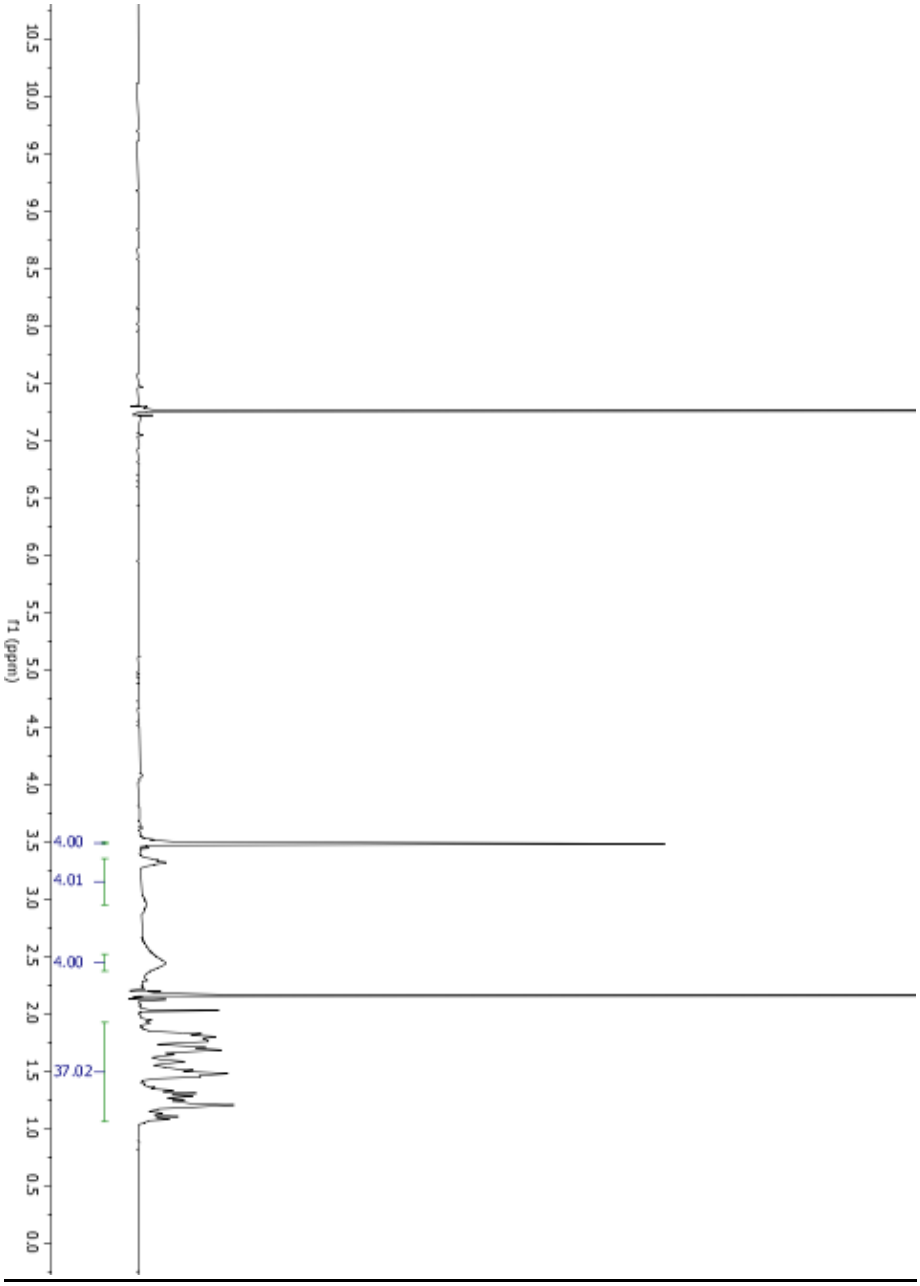

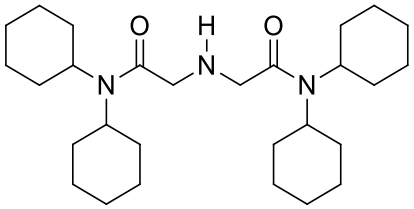

Compound 3-11

^{13}C NMR spectrum ($CDCl_3$, 500 MHz)

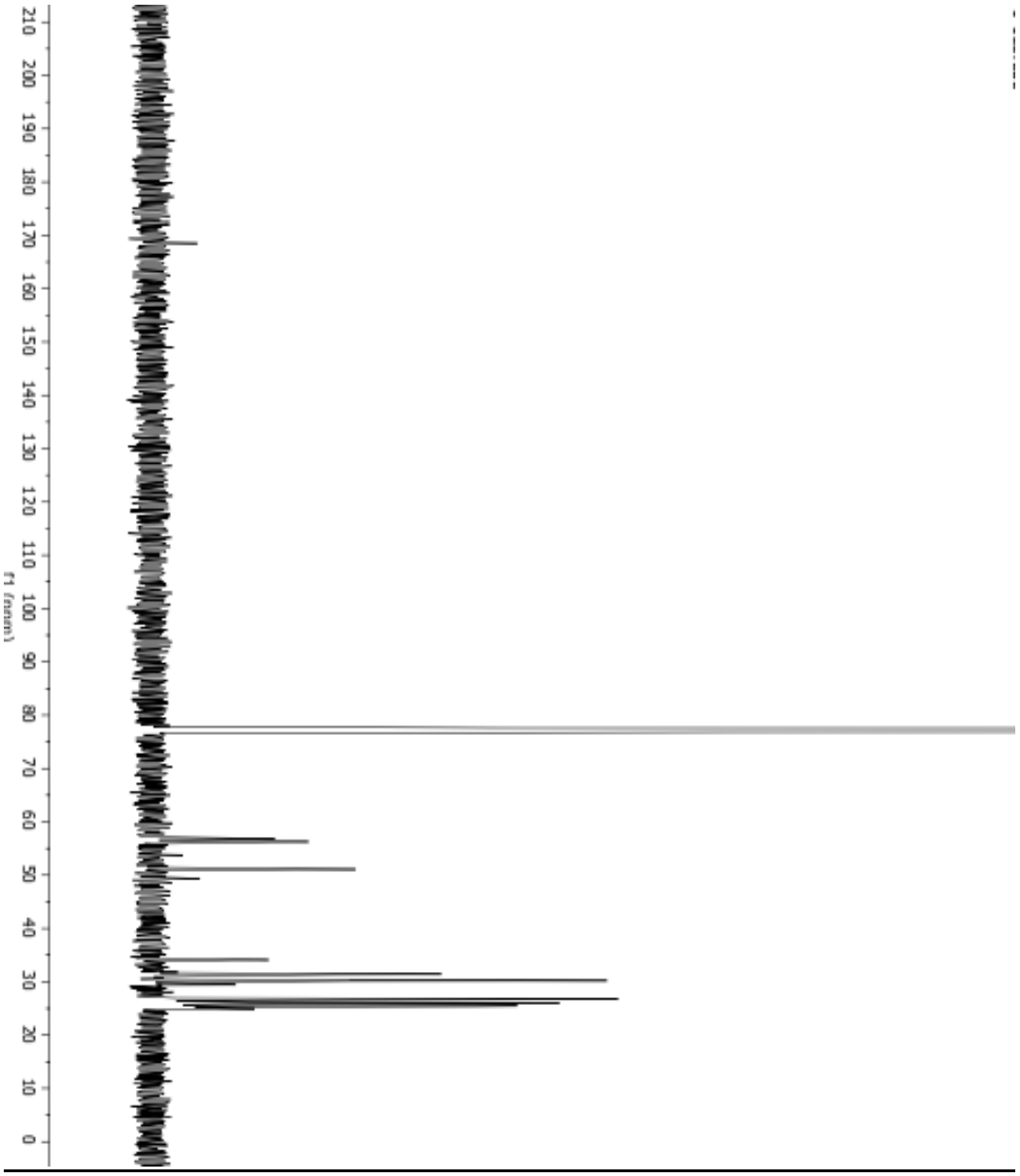

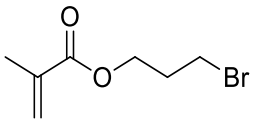

Compound 3-9

^{1}H NMR spectrum ($CDCl_3$, 300 MHz)

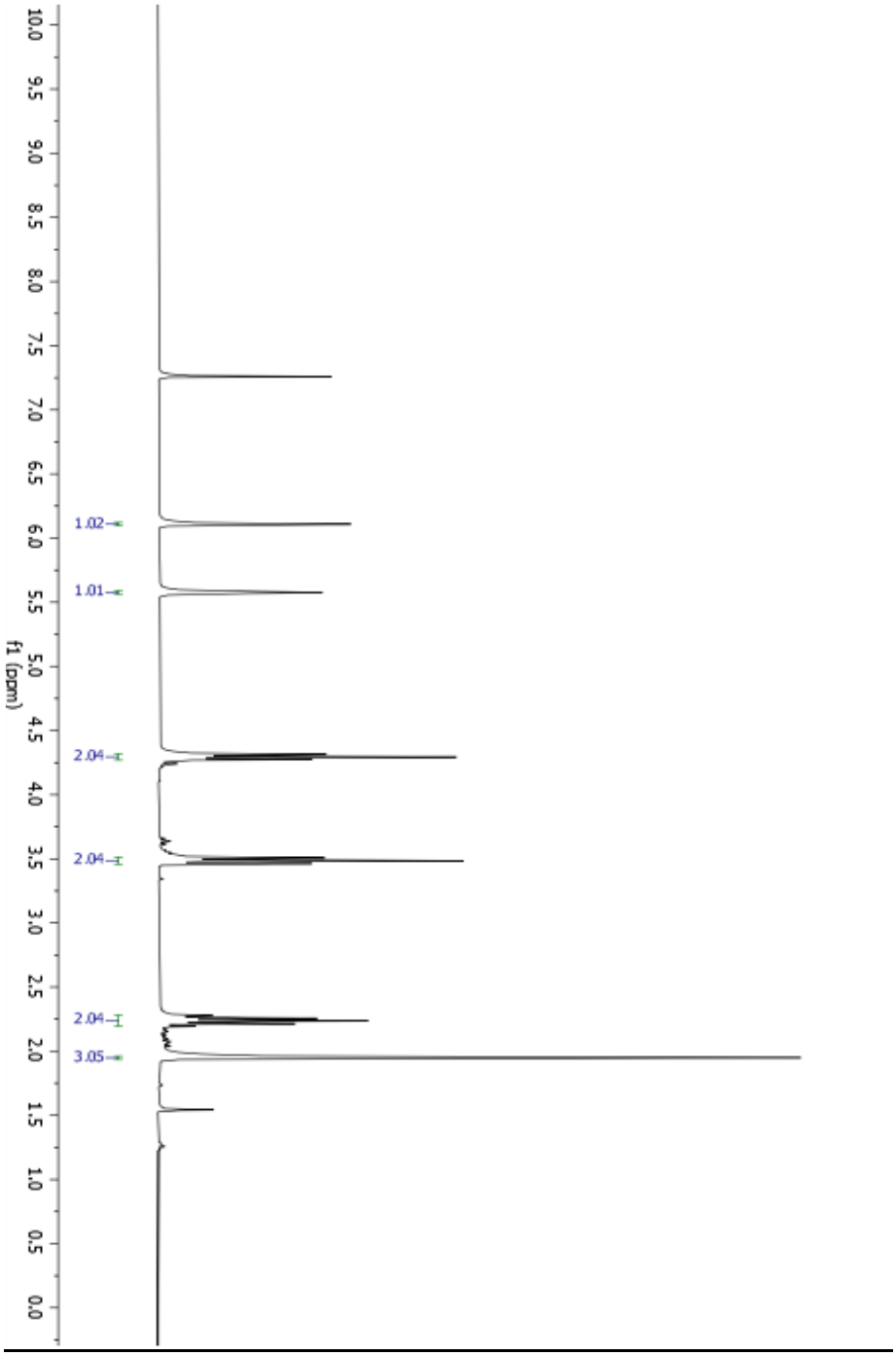

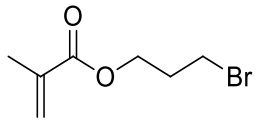

Compound 3-9

^{13}C NMR spectrum ($CDCl_3$, 300 MHz)

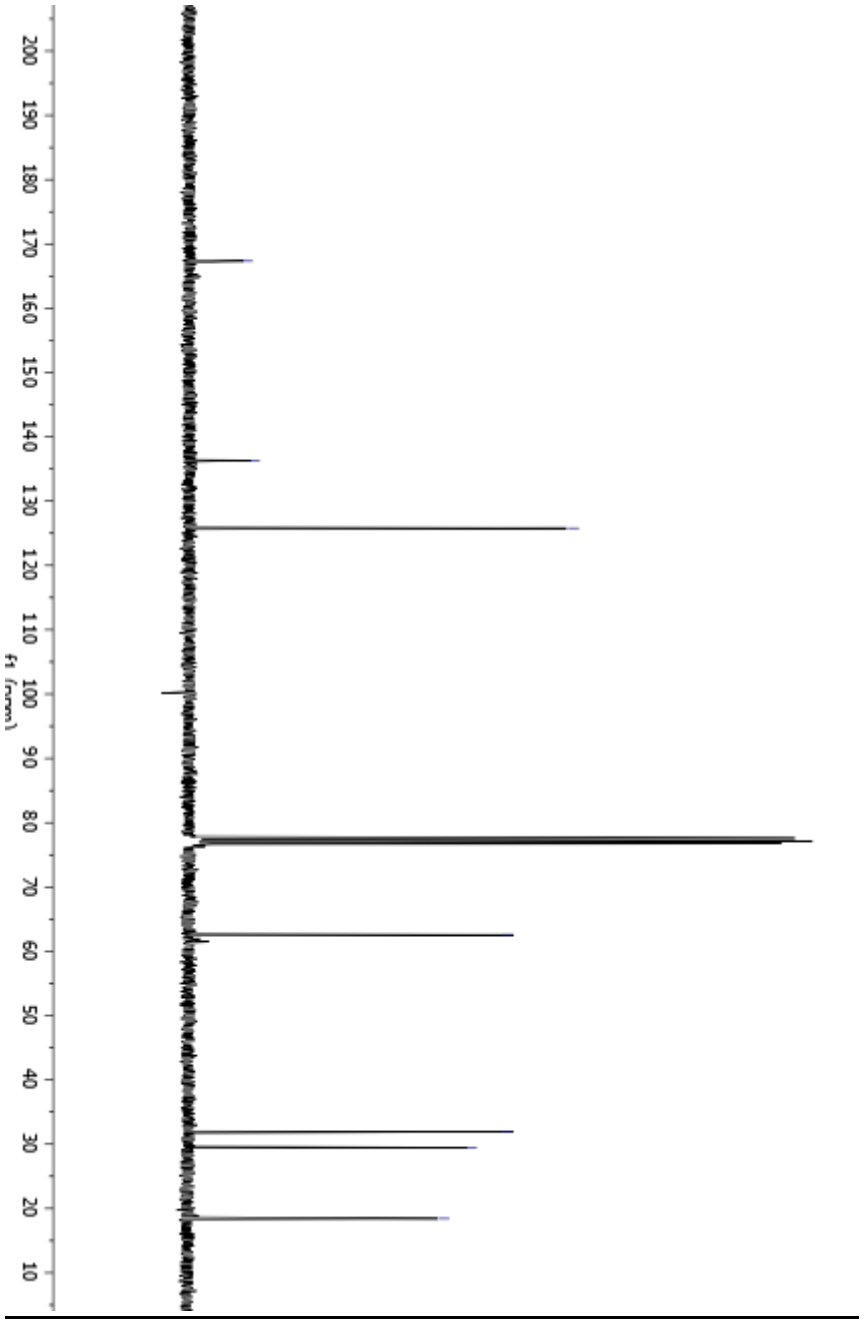

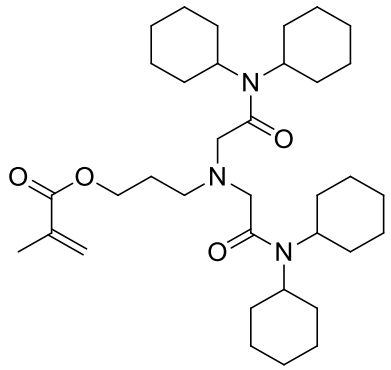

Compound 3-12

^{1}H NMR spectrum ($CDCl_3$, 500 MHz)

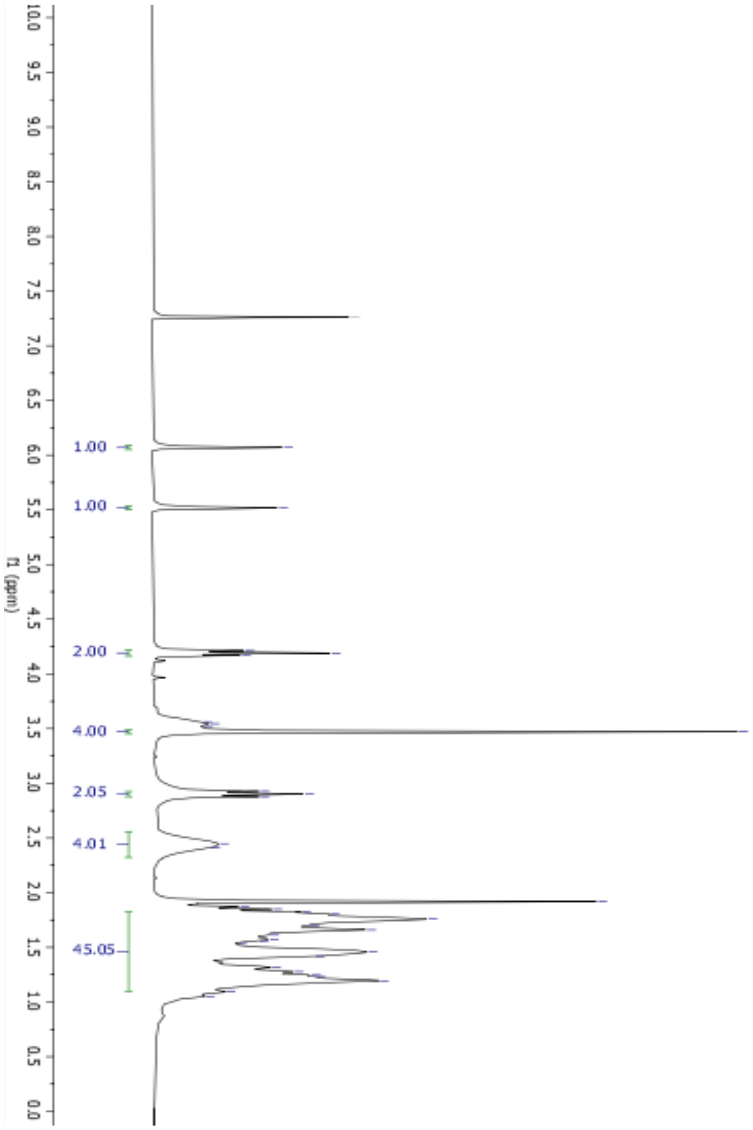

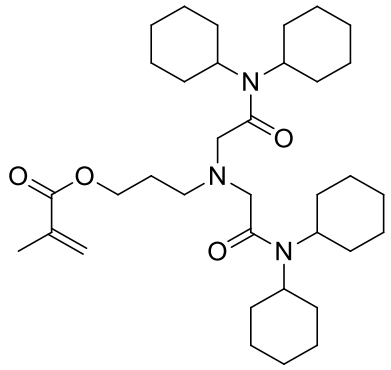

Compound 3-12

^{13}C NMR spectrum ($CDCl_3$, 500 MHz)

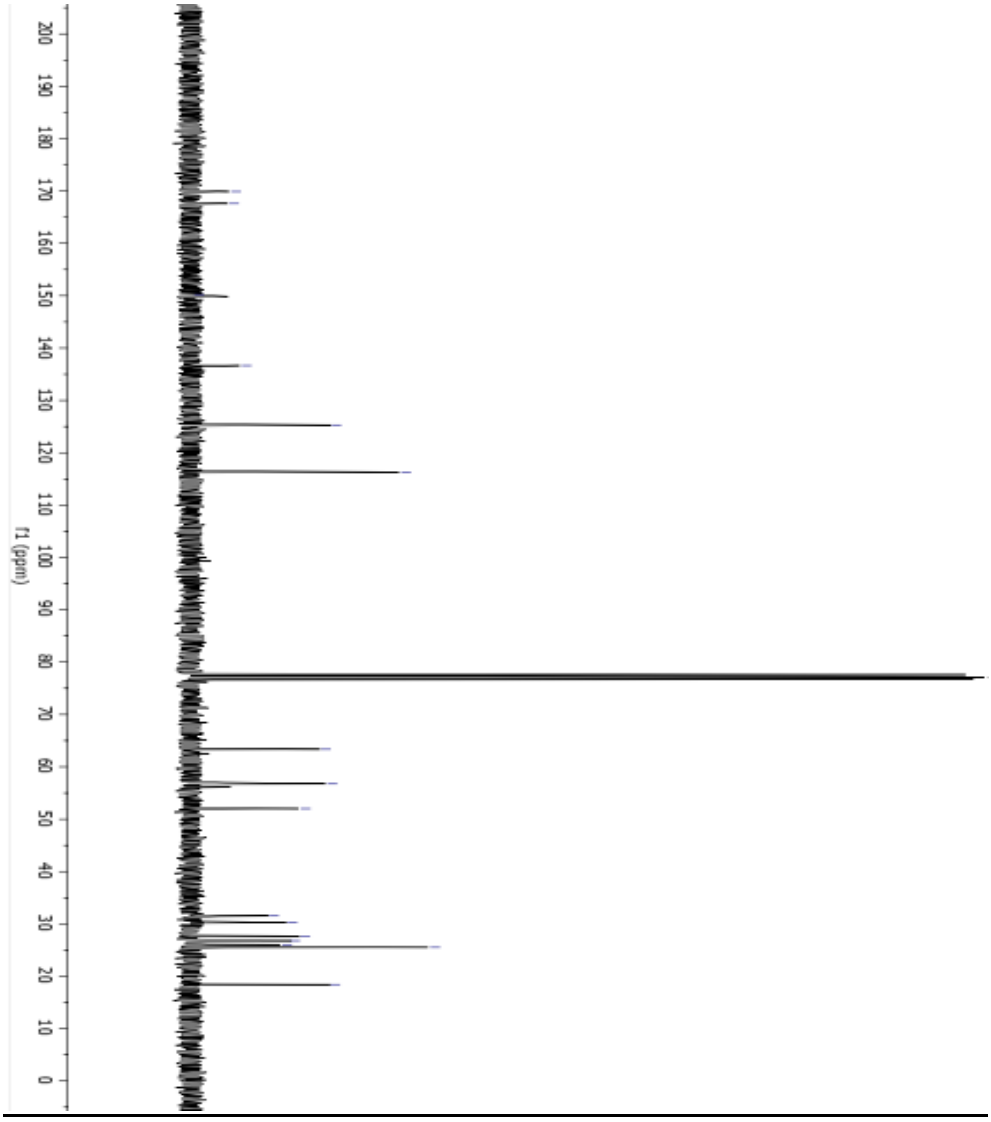

References

1) Sheldrick, G. M. (1996). SADABS: Area Detector Absorption Correction; University of Göttingen, Germany.

2) Dolomanov, O.V.; Bourhis, L.J.; Gildea, R.J.; Howard, J.A.K.; Puschmann, H., (2009). J. Appl. Cryst., 42, 339-341.

3) Sheldrick, G. M. (2015). *Acta Cryst.* A71, 3-8.

4) Sheldrick, G. M. (2015). *Acta Cryst.* C71, 3-8.

5) Bruker (2016). APEX3. Bruker AXS Inc., Madison, Wisconsin, USA.

6) Sheldrick, G.M. (2008). Acta Cryst. A64, 112-122.

Crystal of Compound 3-11 with Calcium perchlorate
Table 1. Crystal data and structure refinement for 3-11.

Identification code	3-11
Empirical formula	$C_{56}H_{102}CaCl_2N_6O_{14}$
Formula weight	1194.41
Temperature/K	100
Crystal system	monoclinic
Space group	C2/c
a/Å	18.3034(10)
b/Å	21.5957(12)
c/Å	16.3153(10)
α/°	90
β/°	101.582(2)
γ/°	90
Volume/Å^3	6317.7(6)
Z	4
ρ_{calc}g/cm^3	1.256
μ/mm^{-1}	0.249
F(000)	2584.0
Crystal size/mm^3	0.41 × 0.04 × 0.01
Radiation	MoKα (λ = 0.71073)
2Θ range for data collection/°	5.098 to 50.12
Index ranges	$-21 \leq h \leq 21$, $-25 \leq k \leq 25$, $-19 \leq l \leq 19$
Reflections collected	91044
Independent reflections	5589 [R_{int} = 0.0920, R_{sigma} = 0.0353]

Data/restraints/parameters	5589/1/369
Goodness-of-fit on F^2	1.027
Final R indexes [I>=2σ (I)]	R_1 = 0.0487, wR_2 = 0.1115
Final R indexes [all data]	R_1 = 0.0754, wR_2 = 0.1257
Largest diff. peak/hole / e $Å^{-3}$	0.86/-0.67

Table 2. Fractional Atomic Coordinates (×10⁴) and Equivalent Isotropic Displacement Parameters (Å²×10³) for 3-11. U_{eq} is defined as 1/3 of the trace of the orthogonalized U_{IJ} tensor.

Atom	*x*	*y*	*z*	U(eq)
Ca1	5000	2931.4(3)	7500	16.83(18)
Cl1	3061.1(4)	1221.1(4)	5577.2(4)	30.33(19)
O1	4246.5(9)	3762.7(9)	7988.5(10)	21.3(4)
O2	4967.7(9)	2582.6(8)	6075.5(10)	20.8(4)
O3	4075.5(13)	2130.2(12)	7436.1(16)	40.2(6)
O4	3712.0(12)	1173.7(12)	6219.6(14)	47.2(6)
O5	2963.6(15)	1877.0(12)	5348(2)	68.2(8)
O6	2413.5(11)	1041.0(10)	5880.0(13)	38.8(5)
O7	3128.7(14)	902.1(15)	4849.5(15)	63.9(8)
N1	4095.4(13)	3503.5(12)	6390.5(14)	27.9(6)
N2	3133.2(11)	4257.4(10)	7899.4(12)	15.7(5)
N3	4501.2(12)	2543.3(10)	4676.7(12)	20.2(5)
C1	3446.2(14)	3789.3(13)	6636.0(15)	21.3(6)
C2	3635.9(14)	3939.4(12)	7569.6(15)	17.9(5)
C3	3907.3(15)	3222.7(12)	5559.3(15)	20.1(6)
C4	4504.1(14)	2755.8(12)	5450.8(15)	17.8(6)
C5	3287.2(13)	4435.2(12)	8798.7(14)	16.3(5)
C6	3367.1(15)	3875.9(12)	9386.7(15)	21.4(6)
C7	3430.3(16)	4095.7(14)	10292.3(16)	26.7(6)
C8	4082.2(15)	4540.0(14)	10544.0(16)	27.9(7)
C9	4008.2(15)	5088.4(13)	9946.5(16)	24.3(6)
C10	3947.8(14)	4879.2(13)	9034.6(15)	20.5(6)
C11	2401.8(13)	4454.8(12)	7394.3(15)	16.7(5)
C12	1750.4(14)	4207.8(15)	7753.5(17)	26.8(6)
C13	1014.6(16)	4383.8(18)	7177(2)	43.7(9)
C14	947.1(19)	5080(2)	7082(2)	56.5(12)
C15	1599(2)	5337.9(17)	6756(2)	51.6(10)
C16	2356.4(17)	5155.9(13)	7289.7(17)	29.2(7)

C17	5077.2(14)	2095.8(12)	4523.1(16)	21.0(6)
C18	5017.4(15)	1465.5(12)	4929.4(16)	21.6(6)
C19	5583.7(15)	1012.1(13)	4688.1(17)	25.5(6)
C20	6372.3(15)	1273.2(14)	4901.6(18)	29.6(7)
C21	6419.8(16)	1900.7(14)	4490.0(19)	31.4(7)
C22	5868.1(15)	2358.2(13)	4744.4(18)	26.2(6)
C23	3948.8(16)	2768.6(13)	3938.1(15)	23.2(6)
C24	3527.1(16)	2247.9(14)	3414.5(17)	30.2(7)
C25	2914.9(17)	2533.0(16)	2733.0(18)	35.9(7)
C26	3250.5(19)	2978.2(15)	2182.3(17)	37.5(8)
C27	3713(2)	3477.9(15)	2696.7(18)	43.0(9)
C28	4304.4(19)	3201.4(14)	3396.3(18)	34.8(7)

Table 3. Anisotropic Displacement Parameters ($Å^2×10^3$) for 3-11. The Anisotropic displacement factor exponent takes the form: $-2\pi^2[h^2a^{*2}U_{11}+2hka^*b^*U_{12}+\ldots]$.

Atom	U_{11}	U_{22}	U_{33}	U_{23}	U_{13}	U_{12}
Ca1	14.1(4)	22.2(4)	14.0(4)	0	2.5(3)	0
Cl1	26.0(4)	43.2(5)	20.8(3)	0.7(3)	2.6(3)	-10.2(3)
O1	17.4(9)	29.9(11)	16.1(9)	-2.9(8)	2.2(7)	6.0(8)
O2	19.1(9)	27.9(11)	15.4(9)	-2.3(8)	3.2(7)	3.2(8)
O3	42.9(14)	48.2(15)	28.6(12)	-6.1(12)	4.9(10)	-25.7(12)
O4	34.2(12)	67.8(17)	34.1(12)	-1.6(11)	-6.3(10)	-9.4(12)
O5	63.2(18)	41.8(16)	101(2)	27.4(15)	20.5(16)	-9.1(13)
O6	30.5(12)	48.7(14)	38.6(12)	11.2(10)	10.6(9)	-11.1(10)
O7	47.8(15)	103(2)	40.5(14)	-32.1(15)	8.8(12)	-10.4(15)
N1	24.4(13)	38.4(15)	21.4(12)	-6.5(11)	5.5(10)	5.5(11)
N2	12.6(10)	22.8(12)	11.2(10)	-3.3(8)	1.3(8)	1.2(9)
N3	25.3(12)	23.0(12)	13.0(11)	-0.9(9)	5.7(9)	5.5(10)
C1	19.4(13)	29.3(16)	15.7(13)	-2.1(11)	4.6(10)	5.8(12)
C2	17.1(13)	20.8(14)	15.8(12)	-0.7(10)	3.3(10)	-1.7(11)
C3	23.9(14)	24.0(14)	12.9(12)	-1.6(10)	4.6(10)	3.0(11)
C4	17.9(13)	18.8(14)	17.9(13)	-1.6(10)	6.2(11)	-2.3(11)
C5	14.5(12)	21.7(14)	12.3(12)	-3.4(10)	1.6(10)	2.0(11)
C6	23.3(14)	23.8(15)	18.0(13)	-1.2(11)	6.6(11)	-0.3(11)
C7	29.0(15)	34.2(17)	17.6(13)	2.8(12)	6.6(11)	5.7(13)
C8	23.8(15)	40.2(18)	17.4(14)	-7.3(12)	-1.3(11)	8.5(13)
C9	16.8(13)	29.3(16)	24.3(14)	-9.9(12)	-1.5(11)	1.9(11)
C10	17.1(13)	23.7(15)	19.0(13)	-3.9(11)	-0.1(10)	0.1(11)

C11	13.5(12)	23.6(14)	12.1(12)	-3.4(10)	0.1(10)	1.7(11)
C12	15.1(13)	43.4(18)	21.4(14)	-6.0(12)	2.1(11)	-6.6(12)
C13	14.4(14)	83(3)	32.1(17)	-19.0(17)	0.4(12)	2.7(16)
C14	33.8(19)	85(3)	41(2)	-24(2)	-15.7(16)	38(2)
C15	66(3)	42(2)	35.9(19)	-4.0(16)	-14.9(17)	30.0(19)
C16	37.7(17)	24.2(16)	23.0(15)	1.0(12)	-0.2(12)	5.7(13)
C17	24.6(14)	23.2(14)	16.7(13)	-3.4(11)	7.7(11)	4.7(12)
C18	21.8(14)	22.9(14)	20.0(13)	-1.9(11)	4.0(11)	-0.2(11)
C19	27.0(15)	23.4(15)	24.6(14)	-0.3(12)	1.4(12)	6.4(12)
C20	23.2(15)	34.6(17)	31.0(16)	-2.4(13)	5.3(12)	8.2(13)
C21	26.9(15)	34.8(17)	36.7(17)	-4.3(13)	16.5(13)	0.0(13)
C22	30.2(16)	21.5(15)	31.2(15)	-3.3(12)	16.7(12)	-2.1(12)
C23	31.4(15)	24.9(15)	13.7(13)	0.4(11)	5.5(11)	10.9(12)
C24	30.2(16)	33.9(17)	24.6(15)	6.4(13)	1.1(12)	-1.3(13)
C25	36.6(18)	45(2)	23.6(15)	1.6(14)	-0.3(13)	6.1(15)
C26	55(2)	37.2(19)	16.7(14)	1.0(13)	-0.3(14)	11.9(16)
C27	78(3)	28.2(18)	20.5(15)	6.6(13)	4.1(16)	5.5(17)
C28	56(2)	23.9(16)	22.0(15)	1.5(12)	1.4(14)	-4.4(15)

Table 4. Bond Lengths for 3-11.

Atom	Atom	Length/Å	Atom	Atom	Length/Å
Ca1	O1	2.4904(18)	C5	C6	1.531(4)
Ca1	O1[1]	2.4903(18)	C5	C10	1.531(4)
Ca1	O2	2.4325(17)	C6	C7	1.534(4)
Ca1	O2[1]	2.4325(17)	C7	C8	1.522(4)
Ca1	O3[1]	2.408(2)	C8	C9	1.523(4)
Ca1	O3	2.408(2)	C9	C10	1.537(3)
Ca1	N1[1]	2.518(2)	C11	C12	1.527(4)
Ca1	N1	2.518(2)	C11	C16	1.524(4)
Cl1	O4	1.424(2)	C12	C13	1.528(4)
Cl1	O5	1.467(3)	C13	C14	1.513(6)
Cl1	O6	1.427(2)	C14	C15	1.508(6)
Cl1	O7	1.399(2)	C15	C16	1.533(4)
O1	C2	1.247(3)	C17	C18	1.528(4)
O2	C4	1.246(3)	C17	C22	1.529(4)
N1	C1	1.464(3)	C18	C19	1.534(4)
N1	C3	1.462(3)	C19	C20	1.523(4)
N2	C2	1.344(3)	C20	C21	1.523(4)

N2	C5	1.488(3)	C21	C22	1.529(4)
N2	C11	1.487(3)	C23	C24	1.525(4)
N3	C4	1.343(3)	C23	C28	1.520(4)
N3	C17	1.488(3)	C24	C25	1.540(4)
N3	C23	1.491(3)	C25	C26	1.527(4)
C1	C2	1.528(3)	C26	C27	1.516(5)
C3	C4	1.523(4)	C27	C28	1.529(4)

[1]1-X,+Y,3/2-Z

Table 5. Bond Angles for 3-11.

Atom	Atom	Atom	Angle/°	Atom	Atom	Atom	Angle/°
O1[1]	Ca1	O1	87.74(9)	C4	N3	C23	121.5(2)
O1	Ca1	N1	63.25(6)	C17	N3	C23	117.66(19)
O1	Ca1	N1[1]	75.09(7)	N1	C1	C2	109.1(2)
O1[1]	Ca1	N1	75.09(7)	O1	C2	N2	123.2(2)
O1[1]	Ca1	N1[1]	63.25(6)	O1	C2	C1	118.7(2)
O2[1]	Ca1	O1[1]	128.33(6)	N2	C2	C1	118.1(2)
O2[1]	Ca1	O1	79.99(6)	N1	C3	C4	110.0(2)
O2	Ca1	O1[1]	79.99(6)	O2	C4	N3	122.7(2)
O2	Ca1	O1	128.33(6)	O2	C4	C3	119.4(2)
O2[1]	Ca1	O2	143.92(9)	N3	C4	C3	117.9(2)
O2[1]	Ca1	N1[1]	65.09(7)	N2	C5	C6	112.9(2)
O2	Ca1	N1[1]	136.47(7)	N2	C5	C10	113.2(2)
O2	Ca1	N1	65.09(7)	C10	C5	C6	111.4(2)
O2[1]	Ca1	N1	136.47(7)	C5	C6	C7	109.8(2)
O3[1]	Ca1	O1	159.03(7)	C8	C7	C6	111.0(2)
O3	Ca1	O1[1]	159.03(7)	C7	C8	C9	110.7(2)
O3[1]	Ca1	O1[1]	95.87(8)	C8	C9	C10	111.8(2)
O3	Ca1	O1	95.87(8)	C5	C10	C9	109.1(2)
O3	Ca1	O2	81.61(8)	N2	C11	C12	111.9(2)
O3	Ca1	O2[1]	72.60(8)	N2	C11	C16	111.7(2)
O3[1]	Ca1	O2	72.60(8)	C16	C11	C12	111.2(2)
O3[1]	Ca1	O2[1]	81.61(8)	C11	C12	C13	109.7(2)
O3	Ca1	O3[1]	88.13(13)	C14	C13	C12	110.7(3)
O3	Ca1	N1	88.08(9)	C15	C14	C13	110.4(3)
O3	Ca1	N1[1]	137.62(8)	C14	C15	C16	113.2(3)
O3[1]	Ca1	N1	137.62(8)	C11	C16	C15	109.9(3)
O3[1]	Ca1	N1[1]	88.07(9)	N3	C17	C18	113.0(2)

N1[1]	Ca1	N1	121.24(12)	N3	C17	C22	112.9(2)
O4	Cl1	O5	107.35(16)	C18	C17	C22	112.0(2)
O4	Cl1	O6	110.86(13)	C17	C18	C19	110.3(2)
O6	Cl1	O5	106.54(15)	C20	C19	C18	111.3(2)
O7	Cl1	O4	112.69(16)	C21	C20	C19	111.3(2)
O7	Cl1	O5	106.60(19)	C20	C21	C22	110.9(2)
O7	Cl1	O6	112.38(15)	C21	C22	C17	110.0(2)
C2	O1	Ca1	122.56(16)	N3	C23	C24	113.4(2)
C4	O2	Ca1	124.79(16)	N3	C23	C28	111.8(2)
C1	N1	Ca1	117.56(16)	C28	C23	C24	110.8(2)
C3	N1	Ca1	117.49(17)	C23	C24	C25	108.8(2)
C3	N1	C1	112.1(2)	C26	C25	C24	110.9(3)
C2	N2	C5	121.2(2)	C27	C26	C25	111.6(2)
C2	N2	C11	122.50(19)	C26	C27	C28	111.6(3)
C11	N2	C5	116.34(18)	C23	C28	C27	110.6(3)
C4	N3	C17	120.8(2)				

[1]1-X,+Y,3/2-Z

Table 6. Hydrogen Bonds for 3-11.

D	H	A	d(D-H)/Å	d(H-A)/Å	d(D-A)/Å	D-H-A/°
O3	H3B	O4	0.87(5)	1.99(5)	2.849(3)	172(4)

Table 7. Hydrogen Atom Coordinates (Å×10^4) and Isotropic Displacement Parameters (Å^2×10^3) for 3-11.

Atom	*x*	*y*	*z*	U(eq)
H3A	4080(20)	1890(20)	7840(30)	64(14)
H3B	3930(20)	1860(20)	7040(30)	67(13)
H1	4465(18)	3794(16)	6410(30)	75(14)
H1A	3016.25	3502.14	6517.93	26
H1B	3308.46	4173.44	6310.41	26
H3C	3869.82	3548.72	5126.28	24
H3D	3417.93	3012.56	5488.98	24
H5	2838.06	4667.61	8891.03	20
H6A	3817.52	3636.55	9337.2	26
H6B	2927.9	3601.86	9227.94	26
H7A	2962.11	4305.5	10349.31	32
H7B	3500.79	3733.38	10671.72	32
H8A	4555.28	4319.3	10538.29	33

H8B	4096.91	4690.76	11120.13	33
H9A	4447.77	5361.72	10108.3	29
H9B	3558.93	5330.38	9993.1	29
H10A	3874.06	5243.68	8659.01	25
H10B	4413.75	4668.69	8971.35	25
H11	2358.45	4271.5	6823.75	20
H12A	1769.08	4384.63	8317.13	32
H12B	1786.93	3751.63	7807.24	32
H13A	989.15	4192.13	6620.78	52
H13B	593.22	4222.92	7411.28	52
H14A	476.64	5184.25	6690.45	68
H14B	931.62	5269.3	7631.14	68
H15A	1560.68	5795.1	6735.88	62
H15B	1571.94	5188.01	6177.14	62
H16A	2761.61	5301.35	7016.62	35
H16B	2420.85	5355.7	7845.76	35
H17	4973.49	2020.83	3905.71	25
H18A	4506.79	1299.47	4743.74	26
H18B	5112.91	1512.61	5545.25	26
H19A	5564.99	616.16	4989.17	31
H19B	5449.29	926.31	4080.37	31
H20A	6526.56	1317.06	5516.11	36
H20B	6720.01	980.86	4710.8	36
H21A	6308.85	1851.24	3874.17	38
H21B	6932.62	2065.86	4658.06	38
H22A	5890.12	2756.55	4450.08	31
H22B	6004.37	2436.68	5353.84	31
H23	3570.29	3017.15	4160.09	28
H24A	3299.86	1969.36	3775.45	36
H24B	3875.06	2001.86	3152.42	36
H25A	2643.87	2198.83	2382.44	43
H25B	2552.94	2758.13	2999.57	43
H26A	3568.94	2743.26	1867.89	45
H26B	2844.29	3173.74	1771.64	45
H27A	3380.41	3751.8	2943.55	52
H27B	3959.37	3732.82	2327.01	52
H28A	4674.8	2970.17	3149.88	42

H28B	4568.75	3538.87	3746.27	42

Table 8. Crystal data and structure refinement for 3-12 (Monomer + calcium)

Identification code	3-12
Empirical formula	$C_{278}H_{486}Ca_4N_{24}O_{73}Cl_8$
Formula weight	5287.15
Temperature/K	298.0
Crystal system	orthorhombic
Space group	$P2_12_12_1$
a/Å	11.7995(6)
b/Å	24.7742(12)
c/Å	28.6649(13)
α/°	90
β/°	90
γ/°	90
Volume/Å^3	8379.4(7)
Z	1
ρ_{calc}g/cm^3	1.0477
μ/mm^{-1}	0.198
F(000)	2639.7
Crystal size/mm^3	0.2 × 0.2 × 0.1
Radiation	Mo Kα (λ = 0.71073)
2Θ range for data collection/°	4.48 to 49.5
Index ranges	-13 ≤ h ≤ 13, -28 ≤ k ≤ 27, -33 ≤ l ≤ 30
Reflections collected	91355
Independent reflections	13790 [R_{int} = 0.1187, R_{sigma} = 0.0827]
Data/restraints/parameters	13790/390/909
Goodness-of-fit on F^2	1.248
Final R indexes [I>=2σ (I)]	R_1 = 0.0933, wR_2 = 0.2355
Final R indexes [all data]	R_1 = 0.1864, wR_2 = 0.3103
Largest diff. peak/hole / e Å^{-3}	0.52/-0.54
Flack parameter	-0.01(7)

Table 9. Fractional Atomic Coordinates (×10^4) and Equivalent Isotropic Displacement Parameters (Å^2×10^3) for 3-12. U_{eq} is defined as 1/3 of of the trace of the orthogonalized U_{IJ} tensor.

Atom	*x*	*y*	*z*	U(eq)
Ca1	6584.4(13)	3556.2(6)	7263.6(5)	65.5(4)
O1	7005(5)	3946(3)	6513.7(16)	83.7(16)

O2	5847(5)	4230(2)	7783.6(16)	75.6(14)
O3	7053(5)	3135(3)	7972.1(17)	82.2(16)
O4	5881(5)	2834(2)	6754.4(16)	79.6(15)
O5	2942(9)	4454(4)	5467(3)	165(4)
O6	4496(16)	4512(9)	5156(8)	291(11)
O7	3988(6)	2797(3)	9038(2)	101.3(19)
O8	2890(10)	3222(5)	9525(3)	179(4)
O9	8240(5)	3000(3)	7038(2)	116(2)
O10	8192(5)	4138(3)	7458(2)	105(2)
N1	7322(6)	4729(3)	6153(2)	78.4(19)
N2	5070(5)	4231(3)	6920.5(18)	66.5(16)
N3	4411(7)	4677(3)	8126(2)	82.1(19)
N4	7500(6)	2341(3)	8304(2)	79.3(19)
N5	5083(5)	2846(2)	7614.3(17)	63.8(15)
N6	4443(7)	2383(3)	6426(2)	81(2)
C1	6772(7)	4424(4)	6466(3)	72(2)
C2	5828(6)	4664(3)	6759(3)	69(2)
C3	4287(7)	4466(3)	7291(2)	72(2)
C4	4905(8)	4455(3)	7753(3)	68.0(19)
C5	4388(8)	3989(3)	6525(3)	81(2)
C6	3673(10)	4394(4)	6247(3)	110(3)
C7	3224(12)	4094(5)	5804(5)	156(6)
C8	3520(20)	4711(8)	5198(5)	183(9)
C9	3100(30)	5109(7)	4891(5)	247(13)
C10	4010(40)	5409(13)	4674(7)	460(30)
C11	1890(40)	5126(18)	4809(17)	540(40)
C12	8158(8)	4480(5)	5838(3)	110(4)
C13B	7629(14)	4047(5)	5530(4)	62(4)
C14A	8870(40)	3944(16)	5267(10)	121(14)
C14B	8300(30)	3776(16)	5109(10)	137(13)
C15A	9780(40)	3727(19)	5580(20)	120(20)
C15B	9200(40)	3560(20)	5380(20)	180(20)
C16A	10210(20)	4185(17)	5828(11)	143(12)
C16B	10050(40)	3890(20)	5568(19)	159(19)
C17	9188(10)	4297(6)	6119(5)	158(6)
C18	7142(8)	5319(4)	6113(3)	93(3)
C19	8252(10)	5633(5)	6164(4)	126(4)

C20	7983(13)	6266(6)	6136(4)	143(5)
C21	7424(13)	6381(5)	5656(5)	147(5)
C22	6298(11)	6057(5)	5613(4)	129(4)
C23	6537(10)	5454(4)	5646(3)	108(3)
C24	5008(10)	4700(4)	8576(3)	98(3)
C25	6060(11)	5064(4)	8551(3)	121(4)
C26	6595(14)	5131(5)	9049(4)	154(6)
C27	6879(15)	4571(6)	9247(4)	155(6)
C28	5805(14)	4230(5)	9282(3)	141(5)
C29	5263(10)	4146(4)	8777(3)	106(3)
C30	3271(8)	4905(4)	8098(3)	93(3)
C31	2435(9)	4574(5)	8413(4)	120(4)
C32	1223(13)	4812(6)	8337(6)	171(6)
C33	1193(11)	5407(6)	8499(5)	148(5)
C34	1974(14)	5739(7)	8162(5)	170(6)
C35	3272(10)	5508(5)	8258(4)	128(4)
C36	6854(7)	2641(4)	8016(2)	68(2)
C37	5882(7)	2403(3)	7751(3)	76(2)
C38	4279(6)	2646(3)	7249(2)	66.7(19)
C39	4915(8)	2633(3)	6782(2)	68(2)
C40	4431(7)	3033(3)	8028(2)	75(2)
C41	3583(8)	2623(4)	8229(3)	90(3)
C42	3119(8)	2846(4)	8688(3)	95(3)
C43	3769(12)	2992(5)	9456(4)	112(3)
C44	4664(13)	2900(6)	9818(3)	124(4)
C45	4556(13)	3240(6)	10241(3)	154(5)
C46	5465(11)	2491(7)	9742(4)	152(6)
C47	8362(8)	2608(4)	8593(3)	94(3)
C48	7842(11)	2992(5)	8943(3)	119(4)
C49	8724(18)	3246(7)	9258(5)	200(8)
C50	9760(30)	3465(11)	8947(12)	260(18)
C51	10203(19)	3075(11)	8644(11)	233(14)
C52	9329(9)	2828(6)	8299(5)	145(5)
C53	7373(9)	1742(4)	8320(3)	97(3)
C54	8561(10)	1490(6)	8194(4)	141(4)
C55	8349(15)	833(6)	8247(7)	182(6)
C56	8063(15)	704(5)	8746(6)	164(6)

C57	6929(13)	963(5)	8852(5)	141(5)
C58	6952(9)	1562(4)	8813(3)	104(3)
C59	5137(9)	2258(4)	5994(3)	94(3)
C60	6092(10)	1876(5)	6104(3)	122(4)
C61	6757(15)	1738(7)	5652(4)	166(6)
C62	7149(16)	2240(9)	5391(4)	178(6)
C63	6096(16)	2610(6)	5262(4)	165(6)
C64	5464(12)	2787(5)	5735(3)	132(4)
C65	3243(8)	2200(4)	6427(3)	87(3)
C66	2568(9)	2490(4)	6053(4)	109(3)
C67	1261(12)	2327(6)	6133(4)	143(4)
C68	1134(10)	1708(6)	6090(4)	134(4)
C69	1895(12)	1429(5)	6450(5)	142(4)
C70	3131(9)	1581(4)	6400(4)	107(3)
Cl1	1222(2)	3614.0(18)	7208.1(11)	139.5(13)
O71	2062(9)	3630(6)	7561(4)	212(3)
O72	1776(9)	3470(6)	6804(5)	212(3)
O73A	557(19)	3068(13)	7221(9)	212(3)
O73B	200(20)	3605(15)	7327(9)	212(3)
O74A	500(20)	4021(13)	7281(10)	212(3)
O74B	1341(18)	4298(12)	7126(9)	212(3)
Cl2	5804(4)	6070.2(12)	7334.8(10)	133.8(12)
O75	6256(11)	5597(3)	7498(3)	190(5)
O76	5103(10)	6328(3)	7679(3)	169(4)
O77	6807(13)	6456(5)	7315(5)	233(6)
O78A	4650(40)	5757(18)	7155(16)	130(20)
O78B	5486(15)	6120(7)	6884(3)	175(9)
O11	8400(30)	5196(16)	7740(30)	320(40)

Table 10. Anisotropic Displacement Parameters ($Å^2×10^3$) for 3-12. The Anisotropic displacement factor exponent takes the form: $-2\pi^2[h^2a^{*2}U_{11}+2hka^*b^*U_{12}+\ldots]$.

Atom	U_{11}	U_{22}	U_{33}	U_{12}	U_{13}	U_{23}
Ca1	76.5(10)	59.8(10)	60.2(8)	1.2(8)	-0.0(7)	4.1(7)
O1	96(4)	90(5)	65(3)	16(3)	20(3)	20(3)
O2	103(4)	65(3)	59(3)	-3(3)	11(3)	-7(2)
O3	88(4)	83(5)	76(3)	-7(3)	-17(3)	19(3)

O4	95(4)	80(4)	64(3)	-4(3)	0(3)	-11(2)
O5	220(10)	155(9)	120(6)	-51(7)	-66(7)	32(6)
O6	211(14)	330(20)	330(20)	-31(16)	-80(16)	62(17)
O7	111(5)	115(5)	78(4)	-5(4)	2(4)	1(3)
O8	182(9)	235(12)	121(7)	44(9)	19(7)	-42(7)
O9	93(4)	116(6)	140(5)	20(4)	2(4)	-25(4)
O10	93(4)	114(5)	108(4)	-27(4)	1(3)	-22(3)
N1	98(5)	67(5)	70(4)	-12(4)	13(4)	19(3)
N2	73(4)	72(4)	54(3)	-5(3)	12(3)	-4(3)
N3	101(5)	73(5)	72(5)	3(4)	18(4)	-7(3)
N4	81(4)	81(5)	76(4)	4(4)	-22(4)	17(3)
N5	79(4)	57(4)	55(3)	7(3)	-14(3)	3(3)
N6	117(6)	62(5)	63(4)	2(4)	-16(4)	-8(3)
C1	77(5)	71(7)	69(5)	-11(5)	1(4)	11(4)
C2	73(5)	50(5)	83(5)	-4(4)	22(4)	1(3)
C3	83(5)	71(5)	63(4)	10(4)	5(4)	-2(4)
C4	88(6)	57(5)	59(5)	-2(4)	9(5)	-5(4)
C5	107(6)	72(6)	65(5)	-9(5)	-7(4)	-11(4)
C6	141(9)	89(7)	101(6)	8(6)	-47(6)	23(5)
C7	207(14)	96(9)	167(11)	-20(9)	-122(10)	36(8)
C8	270(20)	183(16)	96(9)	-91(17)	-64(12)	70(10)
C9	480(40)	167(15)	93(8)	-160(20)	-88(14)	49(9)
C10	810(80)	420(40)	146(15)	-410(50)	-90(30)	110(20)
C11	520(60)	400(50)	720(80)	-100(50)	-460(60)	210(50)
C12	95(7)	135(10)	100(7)	23(6)	56(6)	42(6)
C13B	127(12)	33(9)	24(6)	13(7)	40(7)	-10(5)
C14A	190(40)	90(30)	91(19)	30(20)	20(20)	-7(17)
C14B	180(30)	140(30)	89(18)	-50(20)	78(19)	-41(17)
C15A	70(30)	150(40)	160(40)	10(30)	60(30)	70(40)
C15B	100(30)	160(40)	290(50)	0(30)	110(40)	-70(30)
C16A	90(19)	220(40)	110(20)	50(20)	50(17)	30(20)
C16B	140(40)	210(40)	120(20)	-100(30)	30(20)	-30(20)
C17	91(8)	200(15)	183(12)	45(8)	21(8)	74(11)
C18	113(7)	87(8)	78(5)	-14(6)	2(5)	9(4)
C19	135(9)	112(10)	130(8)	-68(8)	7(7)	17(6)
C20	180(12)	134(12)	113(8)	-59(9)	10(8)	12(7)
C21	189(13)	91(10)	159(11)	-22(9)	5(10)	30(7)

C22	160(11)	68(8)	158(10)	0(7)	3(8)	30(6)
C23	141(8)	86(8)	97(6)	0(6)	-14(6)	19(5)
C24	144(8)	84(7)	68(5)	-4(6)	6(6)	-10(4)
C25	190(11)	88(8)	86(6)	-51(8)	-28(7)	6(5)
C26	258(17)	117(10)	86(7)	-64(10)	-40(9)	1(6)
C27	234(16)	130(12)	101(8)	-64(11)	-60(9)	16(7)
C28	245(15)	101(9)	79(6)	-32(10)	-21(8)	16(5)
C29	181(10)	56(6)	80(6)	-12(6)	-15(6)	11(4)
C30	103(7)	80(7)	95(6)	6(5)	35(5)	-8(4)
C31	98(7)	96(8)	166(10)	5(6)	54(7)	-9(7)
C32	159(12)	147(14)	207(14)	-10(10)	98(11)	-17(10)
C33	144(10)	121(11)	181(11)	28(8)	77(10)	-29(8)
C34	178(14)	151(14)	181(13)	64(11)	34(11)	7(10)
C35	130(9)	87(8)	168(10)	20(7)	54(8)	4(7)
C36	77(5)	65(6)	64(4)	2(4)	-4(4)	11(4)
C37	87(6)	62(5)	79(5)	19(4)	-24(5)	2(4)
C38	78(5)	65(5)	57(4)	4(4)	-9(4)	-3(3)
C39	82(6)	58(5)	62(5)	5(4)	-20(4)	-5(4)
C40	98(6)	73(6)	56(4)	9(4)	2(4)	-7(4)
C41	113(7)	89(7)	68(5)	-21(5)	15(5)	4(4)
C42	78(6)	110(8)	98(6)	2(5)	0(5)	2(5)
C43	123(10)	116(10)	96(9)	-14(7)	24(8)	-1(6)
C44	151(11)	158(12)	63(6)	-61(9)	11(7)	13(6)
C45	190(12)	200(14)	72(6)	-41(10)	22(7)	-4(7)
C46	101(9)	236(18)	120(9)	2(10)	16(7)	44(10)
C47	90(6)	96(7)	95(6)	-10(5)	-36(5)	30(5)
C48	165(10)	97(8)	94(7)	-11(7)	-49(7)	-5(6)
C49	270(20)	175(15)	152(11)	-54(15)	-134(14)	22(10)
C50	260(30)	220(30)	300(30)	-170(20)	-180(30)	100(20)
C51	131(14)	260(30)	310(40)	-67(18)	-105(19)	140(20)
C52	73(6)	193(13)	170(10)	-49(7)	-37(7)	80(9)
C53	121(8)	58(7)	113(7)	18(5)	-7(6)	-7(5)
C54	138(9)	135(11)	149(9)	67(8)	1(8)	-6(7)
C55	210(15)	111(12)	224(16)	85(11)	-42(14)	-18(10)
C56	206(16)	84(9)	201(14)	3(9)	-91(13)	34(9)
C57	172(12)	72(9)	180(11)	0(8)	-49(10)	42(7)
C58	135(8)	76(7)	102(6)	-11(5)	-4(6)	26(5)

C59	143(8)	84(7)	55(5)	16(6)	6(5)	-3(4)
C60	145(9)	123(9)	99(7)	43(8)	7(7)	-43(6)
C61	217(15)	181(16)	100(8)	43(12)	15(10)	-42(9)
C62	231(17)	204(18)	97(9)	16(15)	53(10)	-16(10)
C63	245(17)	166(13)	83(7)	43(12)	28(9)	-15(7)
C64	202(12)	121(10)	72(6)	-36(9)	24(7)	-6(5)
C65	90(7)	82(7)	88(6)	-4(5)	-23(5)	-12(4)
C66	106(8)	98(8)	123(8)	-5(6)	-45(6)	16(6)
C67	149(11)	123(11)	156(10)	-1(8)	-57(9)	8(8)
C68	127(9)	137(12)	138(9)	-16(8)	-51(8)	-7(7)
C69	168(12)	92(9)	166(11)	-31(8)	-9(9)	9(7)
C70	115(8)	67(7)	138(8)	-16(5)	-28(6)	2(5)
Cl1	78.8(17)	218(4)	122(2)	2(2)	7.3(16)	-18(2)
O71	140(5)	247(9)	248(7)	-28(5)	0(5)	22(6)
O72	140(5)	247(9)	248(7)	-28(5)	0(5)	22(6)
O73A	140(5)	247(9)	248(7)	-28(5)	0(5)	22(6)
O73B	140(5)	247(9)	248(7)	-28(5)	0(5)	22(6)
O74A	140(5)	247(9)	248(7)	-28(5)	0(5)	22(6)
O74B	140(5)	247(9)	248(7)	-28(5)	0(5)	22(6)
Cl2	238(4)	65.3(19)	98(2)	5(2)	-12(2)	2.6(14)
O75	320(14)	82(6)	168(7)	42(7)	-107(8)	-5(5)
O76	263(11)	108(7)	135(6)	-3(7)	43(7)	-18(5)
O77	285(15)	146(11)	270(14)	-39(10)	32(11)	21(9)
O78A	170(40)	100(30)	110(40)	10(20)	-60(30)	-50(20)
O78B	227(16)	220(16)	78(7)	78(13)	-38(8)	-5(7)
O11	150(30)	90(30)	710(120)	-40(20)	160(50)	-120(50)

Table 11. Bond Lengths for 3-12.

Atom	Atom	Length/Å	Atom	Atom	Length/Å
Ca1	O1	2.409(5)	C21	C22	1.556(19)
Ca1	O2	2.402(5)	C22	C23	1.524(15)
Ca1	O3	2.349(5)	C24	C25	1.537(15)
Ca1	O4	2.454(6)	C24	C29	1.517(13)
Ca1	O9	2.476(6)	C25	C26	1.569(14)
Ca1	O10	2.447(6)	C26	C27	1.536(19)
Ca1	N2	2.638(6)	C27	C28	1.526(19)
Ca1	N5	2.692(6)	C28	C29	1.594(13)

O1	C1	1.223(9)	C30	C31	1.570(14)
O2	C4	1.246(9)	C30	C35	1.563(14)
O3	C36	1.252(9)	C31	C32	1.563(19)
O4	C39	1.246(9)	C32	C33	1.544(18)
O5	C7	1.357(13)	C33	C34	1.570(19)
O5	C8	1.211(18)	C34	C35	1.657(19)
O6	C8	1.26(3)	C36	C37	1.498(11)
O7	C42	1.440(10)	C38	C39	1.535(11)
O7	C43	1.318(12)	C40	C41	1.538(12)
O8	C43	1.200(14)	C41	C42	1.529(12)
N1	C1	1.340(9)	C43	C44	1.498(16)
N1	C12	1.475(11)	C44	C45	1.482(16)
N1	C18	1.480(11)	C44	C46	1.402(18)
N2	C2	1.471(9)	C47	C48	1.514(15)
N2	C3	1.524(9)	C47	C52	1.520(14)
N2	C5	1.513(9)	C48	C49	1.514(17)
N3	C4	1.335(10)	C49	C50	1.61(3)
N3	C24	1.472(11)	C50	C51	1.40(4)
N3	C30	1.462(12)	C51	C52	1.55(3)
N4	C36	1.347(9)	C53	C54	1.576(14)
N4	C47	1.468(11)	C53	C58	1.561(13)
N4	C53	1.492(11)	C54	C55	1.65(2)
N5	C37	1.498(9)	C55	C56	1.50(2)
N5	C38	1.497(9)	C56	C57	1.51(2)
N5	C40	1.488(9)	C57	C58	1.489(15)
N6	C39	1.317(9)	C59	C60	1.505(14)
N6	C59	1.517(11)	C59	C64	1.555(14)
N6	C65	1.487(11)	C60	C61	1.554(16)
C1	C2	1.517(11)	C61	C62	1.52(2)
C3	C4	1.511(11)	C62	C63	1.59(2)
C5	C6	1.534(12)	C63	C64	1.608(15)
C6	C7	1.565(15)	C65	C66	1.518(13)
C8	C9	1.42(2)	C65	C70	1.541(13)
C9	C10	1.44(4)	C66	C67	1.611(18)
C9	C11	1.44(4)	C67	C68	1.545(17)
C12	C13B	1.522(17)	C68	C69	1.530(17)
C12	C17	1.527(15)	C69	C70	1.514(16)

C13B	C14B	1.59(3)	Cl1	O71	1.416(12)
C14A	C15A	1.49(7)	Cl1	O72	1.378(13)
C14B	C15B	1.42(8)	Cl1	O73A	1.57(3)
C15A	C16A	1.44(7)	Cl1	O73B	1.26(2)
C15B	C16B	1.39(7)	Cl1	O74A	1.33(3)
C16A	C17	1.50(2)	Cl1	O74B	1.72(3)
C16B	C17	2.13(5)	Cl2	O75	1.371(8)
C18	C19	1.530(14)	Cl2	O76	1.437(9)
C18	C23	1.554(13)	Cl2	O77	1.523(14)
C19	C20	1.603(18)	Cl2	O78A	1.65(4)
C20	C21	1.552(17)	Cl2	O78B	1.350(9)

Table 12. Bond Angles for 3-12.

Atom	Atom	Atom	Angle/°	Atom	Atom	Atom	Angle/°
O2	Ca1	O1	110.5(2)	C19	C18	N1	111.8(9)
O3	Ca1	O1	154.3(2)	C23	C18	N1	110.2(7)
O3	Ca1	O2	81.8(2)	C23	C18	C19	111.5(8)
O4	Ca1	O1	80.3(2)	C20	C19	C18	108.8(10)
O4	Ca1	O2	138.9(2)	C21	C20	C19	107.9(10)
O4	Ca1	O3	105.6(2)	C22	C21	C20	109.8(10)
O9	Ca1	O1	80.1(2)	C23	C22	C21	110.0(11)
O9	Ca1	O2	146.6(2)	C22	C23	C18	110.4(9)
O9	Ca1	O3	78.1(2)	C25	C24	N3	111.6(7)
O9	Ca1	O4	72.9(2)	C29	C24	N3	113.2(7)
O10	Ca1	O1	78.9(2)	C29	C24	C25	112.8(9)
O10	Ca1	O2	74.3(2)	C26	C25	C24	110.1(8)
O10	Ca1	O3	83.3(2)	C27	C26	C25	109.2(9)
O10	Ca1	O4	145.8(2)	C28	C27	C26	110.1(13)
O10	Ca1	O9	77.1(2)	C29	C28	C27	110.2(9)
N2	Ca1	O1	63.41(18)	C28	C29	C24	107.9(7)
N2	Ca1	O2	62.95(18)	C31	C30	N3	110.2(8)
N2	Ca1	O3	139.76(19)	C35	C30	N3	110.8(8)
N2	Ca1	O4	90.65(19)	C35	C30	C31	109.4(7)
N2	Ca1	O9	142.2(2)	C32	C31	C30	107.2(10)
N2	Ca1	O10	103.7(2)	C33	C32	C31	109.9(12)
N5	Ca1	O1	136.99(19)	C34	C33	C32	107.5(10)
N5	Ca1	O2	89.12(17)	C35	C34	C33	105.0(11)
N5	Ca1	O3	62.70(18)	C34	C35	C30	106.3(11)

N5	Ca1	O4	61.49(18)	N4	C36	O3	119.7(7)
N5	Ca1	O9	104.6(2)	C37	C36	O3	118.4(7)
N5	Ca1	O10	144.14(19)	C37	C36	N4	121.9(8)
N5	Ca1	N2	96.20(18)	C36	C37	N5	109.1(6)
C1	O1	Ca1	116.2(5)	C39	C38	N5	107.9(6)
C4	O2	Ca1	126.1(5)	N6	C39	O4	121.6(8)
C36	O3	Ca1	118.5(5)	C38	C39	O4	119.6(6)
C39	O4	Ca1	124.3(5)	C38	C39	N6	118.7(8)
C8	O5	C7	131.3(15)	C41	C40	N5	115.3(7)
C43	O7	C42	117.6(9)	C42	C41	C40	108.4(7)
C12	N1	C1	119.8(8)	C41	C42	O7	108.3(7)
C18	N1	C1	122.7(8)	O8	C43	O7	119.6(12)
C18	N1	C12	117.5(7)	C44	C43	O7	115.9(12)
C2	N2	Ca1	99.6(4)	C44	C43	O8	124.6(12)
C3	N2	Ca1	113.1(4)	C45	C44	C43	114.8(13)
C3	N2	C2	108.0(6)	C46	C44	C43	118.5(11)
C5	N2	Ca1	112.9(5)	C46	C44	C45	126.6(13)
C5	N2	C2	112.2(5)	C48	C47	N4	112.1(8)
C5	N2	C3	110.6(6)	C52	C47	N4	111.7(8)
C24	N3	C4	120.6(8)	C52	C47	C48	116.5(11)
C30	N3	C4	121.2(7)	C49	C48	C47	112.2(12)
C30	N3	C24	118.2(7)	C50	C49	C48	109.4(13)
C47	N4	C36	119.3(8)	C51	C50	C49	113(2)
C53	N4	C36	120.7(7)	C52	C51	C50	115(2)
C53	N4	C47	120.0(7)	C51	C52	C47	106.7(14)
C37	N5	Ca1	99.3(4)	C54	C53	N4	107.3(9)
C38	N5	Ca1	111.8(4)	C58	C53	N4	110.2(7)
C38	N5	C37	109.8(5)	C58	C53	C54	112.2(9)
C40	N5	Ca1	115.7(5)	C55	C54	C53	103.5(11)
C40	N5	C37	110.3(5)	C56	C55	C54	109.4(11)
C40	N5	C38	109.4(5)	C57	C56	C55	107.5(11)
C59	N6	C39	120.1(8)	C58	C57	C56	112.9(11)
C65	N6	C39	122.9(7)	C57	C58	C53	111.1(9)
C65	N6	C59	117.0(7)	C60	C59	N6	111.2(7)
N1	C1	O1	120.8(8)	C64	C59	N6	110.6(7)
C2	C1	O1	118.8(7)	C64	C59	C60	116.3(10)
C2	C1	N1	120.4(8)	C61	C60	C59	110.0(9)

C1	C2	N2	109.6(6)	C62	C61	C60	112.5(12)
C4	C3	N2	108.2(6)	C63	C62	C61	110.4(14)
N3	C4	O2	121.1(7)	C64	C63	C62	108.9(10)
C3	C4	O2	120.0(6)	C63	C64	C59	106.7(9)
C3	C4	N3	118.9(8)	C66	C65	N6	110.6(8)
C6	C5	N2	115.0(7)	C70	C65	N6	112.6(8)
C7	C6	C5	107.3(8)	C70	C65	C66	113.0(8)
C6	C7	O5	110.4(10)	C67	C66	C65	106.3(9)
O6	C8	O5	111.9(18)	C68	C67	C66	109.4(11)
C9	C8	O5	124(3)	C69	C68	C67	109.7(9)
C9	C8	O6	123(2)	C70	C69	C68	112.9(10)
C10	C9	C8	111(3)	C69	C70	C65	108.9(9)
C11	C9	C8	118(2)	O72	Cl1	O71	106.0(7)
C11	C9	C10	130(3)	O74A	Cl1	O73A	109.3(14)
C17	C12	N1	109.4(9)	O74B	Cl1	O73B	97.6(17)
C15B	C14B	C13B	96(2)	O76	Cl2	O75	111.7(6)
C16A	C15A	C14A	106(4)	O77	Cl2	O75	104.3(8)
C16B	C15B	C14B	122(6)	O77	Cl2	O76	101.1(7)

Table 13. Atomic Occupancy for 3-12.

Atom	***Occupancy***	**Atom**	***Occupancy***	**Atom**	***Occupancy***
C13B	0.500000	C14A	0.500000	C14B	0.500000
C15A	0.500000	C15B	0.500000	C16A	0.500000
C16B	0.500000	O73A	0.500000	O73B	0.500000
O74A	0.500000	O74B	0.500000	O78A	0.19(3)
O78B	0.81(3)	O11	0.250000		